AN ASYMPTOTIC APPROACH TO MODELING WAVE-GEOMETRY

INTERACTIONS IN AN ELECTROMAGNETIC HEAT EXCHANGER

A Dissertation

Presented to

The Graduate Faculty of Worcester Polytechnic Institute

In Partial Fulfillment

of the Requirements for the Degree

Doctor of Philosophy

Joseph Michael Gaone II

May, 2018
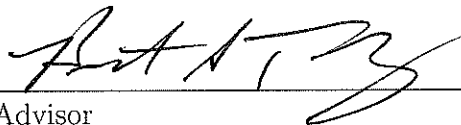
AN ASYMPTOTIC APPROACH TO MODELING WAVE-GEOMETRY

INTERACTIONS IN AN ELECTROMAGNETIC HEAT EXCHANGER
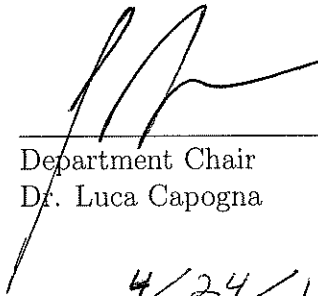
Joseph Michael Gaone II
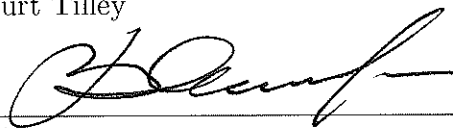
Dissertation

Approved:                                Accepted:

_____                  _____
Advisor                                  Department Chair
Dr. Burt Tilley                          Dr. Luca Capogna

_____                  _____
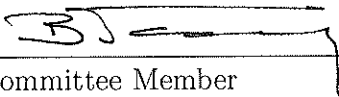Co-Advisor                               Date    4/24/18
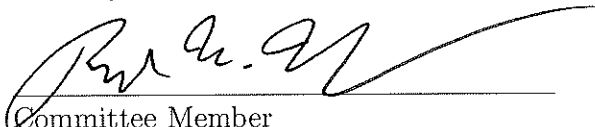Dr. Vadim Yakovlev

_____
Committee Member
Dr. Homer Walker

_____
Committee Member
Dr. Bogdan Vernescu

_____
Committee Member
Dr. Brad Hoff

ii

ABSTRACT

Electromagnetic (EM) heat exchangers are devices that absorb EM radiation and convert its energy to thermal energy for a specific purpose such as to power a turbine. They have recently been of growing interest, yet the field is predominantly studied with thermal resistance network models and is in need of more rigorous continuum modeling. Homogenization has been used in low and high frequency electromagnetics to describe macroscopic behavior of traveling waves. While dielectric material parameters vary with temperature, coupling the energy equation with Maxwell's equations, little effort has been made toward homogenization techniques that capture the effects of this dependence, which is necessary to accurately model porous medium heat exchangers. Firstly, we have examined the effect the wave-geometry interactions of high-frequency illumination has on a triple-layer laminate, which approximates the unit cell of a homogenization problem. Secondly, we develop an extension to a high-frequency homogenization (HFH) method developed for photonics. The extension is made by developing a three-dimensional vector-valued HFH of Maxwell's curl-curl equation that includes dielectric loss. It is validated for a one-dimensional geometry where the exact solution to the scattering problem is known by implementing the Transfer Matrix Method. The HFH model produces perturbation approximations to the dispersion curves showing the nonexistence of band gaps and generates low attenuation outside the band gap regions.

# ACKNOWLEDGEMENTS

Many people deserve my gratitude for their contributions. To the dissertation committee Drs. Tilley, Yakovlev, Walker, Vernescu, and Hoff for serving on the committee and for their help in fashioning the dissertation. To my advisors, Burt Tilley and Vadim Yakovlev, for their support and expertise in guiding me through course work, research, speaking engagements, writing technical papers, interviews, and much preparation for the dissertation and defense. To Brad Hoff, for his time as a mentor during my internship with the Air Force Research Laboratory, for taking the time out of his schedule to personally attend both the proposal and defense, and for continued support and interest in helping me succeed. To fellow students Kyle Dunn, Brian Kodalen, Michael Yereniuk, and Ajit Mohekar for engaging conversations which both solidified and sparked ideas vital to this work. To Matt Porter for acquiring samples of porous Silicon Carbide for use during the defense which brought a renewed excitement to the project. To my parents Karen and Joe, and to my brother Josh, for their unwavering love and support through the years and for encouraging words during my many years as a student. To the love of my life, my wife Traceylee, for her care and friendship, support and encouragement when things got hard, and for her love and understanding during this long and difficult journey, without whom I would never have finished. Finally, to my Lord and savior Jesus Christ, who first loved me.

Almighty God, Who hast created man in Thine own Image, and made him a living soul that he might seek after Thee, and have dominion over Thy creatures, teach us to study the works of Thy hands, that we may subdue the earth to our use, and strengthen our reason for Thy service; and so to receive Thy blessed word, that we may believe on Him whom Thou hast sent, to give us the knowledge of salvation and the remission of our sins. All which we ask in the name of the same Jesus Christ, our Lord.

James Clerk Maxwell (1831-1879)

TABLE OF CONTENTS

LIST OF TABLES

LIST OF FIGURES

In Science, it is when we take some interest in the great discoverers and their lives that it becomes endurable, and only when we begin to trace the development of ideas that it becomes fascinating.

James Clerk Maxwell (1831-1879)

CHAPTER I

INTRODUCTION

A heat exchanger is a device used to efficiently transfer heat from one location to another.
The intended purpose can be to cool a material down or heat it up. They can be found
throughout our everyday lives, the radiator in a car, a radiator in a home, a heat sink in a
circuit board, refrigerators, steam pipes, boilers, computer fans, liquid coolant such as freon
or nitrogen, air conditioning, frying pan, etc. Every application is either trying to heat up
or cool off a system [5–7].

Electromagnetic (EM) heat exchangers involve the heating of a material by an EM
field and the collection of the thermal energy through the use of a fluid. Notable examples
include solar thermal collectors and more recently beamed energy applications. A sample
geometry of a simple heat exchanger is depicted in Figure 1. A material that readily absorbs
EM radiation will heat up, much like how microwaves heat food in a microwave oven. The
heated material is in direct contact with a fluid which will heat up through conduction. The
thermal energy in the fluid is then collected as the fluid flows out of the channel. The energy
in the fluid can be utilized to do work, such as to drive a turbine or produce thrust. The goal
of the current work is to create innovative mathematical models capable of characterizing
and investigating the operation of such a device to further advance the efficiency and utility
of this technology.
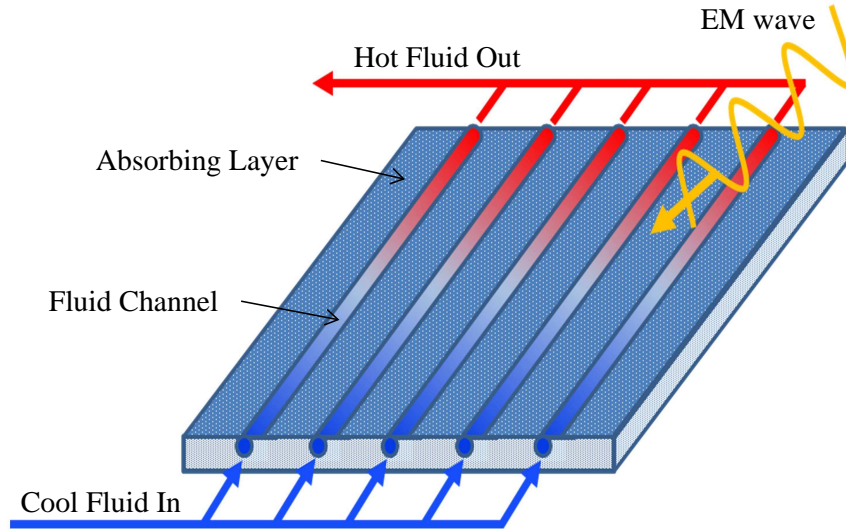
Figure 1.1: An example of a planar EM heat exchanger that heats up the incoming fluid through contact with the surrounding absorbing material.

The dissertation is organized into five chapters. The introduction to EM heat exchangers is further detailed here in Chapter 1. The past and current work into the steady state heating without fluid dynamics is discussed in Chapter 2, particularly for a triple-layer laminate. Chapter 3 introduces fluid flow to the triple-layer geometry which simulates the energy collection aspect of a heat exchanger. Three different approaches are taken to model the physics involved. The first two study the asymptotic regimes of low and high advection while the third directly solves the governing equations with a fully numerical technique. Porous laminate models are considered in Chapter 4 which considers two cases. The first considers the model for a classical long-wave (LW) homogenization, while the second develops an extension to a high-frequency homogenization (HFH) model that now incorporates dielectric losses. The models are compared for validation and conclusions are drawn in Conclusions where we explore possible avenues of future research.

The rest of this Chapter is devoted the background of EM heat exchanger applications and previous models of heat exchangers, a history and analysis of previous microwave heating models, as well as homogenization and effective medium theory of Maxwell's equations. The second part of the Chapter is devoted to reviewing aspects of classical electromagnetic theory required for analyzing EM heat exchangers.

## 1.1    Background

In this section, we present a short history of EM heat exchangers and the current methods of modeling these devices. The fundamental physical phenomena are introduced and the multiphysics coupling is discussed. The primary coupling of electromagnetic heating is examined in more detail and presents select models. Finally, we end with a discussion on porous media and their applicability in heat exchangers.

### 1.1.1    EM Heat Exchangers

Electromagnetic heat exchangers have been around as long as mankind has utilized the sun's power for heating. Solar collection heat exchangers have a long history from Civil War era heating of water filled containers in the sun [8] to the first focused solar fluid heating in the 1940s, which could be fed directly into a home's radiator system [9]. Modern heat exchangers aim to increase in technological advancement, achieving higher temperatures in less time, better efficiency, and use in converting to other energy needs such as running a turbine to generate electricity [10] or beamed-energy propulsion for in atmosphere rocket launches [11].

Mathematical models have been used to describe the operation of EM heat exchangers [12–17]. Most models include complicated geometries and have analyzed the system using thermal resistance networks. This technique models heat transfer as an analogue of electrical circuits and is only valid for systems of steady heat transfer exhibiting no heat generation [18]. Additionally, this limits the ability of models to capture fundamental spatially dependent phenomena. Further mathematical modeling is required in order to understand the physics involved in the operation of EM heat exchangers.

## 1.1.2 Physics Coupling

A main challenge of mathematically modeling an EM heat exchanger is that it is inherently multi-physical and include interactions between three fundamental physics disciplines. The classical physics of electromagnetics, thermodynamics, and fluid dynamics have been developed by scientific patriarchs and throughly studied. Even the bi-coupling fields of electromagnetic heating (EM-Thermal), fluid dynamics (Fluid-Thermal), electro-magneto-hydrodynamics (EM-Fluid) have been studied in recent history. However, multiphysics problems that include a tri-coupling (EM-Fluid-Thermal) are much less understood. Figure 1.2a depicts a possible relationship between the three areas where every coupling is bi-directional. The dependences shown represent only one example and are by no means exhaustive in how the three physics can be coupled together. In order to study EM heat exchangers we must in some way include this coupling, though throughout this work we only consider the coupling described in Figure 1.2b. A material experiences dielectric heating, which is a bi-coupling as the dielectric constant is temperature dependent, changing the electric field, and the tem-
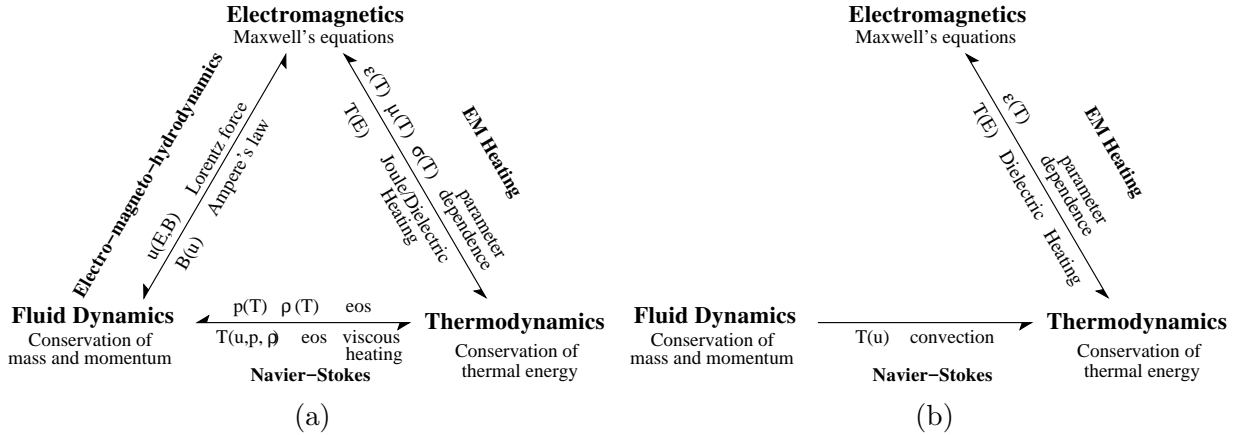
**Figure 1.2:** The coupling of electromagnetics, thermodynamics, and fluid dynamics and how each depends on the other two: A non-exhaustive tri-coupling of the three physical disciplines. Equation of state is abbreviated as (eos), which relates $\rho$, $p$, and $T$ together (a); the present coupling considered throughout this work, where the fluid is uni-coupled only influencing the temperature (b).

perature experiences a volumetric source from the electric field. It is assumed, however, the only coupling to fluid flow is that the fluid velocity induces thermal convection.

It is known that computer simulations can have a tremendous advantage over laboratory experiments in both discovery and design, provided they have been validated through empirical means. There have been several attempts to model the tri-coupling nature of the governing equation using multiphysics solvers such as COMSOL or ANSYS [19–22]. This approach of numerical experimentation reproduces the natural conditions of the device in a simulated environment, which can be beneficial, but it can also make it difficult to identify fundamental physical processes. Additionally, the computational resources required to accurately compute such a model can be expensive. In contrast, mathematical models describe system behavior under certain limiting assumptions. Studying models in various parameter

regimes allows solutions to be more analytically tractable. This approach gleans insight into the underlying physics responsible for particular phenomenon within a system, under these assumed conditions.

### 1.1.3 Electromagnetic Heating

Microwave heating was discovered near the end of World War II [23]. Research increased with the invention of the microwave oven by Percy Spencer in 1945 [23]. The main attribute that microwave heating allows for volumetric heating instead of heating by contact has made its applications almost too numerous to mention, ranging widely from food processing [24–26], microwave assisted combustion [27], chemical vapor infiltration [28], microwave sintering [29–31], material processing [32–35], and much more.

Electromagnetic heating is driven by the work done on electric charges where the dissipated energy is the source to the thermal energy generated within a material. The electromagnetic parameters known as the dielectric constant $\epsilon$ and the magnetic permeability $\mu$ describe, among other interpretations, how resistive electromagnetic energy moves through a particular medium. The materials considered in this work are non-magnetic, $\mu = \mu_0$, where the constant $\mu_0$ is the permeability of free space.

Heating by absorption of electromagnetic radiation is driven by two sources. In the presence of an alternating electric field dipoles oscillate in an attempt to orient themselves with the positive (negative) charge away from (toward) a positive field and toward (away from) a negative field according to the Lorentz force. This rapid movement is the primary source of EM heating for dielectric materials which tend to be insulators. The second source

6

of heating is when an alternating magnetic field induces motion of free charges into eddy currents. The resistivity causes the heat generation and is the primary heating mechanism for conductive materials. Materials may be dominant in one mechanism over the other, but often materials, such as water, exhibit both heating types. It is common when considering monochromatic waves to lump the two losses together as an effective conductivity $\sigma_e = \omega\epsilon'' + \sigma$, or, equivalently, as an effective dielectric loss $\epsilon_e'' = \epsilon'' + \frac{\sigma}{\omega}$, where $\omega$ is the angular frequency, $\sigma$ is the electrical conductivity, and $\epsilon''$ is the dielectric loss. Additional loss mechanisms can be present in other materials [36], but will not be addressed in this work.

Throughout the past 30 years a number of studies have been performed, which have been able to describe fundamental phenomena seen in experiments such as nonuniform heating [37,38] and thermal runaway [4,39,40]. As models progressed with time, applications of microwave heating began to be modeled which have included food treatment [41], chemical vapor infiltration [28], and microwave sintering [30].

Mathematical modeling of microwave heating began in the early 1990s [39, 42–44]. The case of uniformly heating a dielectric half-space was analyzed by Kriegsmann, Brodwin, and Watters in 1990 [39]. In their work they established that the relationship between the steady-state temperature as a function of power, known as the power response curve, was an S-shaped bifurcation diagram or continuation curve, see Figure 1.3. It was shown that positively sloped branches were stable while the negatively sloped branches were unstable [45]. This was the first mathematical model able to describe the phenomenon of thermal runaway and was not experimentally verified until 2002 [46]. Thermal runaway is a natural process in EM heating that causes temperature to increase rapidly, often compromising the
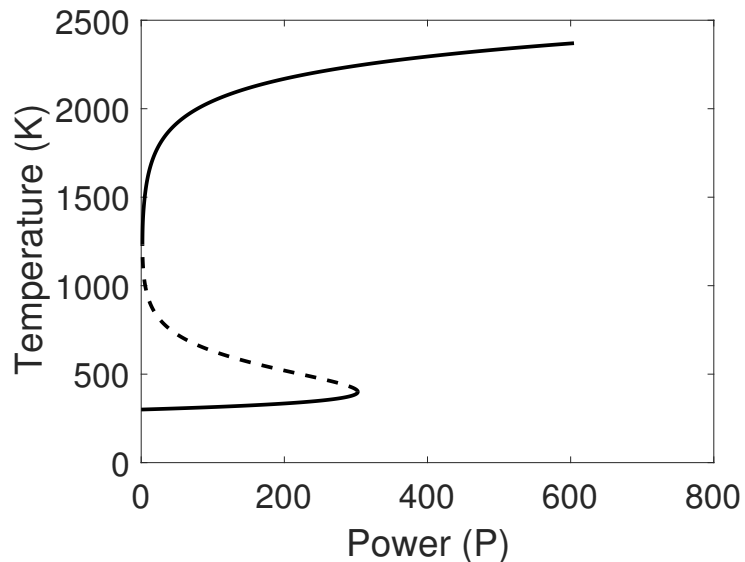
Figure 1.3: Example of an S-curve power response, describing steady state temperature as a function of input EM power; stable branches (solid curve); unstable branches (dashed curve).

integrity of the material either from thermal stress or through melting. The cause is an imbalance where the energy is absorbed at a much larger rate than is dissipated to the environment. This has led to many attempts to find a way to control thermal runaway [47–50].

Models of microwave heating analyze the heat equation with the nonlinear heat source

$$\langle P \rangle = \frac{1}{2}\sigma_e |E|^2, \tag{1.1}$$

where $\langle P \rangle$ is the time averaged power dissipated from the electric field $E$, as it does work to move the bound (dipole) or free (conducting) charges. The derivation of this source is presented in Section 1.2. A lossy material exhibits heat generation from the attenuation of

8

the electric field. The requirement of conservation of energy dictates an advection-diffusion equation govern the transport of thermal energy within a medium,

$$\rho c_p \left[ \frac{\partial T}{\partial t} + \nabla \cdot (\mathbf{u} T) \right] = \nabla \cdot (k \nabla T) + \langle P \rangle, \tag{1.2}$$

where $T$ is temperature, $\mathbf{u}$ is the fluid velocity, and material parameters $\rho$, $c_p$ and $k$ are the density, specific heat, and thermal conductivity of the medium. In general, the energy equation would be coupled to the Navier-Stokes equations to determine an unknown fluid velocity, however, we only consider the uni-directional coupling where fluid velocity is known or solved independently of temperature or the EM field.

There are many relevant parameters that are known empirically to be temperature dependent. These include the permittivity $\epsilon'(\omega, T)$ and dielectric loss $\epsilon''(\omega, T)$ which are also frequency dependent, electrical conductivity $\sigma(T)$, thermal conductivity $k(T)$ and density $\rho(T)$ of both solid and fluid alike. For simplicity, we only consider temperature dependence of the dielectric loss and electrical conductivity. The effective conductivity $\sigma_e$ is then dependent on the temperature making the governing EM and thermal equations bi-coupled. Some models of this dependence have been proposed including polynomial, Arrhenius law, and exponential [51]. However, many dielectric materials have been shown to be in good agreement with an exponential dependence

$$\sigma_e = A e^{bT}, \tag{1.3}$$

9

**Dielectric Loss:** $\epsilon'' = 3.775\text{e-}07e^{3.0324T}$

**Dielectric Loss:** $\epsilon'' = 0.0029128e^{2.3259T}$

(a)  (b)
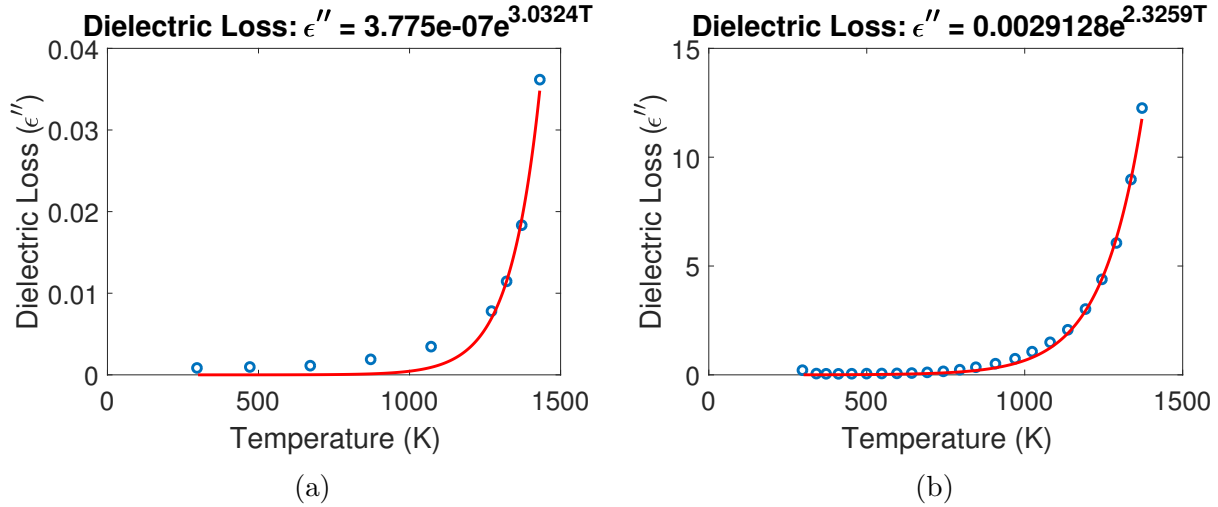
Figure 1.4: Least squares curve fit of an exponential dependence of temperature on the dielectric loss: Silicon Dioxide data taken from [3] (a); Zirconia, data taken from [4] (b).

which is used throughout this work. A justification for the exponential dependence of many dielectric materials is seen from experimental measurement [3]. One such material is Silicon Dioxide ($SiO_2$) for which Figure 1.4a shows an example of a least squares curve fitting.

### 1.1.4 Homogenization Theory

Porous media are ideal materials when a system will benefit from large surface area. Since EM heat exchangers transfer thermal energy from lossy material to a fluid via direct contact, a large surface area will increase the rate of energy transfer. While the large surface area allows for a larger rate of energy transfer, driving fluid through the porous structure to utilize the heat is more difficult as the surface area of the medium increases. Nevertheless, it is a useful material in designing an efficient heat exchanger. A useful mathematical tool to study problems that involve porous media is homogenization.

10

The theory of homogenization is an area of mathematics used to model heterogeneous structures whose true physical processes would be a challenge to model directly. In short, a homogenization method is, in some sense, an averaging technique aimed at approximating the physics of a heterogeneous medium with an "equivalent" homogeneous medium. At its core, this is not a new idea, dating back to work by Poisson [52], Maxwell [53], and Einstein [54]. Prior to 1970 the majority of the work included theory of mixtures [55, 56] and volume averaging methods [57]. The term *homogenization* as a methodological process was first used by Babuska [58]. Homogenization methods via multiscale asymptotics of periodic and random media began in the early 1970s [59–61]. The mathematical formalism of convergence results were developed thereafter [62–65]. The field today is a diverse subject that vary greatly from its beginnings with the simple mixture formulas.

There are several common principles of homogenization with asymptotics. First, there is a disparate difference in two length scales, so one can define the ratio $\eta$ of the characteristic microscale to the macroscale. The method of multiple scales is then applied, where the function $f(x; \eta)$ exhibits scale separation when $\eta \ll 1$, and is approximated by the ansatz $f(x, \xi)$, possessing two independent variables, where $\xi = \frac{x}{\eta}$. Furthermore, a solution is approximated by an asymptotic expansion $f(x, \xi) = f^{(0)}(x, \xi) + \eta f^{(1)}(x, \xi) + \eta^2 f^{(2)}(x, \xi) + ...$ which when applied to the system of equations governing the fundamental physics produces a hierarchy of problems to solve for $f^{(j)}$, $j = 0, 1, 2, ...$ The difficulty arises in making appropriate assumptions so that the sequence of problems are both solvable and meaningful.

The justification of the process above for a leading order approximation is to show

$$\lim_{\eta \to 0} \left\| f(x; \eta) - f^{(0)}\left(x, \frac{x}{\eta}\right) \right\| = 0, \qquad (1.4)$$

over a given norm $\| \cdot \|$ [66]. Classical long-wave homogenization generally has a leading order solution $f^{(0)}(x)$ independent of the microscale variable $\xi$, hence the solution behaves as if it had no microscale structure, a homogenized medium. The long-wave homogenization shown in Chapter 4 exhibits this leading order behavior. However, this is not always the case, for which more sophisticated methods are required to capture microscale effects in a homogenized solution. The high-frequency homogenization of Chapter 4 is one such example.

Homogenization techniques for electromagnetic scattering problems are of particular interest since they can be used to estimate the field in a heterogeneous material. Once an appropriate homogenized scattering problem is solved it can be coupled to a homogenized thermal solution to model the EM heating of a porous media heat exchanger. The EM scattering problem plays an integral role in how the energy is distributed within the material. The classical mixture formulas that determine effective parameters, beginning with that of Maxwell-Garnett, are still widely used today, but are only applicable in limited situations [56]. Scattering in a periodic array of laminates has been extensively studied for their use in lasers as well for their unusual properties such as possessing a negative refractive index [67, 68]. The majority of modern homogenization techniques used to approximate the macroscale EM behavior of these arrays have been restricted to the field of photonics where temperature variations are not considered. The homogenization models can be classified into

12

lossless and low-frequency [69–77], dissipative and low-frequency [78–81], lossless and high-frequency [72, 75, 82], and finally dissipative and high-frequency [80]. There are also a few studies into the transition region between low and high frequency regimes [80,83]. All of these models assume that the dielectric constants are independent of temperature fluctuations and consequently spatially independent. In order to understand the fundamentals of modeling EM heat exchangers, Maxwell's equations with a spatially dependent dielectric loss must be considered in the homogenization.

## 1.2 Classical Electromagnetic Theory

In this Section, we review topics from classical EM theory that will be vital in our understanding of the heat exchanger model. We begin with Maxwell's equations and derive the curl-curl formulation for the electric field, next discuss the associated boundary conditions for a dielectric material, and finally end the review with the derivation of the energy absorbed by a lossy medium.

### 1.2.1 Maxwell's Equations

Starting from Maxwell's equations we derive the curl-curl or Helmholtz-like equations which decouple the electric and magnetic fields. These equations will be referred to throughout the rest of the paper. We assume that the material parameters are not only spatially dependent but depend on temperature and thus implicitly depend on time. Introducing two distinct time scales, a fast time scale describing wave propagation and a slow time scale describing heat transfer we can assume the material parameters are independent of the fast time scale

since they only depend on time implicitly through the temperature. Additionally, we intro-

duce two distinct spatial scales as well, a small scale $l$ characterizing the microscale structure,

and a large scale $L$ characterizing the macroscale structure. Finally, we also assume the inci-

dent field is monochromatic with angular frequency $\omega$ and the current density obeys Ohm's

law, $\mathbf{J}'_f = \sigma \widehat{\mathbf{E}}'$ where the prime denotes dimensional quantity and the hat denotes a time

dependent electric or magnetic field. Maxwell's equations for linear media are given by

$$\nabla' \cdot (\epsilon' \widehat{\mathbf{E}}') = \rho'_f, \qquad\qquad \nabla' \cdot (\mu' \widehat{\mathbf{H}}') = 0, \qquad (1.5)$$

$$\nabla' \times \widehat{\mathbf{E}}' = -\frac{\partial}{\partial \overline{t}'}(\mu' \widehat{\mathbf{H}}'), \qquad\qquad \nabla' \times \widehat{\mathbf{H}}' = \mathbf{J}'_f + \frac{\partial}{\partial \overline{t}'}(\epsilon' \widehat{\mathbf{E}}'). \qquad (1.6)$$

where $\widehat{\mathbf{E}}'(\mathbf{x}', \overline{t}')$ is the electric field, $\widehat{\mathbf{H}}'(\mathbf{x}', \overline{t}')$ is the magnetic field, $\rho'_f$ is the free charge

density.

Before proceeding, we define non-dimensional variables

$$x_i = \frac{x'_i}{l}, \;\; \overline{t} = \omega \overline{t}', \;\; E = \frac{E'}{E_0}, \;\; H = \frac{H'}{H_0}, \;\; \sigma = \frac{\sigma'}{\sigma_0}, \;\; \epsilon = \frac{\epsilon'}{\epsilon_0}, \;\; \mu = \frac{\mu'}{\mu_0}, \;\; \rho_f = \frac{\rho'_f}{\rho_0}, \qquad (1.7)$$

where $H_0 = \frac{E_0}{\mu_0 c}$, $c$ is the speed of light in a vacuum, $\sigma_0 = \omega \epsilon_0$, and $\rho_0 = \frac{\epsilon_0 E_0}{l}$. Next

we introduce the two time scales where $\tau = \overline{t}$ is the fast variable and $t = \delta \overline{t}$ is the slow

variable. We let $\delta = \frac{1}{\omega t_l} \ll 1$, the ratio of the period of EM oscillation $\frac{1}{\omega}$ and $t_l = \frac{l^2}{\alpha}$,

the characteristic heat conduction time of the microstructure, where $\alpha = \frac{k}{\rho c_p}$ is the thermal

diffusivity. Maxwell's equations are rewritten as

$$\nabla \cdot (\epsilon \widehat{\mathbf{E}}) = \rho_f, \quad \nabla \cdot (\mu \widehat{\mathbf{H}}) = 0, \tag{1.8}$$

$$\nabla \times \widehat{\mathbf{E}} = -\frac{\omega l}{c}\frac{\partial}{\partial \tau}(\mu \widehat{\mathbf{H}}) - \delta \frac{\omega l}{c}\frac{\partial}{\partial t}(\mu \widehat{\mathbf{H}}), \quad \nabla \times \widehat{\mathbf{H}} = \frac{\omega l}{c}\sigma \widehat{\mathbf{E}} + \frac{\omega l}{c}\frac{\partial}{\partial \tau}(\epsilon \widehat{\mathbf{E}}) + \delta \frac{\omega l}{c}\frac{\partial}{\partial t}(\epsilon \widehat{\mathbf{E}}). \tag{1.9}$$

We formally consider the leading order problem of an asymptotic expansion in $\delta$. With interest in modeling the lower frequency regime of microwaves $\omega = 2\pi \cdot 10^8 \ rad \cdot Hz$ for Silicon Carbide where we calculate a thermal diffusivity $\alpha = 1.02 \cdot 10^{-4} \ \frac{m^2}{s}$ using parameters $\rho = 3.2 \cdot 10^3 \ \frac{Kg}{m^3}$, $k = 300 \ \frac{W}{mK}$, and $c_p = 920 \ \frac{J}{KgK}$ [84]. Considering a microscale structure on order of millimeters $l = 10^{-3}$ yields $\delta \approx 1.6 \cdot 10^{-7}$. However, this asymptotic assumption is not uniformly valid. Considering a microscale of $l = 1 \ \mu m$ makes $\delta \approx 0.16$ nearly order one, which implies thermal energy is able to diffuse across the microstructure at the same rate one wavelength of the EM wave passes through the sample. Throughout the rest of our work, we assume the asymptotic assumption is valid and moving forward we only consider the leading order EM problem.

It can be shown that for a material with constant conductivity and dielectric parameters the free charge is found by the equation,

$$\rho_f(\overline{t}') = e^{-\frac{\sigma'}{\epsilon'}\overline{t}'}\rho_f(0). \tag{1.10}$$

After a characteristic time of $\frac{\epsilon'}{\sigma'}$, we can assume the free charge density is zero as all charge accumulates at the surface [85]. Since the permittivity and conductivity vary with space it

is no longer clear that the free charge density will dissipate. However by assuming a time harmonic monochromatic wave, Maxwell's equations can be rewritten in terms an effective dielectric constant in which no free pseudo-charges are present. To show this we begin by assuming time harmonic solutions $\widehat{\mathbf{E}} = \mathbf{E}(\mathbf{x})e^{i\omega\tau'} = \mathbf{E}(\mathbf{x})e^{i\tau}$ and $\widehat{\mathbf{H}} = \mathbf{H}(\mathbf{x})e^{i\omega\tau'} = \mathbf{H}(\mathbf{x})e^{i\tau}$. The continuity equation for free charge is

$$\frac{\partial \rho_f}{\partial \tau} = -\nabla \cdot (\sigma \mathbf{E})e^{i\tau}, \tag{1.11}$$

where the free current density is given by Ohm's law. Integrating with respect to time gives

$$\rho_f = -\nabla \cdot (\sigma \widehat{\mathbf{E}})\frac{1}{i}e^{i\tau}. \tag{1.12}$$

Therefore, the free charge density is also time harmonic and satisfies the differential equation

$$\frac{\partial \rho_f}{\partial \tau} = i\rho_f. \tag{1.13}$$

We now transform Gauss' law in terms of an effective dielectric constant which includes the loss from conductivity. Beginning with Gauss' law, multiply both sides by $i$ and substitute in (1.13),

$$i\nabla \cdot (\epsilon \widehat{\mathbf{E}}') = \frac{\partial \rho_f}{\partial \tau}. \tag{1.14}$$

Applying the continuity equation and multiplying through by $e^{-i\tau}$,

$$i\nabla \cdot (\epsilon \mathbf{E}) = -\nabla \cdot (\sigma \mathbf{E}). \tag{1.15}$$

Defining the effective dielectric constant as $\epsilon_e = \epsilon - i\sigma$ the equation for Gauss' law is written as

$$\nabla \cdot (\epsilon_e \mathbf{E}) = 0. \tag{1.16}$$

The time-harmonic leading order Maxwell's equations reduce to

$$\nabla \cdot (\epsilon_e \mathbf{E}) = 0, \qquad\qquad \nabla \cdot (\mu \mathbf{H}) = 0, \tag{1.17}$$

$$\nabla \times \mathbf{E} = -i\gamma\mu\mathbf{H}, \qquad\qquad \nabla \times \mathbf{H} = i\gamma\epsilon_e\mathbf{E}. \tag{1.18}$$

where $\gamma = \frac{\omega l}{c} = 2\pi\frac{l}{\lambda_0}$ is a non-dimensional wavenumber, where $\lambda_0$ is the free-space wavelength. Finally, by taking the curl of the curl of the electric field we are able to derive the Helmholtz-like equation and decouple the fields. The curl-curl is

$$\nabla \times \nabla \times \mathbf{E} = -i\gamma\nabla \times (\mu\mathbf{H}), \tag{1.19}$$

and applying identities from vector calculus it becomes

$$\nabla (\nabla \cdot \mathbf{E}) - \nabla^2\mathbf{E} = -i\gamma [\mu\nabla \times \mathbf{H} + \nabla\mu \times \mathbf{H}], \tag{1.20}$$

17

and finally by substituting in (1.18) we arrive at the system of equations

$$\nabla \cdot (\epsilon_e \mathbf{E}) = 0, \tag{1.21}$$

$$\nabla (\nabla \cdot \mathbf{E}) - \nabla^2 \mathbf{E} = \gamma^2 \epsilon_e \mu \mathbf{E} + \frac{1}{\mu} \nabla \mu \times \nabla \times \mathbf{E}, \tag{1.22}$$

and in general we do not consider any magnetic material so the last term is equal to zero.

### 1.2.2 Boundary Conditions

The boundary conditions on an electromagnetic field at a material interface are given by

$$\mathbf{n} \cdot \mathbf{D}_2 - \mathbf{n} \cdot \mathbf{D}_1 = \sigma_f, \tag{1.23}$$

$$\mathbf{n} \cdot \mathbf{B}_2 - \mathbf{n} \cdot \mathbf{B}_1 = 0, \tag{1.24}$$

$$\mathbf{n} \times \mathbf{E}_2 - \mathbf{n} \times \mathbf{E}_1 = 0, \tag{1.25}$$

$$\mathbf{n} \times \mathbf{H}_2 - \mathbf{n} \times \mathbf{H}_1 = \mathbf{K}, \tag{1.26}$$

where $\mathbf{n}$ is a unit normal pointing from region 1 into region 2, $\sigma_f$ is the free surface charge density, and $\mathbf{K}$ is the surface current density. The derivation of each of these conditions can be found in [85]. From a mathematical perspective, it is known that ohmic conductors with finite conductivity have no free surface current ($\mathbf{K} \equiv 0$) [85, 86]. The current in a conductor will instead be a volumetric current near the surface but not on the surface itself. We make this distinction clear so as to not cause confusion about the immense history of experimental evidence that conductors gather charge at the surface. No free surface current implies there are no free surface charges since the electric field is an alternating field. As with

the continuity of charge equation, one can derive from a pillbox argument the continuity of surface charge equation is given by

$$\frac{\partial \sigma_f}{\partial \tau} = -\nabla \cdot \mathbf{K}. \tag{1.27}$$

The assumption of being an ohmic conductor implies that the surface charge density must be constant in time. However, this is impossible in an alternating field thus it must be that $\sigma \equiv 0$.

### 1.2.3 Energy Absorption

The energy which makes up an electromagnetic field

$$W = \frac{1}{2} \int_{\mathbb{R}^3} \left( \epsilon_0 E^2 + \mu_0 H^2 \right) d^3 r,$$

is determined by the amount of work needed to create it in the first place, which is detailed in [85]. Similarly the work done by an electromagnetic field on a medium is the energy that is dissipated from the field itself and consequently the source of thermal energy. The derivation of the energy dissipation (1.1) is mentioned in [86], but is given below for sake of completeness. Work is defined by

$$W = \int \mathbf{F} \cdot d\mathbf{l}, \tag{1.28}$$

or as a differential $dW = \mathbf{F} \cdot d\mathbf{l}$. The work done by an EM field on a charge is $q$ is given by the distance the charge moves by Lorentz force $\mathbf{F} = q(\mathbf{E} + \mathbf{v} \times \mathbf{B})$. An infinitesimal distance traveled by the charge is $d\mathbf{l} = \mathbf{v}dt$. The work differential on charge $q$ is

$$dW_q = q(\mathbf{E} + \mathbf{v} \times \mathbf{B}) \cdot \mathbf{v}d\tau. \qquad (1.29)$$

Since $\mathbf{v} \times \mathbf{B}$ is perpendicular to $\mathbf{v}$, $(\mathbf{v} \times \mathbf{B}) \cdot \mathbf{v} = 0$. This shows that the magnetic field does no work. The differential is then

$$dW_q = q\mathbf{E} \cdot \mathbf{v}d\tau. \qquad (1.30)$$

We now convert this result to include a general charge density. A point charge is given by $q = \rho dV$, where $dV$ is a differential volume. Current density is also given by $\mathbf{J} = \rho\mathbf{v}$. The differential work is then of the form

$$dW_q = \mathbf{E} \cdot \mathbf{J}dV d\tau. \qquad (1.31)$$

Power is the rate that work is done. Hence the power of a charge $q$ is

$$\frac{dW_q}{d\tau} = \mathbf{E} \cdot \mathbf{J}dV. \qquad (1.32)$$

Summing over all charges in a given volume $V$ the total Power is

$$\frac{dW}{d\tau} = \int_V \mathbf{E} \cdot \mathbf{J} dV. \tag{1.33}$$

The power density is then given by

$$P = \mathbf{E} \cdot \mathbf{J}. \tag{1.34}$$

A sinusoidally oscillating field is given by a linear combination of sines and cosines

$$a(\tau) = a_1 \cos(\omega\tau) + a_2 \sin(\omega\tau), \tag{1.35}$$

where $\omega$ is the angular frequency. This of course can be rewritten in terms of one of the trig functions plus a phase shift and amplitude change.

$$a(\tau) = A \cos(\omega\tau + \alpha), \tag{1.36}$$

which can be written using Euler's formula by

$$a(\tau) = Re\left[\widetilde{A}e^{i\omega\tau}\right], \tag{1.37}$$

where $\widetilde{A} = Ae^{i\alpha}$. Therefore, real measured valued of the electric field $\widehat{\mathbf{E}}(\mathbf{x}, \tau)$, magnetic field $\widehat{\mathbf{H}}(\mathbf{x}, \tau)$, and current density $\widehat{\mathbf{J}}(\mathbf{x}, \tau)$ can be written as

$$\widehat{\mathbf{E}}(\mathbf{x}, \tau) = Re\left[\mathbf{E}(\mathbf{x})e^{i\tau}\right], \tag{1.38}$$

$$\widehat{\mathbf{H}}(\mathbf{x}, \tau) = Re\left[\mathbf{H}(\mathbf{x})e^{i\tau}\right], \tag{1.39}$$

$$\widehat{\mathbf{J}}(\mathbf{x}, \tau) = Re\left[\mathbf{J}(\mathbf{x})e^{i\tau}\right], \tag{1.40}$$

where $\mathbf{E}(\mathbf{x})$, $\mathbf{H}(\mathbf{x})$, and $\mathbf{J}(\mathbf{x})$ are complex valued. Given $z \in \mathbb{C}$, $Re[z] = \frac{z+z^*}{2}$, where $z^*$ is the complex conjugate of $z$. Therefore, the real fields can be written as

$$\widehat{\mathbf{E}}(\mathbf{x}, \tau) = \frac{1}{2}\left[\mathbf{E}(\mathbf{x})e^{i\tau} + \mathbf{E}^*(\mathbf{x})e^{-i\tau}\right], \tag{1.41}$$

$$\widehat{\mathbf{H}}(\mathbf{x}, \tau) = \frac{1}{2}\left[\mathbf{H}(\mathbf{x})e^{i\tau} + \mathbf{H}^*(\mathbf{x})e^{-i\tau}\right], \tag{1.42}$$

$$\widehat{\mathbf{J}}(\mathbf{x}, \tau) = \frac{1}{2}\left[\mathbf{J}(\mathbf{x})e^{i\tau} + \mathbf{J}^*(\mathbf{x})e^{-i\tau}\right]. \tag{1.43}$$

Fields that oscillate sinusoidally are separable in time and space but then the spatial component becomes complex valued as a result from using Euler's formula. The power density written in terms of the complex valued electric field and current density is

$$P = \frac{1}{2}\left[\mathbf{E}e^{i\tau} + \mathbf{E}^*e^{-i\tau}\right] \cdot \frac{1}{2}\left[\mathbf{J}e^{i\tau} + \mathbf{J}^*e^{-i\tau}\right], \tag{1.44}$$

which reduces to

$$P = \frac{1}{2} Re \left[ \mathbf{E} \cdot \mathbf{J} e^{2i\tau} + \mathbf{E} \cdot \mathbf{J}^* \right]. \tag{1.45}$$

Now since the time it takes the heat to dissipate is much longer than the monochromatic period it is useful to consider the time averaged power density over one period of oscillation. Time averaging by definition is

$$\langle f \rangle = \frac{1}{2\pi} \int_0^{2\pi} f(\tau)\, d\tau, \tag{1.46}$$

so the time averaged power density is given by

$$\langle P \rangle = \frac{1}{2\pi} \int_0^{2\pi} \frac{1}{2} Re \left[ \mathbf{E} \cdot \mathbf{J} e^{2i\tau} + \mathbf{E} \cdot \mathbf{J}^* \right]\, d\tau. \tag{1.47}$$

Therefore, the time averaged power density is

$$\langle P \rangle = \frac{1}{2} Re \left[ \mathbf{E} \cdot \mathbf{J}^* \right]. \tag{1.48}$$

This is the power loss to thermal energy due to the electric field doing work on charges in a material.

When given an alternating field and with Ohm's law $\mathbf{J} = \sigma \mathbf{E}$ applicable, and the material is a linear material $\mathbf{D} = \epsilon \mathbf{E}$ an effective conductivity can be defined by using

23

Ampere's law,

$$\nabla \times \mathbf{H} = \gamma \sigma_e \mathbf{E} + i \gamma \epsilon' \mathbf{E}, \tag{1.49}$$

where $\sigma_e = \sigma + \epsilon''$ is now the effective conductivity. Note that $\sigma_e$ is missing the angular frequency $\omega$ since we nondimensionalized the problem. This provides an expression an effective current density when alternating fields are present, $\mathbf{J}_e = \sigma_e \mathbf{E}$. Therefore, the energy dissipated from an electromagnetic field to thermal energy is given by

$$\langle P \rangle = \frac{1}{2} Re \left[ \mathbf{E} \cdot \mathbf{J}_e^* \right] = \frac{1}{2} \sigma_e |\mathbf{E}|^2. \tag{1.50}$$

Thoroughly conscious ignorance is the prelude to every real advance in science

James Clerk Maxwell (1831-1879)

CHAPTER II

TRIPLE LAYER LAMINATE WITHOUT FLUID FLOW

We begin with models which describe the microwave heating of a triple layer laminate of

infinite length, shown in Figure 2.1. The difference between the considered triple-layer

geometry and that of Figure 1 is the incident angle. The simple geometry considered in

this chapter assumes the incident field is normal to the layer boundaries. It is assumed the

inner layer is lossy, possessing a complex-valued dielectric constant, the two outer layers are

lossless, possessing a real-valued dielectric constant, which are all surrounded by free-space.

Two monochromatic plane waves are symmetrically applied and uniform in $x$. Considering

the case when $\nabla \epsilon$ is negligible the equation governing the electric field for this geometry is

the 1-D Helmholtz equation, moreover we assume the field is linearly polarized so it is scalar,

$$\frac{\partial^2 E_j}{\partial z^2} + \gamma^2 \epsilon_j E_j = 0, \tag{2.1}$$

where the index $j$ is in each of the five regions. The internal boundary conditions are given by

continuity and continuity of the derivative which are equivalent conditions to those described

in chapter 1. Since this is an open scattering problem we impose the Sommerfeld radiation
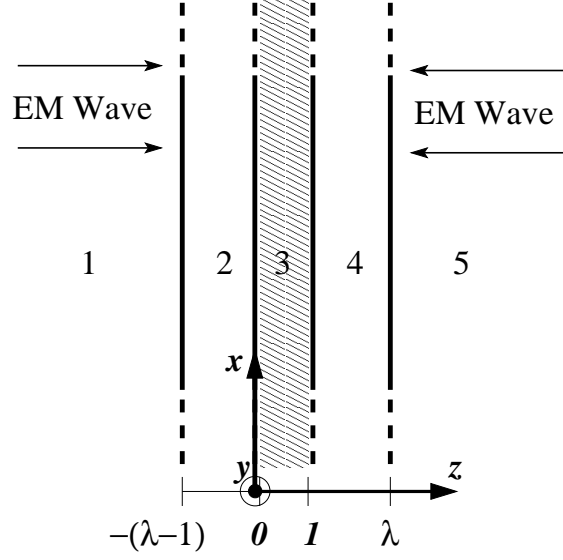
Figure 2.1: Three-layer laminate geometry of infinite length

conditions

$$\lim_{|z| \to \infty} \left( \frac{\partial}{\partial |z|} - i\gamma \right) (E - E_{\text{inc}}) = 0, \tag{2.2}$$

which defines the field entering the system from infinity where the source of the wave is located. The incident field strength is taken to be $E_{\text{inc}} = E_0$ on the left and $E_{\text{inc}} = E_0 e^{i\gamma}$ to maintain symmetry. The electric field is solved exactly and takes the form

$$E_j = a_j e^{i\gamma \sqrt{\epsilon_j} z} + b_j e^{-i\gamma \sqrt{\epsilon_j} z}, \tag{2.3}$$

27

where coefficients $a_j$ and $b_j$ are determined by the boundary conditions. The heat equation in each layer is given by

$$\frac{\partial T_2}{\partial t} = \alpha \left( \frac{\partial^2 T_2}{\partial x^2} + \frac{1}{\eta^2} \frac{\partial^2 T_2}{\partial z^2} \right), \qquad (x,z) \in (-\infty, \infty) \times [-(\lambda - 1), 0], \quad (2.4)$$

$$\frac{\partial T_3}{\partial t} = \frac{\partial^2 T_3}{\partial x^2} + \frac{1}{\eta^2} \frac{\partial^2 T_3}{\partial z^2} + P_L \sigma_e(T_3)|E_3|^2(T_3), \qquad (x,z) \in (-\infty, \infty) \times [0, 1], \quad (2.5)$$

$$\frac{\partial T_4}{\partial t} = \alpha \left( \frac{\partial^2 T_4}{\partial x^2} + \frac{1}{\eta^2} \frac{\partial^2 T_4}{\partial z^2} \right), \qquad (x,z) \in (-\infty, \infty) \times [1, \lambda], \quad (2.6)$$

after nondimensionalizing with

$$x = \frac{x'}{L}, \quad z = \frac{z'}{l}, \quad \bar{t} = \frac{t'}{t_L}, \quad T = \frac{T' - T_A}{T_A}, \quad E = \frac{E'}{E_0}, \quad \sigma = \frac{\sigma'}{\sigma_0}, \qquad (2.7)$$

where $L$ is the characteristic length of the layers, $l$ is the characteristic width, $\eta = \frac{l}{L}$ is the aspect ratio, $t_L = \frac{L^2}{\alpha_3}$ is a macroscale conduction time, $T_A$ is the ambient temperature, $\alpha = \frac{\alpha_2}{\alpha_3}$ is the ratio of thermal diffusivities, and $P_L = \frac{L^2 E_0^2 \epsilon_0 \omega}{2 K_3 T_A}$ is a macroscale non-dimensional power. The thermal boundary and initial conditions are taken to be

$$\frac{\partial T_2}{\partial z} = \overline{Bi}\, T + \overline{R}[(T - 1)^4 + 1], \qquad z = -(\lambda - 1), \qquad (2.8)$$

$$T_2 = T_3, \qquad z = 0, \qquad (2.9)$$

$$K \frac{\partial T_2}{\partial z} = \frac{\partial T_3}{\partial z}, \qquad z = 0, \qquad (2.10)$$

$$T_3 = T_4, \qquad z = 1, \qquad (2.11)$$

28

$$\frac{\partial T_3}{\partial z} = K \frac{\partial T_4}{\partial z}, \hspace{4cm} z = 1, \hspace{2cm} (2.12)$$

$$-\frac{\partial T_4}{\partial z} = \overline{Bi}\, T + \overline{R}[(T-1)^4 + 1], \hspace{2cm} z = \lambda, \hspace{2cm} (2.13)$$

$$T_{2,3,4} \text{ bounded}, \hspace{6cm} (2.14)$$

$$T_{2,3,4}(0, x, z) = 0, \hspace{6cm} (2.15)$$

which include external losses from convection and radiation, where $K = \frac{k_2}{k_3}$ is the ratio of thermal conductivities, $\overline{Bi} = \frac{hl}{k_3}$ is the Biot number, $\overline{R} = \frac{s\varepsilon T_A^3}{h}$ is a radiation parameter, $h$ is a heat transfer coefficient, $s$ is the Stefan-Boltzmann constant, and $\varepsilon$ is the emissivity. We assume the aspect ratio $\eta \ll 1$. Applying the asymptotic expansion

$$T = T^{(0)} + \eta T^{(1)} + \eta^2 T^{(2)} + \dots \hspace{3cm} (2.16)$$

and assuming external losses are small $\overline{Bi} = \eta^2 Bi$, $\overline{R} = \eta^2 R$, the effective temperature is found to be independent of spanwise direction $z$ and is found to be

$$\overline{\rho c_p} \frac{\partial T^{(0)}}{\partial t} = \overline{k} \frac{\partial^2 T^{(0)}}{\partial x^2} + P_L \sigma_e(T^{(0)}) \|E_3\|_2^2 (T^{(0)}) - L(T^{(0)}), \hspace{2cm} (2.17)$$

where $\overline{\rho c_p} = 1 + 2(\lambda - 1)\frac{K}{\alpha}$, is the effective heat capacity per unit volume, $\overline{k} = 1 + 2(\lambda - 1)K$ is an effective thermal conductivity, $\|E_3\|_2$ is the $L_2$ norm of the electric field and $L(T) = 2KBi\,T + 2KR[(T-1)^4 + 1]$. In the following two sections, we investigate two cases considering uniform heating in $x$. In an infinite triple layer the temperature heats up uniformly making the internal flux $\overline{k}\frac{\partial T}{\partial x} = 0$. As a side the same response can be modeled in

29

a finite domain by applying insulating conditions at the top and bottom interfaces. The first case considered is when the wavelength of the alternating field is larger than the microscale structure. This case was first modeled by Kriegsmann, Brodwin, and Watters in 1990 where we review their finding and those of subsequent work [39]. Alternatively, the second is the high-frequency case which considers the wave-geometry interactions that occur when the wavelength is comparable to the microscale.

## 2.1  Long-wave Response

We consider waves whose wavelength is longer than the width of the layers. A power response curve was developed, defined by

$$P_L = \frac{L(T)}{\sigma_e(T)\|E_3\|_2^2},$$  (2.18)

and derived from (2.17). It describes the steady-state temperature of the system provided an incident EM power. It produced the so-called "S-curve" of Figure 2.2a. This bifurcation diagram was the first model capable of describing thermal runaway. As power increases there is a point at which any further increase in power initiates a dramatic increase in temperature as it comes to rest at the temperature associated with the top branch. It was later shown that the branches exhibiting a positive slope were stable while a negative slope is unstable [45]. The S-curve possesses at most two stable steady-state temperatures for any one power, a low temperature, which may be sufficient for certain heating application but is rather inefficient for heat exchangers, and a high temperature, which will damage the

30
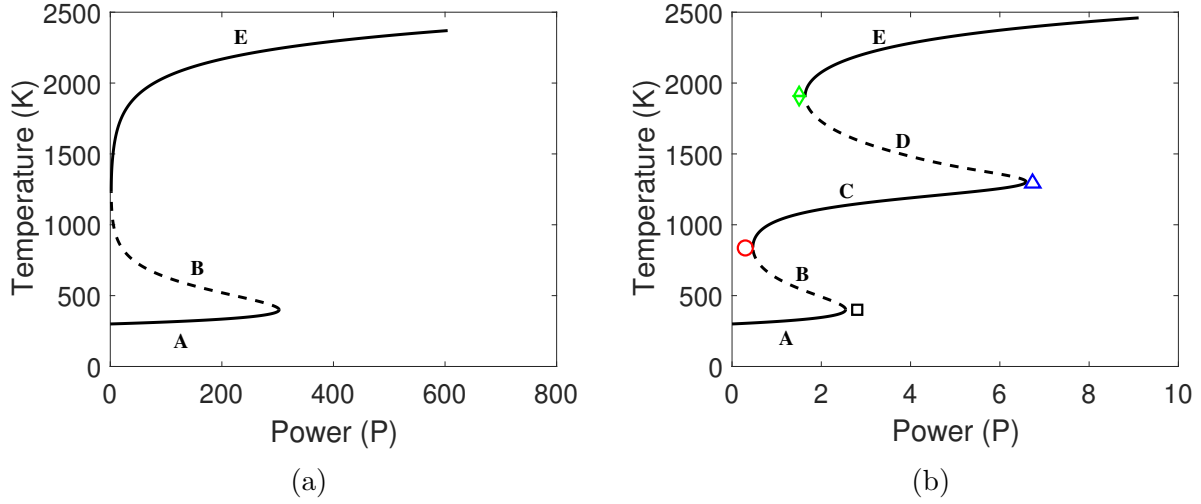
Figure 2.2: S-curve $\epsilon_f = 9\pi^2$ (a), and SS-curve $\epsilon_f = \left(\frac{7\pi}{2}\right)^2$ (b), with common parameters $\epsilon_m = \pi^2$, $K = 0.5$, $Bi = 0.5$, $Q = 0$, $\sigma_e(T) = 10^{-3}e^{3T}$, where the first through fourth turning points are labeled □○△◇ respectively. (solid) stable steady states (dashed) unstable steady states

system. One attempt at controlling this thermal runaway event was to build in a feedback control that increases the device to high powers, increasing the temperature, and then quickly decreases to low powers to bring the temperature back down [87]. The cyclic heating and cooling would oscillate around medium temperatures. This method is difficult to administer in practice. One alternative way to have better control over thermal runaway is to consider how wave-geometry interactions of high-frequency waves might influence the system.

## 2.2   High-Frequency Response

When the electromagnetic wavelength is comparable in size to a materials microstructure, the system can behave like a resonant cavity. This electromagnetic phenomenon has been

known for some time in the field of photonics as a distributed Bragg reflector with a defect layer [88]. This resonance exists when the width of the outer layers are odd multiples of quarter wavelengths and the width of the inner (defect) layer is an odd multiple of half wavelengths

$$(\lambda - 1)l = (2n - 1)\frac{\lambda_2}{4} \qquad n \in \mathbb{Z}^+, \tag{2.19}$$

$$l = (2m - 1)\frac{\lambda_3}{2} \qquad n \in \mathbb{Z}^+. \tag{2.20}$$

The strength of the resonance is increased when the difference in permittivity $\epsilon_2 - \epsilon_3$ is large which is shown by Figure 2.3a. The conditions are such that every return reflection in the defect layer is completely in phase with next transmitted wave. The waves constructively interfere, increasing the electric field strength within the defect. The EM energy capable of being trapped within this layer can significantly exceed the energy of the incident field as shown by Figure 2.3b.

This dramatic change in the electric field transforms the S-curve to an "SS-curve" which possesses an additional stable steady state branch at medium-high temperatures which can be seen in Figure 2.2b. Operating the device on this branch would allow for more efficient heating while avoiding the damaging effects of excessive heating. Notice that thermal runaway is not eliminated nor is it being controlled, but rather is split into two separate thermal runaway events. Additionally, the power level at which these events occurs has been lowered by two orders of magnitude which can be beneficial. A lower incident power leads to better efficiency and the device is able to achieve the first thermal runaway event very
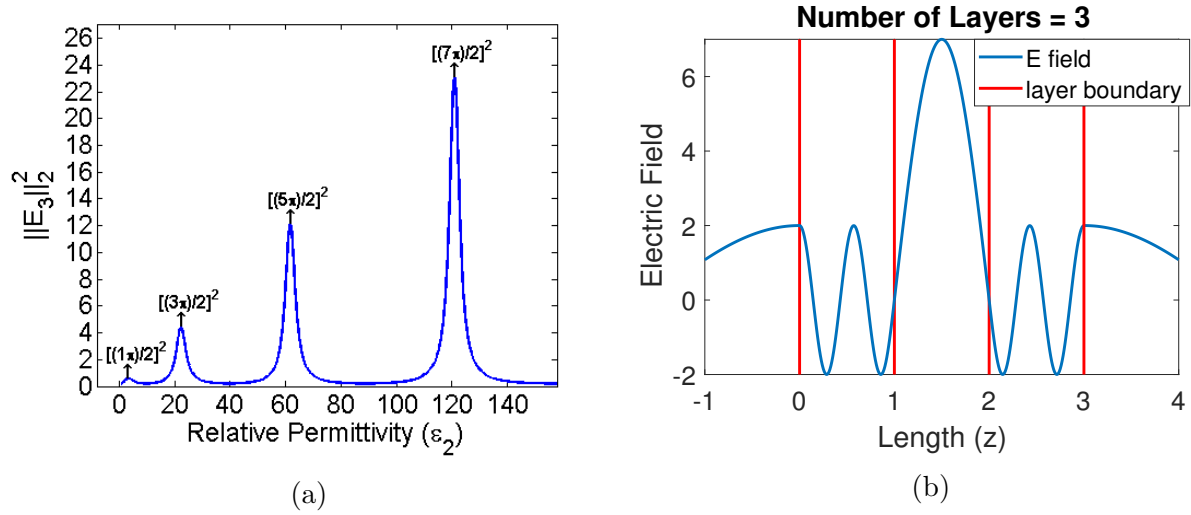
Figure 2.3: A graph of the norm of the electric field as a function of permittivity, which show resonant values (a), and solution of electric field in triple-layer domain exhibiting resonance in the middle defect layer (b).

easily in order to operate on the desired middle branch.

We can partially control the location and range of the branches by varying some fixed system parameters such as $\epsilon_2'$, $\epsilon_3'$, $\gamma$, and $R$ though the greatest control comes from the dynamic parameter $Bi$ which is capable of being altered during operation. Figure 2.4 shows parametric curves for the temperature and power values of the turning points as the permittivity of the outer layers is varied. The regions defining the S-curve, two turning points, from the SS-curve, four turning points, are evident. Figure 2.4a shows that as the permittivity approaches a resonant value the SS-curve is generated by the creation of the two top turning points △◇, which then annihilate together as it moves away from resonance. It also shows the trend of turning points at each successive resonance state, for instance, the temperature of the second turning point ○ decreases while that of the fourth turning point
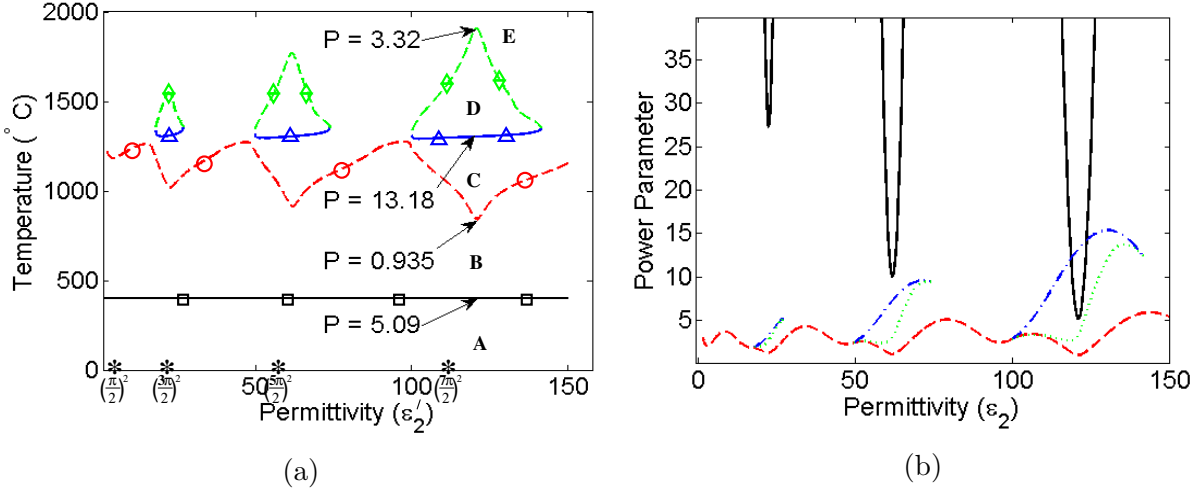
Figure 2.4: Graphs of temperature (a) and power of the turning points of the power response curve (b) as functions of the outer layer permittivity $\epsilon'_2$.

$\Diamond$ increases. Figure 2.4b shows the large variation in the power of the first turning point $\square$ and how, at resonance, the power level is minimized allowing the first thermal runaway event to be initiated using low power.

The parametric curves for the temperature and power values of the turning points as a function of the inner layer permittivity are shown in Figure 2.5. The regions defining the S-curve from the SS-curve are again evident though Figure 2.5a shows that as the permittivity approaches a resonant value the SS-curve is generated by the creation of the middle two turning points $\bigcirc\triangle$, which then annihilate together as it moves away from resonance. The trend of turning points at each successive resonance state show an increase in temperature for the second turning point $\bigcirc$ and third turning point $\triangle$.

We have also considered a parametric curve for temperature with respect to $\gamma$, the

34
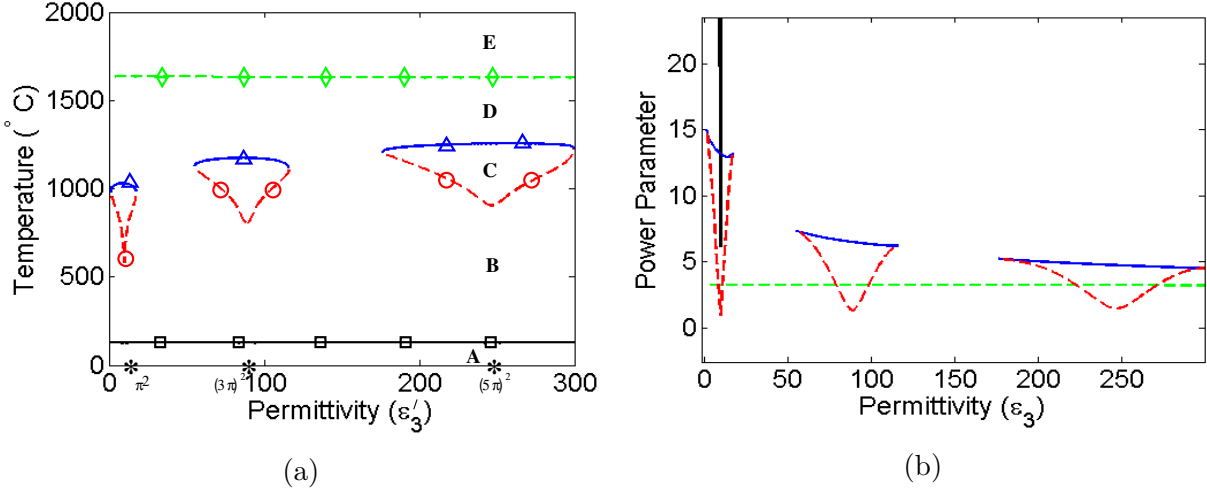
Figure 2.5: Graphs (a) temperature and (b) power of the turning points of the power response curve as a function of the inner layer permittivity $\epsilon_3'$.

non-dimensional wavenumber, which is shown in Figure 2.6a, as well as power response curves if we included attenuation of the electric field in the outer layers as well, depicted in Figure 2.6b. The dynamics of how the power response changes across resonant values is interesting. Unlike the parametric curves of Figures 2.4a and 2.5a, where turning points were created and annihilated in pairs, the top three turning points take turns being created in one pair and annihilated in another pair. Additionally, the turning points change position. A turning point that was originally marked as the second turning point from the bottom ◯ at one resonant state persists through the non-resonance region and become the fourth turning point from the bottom ◇ at the next resonant state. Hence the reason why the curves are not distinctly labeled by color as with the previous parametric curves.

In general, no material is completely lossless as we have assumed but instead absorbs

35
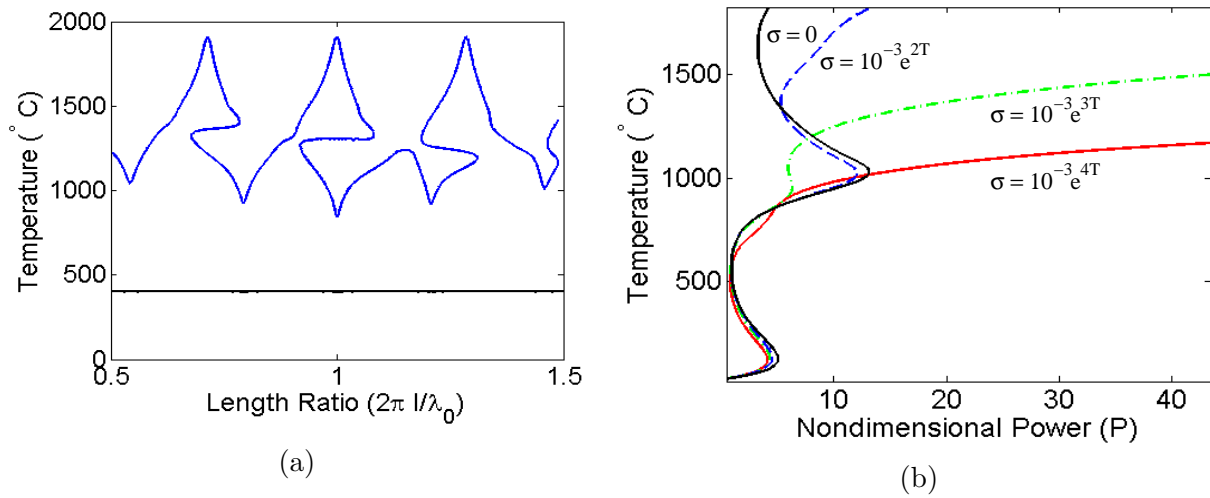
Figure 2.6: Graphs of the temperature of the turning points of the power response curve as a function of wavenumber $\gamma$ (a), and power response curves for non-zero dielectric loss of the outer layers (b).

some electromagnetic energy into heat. Figure 2.6b shows that introducing this absorption in the outer layers lowers the temperature of the top branch. Eventually the loss exceeds that of the inner layer and can take the place of the middle branch in having medium-high temperatures. In the context of an EM heat exchanger, this result suggests a fluid which directly absorbs EM energy may be beneficial if it can be made highly lossy.

Figure 2.7 shows how the external losses affect the power response curve. As the radiation coefficient increases we see the effect of the energy loss on the power response in Figure 2.7b. The figure reflects that the radiation loss is linear in $R$ and quartic in temperature. This results in a lengthening of the middle stable branch which is the only steady state available. The blackbody radiation increases with a material's emissivity which is an intrinsic parameter and cannot be changed once a particular material is chosen. Unlike

radiation, the Biot number can be changed during operation by increasing or decreasing the external convection which makes it a useful control mechanism. Figure 2.7a shows the power response which increases linearly in both $Bi$ and temperature. This effect also increases the power range of the stable middle branch which is needed to safely operate there. If the branch is too short small fluctuations in the system could force the temperature off the middle branch. In addition, it would appear that the transition temperatures at the turning points remain constant as $Bi$ changes. In general this constancy will not occur, however, we can prove this to be true when $R = 0$. Let us examine the slope of the power response curve (2.18) on the logarithmic scale given by

$$\frac{d[\ln(P_L)]}{dT} = \underbrace{-\frac{1}{\|E_3\|_2^2}\frac{\partial\|E_3\|_2^2}{\partial T}}_{(a)} \underbrace{- b}_{(b)} + \underbrace{\frac{1}{L}\frac{dL}{dT}}_{(c)}. \tag{2.21}$$

where $b$ is the exponent in the effective conductivity $\sigma_e(T) = Ae^{bT}$. For the specific case of no radiation the slope reduces to

$$\frac{d[\ln(P_L)]}{dT} = -\frac{1}{\|E_3\|_2^2}\frac{\partial\|E_3\|_2^2}{\partial T} - b + \frac{1}{T}. \tag{2.22}$$

Since this equation is independent of $Bi$, it shows that the slope of the power response is constant for a given temperature, even as the Biot number changes. Specifically, since turning points occur when the slope is zero $\frac{d[\ln(P_L)]}{dT} = 0$, the transition temperatures remain constant.

Next, we ask the question: how does the applied resonance of the electric field create
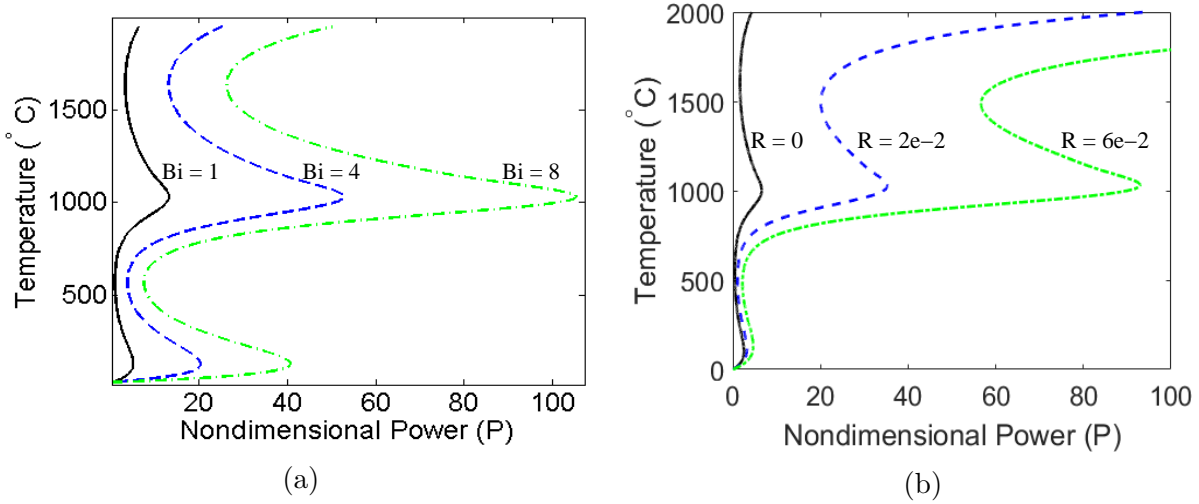
Figure 2.7: Power response curves for different values of external advective $Bi$ losses (a), and radiative $R$ losses (b).

the SS-curve? To answer this, we first provide an explanation of each branch of the power response curves shown in Figure 2.2. We know steady states are defined by the balancing of the sources to losses in (2.18). The turning points are where branches change direction, switching the correlation between parameters. We can determine where turning points occur by setting the slope of the power response (2.21) to zero. Stable (unstable) branches occur when $\frac{d[\ln(P_L)]}{dT} > (<) \, 0$. Since the branch is determined by the balancing of these three terms, we have labeled each term of (2.21), left to right, as $(a)$, $(b)$, and $(c)$ respectively. Prior to discussing each branch in detail, a few notes should be made. First, since $\frac{\partial \|E\|_2^2}{\partial T} < 0$, which can be seen from Figure 2.8, $(a)$ is always positive. Second, since $b$ is a constant, $(b)$ is constant, and thirdly since $L(T)$ is a polynomial, $(c)$ decreases with temperature like $T^{-1}$. Branch labels refer to those shown in Figure 2.2b.

**Branch A:** At these low temperatures, the electric field does not attenuate much from the field at ambient temperature, so $\|E_3\|_2^2$ is large and its derivative is small making $(a)$ negligible. Since the slope is positive $(c) > -(b)$, branch A is *externally stabilized*. The external losses are able to match the rate at which heat is generated internally.

**Branch B:** $(a)$ is still small, but now since $(c)$ decreases with temperature, the external losses can no longer keep up with the rate at which heat is generated making $(c) < -(b)$ yielding a negative slope and an unstable branch.

**Branch E:** $(c)$ is negligible at high temperatures. The electric field having lost most of its energy to the material $\|E_3\|_2^2$ is small, while its derivative is also small since there is not much energy left to lose. This makes $(a)$ comparable with $(b)$, but since it is stable we have that $(a) > -(b)$, so branch E is *conductively stabilized*, since the balance no longer comes from balancing heat generation to heat loss, but rather balancing increased absorption rate (from exponential conductivity) to less available energy (attenuated electric field).

These were the three branches found by Kriegsmann et al. on the S-curve and they are also seen on the SS-curve as well. In order to understand the two new curves associated with the SS-curve we first have to analyze how the electric field changes under resonance. The imaginary part of the wavenumber $k_3 = \sqrt{\epsilon_3}$ is given by

$$\text{Im}(k_3) = \sqrt[4]{\epsilon_3'^2 + A^2 e^{2bT}} \sin\left[\frac{1}{2}\arctan\left(-\frac{Ae^{bT}}{\epsilon_3'}\right)\right]. \tag{2.23}$$

We make two asymptotic approximations for low temperatures and high temperatures. When $T$ is small, $e^{bT} \approx 1$, and when $T$ is large, $\arctan(-Ae^{bT}(\epsilon_3')^{-1}) \approx -\frac{\pi}{2}$, so we define approxi-
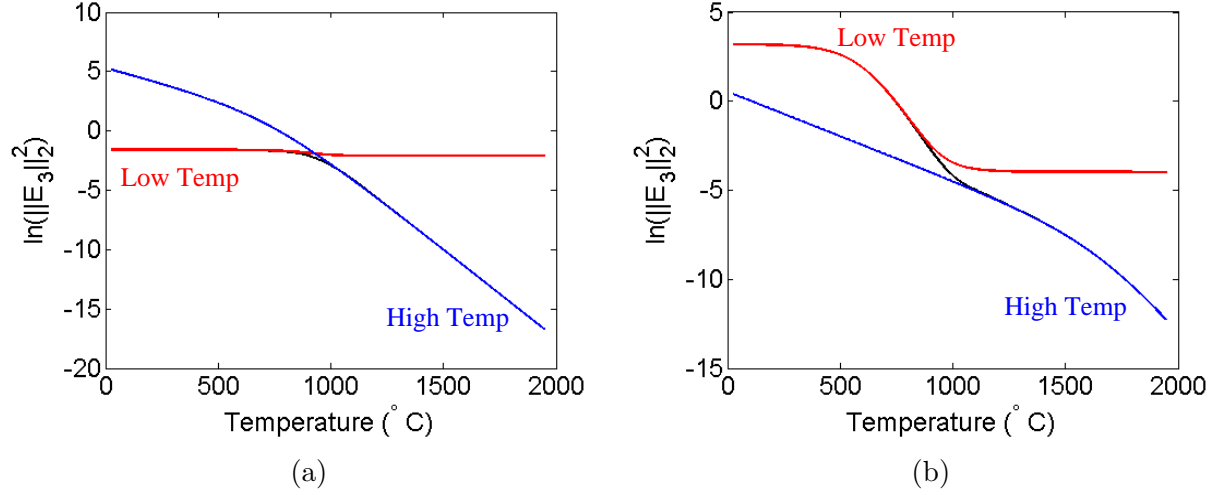
Figure 2.8: Logarithmic scale of the norm of the electric field as a function of temperature for non-resonant (a) and resonant cases (b): exact solution (black), low-temperature approximation (red), high-temperature approximation (blue).

mate wavenumbers, when temperature is small and when it is large as

$$\text{Im}(k_3)_{T \ll 1} = \sqrt[4]{{\epsilon_3'}^2 + A^2} \sin \left[ \frac{1}{2} \arctan \left( -\frac{A e^{bT}}{\epsilon_3'} \right) \right], \tag{2.24}$$

$$\text{Im}(k_3)_{T \gg 1} = -\frac{\sqrt{2}}{2} \sqrt{A} e^{\frac{b}{2} T}. \tag{2.25}$$

Figure 2.8 graphs the logarithm of the square norm of the electric field as a function of temperature using (2.23), given by the black curve, (2.24), given by the red curve, and (2.25) given by the blue curve. Figure 2.8a shows the electric field without resonance while Figure 2.8b is with resonance. Immediately, we notice two distinct differences between the two graphs. Firstly, at resonance we see a rapid decrease in the electric field at medium temperatures, as $T$ increases. Resonance is able to build up the electric field in the middle layer,

40
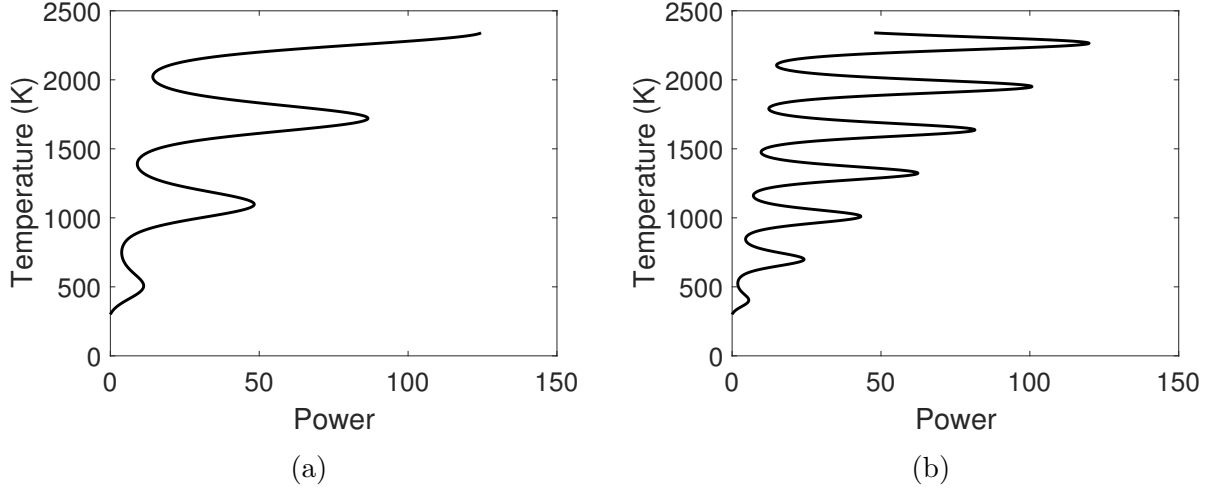
Figure 2.9: Examples of theoretical multiple S-curve power response with parameters $Bi = 1$, $R = 0$, $A = 1e - 3$, $b = 3$, $E_0 = e^5$ and oscillatory parameters $\omega = 1$ (a), and $\omega = 2$ (b).

essentially trapping more energy than usual within its boundary. It is this accumulation of the electric field which allows for this rapid loss of electric energy. Secondly, we notice that the slope at higher temperatures is shallower initially and then becomes more steep at the highest temperatures. Comparing this to the case without resonance and the slope at high temperature remains steep throughout. Since we are able to solve the electric field exactly for this problem the expression governing the high temperature behavior is proportionally

$$\|E_3\|_2^2 = c \left[ k_2^2 M^2 e^{\frac{b}{2}T} + k_2 M e^{bT} + e^{\frac{3}{2}bT} \right]^{-1}, \tag{2.26}$$

where $k_2$ is the wave number in the lossy layer and $M$ is a compound reflection-transmission coefficient. For the case of no resonance $k_2 M \approx 1$ so the largest exponential $e^{\frac{3b}{2}T}$ dominates immediately. During resonance, however, $k_2 M \gg 1$, so the lower-power exponential $e^{\frac{b}{2}T}$

41

affects the solution early on in the high temperature region, but eventually succumbs to the dominating effects of the largest-power exponential $e^{\frac{3}{2}T}$ at the highest temperatures. We can now describe the two new branches.

**Branch C:** At temperatures greater than those of branch B we know the decreasing term (c) is negligible. The temperatures are not yet large enough to completely attenuate the electric field, so $\|E_3\|_2^2$ is still large, however, as we showed from figure 2.8b, its derivative is a large negative value. So large that it forces $(a) > -(b)$ making branch C conductively stable.

**Branch D:** The rapid loss of EM energy that stabilized branch C slows at higher temperature making the derivative of $\|E_3\|_2^2$ smaller in magnitude again. (2.26) shows us in this region $\|E_3\|_2^2 \approx (k_2 M)^{-2} e^{-\frac{b}{2}T}$ which causes $(a) = \frac{b}{2}$ so $(a) < -(b)$ making branch D unstable. Once temperature increases further so that $\|E_3\|_2^2 \approx e^{-\frac{3b}{2}T}$ it makes $(a) = \frac{3b}{2}$ and corresponds to branch E.

In principle, one could attain any number of conductively stable branches, far more than the two generated by the SS-curve. To achieve this, the electric field norm would need to alternate the rate of attenuation between faster and slower than the absorption rate of the conductivity, $\sigma_e(T) = A e^{bT}$. The difficulty would be in designing the device that would produce such a function for the electric field norm. As an example, suppose that $\|E_3\|_2^2 = E_0 e^{-bT - \sin(\omega T)}$; then the power response defined as (2.18) produces the curves shown in Figure 2.9. Multiple stable steady states are created as branches are conductively stabilized. The faster the oscillations, the more branches will be produced which would allow for more precise temperature control.
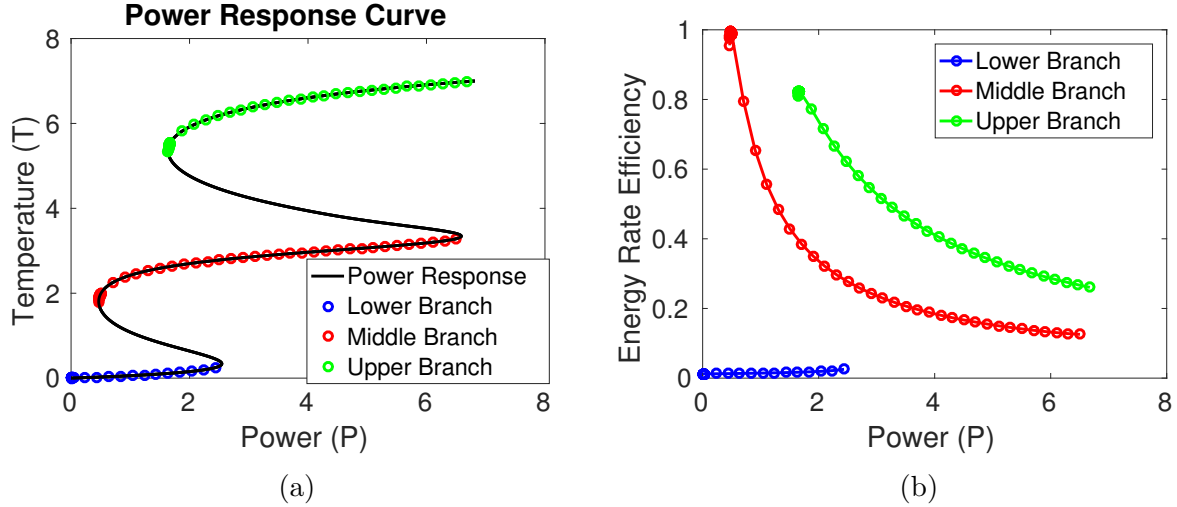
Figure 2.10: Power response curve with selected steady state temperature (a), and efficiency of absorbed power on different branches of the power response curve (b).

The efficiency of a heat exchanger is vital to its overall utility as a means of energy collection. The efficiency of how EM energy transferred is to thermal energy absorbed $\mathcal{E}_{AB}$. The energy absorbed by the EM radiation is given by $P_L \sigma_e(T) \|E_3\|_2^2$. Setting the temperature derivative equal to zero gives a simple relation for the maximum rate energy absorbed,

$$-\frac{1}{\|E_3\|_2^2} \frac{\partial \|E_3\|_2^2}{\partial T} = b, \tag{2.27}$$

where $\sigma_e = Ae^{bT}$. This can be closely related to the location of the turning points derived from the power response (2.21). With term (c) small, we expect the maximum energy absorption to occur near the left turning points. This is confirmed by Figure 2.10, which shows the absorbed efficiency for each branch. There are two left turning points in an SS-curve. Figure 2.10 shows the middle branch can be even more efficient than the upper

43

branch despite having a lower operating temperature. Though the maximum efficiency occurs at the low power regions of the turning points, it is also the first location of regions of nonexistent steady states, which are discussed further in this chapter. Caused by the presence of diffusion in the $x$-direction, a larger thermal conductivity will produce less efficiency. It is therefore beneficial that while we have not discussed the temperature dependence of thermal conductivity it tends to decrease with temperature. The benefit of lower conductivity to gain efficiency of heating is in vital contrast to a desire for larger conductivity to transfer thermal energy to the fluid regions.

## 2.3 Alternating Direction Implicit Method

A COMSOL model was developed in [2] and compared against the no-flow thin-domain model. The COMSOL model was validated by implementing the Peaceman-Rachford Alternating Direction Implicit method (PR-ADI) [89]. The method numerically solves the full non-dimensional system of equations governing the problem,

$$\frac{\partial T_2}{\partial t} = \alpha \left( \frac{\partial^2 T_2}{\partial x^2} + \frac{\partial^2 T_2}{\partial z^2} \right), \qquad\qquad -(\lambda - 1) \leq z \leq 0, \qquad (2.28)$$

$$\frac{\partial T_3}{\partial t} = \frac{\partial^2 T_3}{\partial x^2} + \frac{\partial^2 T_3}{\partial z^2} + P_L |E_3|^2 \sigma(T_3), \qquad\qquad 0 \leq z \leq 1, \qquad (2.29)$$

$$\frac{\partial T_4}{\partial t} = \alpha \left( \frac{\partial^2 T_4}{\partial x^2} + \frac{\partial^2 T_4}{\partial z^2} \right), \qquad\qquad 1 \leq z \leq \lambda, \qquad (2.30)$$

subject to boundary and initial conditions

$$\frac{\partial T_2}{\partial z} = \overline{Bi}\,T + \overline{R}[(T-1)^4 + 1], \qquad\qquad z = -(\lambda - 1), \qquad (2.31)$$

$$T_2 = T_3, \qquad\qquad z = 0, \qquad (2.32)$$

$$K\frac{\partial T_2}{\partial z} = \frac{\partial T_3}{\partial z}, \qquad\qquad z = 0, \qquad (2.33)$$

$$T_3 = T_4, \qquad\qquad z = 1, \qquad (2.34)$$

$$\frac{\partial T_3}{\partial z} = K\frac{\partial T_4}{\partial z}, \qquad\qquad z = 1, \qquad (2.35)$$

$$-\frac{\partial T_4}{\partial z} = \overline{Bi}\,T + \overline{R}[(T-1)^4 + 1], \qquad\qquad z = \lambda, \qquad (2.36)$$

$$\frac{\partial T_{2,3,4}}{\partial x} = 0, \qquad\qquad x = 10, \qquad (2.37)$$

$$T_{2,3,4} = 0, \qquad\qquad x = 0, \qquad (2.38)$$

$$T_{2,3,4}(0, x, z) = 0. \qquad (2.39)$$

For a single numerical simulation we choose the power parameter $P_L$. Sweeping over a range of powers, we can plot a power response curve once a temperature is chosen to be associated with the power. There are several choices one could make from the maximum temperature to the average temperature. In order to best compare this power response curve with that of the low-advection case, we choose to plot the power $P_L$ against the average temperature in the lossy layer $\mathrm{Ave}(T_3) = \frac{1}{10}\int_0^{10}\int_0^1 T_3(z, x)\, dz\, dx$. Figure 2.11 plots three power response curves, one for the thin domain model, one for the ADI method, and one for a model implemented in the COMSOL multiphysics solver detailed in [2]. There is a good agreement between the ADI method and the COMSOL model where the difference between
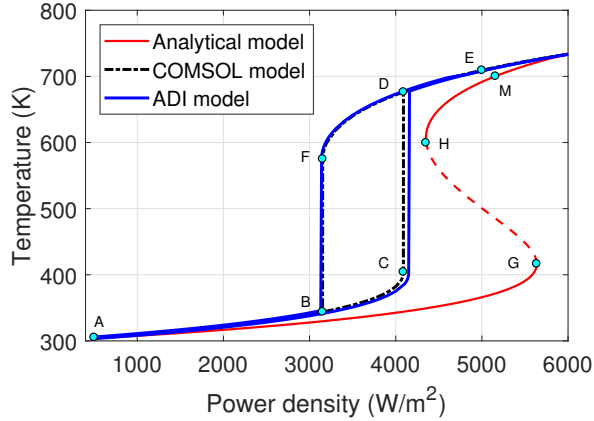
Figure 2.11: Comparison of the thin-domain model of [1] and COMSOL model of [2] to the full numerical solution using the PR-ADI scheme.

the numerical models and the thin domain volumetric average model is due to spatial effects. The power required to initiate thermal runaway events was lower for the ADI and COMSOL model because once the maximum temperature at a given point reached a critical value thermal runaway took over, whereas for the thin-domain model the uniform temperature had to achieve critical temperature to start the event [2]. Therefore, spatial effects play an integral role in the characteristic operation of electromagnetic heat exchangers.

## 2.4  High-Frequency Triple Layer with Diffusive Effects

The previous section discussed the existence of the SS-curve and described the consequences of it in detail. In addition, the model assumed uniform heating in the x-direction on the doubly infinite domain $x \in (-\infty, \infty)$ or equivalently on a finite domain $x \in [0, L]$ with no flux boundary conditions. In this section we consider the domain to be finite and relax the uniform heating assumption by applying a Dirichlet condition at one boundary and a no flux

46
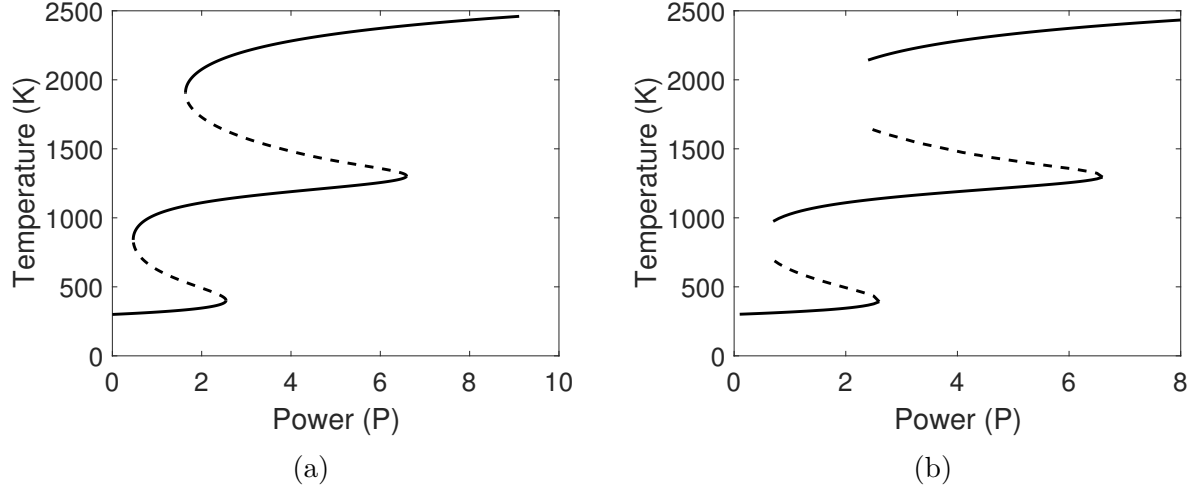
Figure 2.12: Power response curves for the steady state solution at the outlet; nonexistence regions where steady states used appear near the left two turning points; other parameters used to produce these curves include $\epsilon_f = \left(\frac{7\pi}{2}\right)^2$, $\epsilon_m = \pi^2$, $\gamma = 1$, $K = 0.5$, $Bi = 0.5$, $Q = 0$, $\sigma_e(T) = 10^{-3}e^{3T}$; power response for $\overline{k} = 0$ (a); power response for $\overline{k} = 0.5$ (b).

condition at the other. The non-dimensional effective equation is then given by (2.17) with boundary conditions

$$T = 0, \qquad\qquad x = 0, \qquad\qquad (2.40)$$

$$\frac{\partial T}{\partial x} = 0, \qquad\qquad x = 1. \qquad\qquad (2.41)$$

Physically, this models a thin three-layer laminate exposed to cold reservoir at $x = 0$ and sufficiently long enough for the material to heat up at the other boundary allowing the no flux condition to be valid.

While solutions are spatially dependent, since we applied an insulating boundary condition at the outlet, we can define a power response curve for the steady state solution

47

$T(x)$ as

$$P_L = \frac{L(T(1))}{\sigma_e(T(1))\|E_3\|_2^2(T(1))}. \tag{2.42}$$

We are interested in how the power response curve is affected as the diffusive transport changes the heating effects. Figure 2.12a shows the power response for the uniform heating case, while Figure 2.12b shows the power response curve including diffusion effects with $\overline{k} = 0.5$. Increasing the thermal conductivity will produce nonexistence regions, where steady state solutions once existed for the power response of the uniformly heated case. At these low power levels the temperature will no longer have steady states and will decrease until it reaches a lower stable state. These curves are produced by applying numerical continuation and solving the differential equation with an IMEX method described below. By making a parameter sweep over power and initial temperature the steady state solution branches are determined. In order to calculate the unstable branches we increase the initial temperature until the temperature begins to increase toward an upper branch instead of decrease toward a lower branch. This tells us we have two initial temperature on either side of the unstable branch. We can then refine the grid spacing for this parameter until a tolerance of $10^{-6}$ is reached, finding the unstable steady state branches.

We solve the equation for transient solutions with an Implicit-Explicit (IMEX) numerical scheme. The upwinding method [89] is applied to the advection term, Crank-Nicolson [89] is applied to the rest of the linear terms, and Adams-Bashforth [90] is used on the nonlinear source term. It was chosen as a first attempt at a solution however, that there
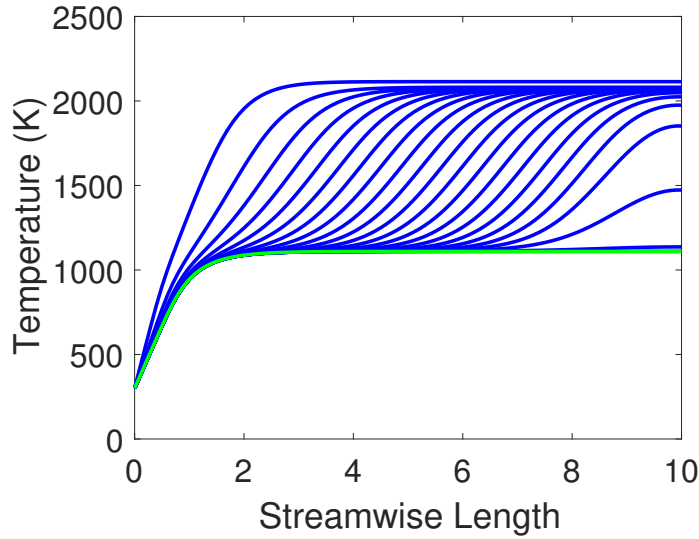
Figure 2.13: Transient solution for $\overline{k} = 0.5$ and $P = 2$

are other more stable IMEX methods one could choose [91]. Figure 2.13 shows the behavior

of solutions in a nonexistence region when the initial temperature is $T(0, x) = 2400\,K$. We

note that the temperature decreases over time and moves downstream until the temperature

comes to rest a lower temperature on the middle branch. This suggests that the existence

of traveling wave solutions is the reason why steady states solutions cease in certain regions

of the power response curve. We first prove that traveling wave solutions exist and then

develop approximations for the wave velocity.

**Theorem 1.** *Equation (2.17) has traveling wave solutions when* $\overline{k}$ *is non-zero.*

*Proof.* Let $T_{S1}$ and $T_{S2}$ denote two stable steady state temperatures and $T_U$ denote the

unstable steady state at the outlet $x = L$, such that $T_{S1} < T_U < T_{S2}$. We show traveling wave

solutions exist between between the two stable temperatures. Since there is the possibility

of two such sets of steady state temperatures for the SS-curve power response there exist two

49

sets of traveling wave solutions. The solutions are monotonically increasing. Transforming (2.17) to the moving reference frame, let $w = x - vt$, so

$$\overline{k}\frac{\partial^2 T}{\partial w^2} + v\overline{\rho c_p}\frac{\partial T}{\partial w} + P_L\sigma_e(T)\|E_3\|_2^2(T) - L(T) = 0. \tag{2.43}$$

We further make the transformation $\widetilde{w} = -\frac{w}{\sqrt{\overline{k}}}$. The negative is to force the solution to be monotonically decreasing which is used in the existence theorem. Furthermore, the scaling on $\sqrt{\overline{k}}$ is to group all the coefficients together. The resulting equation becomes

$$\frac{\partial^2 T}{\partial \widetilde{w}^2} + c\frac{\partial T}{\partial \widetilde{w}} + F(T) = 0, \tag{2.44}$$

where $c = -\frac{v\overline{\rho c_p}}{\sqrt{\overline{k}}}$ and $F(T) = P_L\sigma_e(T)\|E_3\|_2^2(T) - L(T)$. The far field conditions are then given by $\lim_{\widetilde{w}=\infty} T = T_{S1}$ and $\lim_{\widetilde{w}=-\infty} T = T_{S2}$. The source term, an example of which is shown in Figure 2.15, exhibits bi-stability between the low and high temperatures. Bi-stability holds if $F(T) \leq 0$ in a right half neighborhood of $T_{S1}$ and $F(T) \geq 0$ in a left half neighborhood of $T_{S2}$. The remainder of the proof is adopted from [92].

We separate (2.44) into the first order system

$$T' = q \tag{2.45}$$

$$q' = -cq - F(T). \tag{2.46}$$

Solutions to (2.44) satisfying the far field conditions correspond to phase plane trajectories connecting stationary points $(T_{S1}, 0)$ and $(T_{S2}, 0)$. Suppose $c = 0$. Let $(T, q_1^0(T))$ be the

50
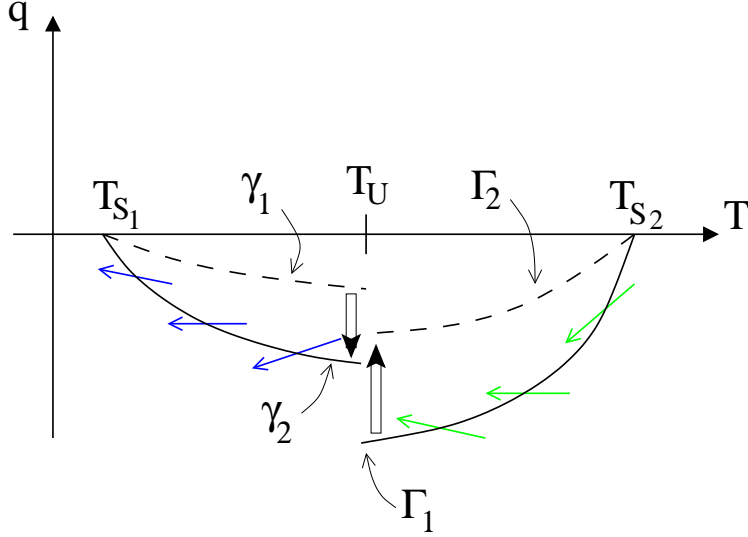
Figure 2.14: Diagram of the phase plane depicting the argument for proof of the existence of traveling wave solutions to the inlet Dirichlet problem.

trajectory approaching the stationary point $(T_{S1}, 0)$ and $(T, q_2^0(T))$ be the trajectory leaving stationary point $(T_{S2}, 0)$. Then $q_1^0(T_{S1}) = 0$, $q_1^0(T_U) < 0$, $q_2^0(T_{S2}) = 0$, and $q_2^0(T_U) < 0$ from bi-stability. If $q_1^0(T_U) = q_2^0(T_U)$ then the trajectories coincide connecting the two stationary points, thus the theorem is proved.

Suppose then that $q_1^0(T_U) \neq q_2^0(T_U)$. Consider a family of trajectories $\gamma_i := (T, q_1^{c_i}(T))$ and $\Gamma_i := (T, q_2^{c_i}(T))$ for $c \neq 0$, where $q_1^c(T_{S1}) = q_2^c(T_{S2}) = 0 \ \forall c$. Next, we prove $q_1^c$ ($q_2^c$) is monotone decreasing (increasing) with respect to $c$. Let $c_2 > c_1$ and divide through (2.46) by $q$, and substitute in (2.45) we have

$$\frac{dq_j}{dT} = -c_k - \frac{F(T)}{q_j^{c_i}}. \tag{2.47}$$

where index $j$ corresponds to trajectories extending from $T_{S1}$ or $T_{S2}$, index $i$ corresponds to

51

a specific trajectory $\gamma_i$ or $\Gamma_i$, and index $k$ for velocity $c_k$ in part determines the slope $\frac{dq}{dT}$ of the vector field $(T', q')$. If $i = k$, then the vector field slope $\frac{dq_j}{dT}$ is the slope of the trajectory $\gamma_i$ or $\Gamma_i$. From this we can conclude that

$$\left.\frac{dq_1}{dT}\right|_{i=2,k=2} < \left.\frac{dq_1}{dT}\right|_{i=2,k=1}, \tag{2.48}$$

$$\left.\frac{dq_2}{dT}\right|_{i=1,k=2} < \left.\frac{dq_2}{dT}\right|_{i=1,k=1}. \tag{2.49}$$

These inequalities are described pictorially in Figure 2.14. $\left.\frac{dq_1}{dT}\right|_{i=2,k=2}$ is given by slope of trajectory $\gamma_2$ while $\left.\frac{dq_1}{dT}\right|_{i=2,k=1}$ is given by the slope of blue vectors. $\left.\frac{dq_2}{dT}\right|_{i=1,k=1}$ is given by the slope of $\Gamma_1$ while $\left.\frac{dq_2}{dT}\right|_{i=1,k=2}$ is given by the slope of the green vectors. (2.48) implies that $\gamma_1$ lies above $\gamma_2$, otherwise since both curves intersect at $(T_{S1}, 0)$, $\gamma_1$ and $\gamma_2$ could intersect a second time. Similarly, (2.49) implies that $\Gamma_2$ lies above $\Gamma_1$, otherwise, since both curves intersect at $(T_{S2}, 0)$, they could intersect a second time. Therefore, $q_1^{c_2} < q_1^{c_1}$ on $T \in [T_{S1}, T_U]$ and $q_2^{c_2} > q_2^{c_1}$ on $T \in [T_U, T_{S2}]$, so $q_1^c$ ($q_2^c$) is monotone decreasing (increasing) with respect to $c$.

Next, we show that $q_j^c$ is continuous with respect to $c$ in the uniform norm. Let $\varepsilon > 0$. Choose $\delta = \frac{\varepsilon}{T_{max}}$, where $T_{max} = T_U$ for $q_1$ on $T \in [T_{S1}, T_U]$ and $T_{max} = T_{S2}$ for $q_2$ on $T \in [T_U, T_{S2}]$. The difference of (2.46) evaluated along $\gamma_1$ and $\gamma_2$ yields

$$q'|_{\gamma_1} - q'|_{\gamma_2} = -c_1\, T'|_{\gamma_1} + c_2\, T'|_{\gamma_2}, \tag{2.50}$$

where (2.45) was substituted for $q$. Integrating both sides and taking the uniform norm
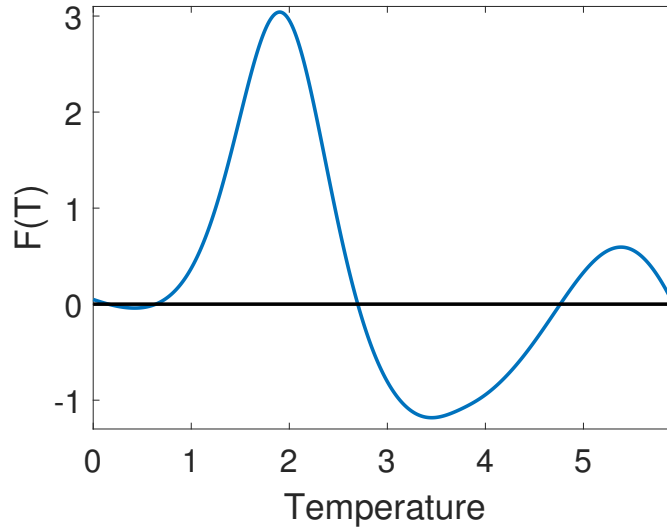
Figure 2.15: Example of the source/loss term $F(T)$ for $P_L = 2$, $\sigma(T) = 10^{-3}e^{3T}$, $\epsilon_2 = \left(\frac{7\pi}{2}\right)^2$, $\epsilon_3 = \pi^2$, $Bi = 0.5$, $R = 0$. It shows two distinct intervals that exhibit bi-stability.

results in $\|q^{c_1} - q^{c_2}\|_\infty = |c_1 - c_2| \|T\|_\infty < \delta T_{max} = \varepsilon$. Therefore, the two trajectories $q_1^c$ and $q_2^c$ are continuous with respect to $c$.

Finally, suppose $q_1^0(T_U) > q_2^0(T_U)$, then by increasing $c$ from zero, $q_1^c(T_U)$ decreases while $q_2^c(T_U)$ increases. Since they are continuous in $c$, there must exist a $c$ such that $q_1^c(T_U) = q_2^c(T_U)$. Suppose instead that $q_1^0(T_U) < q_2^0(T_U)$, then we find equality by decreasing $c$ from zero. Therefore, this implies there does exist a trajectory that connects the two stationary points, hence a wave solution exists. □

Now that we know such traveling wave solutions exist we derive expressions for the wave velocity $v$. We employ the Narrow Reaction Zone (NRZ) method first developed by Zeldovich and Frank-Kamenetskii as an approximation to the speed of flame propagation [93]. The main assumption is that the reaction zone, which in this case is the thermal runaway

event, occurs only on a narrow domain. The approximate equations presented in the narrow reaction zone method in [92] are obtained rigorously as asymptotic solutions in boundary layer theory.

We begin the analysis by scaling (2.44), let $\widetilde{w} = \epsilon^b r$, and $F(T) = \delta \widehat{F}(T)$, where $\epsilon, \delta \ll 1$. The scaled equation becomes

$$\epsilon^{-2b} \frac{\partial^2 T}{\partial r^2} + \epsilon^{-b} c \frac{\partial T}{\partial r} + \delta \widehat{F}(T) = 0. \tag{2.51}$$

The boundary layer theory requires we find the dominant balance between the terms. The first balance we consider is that of the second and third terms which implies $\delta = \epsilon^{-b_1} c$. Consistency requires $\delta = \epsilon^{-b_1} c \gg \epsilon^{-2b_1}$, which implies $c \gg \epsilon^{-b_1}$. The equation for this balance becomes

$$c \frac{\partial T}{\partial r} + \widehat{F}(T) = 0. \qquad \text{(Outer Layer)} \tag{2.52}$$

The second balance is for the first and second terms where $\epsilon^{-2b_2} = \epsilon^{-b_2} c$, which means that $c = \epsilon^{-b_2}$. In order to be consistent, it must be that $\delta \ll \epsilon^{-2b_2}$. The resulting equation is then

$$\frac{\partial^2 T}{\partial r^2} + c \frac{\partial T}{\partial r} = 0. \qquad \text{(Middle Layer)} \tag{2.53}$$

The final balance we consider is of the first and third terms, so that $\epsilon^{-2b_3} = \delta$. To be consistent it further requires that $\delta = \epsilon^{-2b_3} \gg \epsilon^{-b_3} c$, which implies $c \ll \epsilon^{-b_3}$. The governing

equation in this region would be

$$\frac{\partial^2 T}{\partial r^2} + \widehat{F}(T) = 0. \qquad \text{(Inner Layer)} \qquad (2.54)$$

All three of these balances can be consistent if the scales for each region are chosen such that $\epsilon^{-b_1} \ll c = \epsilon^{-b_2} \ll \epsilon^{-b_3}$, which implies that $b_1 < b_2 < b_3$. This provides the order of the nested layers with boundary layer thickness of the regions given by $\epsilon^{b_3} \ll \epsilon^{b_2} \ll \epsilon^{b_1}$.

A quick analysis of the outer most region shows that it is equivalent to the steady state constant solutions. It should be clear that solutions $T(r) \equiv T_{S2}$ and $T(r) \equiv T_{S1}$ satisfy (2.52). Attempting to find non-constant solution, we apply separation of variables to (2.52) producing two implicit solutions in this outer most region,

$$\int_T^{T_{S2}} \frac{c}{\widehat{F}(T)} \, dT = -r, \qquad \lim_{r \to -\infty} T = T_{S2}, \qquad (2.55)$$

$$\int_{T_{S1}}^{T} \frac{c}{\widehat{F}(T)} \, dT = -r, \qquad \lim_{r \to \infty} T = T_{S1}. \qquad (2.56)$$

The integrands are singular since $\widehat{F}(T_{S2}) = \widehat{F}(T_{S1}) = 0$. Since $T_{S2}$ and $T_{S1}$ are simple roots, $\widehat{F}(T)$ approaches the zeros linearly, as shown in Figure 2.15, the integrals diverge for all temperatures $T$. Therefore, the only solutions to (2.52) are the constant solutions.

The main assumption in applying the narrow reaction zone method is that the reaction zone is very small, which is to take the limit as $b_3 \to \infty$. In this limit the matching conditions required to complete the boundary layer theory are to match the two outer solutions together instead of matching to the inner solution.
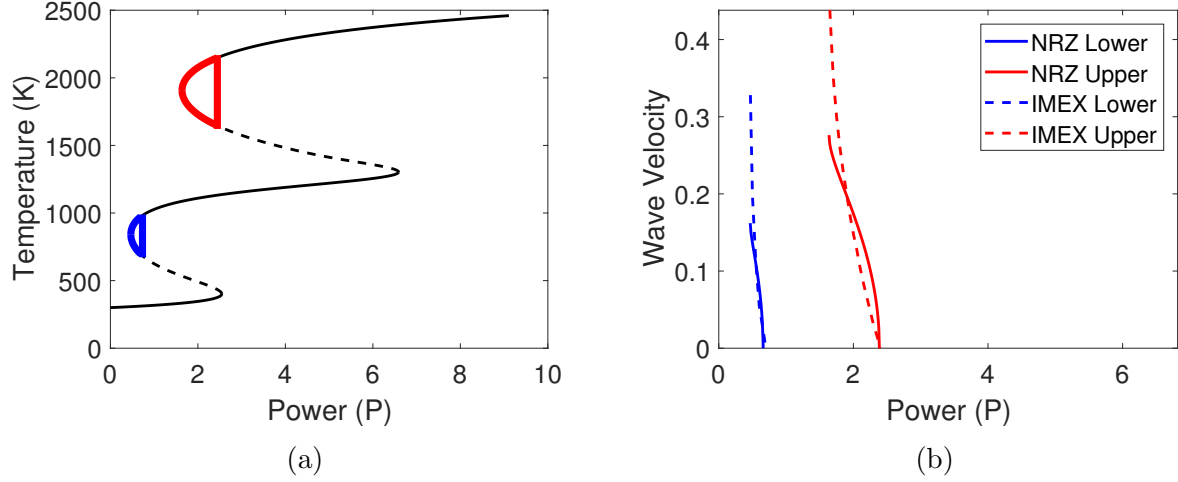
Figure 2.16: Power response for $\overline{k} = 0.5$ where highlighted regions possess traveling wave solutions and no steady states (a), and wave velocity calculated using the Narrow Reaction Zone method and the IMEX method (b).

We find the solution to (2.53) by separation of variables which changes depending on the sign of $c$. Applying the narrow reaction approximation, we match these two solutions of the outer regions together. The solutions for $c \leq 0$ are

$$
T = \begin{cases} T_{S_1}, & w \in (-\infty, 0), \\[2ex] T_{S_2} - (T_{S_2} - T_{S_1})e^{-\frac{v\overline{\rho c_p}}{\overline{k}}w}, & w \in (0, \infty), \end{cases} \tag{2.57}
$$

and the solutions when $c \geq 0$ are

$$
T = \begin{cases} T_{S_1} + (T_{S_2} - T_{S_1})e^{-\frac{v\overline{\rho c_p}}{\overline{k}}w}, & w \in (-\infty, 0), \\[2ex] T_{S_2}, & w \in (0, \infty). \end{cases} \tag{2.58}
$$

56

Next, we integrate (2.54) in terms of $r$ from $(-\infty, \infty)$. In terms of $w$ it yields the jump condition

$$\frac{\overline{k}}{2}\left[\left(\frac{\partial T}{\partial w}\right)^2\bigg|_{0+} - \left(\frac{\partial T}{\partial w}\right)^2\bigg|_{0-}\right] = -\int_{T_{S1}}^{T_{S2}} F(T)\,dT. \tag{2.59}$$

Matching the middle solution to the inner solution and solving for $v$ gives the approximation for the wave velocity

$$v = \sqrt{-\frac{2\overline{k}}{\overline{\rho c_p}^2(T_{S2}-T_{S1})^2}\int_{T_{S1}}^{T_{S2}} F(T)\,dT}, \quad v \geq 0. \tag{2.60}$$

This approximation to the wave velocity can be used to approximate the location of the interface between the existence and nonexistence regions of the power response curves. The IMEX numerical solutions showed that traveling wave solutions occur in the nonexistence regions, and Figure 2.16 shows how the predicted wave velocity decreases as $P$ increases toward the interface. Hence setting the expression for the wave velocity equal to zero we obtain an approximate condition on the location of the interface.

All the mathematical sciences are founded on relations between physical laws and laws of numbers, so that the aim of exact science is to reduce the problems of nature to the determination of quantities by operations with numbers

James Clerk Maxwell (1831-1879)

CHAPTER III

TRIPLE LAYER LAMINATE WITH FLUID FLOW

The examination of the channel cooling problem is essential in understanding fundamental behavior of the transfer of energy from the EM waves to a fluid channel through the intermediate step of a lossy solid material. It will help in understanding more complex problems such as the channel array problem in Chapter 4. A pictorial description of the triple-layer laminate with fluid flow is shown in Figure 3.1. We consider three models that attempt to examine the effects fluid flow has on the operation of an electromagnetic heat exchanger. The first is a simple extension of the effective temperature model of Chapter 2, which is valid for low advection. In contrast, a high-advection model is developed by applying a Galerkin method. Finally, the first two methods are compared against a fully numerical scheme.

We assume that the fluid velocity is given by plane Poiseuille flow with a prescribed pressure gradient, $p_g$, applied to each channel. Fluid velocity is given by

$$u_2'(z') = \frac{1}{2\mu}p_g z'(z' + (\lambda - 1)l), \qquad\qquad -(\lambda - 1)l \leq z' \leq 0, \qquad\qquad (3.1)$$

$$u_4'(z') = \frac{1}{2\mu}p_g(z' - l)(z' - \lambda l), \qquad\qquad l \leq z' \leq \lambda l, \qquad\qquad (3.2)$$

where $\mu$ is the dynamic viscosity and $p_g$ is the prescribed pressure gradient, $u_2'$ is the fluid velocity for the first channel and $u_4'$ is the fluid velocity for the second channel. A positive
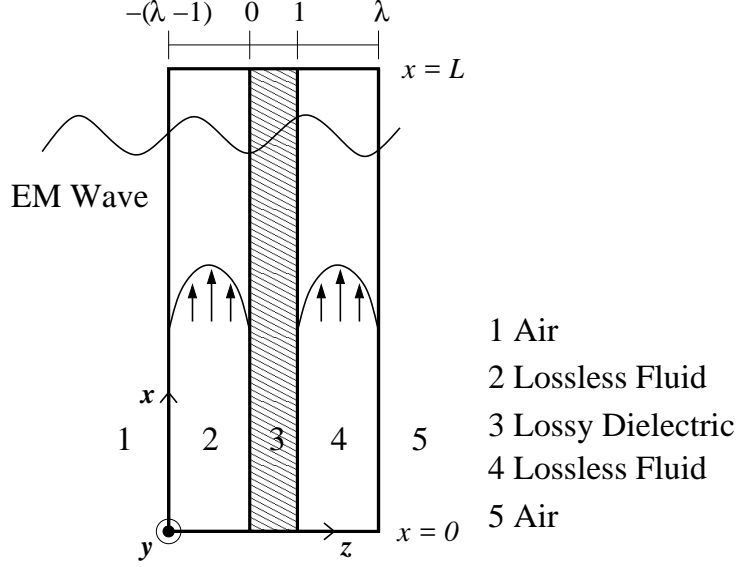
Figure 3.1: Three-layer laminate geometry of finite length

pressure gradient $p_g > 0$ implies $u'(z') < 0$, a downward flow, while a negative pressure gradient $p_g < 0$ implies $u'(z') > 0$, an upward flow. Conservation of energy in each fluid is given by

$$\frac{\partial T_2'}{\partial t'} + u_2'(z')\frac{\partial T_2'}{\partial x'} = \alpha_2 \left( \frac{\partial^2 T_2'}{\partial x'^2} + \frac{\partial^2 T_2'}{\partial z'^2} \right) + \frac{\mu}{\rho_2 c_{p2}} \left( \frac{\partial u_2'}{\partial z'} \right)^2, \quad -(\lambda - 1)l \leq z' \leq 0, \quad (3.3)$$

$$\frac{\partial T_4'}{\partial t'} + u_4'(z')\frac{\partial T_4'}{\partial x'} = \alpha_4 \left( \frac{\partial^2 T_4'}{\partial x'^2} + \frac{\partial^2 T_4'}{\partial z'^2} \right) + \frac{\mu}{\rho_4 c_{p4}} \left( \frac{\partial u_4'}{\partial z'} \right)^2, \quad l \leq z' \leq \lambda l, \quad (3.4)$$

where $T_2'$ and $T_4'$ are the temperature of the fluid for the first and second channel respectively. The second term on the left hand side represents energy transfer by convection. On the right hand side, the first term represents thermal diffusion as we have seen previously. The last term is a viscous heat source generated by friction as the liquid particles move past each other at different speeds. Since the fluid is considered a pure dielectric, no electromagnetic

energy is absorbed directly by the fluid. The heat equation governing energy conservation within the solid is the same as in the previous chapter.

## 3.1 Low Advection Model

We apply the nondimensionalization

$$x = \frac{x'}{L}, \quad z = \frac{z'}{l}, \quad \bar{t} = \frac{t'}{t_L}, \quad T = \frac{T' - T_A}{T_A}, \quad u = \frac{u'}{U}, \quad E = \frac{E'}{E_0}, \quad \sigma = \frac{\sigma'}{\sigma_0}, \quad (3.5)$$

where $U = \frac{|p_g|l^2}{2\mu}$ is the characteristic fluid velocity. Letting $p_\pm = \text{sign}(p_g)$ the resulting equations governing the system are

$$u_2(z) = p_\pm z(z + (\lambda - 1)), \qquad\qquad -(\lambda - 1) \le z \le 0, \qquad (3.6)$$

$$u_4(z) = p_\pm(z - 1)(z - \lambda), \qquad\qquad 1 \le z \le \lambda, \qquad (3.7)$$

$$\frac{\partial T_2}{\partial t} + \alpha Pe_L\, u_2(z)\frac{\partial T_2}{\partial x} = \alpha \left( \frac{\partial^2 T_2}{\partial x^2} + \frac{1}{\eta^2}\frac{\partial^2 T_2}{\partial z^2} \right)$$
$$+ \frac{1}{\eta^2}\alpha Br \left( \frac{\partial u_2}{\partial z} \right)^2, \qquad\qquad -(\lambda - 1) \le z \le 0, \qquad (3.8)$$

$$\frac{\partial T_3}{\partial t} = \frac{\partial^2 T_3}{\partial x^2} + \frac{1}{\eta^2}\frac{\partial^2 T_3}{\partial z^2} + P_L|E_3|^2\sigma(T_3), \qquad\qquad 0 \le z \le 1, \qquad (3.9)$$

$$\frac{\partial T_4}{\partial t} + \alpha Pe_L\, u_4(z)\frac{\partial T_4}{\partial x} = \alpha \left( \frac{\partial^2 T_4}{\partial x^2} + \frac{1}{\eta^2}\frac{\partial^2 T_4}{\partial z^2} \right)$$
$$+ \frac{1}{\eta^2}\alpha Br \left( \frac{\partial u_4}{\partial z} \right)^2, \qquad\qquad 1 \le z \le \lambda, \qquad (3.10)$$

with boundary and initial conditions

$$\frac{\partial T_2}{\partial z} = \eta^2 Bi\, T + \eta^2 R[(T-1)^4 + 1], \qquad z = -(\lambda - 1), \qquad (3.11)$$

$$T_2 = T_3, \qquad K\frac{\partial T_2}{\partial z} = \frac{\partial T_3}{\partial z}, \qquad z = 0, \qquad (3.12)$$

$$T_3 = T_4, \qquad \frac{\partial T_3}{\partial z} = K\frac{\partial T_4}{\partial z}, \qquad z = 1, \qquad (3.13)$$

$$-\frac{\partial T_4}{\partial z} = \eta^2 Bi\, T + \eta^2 R[(T-1)^4 + 1], \qquad z = \lambda, \qquad (3.14)$$

$$\frac{\partial T_{2,3,4}}{\partial x} = 0, \qquad x = \eta^{-1}, \qquad (3.15)$$

$$T_{2,3,4} = 0, \qquad x = 0, \qquad (3.16)$$

$$T_{2,3,4}(0, x, z) = 0, \qquad (3.17)$$

where $Pe_L = \frac{LU}{\alpha_f}$ is the Péclet number, and $Br = \frac{\mu U^2}{k_f T_A}$ is the Brinkman number which are non-dimensional parameters describing the ratio of convection to diffusion and the ratio of viscous heating to conduction respectively. The Dirichlet condition is applied at the inlet $x = 0$ to model an inflow of fluid at ambient temperature, while the insulating condition applied at the outlet $x = \eta^{-1}$ is valid provided the channel is long to for heating to reach steady state, which is assumed.

Understanding the relative size of $Br$ we examine its value for two fluids, water and glycerin. The Brinkman number depends on the pressure gradient which can be controlled during operation. A maximum pressure gradient is determined by insuring a Reynolds number $Re = \frac{\rho_2 Ul}{\mu}$ that corresponds to laminar flow in a channel. The Reynolds number is the ratio of inertial forces to viscous forces and it is generally accepted from empirical

evidence that laminar flow in a channel occurs when $Re < 2000$ [94]. This assumption imposes the following restrictions on the pressure gradient and Brinkman number

$$|p_g| \leq \frac{4 \cdot 10^3 \mu^2}{\rho_2 l^3} \qquad \text{and} \qquad Br \leq \frac{4 \cdot 10^6 \mu^3}{\rho_2^2 k_2 T_A l^2}. \tag{3.18}$$

The material properties for liquid water [95] show that the Brinkman number is negligible. Throughout the remainder of this work, we have assumed viscous heating is negligible and take $Br = 0$.

Once again, by making an asymptotic expansion $T = T^{(0)} + \eta T^{(1)} + \eta^2 T^{(2)} + ...$ and assuming small external losses $\overline{Bi} = \eta^2 Bi$, $\overline{R} = \eta^2 R$, we can find the effective heat equation to be independent of the spanwise direction

$$\overline{\rho c_p} \frac{\partial T}{\partial t} + K Pe_L \overline{u} \frac{\partial T}{\partial x} = \overline{k} \frac{\partial^2 T}{\partial x^2} + P_L \sigma(T) \| E_3^{(0)} \|_2^2 - L(T), \tag{3.19}$$

where $L(T) = 2K Bi\, T + 2K R\,[(T-1)^4 + 1]$, $\overline{\rho c_p} = 1 + 2(\lambda - 1)\frac{K}{\alpha}$, $\overline{k} = 1 + 2(\lambda - 1)K$, $\overline{u} = \widetilde{u}_2 + \widetilde{u}_4 = -\frac{p_\pm}{3}(\lambda - 1)^3$, and

$$\widetilde{u}_2 = \int_{-(\lambda-1)}^{0} u_2(z)\, dz, \tag{3.20}$$

$$\widetilde{u}_4 = \int_{1}^{\lambda} u_4(z)\, dz. \tag{3.21}$$

The effective temperature equation is an advection-diffusion equation with nonlinear sources. The numerical method used to solve it is by using the Crank-Nicolson method

63
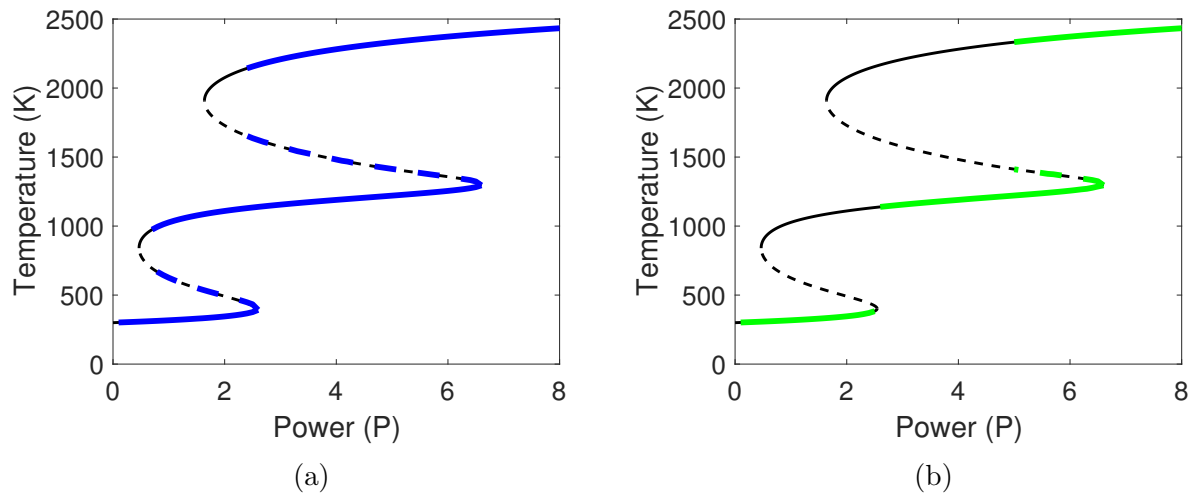
Figure 3.2: SS-curve for fluid flow showing nonexistence regions as $Pe$ increases. The thin black curve is the power response from the uniformly heated case exhibiting no diffusive or advective effects. The colored curves are the power response for diffusive effects $\overline{k} = 0.5$, $Pe = 0$ (a), and for diffusive and advective effects $\overline{k} = 0.5$, $Pe = 12$ (b). Solid lines represent stable steady states and dashed lines represent unstable steady states. Regions of no overlap are where traveling wave solution exist in place of steady states.

with upwinding for the advection term and second order Adams-Bashforth method on the nonlinear parts. The implicit scheme of Crank-Nicolson has the property of being stable and applying the Adams-Bashforth method on the nonlinear source terms allows us to lag the nonlinearities in time. The numerical results show that as with thermal conductivity, increasing Péclet number corresponds to nonexistence regions, where traveling wave solutions develop.

**Theorem 2.** *Equation (3.19) has traveling wave solutions when* $\overline{k}$ *or* $Pe_L$ *are non-zero.*

*Proof.* Let us once again consider a moving reference frame so (3.19) is

$$\overline{k}\frac{\partial^2 T}{\partial w^2} + (v\overline{\rho c_p} - KPe_L\overline{u})\frac{\partial T}{\partial w} + P_L\sigma(T)\|E_3\|_2^2(T) - L(T) = 0. \tag{3.22}$$

Furthermore, scaling $\widetilde{w} = -\frac{w}{\sqrt{\overline{k}}}$ the equation becomes

$$\frac{\partial^2 T}{\partial \widetilde{w}^2} + c\frac{\partial T}{\partial \widetilde{w}} + F(T) = 0, \tag{3.23}$$

where $c = -\frac{v\overline{\rho c_p} - KPe_L\overline{u}}{\sqrt{\overline{k}}}$ and $F(T) = P_L\sigma_e(T)\|E_3\|_2^2(T) - L(T)$. The far field conditions are then given by $\lim_{\widetilde{w}=\infty} T = T_{S1}$ and $\lim_{\widetilde{w}=-\infty} T = T_{S2}$. The remainder of the proof is the same as for Theorem 1. $\qquad\square$

Notice that the addition of advection increases the wave speed. The diffusion-only wave speed is $v_1 = -\frac{c\sqrt{\overline{k}}}{\rho c_p}$ while with advection it becomes $v_2 = -\frac{c\sqrt{\overline{k}} + KPe\overline{u}}{\rho c_p}$. Additionally, we can ask for what value of $Pe$, given two different conductivities $\overline{k}_1$ and $\overline{k}_2$, will produce the same solution. Equating the expressions for $v_1$ and $v_2$ and solving for the Péclet number

reveals that the advection problem with conductivity $\overline{k}_2$ and

$$Pe_L = \frac{(\sqrt{\overline{k}_1} - \sqrt{\overline{k}_2})c}{K\overline{u}}, \tag{3.24}$$

will have the same solution as the diffusion-only solution with conductivity $\overline{k}_1$.

Now that we know such traveling wave solutions exist we derive expressions for the wave velocity $v$ by once again using the Narrow Reaction Zone (NRZ) method. Proceeding as before with the boundary layer analysis we find the approximation to the wave velocity to be

$$v = \begin{cases} \frac{KPe_L\overline{u}}{\overline{\rho c_p}} + \sqrt{-\frac{2\overline{k}}{\overline{\rho c_p}^2(T_{S2}-T_{S1})^2} \int_{T_{S1}}^{T_{S2}} F(T)\, dT}, & v \geq \frac{KPe\overline{u}}{\overline{\rho c_p}}, \\[3mm] \frac{KPe_L\overline{u}}{\overline{\rho c_p}} - \sqrt{\frac{2\overline{k}}{\overline{\rho c_p}^2(T_{S2}-T_{S1})^2} \int_{T_{S1}}^{T_{S2}} F(T)\, dT}, & v \leq \frac{KPe_L\overline{u}}{\overline{\rho c_p}}. \end{cases} \tag{3.25}$$

This approximation to the wave velocity can be used to approximate the location of the interface between the existence and nonexistence regions of the power response curves, depicted in Figure 3.2. The same numerical continuation scheme described in Chapter 2 is used here to plot Figure 3.2. The IMEX numerical solutions showed that traveling wave solutions occur in the nonexistence regions and Figure 2.16 showed how the predicted wave velocity decreases as $P_L$ increases toward the interface between nonexistence and existence of steady-state solutions. Hence setting the expression for the wave velocity equal to zero we obtain an approximate condition on the location of the interface. Table 3.1 compares the predicted power for the interface against the location taken from the power response curve. The error in the prediction worsens as $Pe_L$ increases which is due to the fact that as

| | Lower Wave | | Upper Wave | |
|---|---|---|---|---|
| $Pe_L$ | NRZ | IMEX | NRZ | IMEX |
| 0 | 0.65 | 0.7 | 2.38 | 2.4 |
| 2 | 0.80 | 0.9 | 2.58 | 2.8 |
| 5 | 1.65 | 1.3 | 3.73 | 3.5 |
| 8 | - | 2 | 5.89 | 4.2 |

Table 3.1: Estimation of $P_L$ defining the interface between nonexistence and existence regions of the power response curve for $\overline{k} = 0.5$.

$Pe_L$ increases the width of the boundary layer increases making the narrow reaction zone approximation less applicable.

While the IMEX method is capable of examining transient solutions and studying the traveling wave developed by the nonexistence regions, we seek to find an analytical approximation for steady-state solutions. We consider the steady-state equation of (3.19) in the high power regime $\varepsilon = P_L^{-1} \ll 1$, where the equation becomes

$$\varepsilon \left[ \overline{k}\frac{\partial^2 T}{\partial x^2} - KPe_L\overline{u}\frac{\partial T}{\partial x} \right] + \sigma(T)\|E_3\|_2^2 - \frac{KBi}{P_L}T - \frac{2KR}{P_L}[(T+1)^4 - 1] = 0. \qquad (3.26)$$

We expect a boundary layer at $x = 0$. The order one outer solution is given implicitly by

$$P_L = \frac{L(T)}{\sigma(T)\|E_3\|_2^2(T)}, \qquad (3.27)$$

which is a constant temperature $T_{out}^{(0)}(x) \equiv T^*$ on the power response curve. Next, we define

the inner variable $X = \frac{x-0}{\varepsilon^r}$, where the differential equation becomes

$$\varepsilon^{1-2r}\overline{k}\frac{\partial^2 T}{\partial X^2} - \varepsilon^{1-r}KPe_L\overline{u}\frac{\partial T}{\partial X} + \sigma(T)\|E_3\|_2^2 - \frac{2KBi}{P_L}T - \frac{2KR}{P_L}[(T+1)^4 - 1] = 0. \quad (3.28)$$

Now we identify the dominant balance. The possible balances are $r = \frac{1}{2}$ which is consistent, $r = 1$ which is inconsistent, and $r = 0$ which is the outer solution. The leading order equation for the dominant balance is then

$$\overline{k}\frac{\partial^2 T}{\partial X^2} + \sigma(T)\|E_3\|_2^2 - \frac{2KBi}{P_L}T - \frac{2KR}{P_L}[(T+1)^4 - 1] = 0. \quad (3.29)$$

To continue we linearize the nonlinear parts by taking a Taylor expansion about $T^*$ which will allow us to match the inner and outer solutions. The Taylor expansions are

$$\sigma(T) = Ae^{bT^*} + Abe^{bT^*}(T - T^*), \quad (3.30)$$

$$\|E_3\|_2^2(T) = \|E_3\|_2^2(T^*) + \frac{\partial\|E_3\|_2^2}{\partial T}(T^*)(T - T^*), \quad (3.31)$$

$$[(T+1)^4 - 1] = [(T^* + 1)^4 - 1] + [4(T^* + 1)^3](T - T^*), \quad (3.32)$$

and the linearized differential equation is

$$\overline{k}\frac{\partial^2 T}{\partial X^2} + Ae^{bT^*}\|E_3\|_2^2(T^*) + \left[Abe^{bT^*}\|E_3\|_2^2(T^*) + Ae^{bT^*}\frac{\partial\|E_3\|_2^2}{\partial T}(T^*)\right](T - T^*) - \frac{2KBi}{P_L}T^*$$

$$- \frac{2KBi}{P_L}(T - T^*) - \frac{2KR}{P_L}[(T^* + 1)^4 - 1] - \frac{2KR}{P_L}[4(T^* + 1)^3](T - T^*) = 0. \quad (3.33)$$

68

Since $T^*$ satisfies the power response equation it reduces to

$$\frac{\partial^2 T}{\partial X^2} - \beta T = -\beta T^*, \tag{3.34}$$

where

$$\beta = \frac{1}{k} \left[ -A b e^{bT^*} \|E_3\|_2^2 (T^*) - A e^{bT^*} \frac{\partial \|E_3\|_2^2}{\partial T} (T^*) + \frac{2KR}{P_L} \left[ 4(T^* + 1)^3 \right] + \frac{2KBi}{P_L} \right], \tag{3.35}$$

which can be rewritten as

$$\beta = \frac{\sigma(T^*)\|E_3\|_2^2(T^*)}{k} \frac{1}{P_L} \frac{dP_L}{dT}. \tag{3.36}$$

Hence $\beta > 0$ for all stable steady-state solutions. The solution to the differential equation is then

$$T_{in}^{(0)}(X) = c_1 e^{\sqrt{\beta}X} + c_2 e^{-\sqrt{\beta}X} + T^*. \tag{3.37}$$

Applying the internal boundary condition $T_{in}(0) = 0$ the solution becomes

$$T_{in} = c_1 \left( e^{\sqrt{\beta}X} - e^{-\sqrt{\beta}X} \right) - T^* e^{-\sqrt{\beta}X} + T^*. \tag{3.38}$$

Next, we find the solution in the intermediate region by matching the outer and inner solutions when $x \to 0$ and $X \to \infty$. It requires $c_1 = 0$. This implies $T_{in} = T^* - T^* e^{-\sqrt{\beta}X}$

69

and $T_{match} = T^*$. The general first order solution is given by $T^0 = T_{out} + T_{in} - T_{match}$. Therefore, the solution is

$$T^{(0)}(x) = T^* - T^* e^{-\sqrt{P_L \beta} \, x}, \tag{3.39}$$

after rescaling. This result shows the boundary layer that develops scales with $\sqrt{P}$. We should notice that the solution is independent of advective effects at this scale and will be accurate for lower Péclet numbers. Let us suppose that $Pe_L$ is large enough to scale with diffusion inside the boundary layer. The same analysis will show the solution to be

$$T^{(0)}(x) = T^* - T^* e^{Bx}, \tag{3.40}$$

where

$$B = \frac{KPe_L \overline{u}}{2\overline{k}} - \sqrt{\left(\frac{KPe_L \overline{u}}{2\overline{k}}\right)^2 + P_L \beta}. \tag{3.41}$$

## 3.2   Large Advection Model

The previous model used the fact that everything from the characteristic time, advection, diffusion, and power were $O(1)$ on the macroscale which allowed the solution to be independent of the microscale. The next model that will be investigated considers the case when streamwise advection scales with the spanwise microscale diffusion with mid-range power levels. We define new parameters $Pe_H = \eta^2 Pe_L$ and $P_M = \eta P_L$ where $Pe_H$ and $P_M$ are

70

$O(1)$. Additionally, we assume external conduction losses $\overline{Bi} = O(1)$. On these newly defined scales the non-dimensional system (3.6)-(3.17) at steady state become

$$u_2(z) = p_\pm z(z + (\lambda - 1)), \qquad\qquad -(\lambda - 1) \le z \le 0, \qquad (3.42)$$

$$u_4(z) = p_\pm(z - 1)(z - \lambda), \qquad\qquad 1 \le z \le \lambda, \qquad (3.43)$$

$$\frac{1}{\eta^2} Pe_H \alpha u_2(z) \frac{\partial T_2}{\partial x} = \alpha \left( \frac{\partial^2 T_2}{\partial x^2} + \frac{1}{\eta^2} \frac{\partial^2 T_2}{\partial z^2} \right)$$

$$+ \frac{1}{\eta} \frac{\alpha}{K} P_M |E_2|^2 \sigma_2(T_2), \qquad\qquad -(\lambda - 1) < z < 0, \qquad (3.44)$$

$$0 = \frac{\partial^2 T_3}{\partial x^2} + \frac{1}{\eta^2} \frac{\partial^2 T_3}{\partial z^2} + \frac{1}{\eta} P_M |E_3|^2 \sigma(T_3), \qquad\qquad 0 < z < 1, \qquad (3.45)$$

$$\frac{1}{\eta^2} Pe_H \alpha u_4(z) \frac{\partial T_4}{\partial x} = \alpha \left( \frac{\partial^2 T_4}{\partial x^2} + \frac{1}{\eta^2} \frac{\partial^2 T_4}{\partial z^2} \right)$$

$$+ \frac{1}{\eta} \frac{\alpha}{K} P_M |E_4|^2 \sigma_4(T_4), \qquad\qquad 1 < z < \lambda, \qquad (3.46)$$

with boundary conditions

$$\frac{\partial T_2}{\partial z} = \overline{Bi} T_2 + \eta^2 R \left[ (T_2 + 1)^4 - 1 \right], \qquad\qquad z = -(\lambda - 1), \qquad (3.47)$$

$$T_2 = T_3, \qquad K \frac{\partial T_2}{\partial z} = \frac{\partial T_3}{\partial z}, \qquad\qquad z = 0, \qquad (3.48)$$

$$T_3 = T_4, \qquad \frac{\partial T_3}{\partial z} = K \frac{\partial T_4}{\partial z}, \qquad\qquad z = 1, \qquad (3.49)$$

$$-\frac{\partial T_4}{\partial z} = \overline{Bi} T_4 + \eta^2 R \left[ (T_4 + 1)^4 - 1 \right], \qquad\qquad z = \lambda, \qquad (3.50)$$

71

The solution in the lossy layer after applying boundary conditions $T_3(x,0) = T_2(x,0)$ and $T_3(x,1) = T_4(x,1)$ is

$$T_3(x,z) = [T_4(x,1) - T_2(x,0)]\, z + T_2(x,0). \qquad (3.51)$$

We apply the Galerkin method found in [96] to find the solutions for the temperature in the fluid channels. Define the transformation,

$$\zeta = \begin{cases} \frac{z}{-(\lambda-1)}, & -(\lambda-1) < z < 0, & \Rightarrow & 1 > \xi > 0, \\[2mm] \frac{1-z}{-(\lambda-1)}, & 1 < z < \lambda, & \Rightarrow & 0 < \xi < 1, \end{cases}$$

where $\zeta = 0$ is the interior boundary with region 3 and $\zeta = 1$ is the exterior boundary. The transformed equations are then

$$w(\zeta) = p_{\pm}\zeta(\zeta - 1), \qquad (3.52)$$

$$Pe_H^* \, w(\zeta)\frac{\partial T_2}{\partial x} = \frac{\partial^2 T_2}{\partial \zeta^2}, \qquad (\zeta, x) \in [0,1] \times [0,1], \qquad (3.53)$$

$$Pe_H^* \, w(\zeta)\frac{\partial T_4}{\partial x} = \frac{\partial^2 T_4}{\partial \zeta^2}, \qquad (\zeta, x) \in [0,1] \times [0,1], \qquad (3.54)$$

where $P_{H*} = (\lambda - 1)^2 P_H$ and boundary conditions

$$-\frac{1}{\lambda - 1}\frac{\partial T_2}{\partial \zeta} = \overline{Bi}T_2, \qquad\qquad \zeta = 1, \qquad\qquad (3.55)$$

$$-K\frac{1}{\lambda - 1}\frac{\partial T_2}{\partial \zeta} = T_4(x,0) - T_2(x,0), \qquad\qquad \zeta = 0, \qquad\qquad (3.56)$$

$$K\frac{1}{\lambda - 1}\frac{\partial T_4}{\partial \zeta} = T_4(x,0) - T_2(x,0), \qquad\qquad \zeta = 0, \qquad\qquad (3.57)$$

$$-\frac{1}{\lambda - 1}\frac{\partial T_4}{\partial \zeta} = \overline{Bi}T_4, \qquad\qquad \zeta = 1. \qquad\qquad (3.58)$$

Making another transformation for the dependent variables, the system becomes decoupled. We then define new dependent variables representing the average and difference of the temperatures $T_2$ and $T_4$ as

$$\Theta = \frac{T_2 + T_4}{2}, \qquad\qquad \Delta = \frac{T_2 - T_4}{2}. \qquad\qquad (3.59)$$

The new system of equations to solve is

$$Pe_H^* \, w(\zeta)\frac{\partial \Theta}{\partial x} = \frac{\partial^2 \Theta}{\partial \zeta^2}, \qquad\qquad (\zeta, x) \in [0, 1] \times [0, 1], \qquad\qquad (3.60)$$

$$Pe_H^* \, w(\zeta)\frac{\partial \Delta}{\partial x} = \frac{\partial^2 \Delta}{\partial \zeta^2}, \qquad\qquad (\zeta, x) \in [0, 1] \times [0, 1], \qquad\qquad (3.61)$$

with boundary conditions

$$\frac{\partial \Theta}{\partial \zeta} = -(\lambda - 1)\overline{Bi}\Theta, \qquad\qquad \zeta = 1, \qquad\qquad (3.62)$$

$$\frac{\partial \Delta}{\partial \zeta} = -(\lambda - 1)\overline{Bi}\Delta, \qquad\qquad \zeta = 1, \qquad\qquad (3.63)$$

$$\frac{\partial \Theta}{\partial \zeta} = 0, \qquad\qquad \zeta = 0, \qquad\qquad (3.64)$$

$$\frac{\partial \Delta}{\partial \zeta} = 2\frac{\lambda - 1}{K}\Delta, \qquad\qquad \zeta = 0. \qquad\qquad (3.65)$$

We solve the system using the Galerkin method used in [96]. This is achieved by first solving

the system for plug flow $w(\zeta) \equiv 1$ for an exact solution via eigenfunction expansion. Since

$\theta$ and $\Delta$ are now decoupled the eigenvalues can be different, which we shall call $\mu_1$ and $\mu_2$

respectively. Separation of variables yields a solution of the form

$$\begin{pmatrix} \Theta \\ \Delta \end{pmatrix} = \begin{pmatrix} e^{-\frac{\mu_1}{Pe_H^*}x} & 0 \\ 0 & e^{-\frac{\mu_2}{Pe_H^*}x} \end{pmatrix} \begin{pmatrix} \psi_1(\zeta) \\ \psi_2(\zeta), \end{pmatrix}$$

where the remaining eigenvalue problem is

$$\begin{pmatrix} \psi_1 \\ \psi_2 \end{pmatrix}_{\zeta\zeta} = -\begin{pmatrix} \mu_1 & 0 \\ 0 & \mu_2 \end{pmatrix} \begin{pmatrix} \psi_1 \\ \psi_2 \end{pmatrix}, \qquad\qquad (3.66)$$

with boundary conditions

$$\frac{\partial \psi_1}{\partial \xi} = -(\lambda - 1)\overline{Bi}\psi_1, \qquad\qquad \xi = 1, \qquad\qquad (3.67)$$

$$\frac{\partial \psi_2}{\partial \xi} = -(\lambda - 1)\overline{Bi}\psi_2, \qquad\qquad \xi = 1, \qquad\qquad (3.68)$$

$$\frac{\partial \psi_1}{\partial \xi} = 0, \qquad\qquad \xi = 0, \qquad\qquad (3.69)$$

$$\frac{\partial \psi_2}{\partial \xi} = 2\frac{\lambda - 1}{K}\psi_2, \qquad\qquad \xi = 0. \qquad\qquad (3.70)$$

For completeness, we solve the system together by first finding that the eigenvalues of the matrix which are $\mu_1$ and $\mu_2$. Solving for the eigenvectors we find them to be

$$\begin{pmatrix} 1 \\ 0 \end{pmatrix} \quad \text{and} \quad \begin{pmatrix} 0 \\ 1 \end{pmatrix}, \qquad\qquad (3.71)$$

for each eigenvalue respectively, so the solution is given by

$$\begin{pmatrix} \psi_1 \\ \psi_2 \end{pmatrix} = \begin{pmatrix} 1 \\ 0 \end{pmatrix} [c_1 \cos(\sqrt{\mu_1}\zeta) + c_2 \sin(\sqrt{\mu_1}\zeta)]$$

$$+ \begin{pmatrix} 0 \\ 1 \end{pmatrix} [c_3 \cos(\sqrt{\mu_2}\zeta) + c_4 \sin(\sqrt{\mu_2}\zeta)]. \qquad\qquad (3.72)$$

Applying boundary condition (3.69) implies $c_2 = 0$. Applying boundary condition (3.70) yields $c_4 = 2\frac{\lambda-1}{K\sqrt{\mu_2}}c_3$. Condition (3.67) results in the characteristic equation,

$$\sqrt{\mu_1}\sin(\sqrt{\mu_1}) - (\lambda - 1)\overline{Bi}\cos(\sqrt{\mu_1}) = 0, \qquad\qquad (3.73)$$

for a discrete set of $\mu_{1j}$ and (3.68) yields the characteristic equation

$$\left[K\mu_2 - 2(\lambda - 1)^2\overline{Bi}\right]\sin(\sqrt{\mu_2}) - \left[K\overline{Bi} + 2\right](\lambda - 1)\sqrt{\mu_2}\cos(\sqrt{\mu_2}), \qquad (3.74)$$

for a discrete set of $\mu_{2j}$. By the principle of superposition the series solution is

$$\begin{pmatrix} \Theta \\ \Delta \end{pmatrix} = \sum_{j=1}^{\infty} \begin{pmatrix} e^{-\frac{\mu_{1j}}{Pe_H^*}x} & 0 \\ 0 & e^{-\frac{\mu_{2j}}{Pe_H^*}x} \end{pmatrix} \left[ \begin{pmatrix} 1 \\ 0 \end{pmatrix} a_j\cos(\sqrt{\mu_{1j}}\xi) \right.$$
$$\left. + \begin{pmatrix} 0 \\ 1 \end{pmatrix} b_j \left[\frac{K\sqrt{\mu_{2j}}}{2(\lambda - 1)}\cos(\sqrt{\mu_{2j}}\xi) + \sin(\sqrt{\mu_{2j}}\xi)\right] \right], \qquad (3.75)$$

where we will call

$$\mathbf{\Psi}_{1j} = \begin{pmatrix} 1 \\ 0 \end{pmatrix} \psi_{1j} = \begin{pmatrix} 1 \\ 0 \end{pmatrix} \cos(\sqrt{\mu_{1j}}\xi), \qquad (3.76)$$

$$\mathbf{\Psi}_{2j} = \begin{pmatrix} 0 \\ 1 \end{pmatrix} \psi_{2j} = \begin{pmatrix} 0 \\ 1 \end{pmatrix} \left[\frac{K\sqrt{\mu_{2j}}}{2(\lambda - 1)}\cos(\sqrt{\mu_{2j}}\xi) + \sin(\sqrt{\mu_{2j}}\xi)\right], \qquad (3.77)$$

the basis functions for the plug flow problem. Next, we will use plug flow eigenfunctions to approximate the eigenvalues and eigenfunctions for the Poiseuille flow problem where $w(\zeta) = \zeta(\zeta - 1)$. Once again applying separation of variables to (3.60) and (3.61) the solution has the form

$$\begin{pmatrix} \Theta \\ \Delta \end{pmatrix} = \begin{pmatrix} e^{-\frac{\nu_1}{Pe_H^*}x} & 0 \\ 0 & e^{-\frac{\nu_2}{Pe_H^*}x} \end{pmatrix} \begin{pmatrix} \phi_1(\xi) \\ \phi_2(\xi) \end{pmatrix}, \qquad (3.78)$$

76

where $\nu_1$ and $\nu_2$ are the eigenvalue for the $\Theta$ and $\Delta$ problems respectively. This gives rise to the following eigenvalue problem

$$\begin{pmatrix} \phi_1 \\ \phi_2 \end{pmatrix}_{\xi\xi} = -w(\xi) \begin{pmatrix} \nu_1 & 0 \\ 0 & \nu_2 \end{pmatrix} \begin{pmatrix} \phi_1 \\ \phi_2 \end{pmatrix}, \tag{3.79}$$

with boundary conditions

$$\frac{\partial \phi_1}{\partial \zeta} = -(\lambda - 1)\overline{Bi}\phi_2, \qquad\qquad \zeta = 1, \tag{3.80}$$

$$\frac{\partial \phi_2}{\partial \zeta} = -(\lambda - 1)\overline{Bi}\phi_1, \qquad\qquad \zeta = 1, \tag{3.81}$$

$$\frac{\partial \phi_1}{\partial \zeta} = 0, \qquad\qquad \zeta = 0, \tag{3.82}$$

$$\frac{\partial \phi_2}{\partial \zeta} = 2\frac{\lambda - 1}{K}\phi_2, \qquad\qquad \zeta = 0. \tag{3.83}$$

which can be rewritten as

$$\begin{pmatrix} \phi_1 \\ \phi_2 \end{pmatrix}_{\xi} = -(\lambda - 1)Bi \begin{pmatrix} 1 & 0 \\ 0 & 1 \end{pmatrix} \begin{pmatrix} \phi_1 \\ \phi_2 \end{pmatrix}, \qquad\qquad \xi = 1, \tag{3.84}$$

$$\begin{pmatrix} \phi_1 \\ \phi_2 \end{pmatrix}_{\xi} = 2\frac{\lambda - 1}{K} \begin{pmatrix} 0 & 0 \\ 0 & 1 \end{pmatrix} \begin{pmatrix} \phi_1 \\ \phi_2 \end{pmatrix}, \qquad\qquad \xi = 0. \tag{3.85}$$

We use the plug flow basis functions $\boldsymbol{\Psi}_{1j}$ and $\boldsymbol{\Psi}_{2j}$ to express solutions to the Poiseuille eigenvalue problem for $\phi_1$ and $\phi_2$ as a series expansion

$$\boldsymbol{\Phi} = \sum_{j=1}^{\infty} a_{1j}\boldsymbol{\Psi}_{1j} + a_{2j}\boldsymbol{\Psi}_{2j} = \sum_{j=1}^{\infty} a_{1j} \begin{pmatrix} 1 \\ 0 \end{pmatrix} \psi_{1j} + a_{2j} \begin{pmatrix} 0 \\ 1 \end{pmatrix} \psi_{2j}. \tag{3.86}$$

Applying the boundary condition (3.85) yields,

$$\sum_{j=1}^{\infty} a_{1j} \begin{pmatrix} 1 \\ 0 \end{pmatrix} \psi_{1j\zeta} + a_{2j} \begin{pmatrix} 0 \\ 1 \end{pmatrix} \psi_{2j\zeta} = 2\frac{\lambda-1}{K} \sum_{j=1}^{\infty} a_{2j} \begin{pmatrix} 0 \\ 1 \end{pmatrix} \psi_{2j}, \qquad \zeta = 0. \qquad (3.87)$$

Applying plug flow boundary conditions (3.69) and (3.70) makes the condition

$$2\frac{\lambda-1}{K} \sum_{j=1}^{\infty} a_{2j} \begin{pmatrix} 0 \\ 1 \end{pmatrix} \psi_{2j} = 2\frac{\lambda-1}{K} \sum_{j=1}^{\infty} a_{2j} \begin{pmatrix} 0 \\ 1 \end{pmatrix} \psi_{2j}, \qquad \zeta = 0. \qquad (3.88)$$

Thus this boundary condition on $\phi$ is automatically satisfied. Next, applying the expansion to boundary condition (3.84) produces

$$\sum_{j=1}^{\infty} a_{1j} \begin{pmatrix} 1 \\ 0 \end{pmatrix} \psi_{1j\zeta} + a_{2j} \begin{pmatrix} 0 \\ 1 \end{pmatrix} \psi_{2j\zeta}$$
$$= -(\lambda-1)\overline{Bi} \sum_{j=1}^{\infty} a_{1j} \begin{pmatrix} 1 \\ 0 \end{pmatrix} \psi_{1j} + a_{2j} \begin{pmatrix} 0 \\ 1 \end{pmatrix} \psi_{2j}, \qquad \zeta = 1. \qquad (3.89)$$

Applying plug flow boundary conditions (3.67) and (3.68),

$$-(\lambda-1)\overline{Bi} \sum_{j=1}^{\infty} a_{1j} \begin{pmatrix} 1 \\ 0 \end{pmatrix} \psi_{2j} + a_{2j} \begin{pmatrix} 0 \\ 1 \end{pmatrix} \psi_{1j}$$
$$= -(\lambda-1)\overline{Bi} \sum_{j=1}^{\infty} a_{1j} \begin{pmatrix} 1 \\ 0 \end{pmatrix} \psi_{1j} + a_{2j} \begin{pmatrix} 0 \\ 1 \end{pmatrix} \psi_{2j}, \qquad \zeta = 1, \qquad (3.90)$$

hence this condition too is also satisfied automatically. Plugging the expansion (3.86) into (3.79) the eigenvalue problem becomes

$$\sum_{j=1}^{\infty} a_{1j} \begin{pmatrix} 1 \\ 0 \end{pmatrix} \psi_{1j\xi\xi} + a_{2j} \begin{pmatrix} 0 \\ 1 \end{pmatrix} \psi_{2j\xi\xi} = -w(\xi) \begin{pmatrix} \nu_1 & 0 \\ 0 & \nu_2 \end{pmatrix} \sum_{j=1}^{\infty} a_{1j} \begin{pmatrix} 1 \\ 0 \end{pmatrix} \psi_{1j} + a_{2j} \begin{pmatrix} 0 \\ 1 \end{pmatrix} \psi_{2j}.$$

(3.91)

Applying the plug flow differential equations (3.66) makes the equation algebraic

$$-\sum_{j=1}^{\infty} a_{1j}\mu_{1j} \begin{pmatrix} 1 \\ 0 \end{pmatrix} \psi_{1j} + a_{2j}\mu_{2j} \begin{pmatrix} 0 \\ 1 \end{pmatrix} \psi_{2j} = -w(\xi) \sum_{j=1}^{\infty} a_{1j}\nu_1 \begin{pmatrix} 1 \\ 0 \end{pmatrix} \psi_{1j} + a_{2j}\nu_2 \begin{pmatrix} 0 \\ 1 \end{pmatrix} \psi_{2j}.$$

(3.92)

Next we find two characteristic equations for $\nu_1$ and $\nu_2$ by introducing the inner product

$$\langle u, v \rangle = \int_0^1 u \cdot v \, w(\zeta) \, d\zeta,$$ 

(3.93)

and multiplying through by $\boldsymbol{\Psi_{1i}}$ and $\boldsymbol{\Psi_{2i}}$ respectively for the two equations,

$$\sum_{j=1}^{\infty} \mu_{1j} a_{1j} \psi_{1j} \psi_{1i} = \sum_{j=1}^{\infty} \nu_1 w(\xi) a_{1j} \psi_{1j} \psi_{1i},$$

(3.94)

$$\sum_{j=1}^{\infty} \mu_{2j} a_{2j} \psi_{2j} \psi_{2i} = \sum_{j=1}^{\infty} \nu_2 w(\xi) a_{2j} \psi_{2j} \psi_{2i}.$$

(3.95)

Integrating over each equation from 0 to 1 and applying orthogonality of the plug flow basis functions yields that only the $i$th terms survive on the left hand side,

$$\mu_{1i} a_{1i} \int_0^1 \psi_{1i}^2 \, d\xi = \sum_{j=1}^{\infty} \nu_1 a_{1j} \int_0^1 \psi_{1j} \psi_{1i} w(\xi) \, d\xi, \qquad (3.96)$$

$$\mu_{2j} a_{2j} \int_0^1 \psi_{2i}^2 \, d\xi = \sum_{j=1}^{\infty} \nu_2 a_{2j} \int_0^1 \psi_{2j} \psi_{2i} w(\xi) \, d\xi. \qquad (3.97)$$

These provide us with two sets of algebraic systems $M_1 a_1 = \nu_1 B_1 a_1$ and $M_2 a_2 = \nu_2 B_2 a_2$ where $M_1$ and $M_2$ are diagonal matrices such that $M_{1ii} = \mu_{1i}$ and $M_{2ii} = \mu_{2i}$. The matrices $B_1$ and $B_2$ are given by entries

$$B_{1ij} = \frac{\int_0^1 \psi_{1j} \psi_{1i} \, d\xi}{\int_0^1 \psi_{1i}^2 \, d\xi}, \qquad \text{and} \qquad B_{2ij} = \frac{\int_0^1 \psi_{2j} \psi_{2i} \, d\xi}{\int_0^1 \psi_{2i}^2 \, d\xi}. \qquad (3.98)$$

Since we cannot solve an infinite system of equations for exact eigenvalues $\nu_{1j}$ and $\nu_{2j}$ we will truncate the system so that it only includes the first $N$ equations of the system and we say that the resulting values $\nu_{1j}^N$, $\nu_{2j}^N$, $a_{1i}^N(\nu_{1j})$, and $a_{2i}^N(\nu_{2j})$ are approximations to the exact values. Thus we can define a set of approximate basis functions for the Poiseuille solution which are given by

$$\boldsymbol{\Phi}_{1j}^N = \begin{pmatrix} 1 \\ 0 \end{pmatrix} \phi_{1j}^N = \begin{pmatrix} 1 \\ 0 \end{pmatrix} \sum_{i=1}^{N} a_{1i}^N(\nu_{1j}) \psi_{1i}, \qquad (3.99)$$

$$\boldsymbol{\Phi}_{2j}^N = \begin{pmatrix} 1 \\ 0 \end{pmatrix} \phi_{2j}^N = \begin{pmatrix} 0 \\ 1 \end{pmatrix} \sum_{i=1}^{N} a_{2i}^N(\nu_{2j}) \psi_{2i}. \qquad (3.100)$$

Then with these approximate basis functions $\mathbf{\Phi}_{1j}^N$ and $\mathbf{\Phi}_{2j}^N$ a general solution for $\phi$ is written as the series

$$\mathbf{\Phi} = \sum_{j=1}^{N} c_{1j}\mathbf{\Phi}_{1j}^N + c_{2j}\mathbf{\Phi}_{2j}^N. \tag{3.101}$$

Therefore, the average and difference temperature solution for the Poiseuille Flow are

$$\Theta = \sum_{j=1}^{N} c_{1j}e^{-\frac{\nu_{1j}^N}{Pe_H^*}x}\phi_{1j}^N \tag{3.102}$$

$$\Delta = \sum_{j=1}^{N} c_{2j}e^{-\frac{\nu_{2j}^N}{Pe_H^*}x}\phi_{2j}^N. \tag{3.103}$$

Moreover by taking $\Theta + \Delta$ and $\Theta - \Delta$, we have that

$$T_2^{(0)} = \sum_{j=1}^{N} e^{-\frac{\nu_{1j}^N}{Pe_H^*}x}\left[c_{1j}\phi_{1j}^N + c_{2j}\phi_{2j}^N\right] \tag{3.104}$$

$$T_4^{(0)} = \sum_{j=1}^{N} e^{-\frac{\nu_{2j}^N}{Pe_H^*}x}\left[c_{1j}\phi_{1j}^N - c_{2j}\phi_{2j}^N\right]. \tag{3.105}$$

By applying inlet boundary conditions $T_2(0, z) = f(z)$ and $T_4(0, z) = g(z)$ or rather $\Theta(0, z) = \frac{1}{2}[f(z) + g(z)]$ and $\Delta(0, z) = \frac{1}{2}[f(z) - g(z)]$ the coefficients are given by

$$c_{1j} = \frac{\frac{1}{2}\int_0^1 [f(\zeta) + g(\zeta)]\phi_{1j}(\zeta)w(\zeta)\,d\zeta}{\int_0^1 \phi_{1j}^2(\zeta)w(\zeta)\,d\zeta} \tag{3.106}$$

$$c_{2j} = \frac{\frac{1}{2}\int_0^1 [f(\zeta) - g(\zeta)]\phi_{2j}(\zeta)w(\zeta)\,d\zeta}{\int_0^1 \phi_{2j}^2(\zeta)w(\zeta)\,d\zeta}. \tag{3.107}$$

Notice that in the symmetric case $f(z) \equiv g(z)$, the difference component disappears since $c_{2j} = 0$. Additionally, if we apply the Dirichlet boundary condition $f(z) = 0$, $g(z) = 0$, then we have the trivial solution $T_2^{(0)} = T_4^{(0)} = 0$. Proceeding to the next order solution the governing equation are

$$\alpha Pe_H u_2(z) \frac{\partial T_2^{(1)}}{\partial x} = \alpha \frac{\partial^2 T_2^{(1)}}{\partial z^2} + \frac{\alpha}{K} P_M |E_2(0, z)|^2 \sigma_2(0), \quad (z, x) \in [-(\lambda - 1), 0] \times [0, 1],$$

$$(3.108)$$

$$0 = \frac{\partial^2 T_3^{(1)}}{\partial z^2} + P_M |E_3(0, z)|^2 \sigma(0), \quad (z, x) \in [0, 1] \times [0, 1],$$

$$(3.109)$$

$$\alpha Pe_H u_4(z) \frac{\partial T_4^{(1)}}{\partial x} = \alpha \frac{\partial^2 T_4^{(1)}}{\partial z^2} + \frac{\alpha}{K} P_M |E_4(0, z)|^2 \sigma_4(0), \quad (z, x) \in [1, \lambda] \times [0, 1],$$

$$(3.110)$$

with the same boundary conditions as at leading order

$$\frac{\partial T_2^{(1)}}{\partial z} = \overline{Bi} T_2^{(1)}, \qquad\qquad z = -(\lambda - 1), \qquad (3.111)$$

$$T_2^{(1)} = T_3^{(1)}, \qquad\qquad z = 0, \qquad (3.112)$$

$$K \frac{\partial T_2^{(1)}}{\partial z} = \frac{\partial T_3^{(1)}}{\partial z}, \qquad\qquad z = 0, \qquad (3.113)$$

$$T_3^{(1)} = T_4^{(1)}, \qquad\qquad z = 1, \qquad (3.114)$$

$$\frac{\partial T_3^{(1)}}{\partial z} = K \frac{\partial T_4^{(1)}}{\partial z}, \qquad\qquad z = 1, \qquad (3.115)$$

$$-\frac{\partial T_4^{(1)}}{\partial z} = \overline{Bi} T_4^{(1)}, \qquad\qquad z = \lambda. \qquad (3.116)$$

We notice that the EM heating now appears as source independent of the first correction temperature making the governing equations linear. The solution procedure is the same as at leading order thus we first solve for $T_3^{(1)}$ and applying boundary conditions (3.112) and (3.114) the solution is

$$
T_3^{(1)} = -P_M\sigma(0) \iint |E_3|^2 dz\, dz' + \left[ T_4(x,0) - T_2(x,0) + P_M\sigma(0) \iint |E_3|^2 dz\, dz'\bigg|_{z=1} \right.
$$
$$
\left. -\ P_M\sigma(0) \iint |E_3|^2 dz\, dz'\bigg|_{z=0} \right] z + T_2(x,0) + P_M\sigma(0) \iint |E_3|^2 dz\, dz'\bigg|_{z=0}. \qquad (3.117)
$$

Introducing the transform variables $\zeta$, $\Theta$, and $\Delta$ as defined previously the remaining system becomes,

$$
\begin{pmatrix} \Theta \\ \Delta \end{pmatrix}_{\zeta\zeta} = Pe_H^*\, w(\zeta) \begin{pmatrix} 1 & 0 \\ 0 & 1 \end{pmatrix} \begin{pmatrix} \Theta \\ \Delta \end{pmatrix}_x + \begin{pmatrix} F(x,\zeta) \\ G(x,\zeta) \end{pmatrix}, \qquad (3.118)
$$

where $F(x,\zeta) = -\frac{P_M}{2K}\left[|E_2(0,\zeta)|^2\sigma_2(0) + |E_4(0,\zeta)|^2\sigma_4(0)\right]$ and

$G(x,\zeta) = -\frac{P_M}{2K}\left[|E_2(0,\zeta)|^2\sigma_2(0) - |E_4(0,\zeta)|^2\sigma_4(0)\right]$. The boundary conditions are then given by

$$
\frac{\partial\Theta}{\partial\zeta} = -(\lambda-1)\overline{Bi}\Delta, \qquad\qquad \zeta = 1, \qquad\qquad (3.119)
$$

$$
\frac{\partial\Delta}{\partial\zeta} = -(\lambda-1)\overline{Bi}\Theta, \qquad\qquad \zeta = 1, \qquad\qquad (3.120)
$$

$$
\frac{\partial\Theta}{\partial\zeta} = C, \qquad\qquad \zeta = 0, \qquad\qquad (3.121)
$$

$$
\frac{\partial\Delta}{\partial\zeta} = 2\frac{\lambda-1}{K}\Delta + D, \qquad\qquad \zeta = 0, \qquad\qquad (3.122)
$$

83

where

$$C = \frac{(\lambda - 1)}{2K} P_M \sigma(0) \left[ \int |E_3|^2 dz \Big|_{z=0} - \int |E_3|^2 dz \Big|_{z=1} \right], \tag{3.123}$$

$$D = \frac{\lambda - 1}{K} \left[ \frac{P_M \sigma(0)}{2} \left[ \int |E_3|^2 dz \Big|_{z=0} + \int |E_3|^2 dz \Big|_{z=1} \right] + P_M \sigma(0) \iint |E_3|^2 dz \, dz' \Big|_{z=0} \right.$$

$$\left. - P_M \sigma(0) \iint |E_3|^2 dz \, dz' \Big|_{z=1} \right]. \tag{3.124}$$

We seek a solution by eigenfunction expansion

$$\begin{pmatrix} \Theta \\ \Delta \end{pmatrix} = \sum_{j=1}^{N} \begin{pmatrix} a_j(x) & 0 \\ 0 & b_j(x) \end{pmatrix} \begin{pmatrix} \phi_{1j} \\ \phi_{2j} \end{pmatrix}. \tag{3.125}$$

Taking the dot product of (3.118) with the eigenfunctions and integrate over $\zeta$,

$$\int_0^1 \begin{pmatrix} \Theta \\ \Delta \end{pmatrix}_{\xi\xi} \cdot \begin{pmatrix} \phi_{1m} \\ 0 \end{pmatrix} d\xi = Pe_H^* \int_0^1 \begin{pmatrix} \Theta \\ \Delta \end{pmatrix}_x \cdot \begin{pmatrix} \phi_{1m} \\ 0 \end{pmatrix} w(\xi) \, d\xi$$

$$+ \int_0^1 \begin{pmatrix} F(x,\xi) \\ G(x,\xi) \end{pmatrix} \cdot \begin{pmatrix} \phi_{1m} \\ 0 \end{pmatrix} d\xi, \tag{3.126}$$

$$\int_0^1 \begin{pmatrix} \Theta \\ \Delta \end{pmatrix}_{\xi\xi} \cdot \begin{pmatrix} 0 \\ \phi_{2m} \end{pmatrix} d\xi = Pe_H^* \int_0^1 \begin{pmatrix} \Theta \\ \Delta \end{pmatrix}_x \cdot \begin{pmatrix} 0 \\ \phi_{2m} \end{pmatrix} w(\xi) \, d\xi$$

$$+ \int_0^1 \begin{pmatrix} F(x,\xi) \\ G(x,\xi) \end{pmatrix} \cdot \begin{pmatrix} 0 \\ \phi_{2m} \end{pmatrix} d\xi, \tag{3.127}$$

to find a solvability condition via the Fredholm Alternative Theorem [97]. Apply integration by parts twice,

$$\Theta_\xi \phi_{1m}|_0^1 - \Theta \phi_{1m\xi}|_0^1 + \int_0^1 \Theta \phi_{1m\xi\xi} = Pe_H^* \int_0^1 \Theta_x \phi_{1m} w(\xi) \, d\xi + \int_0^1 F \phi_{1m} \, d\xi, \quad (3.128)$$

$$\Delta_\xi \phi_{2m}|_0^1 - \Delta \phi_{2m\xi}|_0^1 + \int_0^1 \Delta \phi_{2m\xi\xi} \, d\xi = Pe_H^* \int_0^1 \Delta_x \phi_{2m} w(\xi) \, d\xi + \int_0^1 G \phi_{2m} \, d\xi. \quad (3.129)$$

Applying boundary conditions (3.80)-(3.83) and (3.119)-(3.122) yields,

$$-C\phi_{1m}(0) + \int_0^1 \Theta \phi_{1m\xi\xi} \, d\xi = Pe_H^* \int_0^1 \Theta_x \phi_{1m} w(\xi) \, d\xi + \int_0^1 F \phi_{1m} \, d\xi, \quad (3.130)$$

$$-D\phi_{2m}(0) + \int_0^1 \Delta \phi_{2m\xi\xi} \, d\xi = Pe_H^* \int_0^1 \Delta_x \phi_{2m} w(\xi) \, d\xi + \int_0^1 G \phi_{2m} \, d\xi. \quad (3.131)$$

Invoking the governing equation of the eigenfunctions (3.79) it becomes

$$-C\phi_{1m}(0) - \nu_{1m} \int_0^1 \Theta \phi_{1m} w(\xi) \, d\xi = Pe_H^* \int_0^1 \Theta_x \phi_{1m} w(\xi) \, d\xi + \int_0^1 F \phi_{1m} \, d\xi, \quad (3.132)$$

$$-D\phi_{2m}(0) - \nu_{2m} \int_0^1 \Delta \phi_{2m} w(\xi) \, d\xi = Pe_H^* \int_0^1 \Delta_x \phi_{2m} w(\xi) \, d\xi + \int_0^1 G \phi_{2m} \, d\xi. \quad (3.133)$$

Next, we substitute the eigenfunction expansion in for $\Theta$ and $\Delta$

$$-C\phi_{1m}(0) - \nu_{1m} \sum_{j=1}^\infty a_j(x) \langle \phi_{1j}, \phi_{1m} \rangle = Pe_H^* \sum_{j=1}^\infty a_j'(x) \langle \phi_{1j}, \phi_{1m} \rangle + \int_0^1 F \phi_{1m} \, d\xi, \quad (3.134)$$

$$-D\phi_{2m}(0) - \lambda_{2m} \sum_{j=1}^\infty b_j(x) \langle \phi_{2j}, \phi_{2m} \rangle = Pe_H^* \sum_{j=1}^\infty b_j'(x) \langle \phi_{2j}, \phi_{2m} \rangle + \int_0^1 G \phi_{2m} \, d\xi. \quad (3.135)$$

85

Finally by the orthogonality of the eigenfunctions

$$-C\phi_{1m}(0) - \nu_{1m}a_m(x)\langle\phi_{1m}, \phi_{1m}\rangle = Pe_H^* a_m'(x)\langle\phi_{1m}, \phi_{1m}\rangle + \int_0^1 F\phi_{1m}\,d\xi, \qquad (3.136)$$

$$-D\phi_{2m}(0) - \nu_{2m}b_m(x)\langle\phi_{2m}, \phi_{2m}\rangle = Pe_H^* b_m'(x)\langle\phi_{2m}, \phi_{2m}\rangle + \int_0^1 G\phi_{2m}\,d\xi, \qquad (3.137)$$

so the differential equation to solve for $a_m(x)$ and $b_m(x)$ are

$$a_m'(x) + \frac{\nu_{1m}}{Pe_H^*}a_m(x) = \overbrace{\frac{-C\phi_{1m}(0)}{Pe_H^*\langle\phi_{1m}, \phi_{1m}\rangle} - \int_0^1 \frac{F\phi_{1m}}{Pe_H^*\langle\phi_{1m}, \phi_{1m}\rangle}\,d\xi}^{\text{Call this constant } S_{1m}}, \qquad (3.138)$$

$$b_m'(x) + \frac{\nu_{2m}}{Pe}b_m(x) = \overbrace{\frac{-D\phi_{2m}(0)}{Pe_H^*\langle\phi_{2m}, \phi_{2m}\rangle} - \int_0^1 \frac{G\phi_{2m}}{Pe_H^*\langle\phi_{2m}, \phi_{2m}\rangle}\,d\xi}^{\text{Call this constant } S_{2m}}. \qquad (3.139)$$

The solutions to these ODEs are

$$a_m(x) = c_{1m}e^{-\frac{\nu_{1m}}{Pe_H^*}x} + \frac{Pe_H^*}{\nu_{1m}}S_{1m}, \qquad (3.140)$$

$$b_m(x) = c_{2m}e^{-\frac{\nu_{2m}}{Pe_H^*}x} + \frac{Pe_H^*}{\nu_{2m}}S_{2m}. \qquad (3.141)$$

The general solution to the eigenfunction expansion problem is

$$\Theta(x, \xi) = \sum_{j=1}^{\infty}\left[c_{1j}e^{-\frac{\nu_{1j}}{Pe_H^*}x} + \frac{Pe_H^*}{\nu_{1j}}S_{1j}\right]\phi_{1m}(\xi), \qquad (3.142)$$

$$\Delta(x, \xi) = \sum_{j=1}^{\infty}\left[c_{2j}e^{-\frac{\nu_{2j}}{Pe_H^*}x} + \frac{Pe_H^*}{\nu_{2j}}S_{2j}\right]\phi_{2m}(\xi). \qquad (3.143)$$

86

For the inlet conditions $T_2(0, z) = f(z)$ and $T_4(0, z) = g(z)$, the inlet conditions for the average and difference are $\Theta(0, \xi) = \frac{1}{2}[f + g]$ and $\Delta(0, \xi) = \frac{1}{2}[f - g]$. Then the inlet condition becomes

$$\frac{1}{2}[f + g] = \sum_{j=1}^{\infty} \left[ c_{1j} + \frac{Pe_H^*}{\nu_{1j}} S_{1j} \right] \phi_{1j}, \tag{3.144}$$

$$\frac{1}{2}[f - g] = \sum_{j=1}^{\infty} \left[ c_{2j} + \frac{Pe_H^*}{\nu_{2j}} S_{2j} \right] \phi_{2j}. \tag{3.145}$$

To find constants $c_{1j}$ and $c_{2j}$, we take the dot product with the eigenvector, multiply by $w(\xi)$, and integrate in $\xi$,

$$\int_0^1 \frac{1}{2}[f + g] \phi_{1m} w(\xi) \, d\xi = \sum_{j=1}^{\infty} \left[ c_{1j} + \frac{Pe_H^*}{\nu_{1j}} S_{1j} \right] \int_0^1 \phi_{1j} \phi_{1m} w(\xi) \, d\xi, \tag{3.146}$$

$$\int_0^1 \frac{1}{2}[f - g] \phi_{2m} w(\xi) \, d\xi = \sum_{j=1}^{\infty} \left[ c_{2j} + \frac{Pe_H^*}{\nu_{2j}} S_{2j} \right] \int_0^1 \phi_{2j} \phi_{2m} w(\xi) \, d\xi. \tag{3.147}$$

Therefore, by orthogonality the constants are given by

$$c_{1m} = \frac{\langle \frac{1}{2}[f + g], \phi_{1m} \rangle}{\langle \phi_{1m}, \phi_{1m} \rangle} - \frac{Pe_H^*}{\nu_{1m}} S_{1m}, \tag{3.148}$$

$$c_{2m} = \frac{\langle \frac{1}{2}[f - g], \phi_{2m} \rangle}{\langle \phi_{2m}, \phi_{2m} \rangle} - \frac{Pe_H^*}{\nu_{2m}} S_{2m}. \tag{3.149}$$
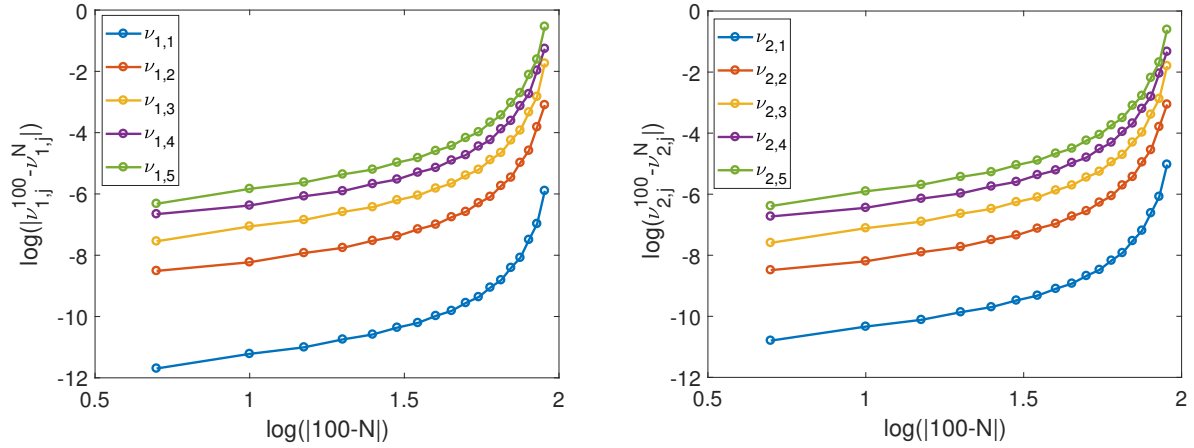
Figure 3.3: Convergence of the first five eigenvalue approximations $\nu_{1,j}^N$ and $\nu_{2,j}^N$, $j = 1, 2, 3, 4, 5$, as the number of Galerkin modes increases by 5 from $N = 15$ to $N = 95$: convergence of eigenvalues $\nu_{1,j}$ for $\Theta$ (a); and convergence of eigenvalues $\nu_{2,j}$ for $\Delta$ (b).

The original temperature solution are then given by

$$T_2^{(1)}(x, \xi) = \sum_{j=1}^{\infty} \left[ c_{1j} e^{-\frac{\nu_{1j}}{Pe_H^*}x} + \frac{Pe_H^*}{\nu_{1j}} S_{1j} \right] \phi_{1j}(\xi) + \left[ c_{2j} e^{-\frac{\nu_{2j}}{Pe_H^*}x} + \frac{Pe_H^*}{\nu_{2j}} S_{2j} \right] \phi_{2j}(\xi), \quad (3.150)$$

$$T_4^{(1)}(x, \xi) = \sum_{j=1}^{\infty} \left[ c_{1j} e^{-\frac{\nu_{1j}}{Pe_H^*}x} + \frac{Pe_H^*}{\nu_{1j}} S_{1j} \right] \phi_{1j}(\xi) - \left[ c_{2j} e^{-\frac{\nu_{2j}}{Pe_H^*}x} + \frac{Pe_H^*}{\nu_{2j}} S_{2j} \right] \phi_{2j}(\xi). \quad (3.151)$$

Figure 3.3 shows the convergence of the eigenvalues as the number of Galerkin modes $N$ increases, where the mode for $N = 100$ was used as the converged solution. It demonstrates that this method converges rapidly requiring only a few modes to be accurate.

## 3.3 Alternating Direction Implicit (ADI) Method

In order to validate the high-advection model we implement a scheme to numerically solve the full non-dimensional system of equations governing the problem. We solve the non-dimensional system

$$\frac{\partial T_2}{\partial t} + \alpha Pe_L \, u_2(z) \frac{\partial T_2}{\partial x} = \alpha \left( \frac{\partial^2 T_2}{\partial x^2} + \frac{\partial^2 T_2}{\partial z^2} \right), \qquad -(\lambda - 1) \le z \le 0, \quad (3.152)$$

$$\frac{\partial T_3}{\partial t} = \frac{\partial^2 T_3}{\partial x^2} + \frac{\partial^2 T_3}{\partial z^2} + P_L |E_3|^2 \sigma(T_3), \qquad 0 \le z \le 1, \quad (3.153)$$

$$\frac{\partial T_4}{\partial t} + \alpha Pe_L \, u_4(z) \frac{\partial T_4}{\partial x} = \alpha \left( \frac{\partial^2 T_4}{\partial x^2} + \frac{\partial^2 T_4}{\partial z^2} \right), \qquad 1 \le z \le \lambda, \quad (3.154)$$

subject to boundary and initial conditions

$$\frac{\partial T_2}{\partial z} = \overline{Bi} \, T + \overline{R}[(T-1)^4 + 1], \qquad z = -(\lambda - 1), \qquad (3.155)$$

$$T_2 = T_3, \qquad K \frac{\partial T_2}{\partial z} = \frac{\partial T_3}{\partial z}, \qquad z = 0, \qquad (3.156)$$

$$T_3 = T_4, \qquad \frac{\partial T_3}{\partial z} = K \frac{\partial T_4}{\partial z}, \qquad z = 1, \qquad (3.157)$$

$$-\frac{\partial T_4}{\partial z} = \overline{Bi} \, T + \overline{R}[(T-1)^4 + 1], \qquad z = \lambda, \qquad (3.158)$$

$$\frac{\partial T_{2,3,4}}{\partial x} = 0, \qquad x = 10, \qquad (3.159)$$

$$T_{2,3,4} = 0, \qquad x = 0, \qquad (3.160)$$

$$T_{2,3,4}(0, x, z) = 0, \qquad (3.161)$$

by using the Peaceman-Rachford Alternating Direction Implicit numerical method [89]. Steady-state solutions are taken with an relative error tolerance of $10^{-6}$. We can now use

this method to compare the numerical solution to those achieved by the Galerkin method of the high-advection case. Figure 3.4 plots the temperature profile using both methods for a lower advection case $Pe = 5$, and a higher advection case $Pe = 50$. The solutions for $Pe = 50$ are in very good agreement, while $Pe = 5$ is still in good agreement, but not as well as the higher advection case. This is expected since the Galerkin model was developed for high-advection and will be a poor model as lower advection where streamwise diffusion becomes more dominant.
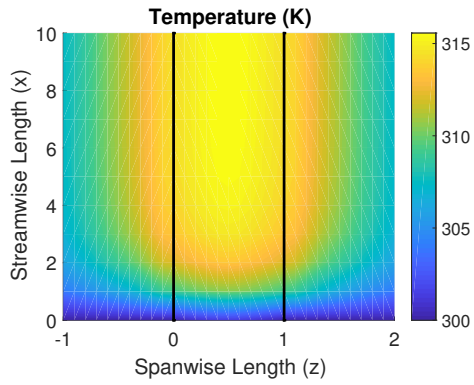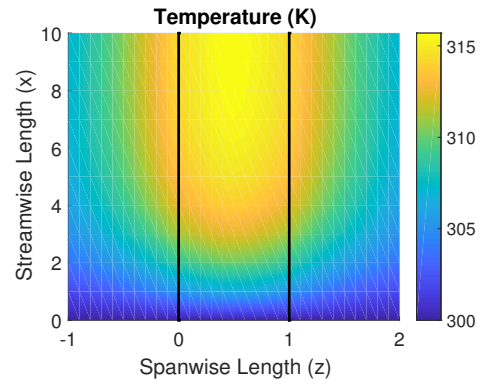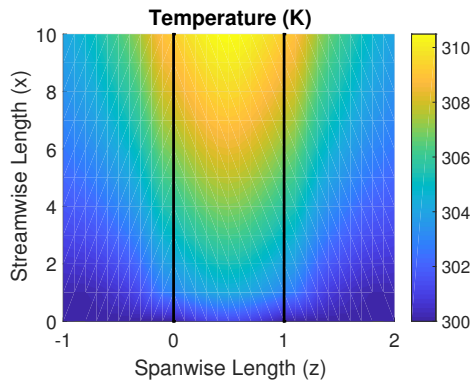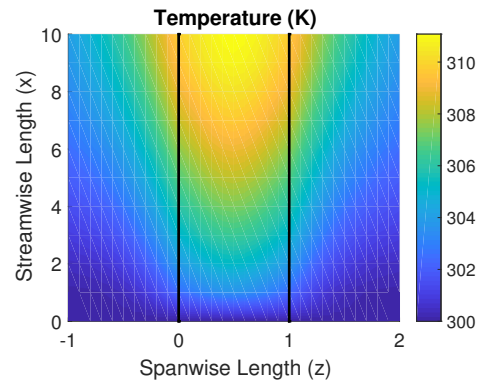
Figure 3.4: Temperature profiles for solutions with power $P = 1$ using the Galerkin method with $Pe_L = 5$, (a); PR-ADI method with $Pe_L = 5$ (b); Galerkin method with $Pe_L = 50$ (c); and PR-ADI method with $Pe_L = 50$ (d).

The chief philosophical value of physics is that it gives the mind something distinct to lay hold of, which if you don't, Nature at once tells you you are wrong.

<div align="right">James Clerk Maxwell (1831-1879)</div>

# CHAPTER IV

## POROUS MEDIA LAMINATE MODELS

We now consider the case of multi-layered two-phase dielectric material in the homogenization limit. This geometry is known as a one-dimensional photonic crystal, especially when the layers alternate high and low permittivity. Traditionally, photonic crystals have been studied for their optical properties, both visible and sub-visible, but have not been well studied with the inclusion of lossy materials. In contrast, there have been numerous studies considering a heat exchanger with a porous medium as the target material [17, 35, 98–102], however, they do not consider the high-frequency interactions of a photonic crystal. It is these interactions we are interested in studying in the context of a porous heat exchanger since it was precisely these interactions that produced the SS-curve discussed in Chapter 2.

The first section of the present Chapter details the homogenization of the thermal system which can be coupled to one of the EM models that follow. There are two models for the EM problem that we have considered. The first is the familiar long-wave approach, considering wavelengths much longer than the microscale, which is the classical homogenization of Maxwell's equations and will be a limiting case of the following high-frequency homogenization. The high-frequency case, where the wavelength is comparable to the microscale, is the regime where the unique optical effects associated with photonic crystals are present. We extend the homogenization technique of [82] to include material loss. The scattering
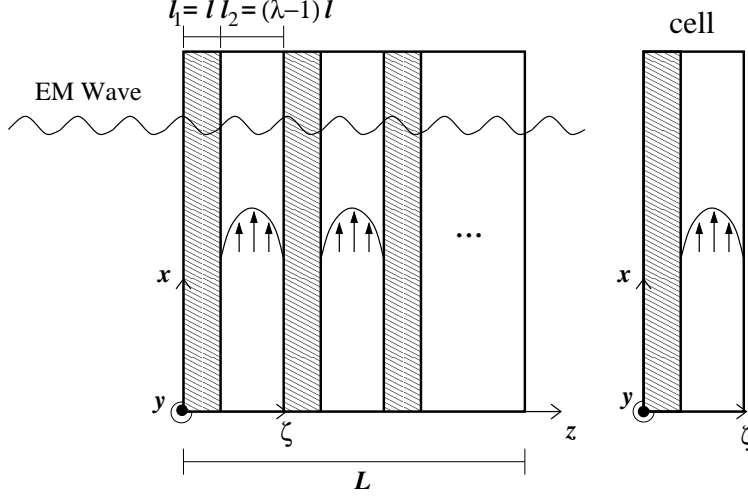
Figure 4.1: Porous laminate geometry

problem is compared to the exact solutions of the Transform Matrix Method (TMM).

4.1 Homogenization of the Thermal Problem

We start this Chapter with the energy equation homogenization for the laminate geometry of Figure 4.1. It is a two phase laminate so we can define the non-dimensional energy equation for each of the two layers

$$\frac{\partial T_1}{\partial 1} + \alpha P e_L\, u(z)\frac{\partial T_1}{\partial x} = \alpha\frac{\partial^2 T_1}{\partial x^2} + \frac{1}{\eta^2}\alpha\frac{\partial^2 T_1}{\partial \zeta^2}, \qquad (x,z) \in [0,1] \times [-(\lambda-1),0], \qquad (4.1)$$

$$\frac{\partial T_2}{\partial t} = \frac{\partial^2 T_2}{\partial x^2} + \frac{1}{\eta^2}\frac{\partial^2 T_2}{\partial \zeta^2} + P_L|E_2|^2\sigma(T_2), \qquad (x,z) \in [0,1] \times [0,1]. \qquad (4.2)$$

Consider a single heat equation indexed by $i = 1, 2$ corresponding to the two regions, where $\alpha_1 = \alpha$, $\alpha_2 = 1$, $u_1 = u$, $u_2 = 0$, $\sigma_1 = 0$, and $\sigma_2 = \sigma$. Next, we introduce the multiple scales given by $z = \eta\zeta$, where $z$ is the macroscale variable and $\zeta$ is the microscale variable. The

system with cell boundary conditions becomes

$$\frac{\partial T_i}{\partial \tau} + \alpha_i Pe_L \, u_i(\zeta) \frac{\partial T_i}{\partial x} = \alpha_i \frac{\partial^2 T_i}{\partial x^2} + \alpha_i \frac{\partial^2 T_i}{\partial z^2} + \frac{2}{\eta} \alpha_i \frac{\partial^2 T_i}{\partial \zeta \partial z} + \frac{1}{\eta^2} \alpha_i \frac{\partial^2 T_i}{\partial \zeta^2} + P_L |E_i|^2 \sigma_i(T_i), \quad (4.3)$$

$$T_1(x, z, 0) = T_2(x, z, 0), \tag{4.4}$$

$$\alpha_1 \frac{\partial T_1}{\partial \zeta} + \eta \alpha_1 \frac{\partial T_1}{\partial z} = \alpha_2 \frac{\partial T_2}{\partial \zeta} + \eta \alpha_2 \frac{\partial T_2}{\partial z}, \quad \zeta = 0, \tag{4.5}$$

$$T_1(x, z, -(\lambda - 1)) = T_2(x, z, 1). \tag{4.6}$$

Finally, we assume an asymptotic expansion $T_i = T_i^{(0)} + \eta T_i^{(1)} + \eta^2 T_i^{(2)} + ...$, $\eta \ll 1$, and solve the hierarchy of problems in each order of $\eta$. The first order problem is given by

$$\alpha_i \frac{\partial^2 T_i^{(0)}}{\partial \zeta^2} = 0, \tag{4.7}$$

which yields the solution

$$T_i^{(0)}(x, \zeta, z) = A_i(x, z)\zeta + B_i(x, z). \tag{4.8}$$

Applying the periodicity condition (4.6), coefficient $A_i(x, z) \equiv 0$. Applying continuity boundary condition (4.4), $T_1^{(0)}(x, z, 0) = T_2^{(0)}(x, z, 0)$ implies that $B_1(x, z) \equiv B_2(x, z)$, hence the leading order solution is independent of the microscale variable $\zeta$,

$$T^{(0)}(x, z) = T_1^{(0)} = T_2^{(0)}. \tag{4.9}$$

Proceeding to the next order for the cell problem, it is given by

$$0 = \alpha_i \frac{\partial^2 T_i^{(1)}}{\partial \zeta^2} + 2\alpha_i \frac{\partial^2 T_i^{(0)}}{\partial \zeta \partial z}, \tag{4.10}$$

which reduces to

$$\frac{\partial^2 T_i^{(1)}}{\partial \zeta^2} = 0, \tag{4.11}$$

and results in the general solution

$$T_i^{(1)} = C_i(x, z)\zeta + D_i(x, z). \tag{4.12}$$

Since the cell problem is unique up to a constant, we choose $D_2(x, z) \equiv 0$. Applying the continuity (4.4) yields the condition

$$D_1(x, z) = 0, \tag{4.13}$$

then applying periodicity (4.6) along the cell outer boundary, we have that

$$-(\lambda - 1)C_1(x, z) = C_2(x, z). \tag{4.14}$$

Applying the flux boundary condition (4.5) gives the cell problems dependence on the leading order solution,

$$\alpha_1 C_1(x, z) - \alpha_2 C_2(x, z) = (\alpha_2 - \alpha_1) \frac{\partial T^{(0)}}{\partial z}. \tag{4.15}$$

By substituting (4.14) into (4.15) we find each of the coefficients to be

$$C_1(x, z) = \frac{(\alpha_2 - \alpha_1)}{\alpha_1 + \alpha_2(\lambda - 1)} \frac{\partial T^{(0)}}{\partial z}, \tag{4.16}$$

$$C_2(x, z) = -\frac{(\alpha_2 - \alpha_1)(\lambda - 1)}{\alpha_1 + \alpha_2(\lambda - 1)} \frac{\partial T^{(0)}}{\partial z}. \tag{4.17}$$

Therefore, the second order solution in terms of the first order solution is given by,

$$T_1^{(1)}(x, z, \zeta) = \left( \frac{(\alpha_2 - \alpha_1)}{\alpha_1 + \alpha_2(\lambda - 1)} \zeta \right) \frac{\partial T^{(0)}}{\partial z}, \tag{4.18}$$

$$T_2^{(1)}(x, z, \zeta) = \left( -\frac{(\alpha_2 - \alpha_1)(\lambda - 1)}{\alpha_1 + \alpha_2(\lambda - 1)} \zeta \right) \frac{\partial T^{(0)}}{\partial z}. \tag{4.19}$$

Finally, we proceed to the $O(\eta^2)$ problem, where we have closure finding an effective equation for the leading order solution. The second order energy equation is

$$\frac{\partial T^{(0)}}{\partial t} + \alpha_i Pe_L \, u_i \frac{\partial T^{(0)}}{\partial x} = \alpha_i \frac{\partial^2 T^{(0)}}{\partial x^2} + \alpha_i \frac{\partial^2 T_i^{(2)}}{\partial \zeta^2} + 2\alpha_i \frac{\partial T_i^{(1)}}{\partial \zeta \partial z} + \alpha_i \frac{\partial^2 T^{(0)}}{\partial z^2} + P_L |E_i|^2 \sigma_i(T^{(0)})$$

$$\tag{4.20}$$

$$T_1^{(2)}(x, z, 0) = T_2^{(2)}(x, z, 0) \tag{4.21}$$

$$\alpha_1 \frac{\partial T_1^{(2)}}{\partial \zeta} + \alpha_1 \frac{\partial T_1^{(1)}}{\partial z} = \alpha_2 \frac{\partial T_2^{(2)}}{\partial \zeta} + \alpha_2 \frac{\partial T_2^{(1)}}{\partial z}, \quad \zeta = 1 \tag{4.22}$$

The effective equation governing the order one solution is determined by integrating each PDE in $\zeta$ over the respective domains and adding them together,

$$\int_{-(\lambda-1)}^{0} \left[ \frac{\partial T^{(0)}}{\partial t} + \alpha_1 Pe_L u \frac{\partial T^{(0)}}{\partial x} \right] d\zeta + \int_{0}^{1} \frac{\partial T^{(0)}}{\partial t} \zeta$$

$$= \int_{-(\lambda-1)}^{0} \left[ \alpha_1 \frac{\partial^2 T^{(0)}}{\partial x^2} + \alpha_1 \frac{\partial^2 T_1^{(2)}}{\partial \zeta^2} + 2\alpha_1 \frac{\partial^2 T_1^{(1)}}{\partial \zeta \partial z} + \alpha_1 \frac{\partial^2 T^{(0)}}{\partial z^2} \right] d\zeta$$

$$+ \int_{0}^{1} \left[ \alpha_2 \frac{\partial^2 T^{(0)}}{\partial x^2} + \alpha_2 \frac{\partial^2 T_2^{(2)}}{\partial \zeta^2} + 2\alpha_2 \frac{\partial^2 T_2^{(1)}}{\partial \zeta \partial z} + \alpha_2 \frac{\partial^2 T^{(0)}}{\partial z^2} + P_L |E|^2 \sigma(T^{(0)}) \right] d\zeta. \quad (4.23)$$

Evaluating each integral, the equation becomes

$$\lambda \frac{\partial T^{(0)}}{\partial t} + \alpha_1 Pe_L \lambda \overline{u} \frac{\partial T^{(0)}}{\partial x} = [\alpha_2 + (\lambda - 1)\alpha_1] \frac{\partial^2 T^{(0)}}{\partial x^2} + \alpha_1 \left[ \left. \frac{\partial T_1^{(2)}}{\partial \zeta} \right|_0 - \left. \frac{\partial T_1^{(2)}}{\partial \zeta} \right|_{-(\lambda-1)} \right]$$

$$+ 2\alpha_1 \left[ \left. \frac{\partial T_1^{(1)}}{\partial z} \right|_0 - \left. \frac{\partial T_1^{(1)}}{\partial z} \right|_{-(\lambda-1)} \right] + [\alpha_2 + (\lambda - 1)\alpha_1] \frac{\partial^2 T^{(0)}}{\partial z^2} + \alpha_2 \left[ \left. \frac{\partial T_2^{(2)}}{\partial \zeta} \right|_1 - \left. \frac{\partial T_2^{(2)}}{\partial \zeta} \right|_0 \right]$$

$$+ 2\alpha_2 \left[ \left. \frac{\partial T_2^{(1)}}{\partial z} \right|_1 - \left. \frac{\partial T_2^{(1)}}{\partial z} \right|_0 \right] + P_L \|E\|_2^2 \sigma(T^{(0)}), \quad (4.24)$$

which can be rearranged as

$$\lambda \frac{\partial T^{(0)}}{\partial t} + \alpha_1 Pe_L \lambda \overline{u} \frac{\partial T^{(0)}}{\partial x} = [\alpha_2 + (\lambda - 1)\alpha_1] \frac{\partial^2 T^{(0)}}{\partial x^2} + [\alpha_2 + (\lambda - 1)\alpha_1] \frac{\partial^2 T^{(0)}}{\partial z^2}$$

$$+ P_L \|E\|_2^2 \sigma(T^{(0)}) + \left[ \alpha_1 \left. \frac{\partial T_1^{(2)}}{\partial \zeta} \right|_0 - \alpha_2 \left. \frac{\partial T_2^{(2)}}{\partial \zeta} \right|_0 \right] + \left[ 2\alpha_1 \left. \frac{\partial T_1^{(1)}}{\partial z} \right|_0 - 2\alpha_2 \left. \frac{\partial T_2^{(1)}}{\partial z} \right|_0 \right]$$

$$+ \left[ \alpha_2 \left. \frac{\partial T_2^{(2)}}{\partial \zeta} \right|_1 - \alpha_1 \left. \frac{\partial T_1^{(2)}}{\partial \zeta} \right|_{-(\lambda-1)} \right] + \left[ 2\alpha_2 \left. \frac{\partial T_2^{(1)}}{\partial z} \right|_1 - 2\alpha_1 \left. \frac{\partial T_1^{(1)}}{\partial z} \right|_{-(\lambda-1)} \right]. \quad (4.25)$$

Applying the flux conditions (4.5) at second order, it becomes,

$$
\lambda \frac{\partial T^{(0)}}{\partial t} + \alpha_1 Pe_L \, \lambda \overline{u} \frac{\partial T^{(0)}}{\partial x} = [\alpha_2 + (\lambda - 1)\alpha_1] \frac{\partial^2 T^{(0)}}{\partial x^2} + [\alpha_2 + (\lambda - 1)\alpha_1] \frac{\partial^2 T^{(0)}}{\partial z^2}
$$

$$
+ \quad P_L \|E\|_2^2 \sigma(T^{(0)}) - \left[ \alpha_1 \left. \frac{\partial T_1^{(1)}}{\partial z} \right|_0 - \alpha_2 \left. \frac{\partial T_2^{(1)}}{\partial z} \right|_0 \right] + \left[ 2\alpha_1 \left. \frac{\partial T_1^{(1)}}{\partial z} \right|_0 - 2\alpha_2 \left. \frac{\partial T_2^{(1)}}{\partial z} \right|_0 \right]
$$

$$
+ \quad \left[ \alpha_2 \left. \frac{\partial T_2^{(2)}}{\partial \zeta} \right|_1 - \alpha_1 \left. \frac{\partial T_1^{(2)}}{\partial \zeta} \right|_{-(\lambda-1)} \right] + \left[ 2\alpha_2 \left. \frac{\partial T_2^{(1)}}{\partial z} \right|_1 - 2\alpha_1 \left. \frac{\partial T_1^{(1)}}{\partial z} \right|_{-(\lambda-1)} \right]. \qquad (4.26)
$$

Applying periodicity on the flux boundary condition at the outer boundaries $\zeta = -(\lambda - 1), 1$

the equation becomes,

$$
\lambda \frac{\partial T^{(0)}}{\partial t} + \alpha_1 Pe_L \, \lambda \overline{u} \frac{\partial T^{(0)}}{\partial x} = [\alpha_2 + (\lambda - 1)\alpha_1] \frac{\partial^2 T^{(0)}}{\partial x^2} + [\alpha_2 + (\lambda - 1)\alpha_1] \frac{\partial^2 T^{(0)}}{\partial z^2}
$$

$$
+ \quad P_L \|E\|_2^2 \sigma(T^{(0)}) - \left[ \alpha_1 \left. \frac{\partial T_1^{(1)}}{\partial z} \right|_0 - \alpha_2 \left. \frac{\partial T_2^{(1)}}{\partial z} \right|_0 \right] + \left[ 2\alpha_1 \left. \frac{\partial T_1^{(1)}}{\partial z} \right|_0 - 2\alpha_2 \left. \frac{\partial T_2^{(1)}}{\partial z} \right|_0 \right]
$$

$$
- \quad \left[ \alpha_2 \left. \frac{\partial T_2^{(1)}}{\partial z} \right|_1 - \alpha_1 \left. \frac{\partial T_1^{(1)}}{\partial z} \right|_{-(\lambda-1)} \right] + \left[ 2\alpha_2 \left. \frac{\partial T_2^{(1)}}{\partial z} \right|_1 - 2\alpha_1 \left. \frac{\partial T_1^{(1)}}{\partial z} \right|_{-(\lambda-1)} \right], \qquad (4.27)
$$

which reduces to

$$
\lambda \frac{\partial T^{(0)}}{\partial t} + \alpha_1 Pe_L \, \lambda \overline{u} \frac{\partial T^{(0)}}{\partial x} = [\alpha_2 + (\lambda - 1)\alpha_1] \frac{\partial^2 T^{(0)}}{\partial x^2} + [\alpha_2 + (\lambda - 1)\alpha_1] \frac{\partial^2 T^{(0)}}{\partial z^2}
$$

$$
+ P_L \|E\|_2^2 \sigma(T^{(0)}) + \left[ \alpha_1 \left. \frac{\partial T_1^{(1)}}{\partial z} \right|_0 - \alpha_1 \left. \frac{\partial T_1^{(1)}}{\partial z} \right|_{-(\lambda-1)} \right] + \left[ \alpha_2 \left. \frac{\partial T_2^{(1)}}{\partial z} \right|_1 - \alpha_2 \left. \frac{\partial T_2^{(1)}}{\partial z} \right|_0 \right]. \qquad (4.28)
$$

Next, the difference in derivatives of the first correction solution are

$$\left.\frac{\partial T_2^{(1)}}{\partial z}\right|_1 - \left.\frac{\partial T_2^{(1)}}{\partial z}\right|_0 = -\frac{(\alpha_2 - \alpha_1)(\lambda - 1)}{\alpha_1 + \alpha_2(\lambda - 1)}\frac{\partial^2 T^{(0)}}{\partial z^2}, \qquad (4.29)$$

$$\left.\frac{\partial T_1^{(1)}}{\partial z}\right|_0 - \left.\frac{\partial T_1^{(1)}}{\partial z}\right|_{-(\lambda-1)} = \frac{(\alpha_2 - \alpha_1)(\lambda - 1)}{\alpha_1 + \alpha_2(\lambda - 1)}\frac{\partial^2 T^{(0)}}{\partial z^2}. \qquad (4.30)$$

Then, by applying these to the equation and dividing through by $\lambda$, the effective equation that governs the leading order temperature appears in the form

$$\frac{\partial T^{(0)}}{\partial t} + \alpha_1 Pe_L \,\overline{u}\frac{\partial T^{(0)}}{\partial x} = A_{ari}\frac{\partial^2 T^{(0)}}{\partial x^2} + A_{har}\frac{\partial^2 T^{(0)}}{\partial z^2} + \frac{P_L}{\lambda}\|E\|_2^2\sigma(T^{(0)}), \qquad (4.31)$$

where $\overline{u} = \frac{1}{\lambda}\int_{-(\lambda-1)}^0 u(\zeta)\,d\zeta$, $A_{ari} = \frac{\alpha_1 + (\lambda-1)\alpha_2}{\lambda}$, $A_{har} = \frac{\alpha_1\alpha_2\lambda}{\alpha_1+\alpha_2(\lambda-1)}$, and $\|E\|_2^2 = \int_0^1 |E(x,\zeta,z)|^2\,d\zeta$. Coefficients $A_{ari}$ and $A_{har}$, the arithmetic and harmonic means respectively, define the anisotropy of the effective thermal diffusivities in the $x$- and $z$-direction. This effective temperature equation is be solved by applying the PR-ADI method used previously. It first requires to be coupled with a model that solves for the electric field inside the multi-layered material.

The rest of this work is dedicated to two such models in two distinct asymptotic regimes. The first model is a classical homogenization of Maxwell's equations which, as we will show, only under certain assumption is equivalent to simple mixture formula. The restriction for classical homogenization is that the wavelength must be long comparable to the microstructure. Since we are interested in the high-frequency interactions associated with the SS-curve, we consider the high-frequency homogenization by [82] which was developed

for lossless material, and we include a low-loss parameter that models attenuation over the macroscale length of the material. Since the geometry under consideration is a multi-layer laminate, these models can be compared against the exact solution found by the Transfer Matrix Method (TMM). The Transfer Matrix Method is used to solve the 1D Helmholtz equation of a layered geometry. Discussed in [68] and detailed in Appendix B, it easily implemented as particular matrices known as transfer matrices determine how waves behave across an interface.

4.2   Long-wave Homogenization Model

We begin the derivation for the long-wave homogenization of Maxwell's equations by starting with (1.17) and (1.18) and make the transformation $\gamma = \eta\gamma_L$, $\eta \ll 1$, where $\gamma_L = \frac{\omega L}{c}$ is a non-dimensional wavenumber that is $O(1)$ when the wavelength is comparable to the macroscale length $L$. This is the long-wave assumption made to perform the classical homogenization technique. We have assumed in this case that phase one is the lossless medium, but it is trivial to swap the two layers. Additionally, we want the macroscale variables $x$ and $z$ to be scaled on the macroscale to model long-wave propagation. Applying this, rescaling (1.17) and (1.18) become

$$\eta\widetilde{\nabla} \cdot (\epsilon\mathbf{E}) = 0, \qquad\qquad \eta\widetilde{\nabla} \cdot (\mu\mathbf{H}) = 0, \qquad (4.32)$$

$$\eta\widetilde{\nabla} \times \mathbf{E} = -i\eta\gamma_L\mu\mathbf{H}, \qquad\qquad \eta\widetilde{\nabla} \times \mathbf{H} = i\eta\gamma_L\epsilon\mathbf{E}. \qquad (4.33)$$

Then we apply multiple scales defined by $z = \eta\zeta$. The divergence and curl operators are consequently

$$\widetilde{\nabla} \cdot \mathbf{A} = \frac{\partial A_x}{\partial x} + \frac{\partial A_y}{\partial y} + \frac{\partial A_z}{\partial z} + \frac{1}{\eta}\frac{\partial A_\zeta}{\partial \zeta} = \nabla \cdot \mathbf{A} + \frac{1}{\eta}\frac{\partial A_\zeta}{\partial \zeta}, \tag{4.34}$$

$$\widetilde{\nabla} \times \mathbf{A} = \begin{vmatrix} \widehat{i} & \widehat{j} & \widehat{k} \\ \frac{\partial}{\partial x} & \frac{\partial}{\partial y} & \frac{\partial}{\partial z} \\ A_x & A_y & A_z \end{vmatrix} = \left(\frac{\partial A_z}{\partial y} - \frac{\partial A_y}{\partial z}\right)\widehat{i} + \left(\frac{\partial A_x}{\partial z} - \frac{\partial A_z}{\partial x}\right)\widehat{j} + \left(\frac{\partial A_y}{\partial x} - \frac{\partial A_x}{\partial y}\right)\widehat{k}$$

$$\tag{4.35}$$

$$= \left[\left(\frac{\partial A_z}{\partial y} - \frac{\partial A_y}{\partial z}\right)\widehat{i} + \left(\frac{\partial A_x}{\partial z} - \frac{\partial A_z}{\partial x}\right)\widehat{j} + \left(\frac{\partial A_y}{\partial x} - \frac{\partial A_x}{\partial y}\right)\widehat{k}\right] + \frac{1}{\eta}\left[-\frac{\partial A_y}{\partial \zeta}\widehat{i} + \frac{\partial A_x}{\partial \zeta}\widehat{j}\right]$$

$$\tag{4.36}$$

$$= \nabla \times \mathbf{A} + \frac{1}{\eta}\left[-\frac{\partial A_y}{\partial \zeta}\widehat{i} + \frac{\partial A_x}{\partial \zeta}\widehat{j}\right]. \tag{4.37}$$

The governing equations for each phase are given by

$$\nabla \cdot (\epsilon_1 \mathbf{E}_1) + \frac{1}{\eta}\frac{\partial(\epsilon_1 E_{1z})}{\partial \zeta} = 0, \tag{4.38}$$

$$\nabla \cdot (\epsilon_2 \mathbf{E}_2) + \frac{1}{\eta}\frac{\partial(\epsilon_2 E_{2z})}{\partial \zeta} = 0, \tag{4.39}$$

$$\nabla \times \mathbf{E}_1 + \frac{1}{\eta}\left(-\frac{\partial E_{1y}}{\partial \zeta} \quad , \quad \frac{\partial E_{1x}}{\partial \zeta} \quad , \quad 0\right) = -i\gamma_L\mu_1\mathbf{H}_1, \tag{4.40}$$

$$\nabla \times \mathbf{E}_2 + \frac{1}{\eta}\left(-\frac{\partial E_{2y}}{\partial \zeta} \quad , \quad \frac{\partial E_{2x}}{\partial \zeta} \quad , \quad 0\right) = -i\gamma_L\mu_2\mathbf{H}_2, \tag{4.41}$$

$$\nabla \cdot (\mu_1 \mathbf{H}_1) + \frac{1}{\eta} \frac{\partial(\mu_1 H_{1z})}{\partial \zeta} = 0, \tag{4.42}$$

$$\nabla \cdot (\mu_2 \mathbf{H}_2) + \frac{1}{\eta} \frac{\partial(\mu_2 H_{2z})}{\partial \zeta} = 0, \tag{4.43}$$

$$\nabla \times \mathbf{H}_1 + \frac{1}{\eta} \left( -\frac{\partial H_{1y}}{\partial \zeta} \ , \ \frac{\partial H_{1x}}{\partial \zeta} \ , \ 0 \right) = i\gamma_L \epsilon_1 \mathbf{E}_1, \tag{4.44}$$

$$\nabla \times \mathbf{H}_2 + \frac{1}{\eta} \left( -\frac{\partial H_{2y}}{\partial \zeta} \ , \ \frac{\partial H_{2x}}{\partial \zeta} \ , \ 0 \right) = i\gamma_L \epsilon_2 \mathbf{E}_2, \tag{4.45}$$

and the interface boundary conditions (1.23)-(1.26) for this geometry reduce to

$$E_{1x} = E_{2x}, \qquad\qquad H_{1x} = H_{2x}, \tag{4.46}$$

$$E_{1y} = E_{2y}, \qquad\qquad H_{1y} = H_{2y}, \tag{4.47}$$

$$\epsilon_1 E_{1z} = \epsilon_2 E_{2z}, \qquad\qquad \mu_1 H_{1z} = \mu_2 H_{2z}. \tag{4.48}$$

The leading order problem for each component is

$$\frac{\partial E_{1x}^{(0)}}{\partial \zeta} = 0, \qquad \frac{\partial E_{1y}^{(0)}}{\partial \zeta} = 0, \qquad \frac{\partial(\epsilon_1 E_{1z}^{(0)})}{\partial \zeta} = 0, \tag{4.49}$$

$$\frac{\partial E_{2x}^{(0)}}{\partial \zeta} = 0, \qquad \frac{\partial E_{2y}^{(0)}}{\partial \zeta} = 0, \qquad \frac{\partial(\epsilon_2 E_{2z}^{(0)})}{\partial \zeta} = 0, \tag{4.50}$$

$$\frac{\partial H_{1x}^{(0)}}{\partial \zeta} = 0, \qquad \frac{\partial H_{1y}^{(0)}}{\partial \zeta} = 0, \qquad \frac{\partial(\mu_1 H_{1z}^{(0)})}{\partial \zeta} = 0, \tag{4.51}$$

$$\frac{\partial H_{2x}^{(0)}}{\partial \zeta} = 0, \qquad \frac{\partial H_{2y}^{(0)}}{\partial \zeta} = 0, \qquad \frac{\partial(\mu_2 H_{2z}^{(0)})}{\partial \zeta} = 0, \tag{4.52}$$

with boundary conditions

$$E_{1x}^{(0)}(x, y, z, 1) = E_{2x}^{(0)}(x, y, z, 1), \qquad H_{1x}^{(0)}(x, y, z, 1) = H_{2x}^{(0)}(x, y, z, 1), \qquad (4.53)$$

$$E_{1y}^{(0)}(x, y, z, 1) = E_{2y}^{(0)}(x, y, z, 1), \qquad H_{1y}^{(0)}(x, y, z, 1) = H_{2y}^{(0)}(x, y, z, 1), \qquad (4.54)$$

$$\epsilon_1 E_{1z}^{(0)}(x, y, z, 1) = \epsilon_2 E_{2z}^{(0)}(x, y, z, 1), \qquad \mu_1 H_{1z}^{(0)}(x, y, z, 1) = \mu_2 H_{2z}^{(0)}(x, y, z, 1). \quad (4.55)$$

Each component of the field is independent of $\zeta$ within each region. Applying the boundary conditions, the leading order solutions have the form

$$\mathbf{E}^{(0)}(x, y, z) = \begin{cases} \left( E_x^{(0)}, & E_y^{(0)}, & E_{1z}^{(0)} \right), & 0 \le \zeta < 1, \\ \left( E_x^{(0)}, & E_y^{(0)}, & \frac{\epsilon_1}{\epsilon_2} E_{1z}^{(0)} \right), & 1 \le \zeta < \lambda, \end{cases} \qquad (4.56)$$

$$\mathbf{H}^{(0)}(x, y, z) = \begin{cases} \left( H_x^{(0)}, & H_y^{(0)}, & H_{1z}^{(0)} \right), & 0 \le \zeta < 1, \\ \left( H_x^{(0)}, & H_y^{(0)}, & \frac{\mu_1}{\mu_2} H_{1z}^{(0)} \right), & 1 \le \zeta < \lambda. \end{cases} \qquad (4.57)$$

The equations governing the first correction are

$$\nabla \cdot (\epsilon_1 \mathbf{E}_1^{(0)}) + \frac{\partial (\epsilon_1 E_{1z}^{(1)})}{\partial \zeta} = 0, \qquad (4.58)$$

$$\nabla \cdot (\epsilon_2 \mathbf{E}_2^{(0)}) + \frac{\partial (\epsilon_2 E_{2z}^{(1)})}{\partial \zeta} = 0, \qquad (4.59)$$

$$\nabla \times \mathbf{E}_1^{(0)} + \left( -\frac{\partial E_{1y}^{(1)}}{\partial \zeta}, \quad \frac{\partial E_{1x}^{(1)}}{\partial \zeta}, \quad 0 \right) = -i\gamma_L \mu_1 \mathbf{H}_1^{(0)}, \qquad (4.60)$$

$$\nabla \times \mathbf{E}_2^{(0)} + \left( -\frac{\partial E_{2y}^{(1)}}{\partial \zeta}, \quad \frac{\partial E_{2x}^{(1)}}{\partial \zeta}, \quad 0 \right) = -i\gamma_L \mu_2 \mathbf{H}_2^{(0)}, \qquad (4.61)$$

104

$$\nabla \cdot (\mu_1 \mathbf{H}_1^{(0)}) + \frac{\partial(\mu_1 H_{1z}^{(1)})}{\partial \zeta} = 0, \tag{4.62}$$

$$\nabla \cdot (\mu_2 \mathbf{H}_2^{(0)}) + \frac{\partial(\mu_2 H_{2z}^{(1)})}{\partial \zeta} = 0, \tag{4.63}$$

$$\nabla \times \mathbf{H}_1^{(0)} + \left( -\frac{\partial H_{1y}^{(1)}}{\partial \zeta} \quad , \quad \frac{\partial H_{1x}^{(1)}}{\partial \zeta} \quad , \quad 0 \right) = i\gamma_L \epsilon_1 \mathbf{E}_1^{(0)}, \tag{4.64}$$

$$\nabla \times \mathbf{H}_2^{(0)} + \left( -\frac{\partial H_{2y}^{(1)}}{\partial \zeta} \quad , \quad \frac{\partial H_{2x}^{(1)}}{\partial \zeta} \quad , \quad 0 \right) = i\gamma_L \epsilon_2 \mathbf{E}_2^{(0)}, \tag{4.65}$$

with boundary conditions

$$E_{1x}^{(1)}(x,y,z,1) = E_{2x}^{(1)}(x,y,z,1), \qquad\qquad H_{1x}^{(1)}(x,y,z,1) = H_{2x}^{(1)}(x,y,z,1), \tag{4.66}$$

$$E_{1y}^{(1)}(x,y,z,1) = E_{2y}^{(1)}(x,y,z,1), \qquad\qquad H_{1y}^{(1)}(x,y,z,1) = H_{2y}^{(1)}(x,y,z,1), \tag{4.67}$$

$$\epsilon_1 E_{1z}^{(1)}(x,y,z,1) = \epsilon_2 E_{2z}^{(1)}(x,y,z,1), \qquad \mu_1 H_{1z}^{(1)}(x,y,z,1) = \mu_2 H_{2z}^{(1)}(x,y,z,1), \tag{4.68}$$

and periodicity conditions

$$E_{1x}^{(1)}(x,y,z,0) = E_{2x}^{(1)}(x,y,z,\lambda), \qquad\qquad H_{1x}^{(1)}(x,y,z,0) = H_{2x}^{(1)}(x,y,z,\lambda), \tag{4.69}$$

$$E_{1y}^{(1)}(x,y,z,0) = E_{2y}^{(1)}(x,y,z,\lambda), \qquad\qquad H_{1y}^{(1)}(x,y,z,0) = H_{2y}^{(1)}(x,y,z,\lambda), \tag{4.70}$$

$$\epsilon_1 E_{1z}^{(1)}(x,y,z,0) = \epsilon_2 E_{2z}^{(1)}(x,y,z,\lambda), \qquad \mu_1 H_{1z}^{(1)}(x,y,z,0) = \mu_2 H_{2z}^{(1)}(x,y,z,\lambda). \tag{4.71}$$

First, we determine the effective divergence equations starting with the magnetic field. Averaging each equation by integrating over the region domain and dividing by cell volume $\lambda$

yields,

$$\frac{1}{\lambda} \int_0^1 \nabla \cdot (\mu_1 \mathbf{H}_1^{(0)}) \, d\zeta + \frac{1}{\lambda} \int_0^1 \frac{\partial(\mu_1 H_{1z}^{(1)})}{\partial \zeta} \, d\zeta = 0, \tag{4.72}$$

$$\frac{1}{\lambda} \int_1^\lambda \nabla \cdot (\mu_2 \mathbf{H}_2^{(0)}) \, d\zeta + \frac{1}{\lambda} \int_1^\lambda \frac{\partial(\mu_2 H_{2z}^{(1)})}{\partial \zeta} \, d\zeta = 0. \tag{4.73}$$

Evaluating the integrals the equations become

$$\frac{1}{\lambda} \nabla \cdot (\mu_1 \mathbf{H}_1^{(0)}) = -\frac{1}{\lambda} \left[ \mu_1 H_{1z}^{(1)} \Big|_1 - \mu_1 H_{1z}^{(1)} \Big|_0 \right], \tag{4.74}$$

$$\frac{\lambda - 1}{\lambda} \nabla \cdot (\mu_2 \mathbf{H}_2^{(0)}) = -\frac{1}{\lambda} \left[ \mu_2 H_{2z}^{(1)} \Big|_\lambda - \mu_2 H_{2z}^{(1)} \Big|_1 \right], \tag{4.75}$$

and by adding them together and applying boundary and periodic conditions,

$$\frac{1}{\lambda} \nabla \cdot (\mu_1 \mathbf{H}_1^{(0)}) + \frac{\lambda - 1}{\lambda} \nabla \cdot (\mu_2 \mathbf{H}_2^{(0)}) = 0. \tag{4.76}$$

The effective equation can then be written down in terms of phase 1 $\nabla \cdot (M_1 \mathbf{H}_1^{(0)}) = 0$ or

phase 2 $\nabla \cdot (M_2 \mathbf{H}_2^{(0)}) = 0$, where the effective permeability matrix $M_1$ and $M_2$ are

$$M_1 = \begin{bmatrix} \mu_{ari} & 0 & 0 \\ 0 & \mu_{ari} & 0 \\ 0 & 0 & \mu_1 \end{bmatrix}, \qquad M_2 = \begin{bmatrix} \mu_{ari} & 0 & 0 \\ 0 & \mu_{ari} & 0 \\ 0 & 0 & \mu_2 \end{bmatrix}, \tag{4.77}$$

where the arithmetic mean of permeability is $\mu_{ari} = \frac{\mu_1 + (\lambda - 1)\mu_2}{\lambda}$. The reason we do not obtain

a single effective equation is because the $z$-component is not continuous across the boundary

interface, but rather it is the magnetic flux $\mathbf{B}$ that is continuous. Next, we can do the same

thing for the divergence of the electric field. Average each equation by integrating over the

region domain and dividing by cell volume $\lambda$, we find that,

$$\frac{1}{\lambda} \int_0^1 \nabla \cdot (\epsilon_1 \mathbf{E}_1^{(0)}) \, d\zeta + \frac{1}{\lambda} \int_0^1 \frac{\partial (\epsilon_1 E_{1z}^{(1)})}{\partial \zeta} \, d\zeta = 0, \tag{4.78}$$

$$\frac{1}{\lambda} \int_1^\lambda \nabla \cdot (\epsilon_2 \mathbf{E}_2^{(0)}) \, d\zeta + \frac{1}{\lambda} \int_1^\lambda \frac{\partial (\epsilon_2 E_{2z}^{(1)})}{\partial \zeta} \, d\zeta = 0. \tag{4.79}$$

Evaluating the integrals, the equations become

$$\frac{1}{\lambda} \nabla \cdot (\epsilon_1 \mathbf{E}_1^{(0)}) = -\frac{1}{\lambda} \left[ \epsilon_1 E_{1z}^{(1)} \Big|_1 - \epsilon_1 E_{1z}^{(1)} \Big|_0 \right], \qquad \frac{\lambda - 1}{\lambda} \nabla \cdot (\epsilon_2 \mathbf{E}_2^{(0)}) = -\frac{1}{\lambda} \left[ \epsilon_2 E_{2z}^{(1)} \Big|_\lambda - \epsilon_2 E_{2z}^{(1)} \Big|_1 \right].$$
$$\tag{4.80}$$

The phase 1 equation can be rewritten as

$$\frac{1}{\lambda} \nabla \cdot (\epsilon_1 \mathbf{E}_1^{(0)}) = -\frac{1}{\lambda} \left[ \epsilon_1 E_{1z}^{(1)} \Big|_1 - \epsilon_1 E_{1z}^{(1)} \Big|_0 \right]. \tag{4.81}$$

Finally, adding the equations together and applying the boundary and periodic conditions, we arrive at the effective equation

$$\frac{1}{\lambda} \nabla \cdot (\epsilon_1 \mathbf{E}_1^{(0)}) + \frac{\lambda - 1}{\lambda} \nabla \cdot (\epsilon_2 \mathbf{E}_2^{(0)}) = 0. \tag{4.82}$$

This equation is different from the magnetic field which is due to the fact that the boundary condition for the lossy medium uses the real part of the dielectric constant $\epsilon_1$ and not the effective complex dielectric constant $\epsilon_1$. For the specific case of a lossy medium with a dielectric constant that is spatially invariant, we have $\nabla \cdot (P_1 \mathbf{E}_1^{(0)}) = 0$ and $\nabla \cdot (P_2 \mathbf{E}_2^{(0)}) = 0$,

where the effective permittivity matrix $P_1$ and $P_2$ are

$$P_1 = \begin{bmatrix} \epsilon_{ari} & 0 & 0 \\ 0 & \epsilon_{ari} & 0 \\ 0 & 0 & \epsilon_1 \end{bmatrix}, \qquad P_2 = \begin{bmatrix} \epsilon_{ari} & 0 & 0 \\ 0 & \epsilon_{ari} & 0 \\ 0 & 0 & \epsilon_2 \end{bmatrix}, \qquad (4.83)$$

and the arithmetic mean of permittivity is $\epsilon_{ari} = \frac{\epsilon_1 + (\lambda-1)\epsilon_2}{\lambda}$. We now find the effective curl

equations. Starting with the curl of the electric field, we take the average over each phase,

$$\frac{1}{\lambda}\nabla \times \mathbf{E}_1^{(0)} + i\frac{1}{\lambda}\gamma_L\mu_1\mathbf{H}_1^{(0)} = -\frac{1}{\lambda}\left(-\left.E_{1y}^{(1)}\right|_1 + \left.E_{1y}^{(1)}\right|_0 \quad , \quad \left.E_{1x}^{(1)}\right|_1 - \left.E_{1x}^{(1)}\right|_0 \quad , \quad 0\right),$$

$$(4.84)$$

$$\frac{\lambda-1}{\lambda}\nabla \times \mathbf{E}_2^{(0)} + i\frac{\lambda-1}{\lambda}\gamma_L\mu_2\mathbf{H}_2^{(0)} = -\frac{1}{\lambda}\left(-\left.E_{2y}^{(1)}\right|_\lambda + \left.E_{2y}^{(1)}\right|_1 \quad , \quad \left.E_{2x}^{(1)}\right|_\lambda - \left.E_{2x}^{(1)}\right|_1 \quad , \quad 0\right).$$

$$(4.85)$$

Adding equations together and applying boundary and periodic conditions, we end with

$$\frac{1}{\lambda}\nabla \times \mathbf{E}_1^{(0)} + \frac{\lambda-1}{\lambda}\nabla \times \mathbf{E}_2^{(0)} + i\frac{1}{\lambda}\gamma_L\mu_1\mathbf{H}_1^{(0)} + i\frac{\lambda-1}{\lambda}\gamma_L\mu_2\mathbf{H}_2^{(0)} = 0, \qquad (4.86)$$

which can be rewritten as $\nabla \times (\widetilde{P}_1\mathbf{E}_1^{(0)}) + i\gamma_L M_1\mathbf{H}_1^{(0)} = 0$ or $\nabla \times (\widetilde{P}_2\mathbf{E}_2^{(0)}) + i\gamma_L M_2\mathbf{H}_2^{(0)} = 0$,

where $\widetilde{P}_1$ and $\widetilde{P}_2$ are

$$\widetilde{P}_1 = \begin{bmatrix} 1 & 0 & 0 \\ 0 & 1 & 0 \\ 0 & 0 & \frac{1+(\lambda-1)\frac{\epsilon_1}{\epsilon_2}}{\lambda} \end{bmatrix}, \qquad \widetilde{P}_2 = \begin{bmatrix} 1 & 0 & 0 \\ 0 & 1 & 0 \\ 0 & 0 & \frac{\frac{\epsilon_2}{\epsilon_1}+(\lambda-1)}{\lambda} \end{bmatrix}. \qquad (4.87)$$

108

Similarly, taking the average over each region for the curl of the magnetic fields,

$$\frac{1}{\lambda}\nabla \times \mathbf{H}_1^{(0)} - i\frac{1}{\lambda}\gamma_L\epsilon_1\mathbf{E}_1^{(0)} = -\frac{1}{\lambda}\left(-H_{1y}^{(1)}\Big|_1 + H_{1y}^{(1)}\Big|_0 \quad , \quad H_{1x}^{(1)}\Big|_1 - H_{1x}^{(1)}\Big|_0 \quad , \quad 0\right),$$

(4.88)

$$\frac{\lambda-1}{\lambda}\nabla \times \mathbf{H}_2^{(0)} - i\frac{\lambda-1}{\lambda}\gamma_L\epsilon_2\mathbf{E}_2^{(0)} = -\frac{1}{\lambda}\left(-H_{2y}^{(1)}\Big|_\lambda + H_{2y}^{(1)}\Big|_1 \quad , \quad H_{2x}^{(1)}\Big|_\lambda - H_{2x}^{(1)}\Big|_1 \quad , \quad 0\right).$$

(4.89)

Adding equations together and applying boundary and periodic conditions,

$$\frac{1}{\lambda}\nabla \times \mathbf{H}_1^{(0)} + \frac{\lambda-1}{\lambda}\nabla \times \mathbf{H}_2^{(0)} - i\frac{1}{\lambda}\gamma_L\epsilon_1\mathbf{E}_1^{(0)} - i\frac{\lambda-1}{\lambda}\gamma_L\epsilon_2\mathbf{E}_2^{(0)} = 0, \quad (4.90)$$

which can be given by $\nabla \times (\widetilde{M_1}\mathbf{H}_1^{(0)}) - i\gamma_L P_1\mathbf{E}_1^{(0)} = 0$ or $\nabla \times (\widetilde{M_2}\mathbf{H}_2^{(0)}) - i\gamma_L P_2\mathbf{E}_2^{(0)} = 0$,

where the matrices are

$$\widetilde{M_1} = \begin{bmatrix} 1 & 0 & 0 \\ 0 & 1 & 0 \\ 0 & 0 & \frac{1+(\lambda-1)\frac{\mu_1}{\mu_2}}{\lambda} \end{bmatrix}, \qquad \widetilde{M_2} = \begin{bmatrix} 1 & 0 & 0 \\ 0 & 1 & 0 \\ 0 & 0 & \frac{\frac{\mu_2}{\mu_1}+(\lambda-1)}{\lambda} \end{bmatrix}. \quad (4.91)$$

The homogenized system of Maxwell's equation is given by

$$\nabla \cdot (P_1\mathbf{E}_1^{(0)}) = 0, \qquad \nabla \cdot (M_1\mathbf{H}_1^{(0)}) = 0, \quad (4.92)$$

$$\nabla \times (\widetilde{P_1}\mathbf{E}_1^{(0)}) + i\gamma_L M_1\mathbf{H}_1^{(0)} = 0, \qquad \nabla \times (\widetilde{M_1}\mathbf{H}_1^{(0)}) - i\gamma_L P_1\mathbf{E}_1^{(0)} = 0. \quad (4.93)$$

Next, we wish to decouple the electric and magnetic field by employing the curl-curl formulation. Applying matrices $\widetilde{M_1}M_1^{-1}$ and $\widetilde{P_1}P_1^{-1}$ to (4.93) respectively, yields

$$\widetilde{M_1}M_1^{-1}\nabla \times (\widetilde{P_1}\mathbf{E}_1^{(0)}) + i\gamma_L\widetilde{M_1}\mathbf{H}_1^{(0)} = 0, \tag{4.94}$$

$$\widetilde{P_1}P_{1e}^{-1}\nabla \times (\widetilde{M_1}\mathbf{H}_1^{(0)}) - i\gamma_L\widetilde{P_1}\mathbf{E}_1^{(0)} = 0. \tag{4.95}$$

We take the curl of each side to get

$$\nabla \times [\widetilde{M_1}M_1^{-1}\nabla \times (\widetilde{P_1}\mathbf{E}_1^{(0)})] + i\gamma_L\nabla \times (\widetilde{M_1}\mathbf{H}_1^{(0)}) = 0, \tag{4.96}$$

$$\nabla \times [\widetilde{P_1}P_{1e}^{-1}\nabla \times (\widetilde{M_1}\mathbf{H}_1^{(0)})] - i\gamma_L\nabla \times (\widetilde{P_1}\mathbf{E}_1^{(0)}) = 0, \tag{4.97}$$

and substituting (4.93) into (4.96) and (4.97), the equations decouple

$$\nabla \times [M^{-1}\nabla \times (\widetilde{P_1}\mathbf{E}_1^{(0)})] - \gamma_L^2 P_1\mathbf{E}_1^{(0)} = 0, \tag{4.98}$$

$$\nabla \times [P^{-1}\nabla \times (\widetilde{M_1}\mathbf{H}_1^{(0)})] - \gamma_L^2 M_1\mathbf{H}_1^{(0)} = 0, \tag{4.99}$$

where we have defined new matrices $M = M_1\widetilde{M_1}^{-1}$ and $P = P_1\widetilde{P_1}^{-1}$,

$$M = \begin{bmatrix} \mu_{ari} & 0 & 0 \\ 0 & \mu_{ari} & 0 \\ 0 & 0 & \mu_{har} \end{bmatrix}, \qquad \text{and} \qquad P = \begin{bmatrix} \epsilon_{ari} & 0 & 0 \\ 0 & \epsilon_{ari} & 0 \\ 0 & 0 & \epsilon_{har} \end{bmatrix}. \tag{4.100}$$

We can compare this result to the effective equations one would get from using standard mixing rules. The mixing rules determine that the effective parameters are given by $M$ and

$P$ [56], which result in Maxwell's equations of the form

$$\nabla \cdot (P\mathbf{E}) = 0, \qquad \nabla \cdot (M\mathbf{H}) = 0, \tag{4.101}$$

$$\nabla \times \mathbf{E} = -i\gamma_L M\mathbf{H}, \qquad \nabla \times \mathbf{H} = i\gamma_L P\mathbf{E}, \tag{4.102}$$

The curl-curl formulation can be written as

$$\nabla \times [M^{-1}\nabla \times \mathbf{E}] = \gamma_L^2 P\mathbf{E}, \qquad \nabla \times [P^{-1}\nabla \times \mathbf{H}] = \gamma_L^2 M\mathbf{H}. \tag{4.103}$$

The long-wave homogenization is only equivalent to the standard mixing formulas if the electromagnetic parameters are spatially invariant, which is not the case for temperature dependent dielectric loss. However, for dielectric heating in which the material is non-magnetic, $M \equiv I$, so the electric field equation reduces to

$$\nabla(\nabla \cdot \mathbf{E}) - \nabla^2\mathbf{E} = \gamma_L^2 P\mathbf{E}. \tag{4.104}$$

Furthermore, for the specific case of a plane wave at normal incidence to a laminated material with constant permittivity the homogenized equation is

$$-\frac{\partial^2 E}{\partial z^2} = \gamma_L^2 \epsilon_{ari} E, \tag{4.105}$$

which can be solve by applying the Transform Matrix Method. Mathematically, the long-wave homogenization is equivalent to an "effective medium" and behaves no differently than

(a)

(b)
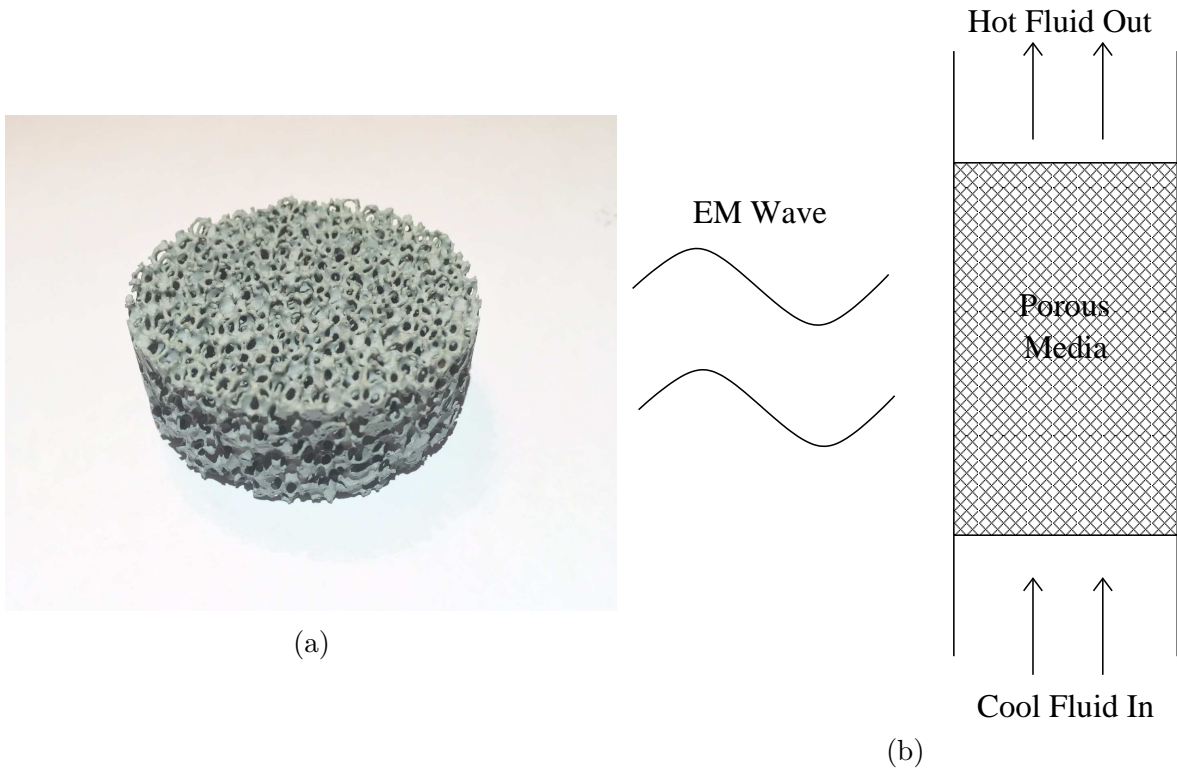
Figure 4.2: Silicon carbide foam (sample courtesy of Matt Porter) (a), diagram of a porous electromagnetic heat exchanger where the porous material heats up from attenuation of EM energy which transfers the energy to a fluid passing through the material (b).

a homogeneous medium. Instead, we now seek solutions for the case of high-frequency waves where the wavelengths are comparable to the microscale. The wave-geometry interactions mean it will not behave as an "effective medium" but requires a different homogenization approach.

## 4.3  High-Frequency Homogenization Model

In this Section, we extend the work of [82] to include dielectric loss on a three dimensional domain. The full three-dimensional HFH models the electric field problem associated with

112

the scenario in Figure 4.2. We consider a lossy material, such as silicon carbide, in a porous

structure to be placed in a fluid channel. The homogenization determines the electric field

solution to leading order which can then be coupled to the thermal problem to model a heat

exchanger. The wavelength is comparable to the microscale, which implies $\epsilon' = O(1)$, while

we assume the dielectric loss is small so that energy is absorbed on the macroscale, which

implies $\epsilon'' = O(\eta^2)$. A small dielectric loss is well validated for many dielectric materials as

is demonstrated by Figure 1.4, where even as high temperatures increase the dielectric loss

it is still less than one.

### 4.3.1 Three Dimensional Derivation

We begin by deriving the homogenization for a general electric field in three dimensions and

then consider the one dimensional laminate case as a specific example. According to the

curl-curl formulation of Maxwell's equations from Chapter 1, the electric field is governed

by the set of equations

$$\nabla' \cdot (\epsilon \mathbf{E}) = 0, \tag{4.106}$$

$$-\nabla'(\nabla' \cdot \mathbf{E}) + \nabla'^2 \mathbf{E} + \gamma^2 \epsilon \mathbf{E} = 0, \tag{4.107}$$

where $\mathbf{E}$ is the electric field vector, $\gamma^2$ is the non-dimensional wavenumber, and the complex

dielectric constant is $\epsilon = \epsilon' - i\eta^2 \epsilon''$. We expand the electric field and wave number in

asymptotic expansions $\mathbf{E} = \mathbf{E}^{(0)} + \eta \mathbf{E}^{(1)} + \eta^2 \mathbf{E}^{(2)} + \cdots$ and $\gamma^2 = \gamma_0^2 + \eta \gamma_1^2 + \eta^2 \gamma_2^2 + \cdots$, $\eta \ll 1$.

We also apply multiple scales so $\mathbf{x}' = \eta \mathbf{x}$ and $\mathbf{x}' = \boldsymbol{\zeta}$, where $\mathbf{x}$ is the macroscale and $\boldsymbol{\zeta}$ is the

microscale, thus derivatives become $\nabla' = \eta \nabla_x + \nabla_\zeta$ and $\nabla'^2 = \eta^2 \nabla_x^2 + \eta \left( \text{div}_x \nabla_\zeta + \text{div}_\zeta \nabla_x \right) +$

$\nabla_\zeta^2$. The domain is assumed be a periodic array of cells, where the domain of a single cell is taken to be $V = \{\zeta_1\widehat{e}_1| -1 \le \zeta \le 1\} \times \{\zeta_2\widehat{e}_2| -1 \le \zeta \le 1\} \times \{\zeta_3\widehat{e}_3| -1 \le \zeta \le 1\}$. The governing equations are then expanded to be

$$(\eta\nabla_x + \nabla_\zeta) \cdot \left[(\epsilon' - i\eta^2\epsilon'')(\mathbf{E}^{(0)} + \eta\mathbf{E}^{(1)} + \eta^2\mathbf{E}^{(2)} + \cdots)\right] = 0, \tag{4.108}$$

for the divergence equation, and

$$-(\eta\nabla_x + \nabla_\zeta)\left[(\eta\nabla_x + \nabla_\zeta) \cdot (\mathbf{E}^{(0)} + \eta\mathbf{E}^{(1)} + \eta^2\mathbf{E}^{(2)} + \cdots)\right]+$$

$$(\eta^2\nabla_x^2 + 2\eta\,\mathrm{div}_x\nabla_\zeta + \nabla_\zeta^2)(\mathbf{E}^{(0)} + \eta\mathbf{E}^{(1)} + \eta^2\mathbf{E}^{(2)} + \cdots)+$$

$$(\gamma_0^2 + \eta\gamma_1^2 + \eta^2\gamma_2^2 + \cdots)(\epsilon' - i\eta^2\epsilon'')(\mathbf{E}^{(0)} + \eta\mathbf{E}^{(1)} + \eta^2\mathbf{E}^{(2)} + \cdots) = 0, \tag{4.109}$$

for the curl-curl equation. The equations governing the leading order problem are

$$\nabla_\zeta \cdot (\epsilon'\mathbf{E}^{(0)}) = 0, \tag{4.110}$$

$$-\nabla_\zeta(\nabla_\zeta \cdot \mathbf{E}^{(0)}) + \nabla_\zeta^2\mathbf{E}^{(0)} + \gamma_0^2\epsilon'\mathbf{E}^{(0)} = 0. \tag{4.111}$$

We assume, as we have before, that $\epsilon'$ is constant within each phase of the material, which implies (4.110) reduces to

$$\nabla_\zeta \cdot \mathbf{E}^{(0)} = 0, \tag{4.112}$$

showing to leading order the electric field is divergence free on the microscale. Equation (4.112) then implies that (4.111) reduces to

$$\nabla_{\zeta}^2 \mathbf{E}^{(0)} + \gamma_0^2 \epsilon' \mathbf{E}^{(0)} = 0. \tag{4.113}$$

Floquet-Bloch theory yields a solution of the form

$$\mathbf{E}^{(0)} = f^{(0)}(\mathbf{x})\mathbf{U}^{(0)}(\boldsymbol{\zeta}, \gamma_0), \tag{4.114}$$

where $\mathbf{U}^{(0)}(\zeta, \gamma_0)$ is a periodic solution on the microscale and $f^{(0)}(\mathbf{x})$ is the dependence on the macroscale [82]. There is no reason to suggest that the macroscale response is isotropic with respect the homogenized medium, hence in general $f^{(0)}(\mathbf{x})$ is a second order tensor, for now, however, we assume it is a scalar.

The manner in which this homogenization procedure works is that we first solve for the leading order problem applying periodic or antiperiodic boundary conditions over the unit cell. Three dimensions and two possible boundary conditions yields $2^3$ base states to be solved at leading order. We find a set of discrete wavenumbers (eigenfrequencies) $\gamma_0$ for each of the base states. In general the leading order cell problem must be solved numerically which can then be applied in the homogenization solution. Figure 4.3 shows an example of how one would solve the cell problem for a three-dimensional porous media, taken from [103]. Figure 4.3a shows a $\mu CT$ scan of a metal foam which is used to develop the 3D periodic cell geometry in Figure 4.3b and can be used to solve the leading order problem

(a)

(b)
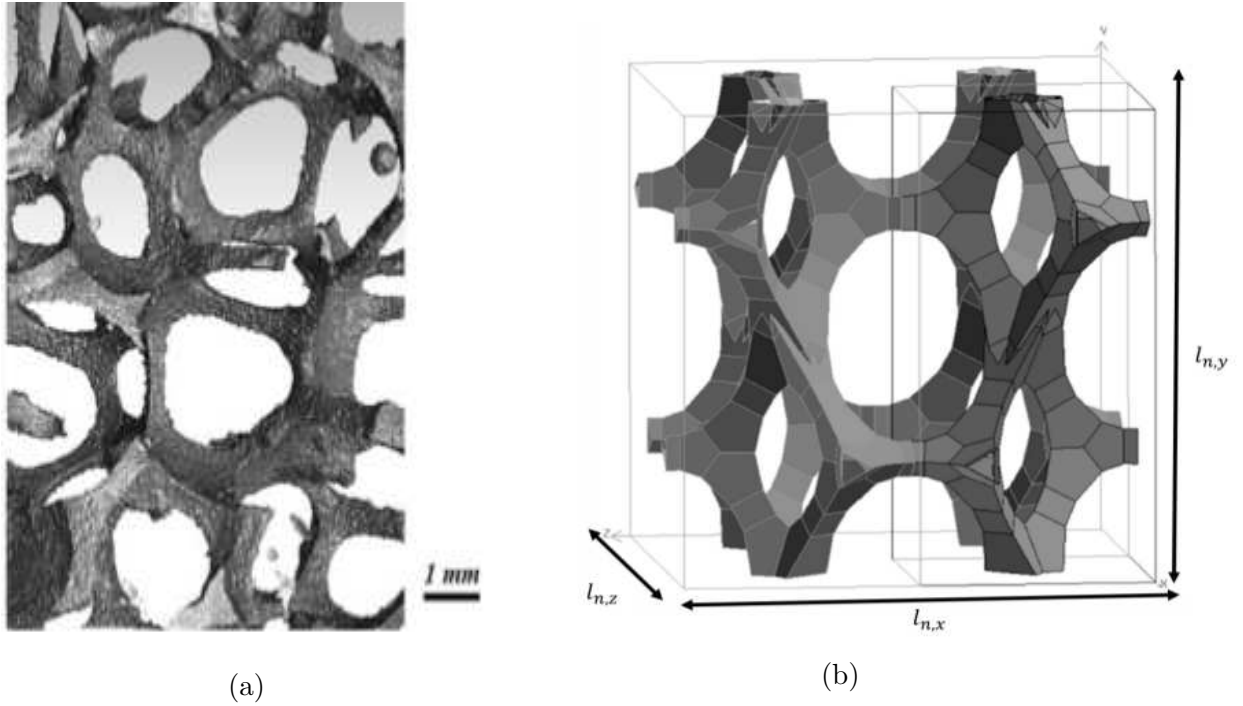
Figure 4.3: $\mu CT$ scan of a metal foam with 8.5 $\mu m$ voxel (3d pixel) size (a), periodic cell of a numerical geometry approximating the metal foam from $\mu CT$ scan (b).

numerically. Solutions that are neither periodic, nor antiperiodic are found by perturbing the solution away from the base states by finding the corrections to $\gamma_1$ and $\gamma_2$ for the lossy case. The macroscale dependence $f^{(0)}$ is determined in the classical homogenization technique of obtaining a compatibility condition by applying the Fredholm Alternative Theorem at each successive order until the system closes.

Prior to proceeding with the homogenization procedure we first note that the Helmholtz operator with periodic boundary conditions is self-adjoint, the proof is shown in Appendix A, which is required for the use of the Fredholm Alternative, presented by Theorem 3 also in Appendix A. We define the inner product

$$\langle \mathbf{u}, \mathbf{v} \rangle = \int_V \mathbf{u} \cdot \overline{\mathbf{v}} \, dV, \tag{4.115}$$

where $\overline{\mathbf{v}}$ is the complex conjugate of vector $\mathbf{v}$. An adjoint operator $L^*$ is defined such that $\langle L\mathbf{u}, \mathbf{v} \rangle = \langle \mathbf{u}, L^*\mathbf{v} \rangle$, and the operator $L$ is called self-adjoint provided $L^* = L$.

Next, we consider the first correction problem to proceed with the homogenization. As the Fredholm Alternative Theorem is used in the homogenization process, it is stated above without proof and describes an alternative condition for the existence of solutions to linear differential equations [97]. This alternative condition will determine the corrections

for $\gamma_1$ and $\gamma_2$. The equations for the first correction are

$$\nabla_x \cdot (\epsilon' \mathbf{E}^{(0)}) + \nabla_\zeta \cdot (\epsilon' \mathbf{E}^{(1)}) = 0, \tag{4.116}$$

$$-\nabla_x(\nabla_\zeta \cdot \mathbf{E}^{(0)}) - \nabla_\zeta(\nabla_x \cdot \mathbf{E}^{(0)}) - \nabla_\zeta(\nabla_\zeta \cdot \mathbf{E}^{(1)}) + 2\operatorname{div}(\nabla_\zeta \mathbf{E}^{(0)}) +$$

$$\nabla_\zeta^2 \mathbf{E}^{(1)} + \gamma_0^2 \epsilon' \mathbf{E}^{(1)} + \gamma_1^2 \epsilon' \mathbf{E}^{(0)} = 0. \tag{4.117}$$

Again, since $\epsilon'$, is constant the (4.116) yields

$$\nabla_\zeta \cdot \mathbf{E}^{(1)} = -\nabla_x \cdot \mathbf{E}^{(0)}. \tag{4.118}$$

Then, applying (4.112) and (4.118) to (4.117) it reduces to

$$\nabla_\zeta^2 \mathbf{E}^{(1)} + \gamma_0^2 \epsilon' \mathbf{E}^{(1)} = -2\nabla_x \cdot \left(\nabla_\zeta \mathbf{E}^{(0)}\right)^T - \gamma_1^2 \epsilon' \mathbf{E}^{(0)}. \tag{4.119}$$

Substituting in (4.114) the equation for the first correction is

$$\nabla_\zeta^2 \mathbf{E}^{(1)} + \gamma_0^2 \epsilon' \mathbf{E}^{(1)} = -2\nabla_x f^{(0)} \cdot \left(\nabla_\zeta \mathbf{U}^{(0)}\right)^T - f^{(0)} \gamma_1^2 \epsilon' \mathbf{U}^{(0)}. \tag{4.120}$$

Applying the Fredholm Alternative Theorem the compatibility condition is

$$-2\int_V \nabla_x f^{(0)} \cdot \left(\nabla_\zeta \mathbf{U}^{(0)}\right)^T \cdot \mathbf{U}^{(0)} \, dV - \gamma_1^2 f^{(0)} \epsilon' \int_V \mathbf{U}^{(0)} \cdot \mathbf{U}^{(0)} \, dV = 0. \tag{4.121}$$

We evaluate the first integral of (4.121). It first reduces to

$$-\int_V \nabla f^{(0)} \cdot (\nabla_\zeta \mathbf{U}^{(0)})^T \cdot \mathbf{U}^{(0)} \, dV = -\sum_{i=1}^{3} \int_V U_i^{(0)} \nabla_\zeta U_i^{(0)} \, dV \cdot \nabla f^{(0)}. \tag{4.122}$$

Next, applying identity (I.16),

$$-2\int_V \nabla_x f^{(0)} \cdot (\nabla_\zeta \mathbf{U}^{(0)})^T \cdot \mathbf{U}^{(0)} \, dV = -\sum_{i=1}^{3} \frac{1}{2} \left[ \int_{\partial V} (U_i^{(0)})^2 \mathbf{n} \, dS \right] \cdot \nabla f^{(0)}, \tag{4.123}$$

where the right hand side is zero from periodicity. This reduces the compatibility condition (4.121) to

$$\gamma_1^2 f^{(0)} \epsilon' \int_V |\mathbf{U}^{(0)}|^2 \, dV = 0, \tag{4.124}$$

which requires $\gamma_1^2 = 0$ since the integrand is strictly positive. Next, we determine the solution to the first correction problem. Substituting $\gamma_1 = 0$ in (4.120), the first correction problem becomes

$$\nabla_\zeta^2 \mathbf{E}^{(1)} + \gamma_0^1 \epsilon' \mathbf{E}^{(1)} = -2 \left[ \frac{\partial f^{(0)}}{\partial x_1}, \frac{\partial f^{(0)}}{\partial x_2}, \frac{\partial f^{(0)}}{\partial x_3} \right] \begin{bmatrix} \frac{\partial U_1^{(0)}}{\partial \zeta_1} & \frac{\partial U_2^{(0)}}{\partial \zeta_1} & \frac{\partial U_3^{(0)}}{\partial \zeta_1} \\ \frac{\partial U_1^{(0)}}{\partial \zeta_2} & \frac{\partial U_2^{(0)}}{\partial \zeta_2} & \frac{\partial U_3^{(0)}}{\partial \zeta_2} \\ \frac{\partial U_1^{(0)}}{\partial \zeta_3} & \frac{\partial U_2^{(0)}}{\partial \zeta_3} & \frac{\partial U_3^{(0)}}{\partial \zeta_3} \end{bmatrix}, \tag{4.125}$$

119

which equals

$$\nabla_\zeta^2 \mathbf{E}^{(1)} + \gamma_0^1 \epsilon' \mathbf{E}^{(1)} = -2 \left[ \frac{\partial f^{(0)}}{\partial x_1} \frac{\partial U_1^{(0)}}{\partial \zeta_1} + \frac{\partial f^{(0)}}{\partial x_2} \frac{\partial U_1^{(0)}}{\partial \zeta_2} + \frac{\partial f^{(0)}}{\partial x_3} \frac{\partial U_1^{(0)}}{\partial \zeta_3} \, , \right.$$
$$\frac{\partial f^{(0)}}{\partial x_1} \frac{\partial U_2^{(0)}}{\partial \zeta_1} + \frac{\partial f^{(0)}}{\partial x_2} \frac{\partial U_2^{(0)}}{\partial \zeta_2} + \frac{\partial f^{(0)}}{\partial x_3} \frac{\partial U_2^{(0)}}{\partial \zeta_3} \, ,$$
$$\left. \frac{\partial f^{(0)}}{\partial x_1} \frac{\partial U_3^{(0)}}{\partial \zeta_1} + \frac{\partial f^{(0)}}{\partial x_2} \frac{\partial U_3^{(0)}}{\partial \zeta_2} + \frac{\partial f^{(0)}}{\partial x_3} \frac{\partial U_3^{(0)}}{\partial \zeta_3} \right] , \qquad (4.126)$$

and can be rewritten as

$$\nabla_\zeta^2 \mathbf{E}^{(1)} + \gamma_0^1 \epsilon' \mathbf{E}^{(1)} = -2 \left[ \nabla_x f^{(0)} \cdot \nabla_\zeta U_1^{(0)} \, , \, \nabla_x f^{(0)} \cdot \nabla_\zeta U_2^{(0)} \, , \, \nabla_x f^{(0)} \cdot \nabla_\zeta U_3^{(0)} \right] . \qquad (4.127)$$

Each component of the first correction $\mathbf{E}^{(1)}$ is given by

$$E_i^{(1)} = f^{(1)} U_i^{(0)} + \nabla_x f^{(0)} \cdot \left[ \mathbf{V}_i - \boldsymbol{\zeta} U_i^{(0)} \right] , \qquad (4.128)$$

which includes a homogeneous solution and a particular solution. The vector valued solution can be written as

$$\mathbf{E}^{(1)} = f^{(1)} \mathbf{U}^{(0)} + \nabla_x f^{(0)} \cdot \left[ \underline{\underline{V}}^T - \boldsymbol{\zeta} \mathbf{U}^{(0)T} \right] , \qquad (4.129)$$

where $\mathbf{V}_i(\boldsymbol{\zeta})$ is row vector $i$ of the tensor $\underline{\underline{V}}(\boldsymbol{\zeta})$. Here, $\mathbf{V}_i(\boldsymbol{\zeta})$ are non-triple periodic solutions of the homogeneous equation. Since we require that $\mathbf{E}^{(1)}$ is periodic, it implies that $v_{ij} - \zeta_j U_i^{(0)}$ is periodic in each variable $\zeta_k$, $\forall i, j = 1, 2, 3$. When $k \neq j$, we only require $v_{ij}$ to be periodic

120

in $\zeta_k$ to satisfy periodicity. When $k = j$, the periodicity condition

$$\left( v_{ik} - \zeta_k U_i^{(0)} \right)\Big|_{\zeta_k=1} = \left( v_{ik} - \zeta_k U_i^{(0)} \right)\Big|_{\zeta_k=-1}, \tag{4.130}$$

implies that

$$v_{ik}\big|_{\zeta_k=1} - v_{ik}\big|_{\zeta_k=-1} = U_i^{(0)}\Big|_{\zeta_k=1} + (\lambda - 1)\, U_i^{(0)}\Big|_{\zeta_k=-1}, \tag{4.131}$$

and applying periodicity on $U_i^{(0)}$, the condition to guarantee periodicity becomes

$$v_{ik}\big|_{\zeta_k=1} - v_{ik}\big|_{\zeta_k=-1} = \lambda\, U_i^{(0)}\Big|_{\zeta_k=1}. \tag{4.132}$$

Therefore, to summarize, the row vectors of $\underline{\underline{V}}$ are solutions of the homogeneous problem that satisfy the following conditions for the periodicity of entries $v_{ij}$

| Periodic in $\zeta_1$ | $v_{12}$ | $v_{13}$ | $v_{22}$ | $v_{23}$ | $v_{32}$ | $v_{33}$ |
|---|---|---|---|---|---|---|
| Periodic in $\zeta_2$ | $v_{11}$ | $v_{13}$ | $v_{21}$ | $v_{23}$ | $v_{31}$ | $v_{33}$ |
| Periodic in $\zeta_3$ | $v_{11}$ | $v_{12}$ | $v_{21}$ | $v_{22}$ | $v_{31}$ | $v_{32}$ |

and jump conditions

$$v_{11}\big|_{\zeta_1=1} - v_{11}\big|_{\zeta_1=-1} = \lambda\, U_1^{(0)}\Big|_{\zeta_1=1}, \tag{4.133}$$

$$v_{12}\big|_{\zeta_2=1} - v_{12}\big|_{\zeta_2=-1} = \lambda\, U_1^{(0)}\Big|_{\zeta_2=1}, \tag{4.134}$$

$$v_{13}\big|_{\zeta_3=1} - v_{13}\big|_{\zeta_3=-1} = \lambda\, U_1^{(0)}\Big|_{\zeta_3=1}, \tag{4.135}$$

121

$$v_{21}\big|_{\zeta_1=1} - v_{21}\big|_{\zeta_1=-1} = \lambda\, U_2^{(0)}\Big|_{\zeta_1=1}, \tag{4.136}$$

$$v_{22}\big|_{\zeta_2=1} - v_{22}\big|_{\zeta_2=-1} = \lambda\, U_2^{(0)}\Big|_{\zeta_2=1}, \tag{4.137}$$

$$v_{23}\big|_{\zeta_3=1} - v_{23}\big|_{\zeta_3=-1} = \lambda\, U_2^{(0)}\Big|_{\zeta_3=1}, \tag{4.138}$$

$$v_{31}\big|_{\zeta_1=1} - v_{31}\big|_{\zeta_1=-1} = \lambda\, U_3^{(0)}\Big|_{\zeta_1=1}, \tag{4.139}$$

$$v_{32}\big|_{\zeta_2=1} - v_{32}\big|_{\zeta_2=-1} = \lambda\, U_3^{(0)}\Big|_{\zeta_2=1}, \tag{4.140}$$

$$v_{33}\big|_{\zeta_3=1} - v_{33}\big|_{\zeta_3=-1} = \lambda\, U_3^{(0)}\Big|_{\zeta_3=1}. \tag{4.141}$$

We also require that $\frac{\partial \mathbf{E}^{(1)}}{\partial \zeta_k}$ is periodic in $\zeta_k$. We have that

$$\frac{\partial}{\partial \zeta_k}\left(v_{ij} - \zeta_j U_i^{(0)}\right) = \begin{cases} \frac{\partial v_{ij}}{\partial \zeta_k} - \zeta_j \frac{\partial U^{(0)}}{\partial \zeta_k}, & k \neq j, \\[2mm] \frac{\partial v_{ik}}{\partial \zeta_k} - U_i^{(0)} - \zeta_k \frac{\partial U^{(0)}}{\partial \zeta_k}, & k = j, \end{cases} \tag{4.142}$$

and require periodicity in $\zeta_k$. This implies that $\frac{\partial v_{ij}}{\partial \zeta_k}$ is periodic in $\zeta_k$ for $k \neq j$ and for $k = j$

periodicity

$$\left(\frac{\partial v_{ik}}{\partial \zeta_k} - U_i^{(0)} - \zeta_k \frac{\partial U_i^{(0)}}{\partial \zeta_k}\right)\Bigg|_{\zeta_k=1} = \left(\frac{\partial v_{ik}}{\partial \zeta_k} - U_i^{(0)} - \zeta_k \frac{\partial U_i^{(0)}}{\partial \zeta_k}\right)\Bigg|_{\zeta_k=-1} \tag{4.143}$$

requires that

$$\frac{\partial v_{ik}}{\partial \zeta_k}\Bigg|_{\zeta_k=1} - \frac{\partial v_{ik}}{\partial \zeta_k}\Bigg|_{\zeta_k=-1} = \lambda \frac{\partial U_i^{(0)}}{\partial \zeta_k}\Bigg|_{\zeta_k=1}. \tag{4.144}$$

To summarize, we require the following conditions on $\underline{\underline{V}}$ for periodicity

| Periodic in $\zeta_1$ | $\frac{\partial v_{12}}{\partial \zeta_1}$ | $\frac{\partial v_{13}}{\partial \zeta_1}$ | $\frac{\partial v_{22}}{\partial \zeta_1}$ | $\frac{\partial v_{23}}{\partial \zeta_1}$ | $\frac{\partial v_{32}}{\partial \zeta_1}$ | $\frac{\partial v_{33}}{\partial \zeta_1}$, |
|---|---|---|---|---|---|---|
| Periodic in $\zeta_2$ | $\frac{\partial v_{11}}{\partial \zeta_2}$ | $\frac{\partial v_{13}}{\partial \zeta_2}$ | $\frac{\partial v_{21}}{\partial \zeta_2}$ | $\frac{\partial v_{23}}{\partial \zeta_2}$ | $\frac{\partial v_{31}}{\partial \zeta_2}$ | $\frac{\partial v_{33}}{\partial \zeta_2}$, |
| Periodic in $\zeta_3$ | $\frac{\partial v_{11}}{\partial \zeta_3}$ | $\frac{\partial v_{12}}{\partial \zeta_3}$ | $\frac{\partial v_{21}}{\partial \zeta_3}$ | $\frac{\partial v_{22}}{\partial \zeta_3}$ | $\frac{\partial v_{31}}{\partial \zeta_3}$ | $\frac{\partial v_{32}}{\partial \zeta_3}$, |

and jump conditions

$$\left.\frac{\partial v_{11}}{\partial \zeta_1}\right|_{\zeta_1=1} - \left.\frac{\partial v_{11}}{\partial \zeta_1}\right|_{\zeta_1=-1} = \lambda \left.\frac{\partial U_1^{(0)}}{\partial \zeta_1}\right|_{\zeta_1=1}, \tag{4.145}$$

$$\left.\frac{\partial v_{12}}{\partial \zeta_2}\right|_{\zeta_2=1} - \left.\frac{\partial v_{12}}{\partial \zeta_2}\right|_{\zeta_2=-1} = \lambda \left.\frac{\partial U_1^{(0)}}{\partial \zeta_2}\right|_{\zeta_2=1}, \tag{4.146}$$

$$\left.\frac{\partial v_{13}}{\partial \zeta_3}\right|_{\zeta_3=1} - \left.\frac{\partial v_{13}}{\partial \zeta_3}\right|_{\zeta_3=-1} = \lambda \left.\frac{\partial U_1^{(0)}}{\partial \zeta_3}\right|_{\zeta_3=1}, \tag{4.147}$$

$$\left.\frac{\partial v_{21}}{\partial \zeta_1}\right|_{\zeta_1=1} - \left.\frac{\partial v_{21}}{\partial \zeta_1}\right|_{\zeta_1=-1} = \lambda \left.\frac{\partial U_2^{(0)}}{\partial \zeta_1}\right|_{\zeta_1=1}, \tag{4.148}$$

$$\left.\frac{\partial v_{22}}{\partial \zeta_2}\right|_{\zeta_2=1} - \left.\frac{\partial v_{22}}{\partial \zeta_2}\right|_{\zeta_2=-1} = \lambda \left.\frac{\partial U_2^{(0)}}{\partial \zeta_2}\right|_{\zeta_2=1}, \tag{4.149}$$

$$\left.\frac{\partial v_{23}}{\partial \zeta_3}\right|_{\zeta_3=1} - \left.\frac{\partial v_{23}}{\partial \zeta_3}\right|_{\zeta_3=-1} = \lambda \left.\frac{\partial U_2^{(0)}}{\partial \zeta_3}\right|_{\zeta_3=1}, \tag{4.150}$$

$$\left.\frac{\partial v_{31}}{\partial \zeta_1}\right|_{\zeta_1=1} - \left.\frac{\partial v_{31}}{\partial \zeta_1}\right|_{\zeta_1=-1} = \lambda \left.\frac{\partial U_3^{(0)}}{\partial \zeta_1}\right|_{\zeta_1=1}, \tag{4.151}$$

$$\left.\frac{\partial v_{32}}{\partial \zeta_2}\right|_{\zeta_2=1} - \left.\frac{\partial v_{32}}{\partial \zeta_2}\right|_{\zeta_2=-1} = \lambda \left.\frac{\partial U_3^{(0)}}{\partial \zeta_2}\right|_{\zeta_2=1}, \tag{4.152}$$

$$\left.\frac{\partial v_{33}}{\partial \zeta_3}\right|_{\zeta_3=1} - \left.\frac{\partial v_{33}}{\partial \zeta_3}\right|_{\zeta_3=-1} = \lambda \left.\frac{\partial U_3^{(0)}}{\partial \zeta_3}\right|_{\zeta_3=1}. \tag{4.153}$$

Next, we proceed to the second-order correction. The equations for the second correction are given by

$$\nabla_x \cdot (\epsilon' \mathbf{E}^{(1)}) + \nabla_\zeta \cdot (\epsilon' \mathbf{E}^{(2)}) - i\nabla_\zeta \cdot (\epsilon'' \mathbf{E}^{(0)}) = 0, \tag{4.154}$$

$$-\nabla_x(\nabla_x \cdot \mathbf{E}^{(0)}) - \nabla_x(\nabla_\zeta \cdot \mathbf{E}^{(1)}) - \nabla_\zeta(\nabla_x \cdot \mathbf{E}^{(1)}) - \nabla_\zeta(\nabla_\zeta \cdot \mathbf{E}^{(2)}) + \nabla_x^2 \mathbf{E}^{(0)} + \tag{4.155}$$

$$2\operatorname{div}_x(\nabla_\zeta \mathbf{E}^{(1)}) + \nabla_\zeta^2 \mathbf{E}^{(2)} + \gamma_0^2 \epsilon' \mathbf{E}^{(2)} - \gamma_0^2 i\epsilon'' \mathbf{E}^{(0)} + \gamma_1^2 \epsilon' \mathbf{E}^{(1)} + \gamma_2^2 \epsilon' \mathbf{E}^{(0)} = 0. \tag{4.156}$$

Since $\epsilon'$ is constant and $\epsilon''$ is spatially dependent on the microscale variables $\boldsymbol{\zeta}$, (4.154) becomes

$$\epsilon' \nabla_x \cdot \mathbf{E}^{(1)} + \epsilon' \nabla_\zeta \cdot \mathbf{E}^{(2)} - i\nabla_\zeta \epsilon'' \cdot \mathbf{E}^{(0)} - i\epsilon'' \nabla_\zeta \cdot \mathbf{E}^{(0)} = 0, \tag{4.157}$$

and applying (4.112), it reduces to

$$\nabla_\zeta \cdot \mathbf{E}^{(2)} = -\nabla_x \cdot \mathbf{E}^{(1)} + \frac{i}{\epsilon'} \nabla_\zeta \epsilon'' \cdot \mathbf{E}^{(0)}. \tag{4.158}$$

124

Applying (4.118), (4.158), and since $\gamma_1^2 = 0$, (4.156) reduces to

$$\nabla_\zeta^2 \mathbf{E}^{(2)} + \gamma_0^2 \epsilon' \mathbf{E}^{(2)} = -2\nabla_x \cdot \left(\nabla_\zeta \mathbf{E}^{(1)}\right)^T + \nabla_\zeta \left(\frac{i}{\epsilon'} \nabla_\zeta \epsilon'' \cdot \mathbf{E}^{(0)}\right) - \nabla_x^2 \mathbf{E}^{(0)}$$

$$+ \gamma_0^2 i \epsilon'' \mathbf{E}^{(0)} - \gamma_2^2 \epsilon' \mathbf{E}^{(0)}. \tag{4.159}$$

Substituting (4.114), the equation becomes

$$\nabla_\zeta^2 \mathbf{E}^{(2)} + \gamma_0^2 \epsilon' \mathbf{E}^{(2)} = -2\nabla_x \cdot \left(\nabla_\zeta \mathbf{E}^{(1)}\right)^T + f^{(0)} \nabla_\zeta \left(\frac{i}{\epsilon'} \nabla_\zeta \epsilon'' \cdot \mathbf{U}^{(0)}\right) - \nabla_x^2 f^{(0)} \mathbf{U}^{(0)}$$

$$+ f^{(0)} \gamma_0^2 i \epsilon'' \mathbf{U}^{(0)} - f^{(0)} \gamma_2^2 \epsilon' \mathbf{U}^{(0)}. \tag{4.160}$$

Next, we find the compatibility condition by applying the Fredholm Alternative Theorem, which results in a differential equation for $f^{(0)}$,

$$2\int_V \nabla_x \cdot \left(\nabla_\zeta \mathbf{E}^{(1)}\right)^T \cdot \mathbf{U}^{(0)} \, dV - f^{(0)} \int_V \nabla_\zeta \left(\frac{i}{\epsilon'} \nabla_\zeta \epsilon'' \cdot \mathbf{U}^{(0)}\right) \cdot \mathbf{U}^{(0)} \, dV +$$

$$\nabla_x^2 f^{(0)} \int_V \mathbf{U}^{(0)} \cdot \mathbf{U}^{(0)} \, dV - f^{(0)} i \gamma_0^2 \int_V \epsilon'' \mathbf{U}^{(0)} \cdot \mathbf{U}^{(0)} \, dV + f^{(0)} \gamma_2^2 \int_V \epsilon' \mathbf{U}^{(0)} \cdot \mathbf{U}^{(0)} \, dV = 0. \tag{4.161}$$

We simplify the compatibility condition by reducing some of the integrals. Applying identity (I.13) to the second term of (4.161) we have that

$$\int_V \nabla_\zeta \left(\frac{i}{\epsilon'} \nabla_\zeta \epsilon'' \cdot \mathbf{U}^{(0)}\right) \cdot \mathbf{U}^{(0)} \, dV = \int_{\partial V} \frac{i}{\epsilon'} \left(\nabla_\zeta \epsilon'' \cdot \mathbf{U}^{(0)}\right) \left(\mathbf{U}^{(0)} \cdot \mathbf{n}\right) \, dS$$

$$- \int_V \frac{i}{\epsilon'} \left(\nabla_\zeta \epsilon'' \cdot \mathbf{U}^{(0)}\right) \left(\nabla_\zeta \cdot \mathbf{U}^{(0)}\right) \, dV, \tag{4.162}$$

125

and applying (4.112) this volume integral equals a surface integral,

$$\int_V \nabla_\zeta \left( \frac{i}{\epsilon'} \nabla_\zeta \epsilon'' \cdot \mathbf{U}^{(0)} \right) \cdot \mathbf{U}^{(0)} \, dV = \int_{\partial V} \frac{i}{\epsilon'} \left( \nabla_\zeta \epsilon'' \cdot \mathbf{U}^{(0)} \right) \left( \mathbf{U}^{(0)} \cdot \mathbf{n} \right) \, dS. \tag{4.163}$$

Next, we determine the first integral of (4.161) by substituting in the first correction solution.

Using index notation, (4.129) is

$$E_i^{(1)} = f^{(0)} U_i^{(0)} + \frac{\partial f^{(0)}}{\partial x_k} \left[ v_{ik} - \zeta_k U_i^{(0)} \right], \tag{4.164}$$

where the gradient is then given by

$$\left( \nabla_\zeta \mathbf{E}^{(1)} \right)_{ij} = \frac{\partial E_i^{(1)}}{\partial \zeta_j} = f^{(0)} \frac{\partial U_i^{(0)}}{\partial \zeta_j} + \frac{\partial f^{(0)}}{\partial x_k} \left[ \frac{\partial v_{ik}}{\partial \zeta_j} - \frac{\partial}{\partial \zeta_j} \left( \zeta_k U_i^{(0)} \right) \right], \tag{4.165}$$

which equals

$$\left( \nabla_\zeta \mathbf{E}^{(1)} \right)_{ij} = f^{(0)} \frac{\partial U_i^{(0)}}{\partial \zeta_j} + \frac{\partial f^{(0)}}{\partial x_k} \left[ \frac{\partial v_{ik}}{\partial \zeta_j} - \delta_{jk} U_i^{(0)} - \zeta_k \frac{\partial U_i^{(0)}}{\partial \zeta_j} \right]. \tag{4.166}$$

Taking the transpose switches, the indices

$$\left( \nabla_\zeta \mathbf{E}^{(1)} \right)_{ij}^T = \left( \nabla_\zeta \mathbf{E}^{(1)} \right)_{ji} = f^{(0)} \frac{\partial U_j^{(0)}}{\partial \zeta_i} + \frac{\partial f^{(0)}}{\partial x_k} \left[ \frac{\partial v_{jk}}{\partial \zeta_i} - \delta_{ik} U_j^{(0)} - \zeta_k \frac{\partial U_j^{(0)}}{\partial \zeta_i} \right]. \tag{4.167}$$

Since $(\nabla_x \cdot \underline{\underline{A}})_i = \frac{\partial}{\partial x_j} a_{ji}$, where $a_{ij}$ are the entries of tensor $\underline{\underline{A}}$, we have that

$$\left[ \nabla_x \cdot \left( \nabla_\zeta \mathbf{E}^{(1)} \right)^T \right]_i = \frac{\partial}{\partial x_j} \left( \nabla_\zeta \mathbf{E}^{(1)} \right)^T_{ji} = \frac{\partial}{\partial x_j} \left( \nabla_\zeta \mathbf{E}^{(1)} \right)_{ij}$$
$$= \frac{\partial f^{(0)}}{\partial x_j} \frac{\partial U_i^{(0)}}{\partial \zeta_j} + \frac{\partial^2 f^{(0)}}{\partial x_j \partial x_k} \left[ \frac{\partial v_{ik}}{\partial \zeta_j} - \delta_{jk} U_i^{(0)} - \zeta_k \frac{\partial U_i^{(0)}}{\partial \zeta_j} \right], \qquad (4.168)$$

hence

$$\nabla_x \cdot \left( \nabla_\zeta \mathbf{E}^{(1)} \right)^T \cdot \mathbf{U} = U_i^{(0)} \frac{\partial f^{(0)}}{\partial x_j} \frac{\partial U_i^{(0)}}{\partial \zeta_j} + U_i^{(0)} \frac{\partial^2 f^{(0)}}{\partial x_j \partial x_k} \left[ \frac{\partial v_{ik}}{\partial \zeta_j} - \delta_{jk} U_i^{(0)} - \zeta_k \frac{\partial U_i^{(0)}}{\partial \zeta_j} \right]. \quad (4.169)$$

Therefore, the integral in index notation is given by

$$2 \int_V \nabla_x \cdot \left( \nabla_\zeta \mathbf{E}^{(0)} \right)^T \cdot \mathbf{U}^{(0)} \, dV = 2 \frac{\partial f^{(0)}}{\partial x_j} \int_V \frac{\partial U_i^{(0)}}{\partial \zeta_j} U_i^{(0)} \, dV$$
$$+ 2 \frac{\partial^2 f^{(0)}}{\partial x_j \partial x_k} \int_V \left[ \frac{\partial v_{ik}}{\partial \zeta_j} U_i^{(0)} - \delta_{jk} U_i^{(0)2} - \zeta_k \frac{\partial U_i^{(0)}}{\partial \zeta_j} U_i^{(0)} \right] \, dV.$$
$$(4.170)$$

This is the expression defining the first integral of the compatibility condition (4.161). Now, the first integral of (4.170) is evaluated as

$$\frac{\partial f^{(0)}}{\partial x_j} \int_V \frac{\partial U_i^{(0)}}{\partial \zeta_j} U_i^{(0)} \, dV = \nabla_x \cdot \int_V \nabla_\zeta U_i^{(0)} U_i^{(0)} \, dV = \nabla_x f^{(0)} \cdot \frac{1}{2} \int_{\partial V} U_i^{(0)2} \mathbf{n} \, dS = 0, \quad (4.171)$$

by (I.16) and periodicity of $\mathbf{U}^{(0)}$. The compatibility condition can finally be written down

127

as

$$2\frac{\partial^2 f^{(0)}}{\partial x_j \partial x_k} \int_V \left[ \frac{\partial v_{ik}}{\partial \zeta_j} U_i^{(0)} - \delta_{jk} U_i^{(0)2} - \zeta_k \frac{\partial U_i^{(0)}}{\partial \zeta_j} U_i^{(0)} \right] dV + \frac{\partial^2 f^{(0)}}{\partial x_j^2} \int_V |\mathbf{U}^{(0)}|^2 \, dV$$

$$+ f^{(0)} \left[ -\int_{\partial V} \frac{i}{\epsilon'} \left( \nabla_\zeta \epsilon'' \cdot \mathbf{U}^{(0)} \right) \left( \mathbf{U}^{(0)} \cdot \mathbf{n} \right) \, dS + i\gamma_0^2 \int_V \epsilon'' |\mathbf{U}^{(0)}|^2 \, dV + \gamma_2^2 \int_V \epsilon' |\mathbf{U}^{(0)}|^2 \, dV \right] = 0,$$

$$(4.172)$$

which defines the differential equation for $f^{(0)}\mathbf{x}$,

$$\nabla_x \cdot \left[ \underline{T} \nabla_x f^{(0)} \right] + \left[ \gamma_2^2 + iD \right] f^{(0)} = 0, \tag{4.173}$$

where

$$D = \frac{-\int_{\partial V} \frac{1}{\epsilon'} \left( \nabla_\zeta \epsilon'' \cdot \mathbf{U}^{(0)} \right) \left( \mathbf{U}^{(0)} \cdot \mathbf{n} \right) \, dS + \gamma_0^2 \int_V \epsilon'' |\mathbf{U}^{(0)}|^2 \, dV}{\int_V \epsilon' |\mathbf{U}^{(0)}|^2 \, dV}, \tag{4.174}$$

and

$$T_{jk} = \frac{t_{jk}}{\int_V \epsilon' |\mathbf{U}^{(0)}|^2 \, dV}. \tag{4.175}$$

We wish to make this tensor symmetric. Fixing $j \neq k$ we consider the sum of the two mixed derivatives present in the differential equation

$$2\frac{\partial^2 f^{(0)}}{\partial x_j \partial x_k} \int_V \left[ \frac{\partial v_{ik}}{\partial \zeta_j} U_i^{(0)} - \zeta_k \frac{\partial U_i^{(0)}}{\partial \zeta_j} U_i^{(0)} \right] dV + 2\frac{\partial^2 f^{(0)}}{\partial x_k \partial x_j} \int_V \left[ \frac{\partial v_{ij}}{\partial \zeta_k} U_i^{(0)} - \zeta_j \frac{\partial U_i^{(0)}}{\partial \zeta_k} U_i^{(0)} \right] dV.$$

$$(4.176)$$

128

Since $\frac{\partial^2 f^{(0)}}{\partial x_j \partial x_k} = \frac{\partial^2 f^{(0)}}{\partial x_k \partial x_j}$, they combine to make one coefficient

$$2\frac{\partial^2 f^{(0)}}{\partial x_j \partial x_k}\int_V \left[ \frac{\partial v_{ik}}{\partial \zeta_j}U_i^{(0)} + \frac{\partial v_{ij}}{\partial \zeta_k}U_i^{(0)} - \zeta_k \frac{\partial U_i^{(0)}}{\partial \zeta_j}U_i^{(0)} - \zeta_j \frac{\partial U_i^{(0)}}{\partial \zeta_k}U_i^{(0)} \right] dV. \qquad (4.177)$$

However, since we want the tensor to be symmetric, we apply half of this coefficient to both symmetric derivatives so that

$$t_{jk} = \int_V \left[ \frac{\partial v_{ik}}{\partial \zeta_j}U_i^{(0)} + \frac{\partial v_{ij}}{\partial \zeta_k}U_i^{(0)} - \zeta_k \frac{\partial U_i^{(0)}}{\partial \zeta_j}U_i^{(0)} - \zeta_j \frac{\partial U_i^{(0)}}{\partial \zeta_k}U_i^{(0)} \right] dV. \qquad (4.178)$$

We can also write down the diagonal elements which are given by

$$t_{kk} = 2\int_V \left[ \frac{\partial v_{ik}}{\partial \zeta_k}U_i^{(0)} - U_i^{(0)\,2} - \zeta_k \frac{\partial U_i^{(0)}}{\partial \zeta_k}U_i^{(0)} \right] dV + \int_V |\mathbf{U}^{(0)}|^2 \, dV, \qquad (4.179)$$

and can be rewritten as

$$t_{kk} = 2\int_V \left[ \frac{\partial v_{ik}}{\partial \zeta_k}U_i^{(0)} - \zeta_k \frac{\partial U_i^{(0)}}{\partial \zeta_k}U_i^{(0)} \right] dV - \int_V U_i^{(0)\,2} \, dV. \qquad (4.180)$$

The symmetric entries can be reduced further. Let $S_k$ be the domain such that $S_1 = \{\zeta_2\widehat{e}_2|-1 \le \zeta_2 \le 1\} \times \{\zeta_3\widehat{e}_3|-1 \le \zeta_3 \le 1\}$, $S_2 = \{\zeta_1\widehat{e}_1|-1 \le \zeta_1 \le 1\} \times \{\zeta_3\widehat{e}_3|-1 \le \zeta_3 \le 1\}$, and $S_3 = \{\zeta_1\widehat{e}_1|-1 \le \zeta_1 \le 1\} \times \{\zeta_2\widehat{e}_2|-1 \le \zeta_2 \le 1\}$. Then the integral from the diagonal

entries is

$$\int_V \zeta_k \frac{\partial U_i^{(0)}}{\partial x_k} U_i^{(0)} \, dV = \int_{S_k} \int_{-1}^{1} \zeta_k \frac{\partial U_i^{(0)}}{\partial \zeta_k} U_i^{(0)} \, d\zeta_k \, dS_k = \int_{S_k} \int_{-1}^{1} \zeta_k \frac{1}{2} \frac{\partial}{\partial \zeta_k} \left( U_i^{(0)} \right)^2 d\zeta_k \, dS_k$$

$$(4.181)$$

Applying integration by parts, it becomes

$$\int_V \zeta_k \frac{\partial U_i^{(0)}}{\partial x_k} U_i^{(0)} \, dV = \frac{1}{2} \int_{S_k} \zeta_k U_i^{(0)\,2} \bigg|_{\zeta_k=-1}^{\zeta_k=1} dS_k - \frac{1}{2} \int_V U_i^{(0)\,2} \, dV, \qquad (4.182)$$

which evaluates to be

$$\int_V \zeta_k \frac{\partial U_i^{(0)}}{\partial x_k} U_i^{(0)} \, dV = \int_{S_k} U_i^{(0)\,2} \bigg|_{\zeta_k=1} dS_k - \frac{1}{2} \int_V U_i^{(0)\,2} \, dV \qquad (4.183)$$

by periodicity. Therefore, the symmetric components are given by

$$t_{kk} = 2 \int_V \frac{\partial v_{ik}}{\partial \zeta_k} U_i^{(0)} \, dV - 2 \int_{S_k} U_i^{(0)\,2} \bigg|_{\zeta_k=1} dS_k. \qquad (4.184)$$

Similarly, we can simplify the off diagonal elements, since

$$-2 \int_V \zeta_l \frac{\partial U_i^{(0)}}{\partial \zeta_j} U_i^{(0)} \, dV = - \int_{S_j} \int_{-1}^{1} \zeta_k \frac{\partial}{\partial \zeta_j} U_i^{(0)\,2} \, d\zeta_j \, dS_j = - \int_{S_j} \zeta_k U_i^{(0)\,2} \bigg|_{\zeta_j=-1}^{\zeta_j=1} dS_j = 0,$$

$$(4.185)$$

130

by periodicity of $U_i^{(0)}$ in $\zeta_j$. Therefore, the off diagonal elements are given by

$$t_{jk} = \int_V \left[ \frac{\partial v_{ik}}{\partial \zeta_j} U_i^{(0)} + \frac{\partial v_{ij}}{\partial \zeta_k} U_i^{(0)} \right] dV. \tag{4.186}$$

To summarize, the tensor components are given by

$$t_{11} = 2 \int_V \sum_{i=1}^{3} \frac{\partial v_{i1}}{\partial \zeta_1} U_i^{(0)} \, dV - 2 \iint_{S_1} \sum_{i=1}^{3} U_i^{(0)\,2} \Bigg|_{\zeta_1=1} d\zeta_2 \, d\zeta_3, \tag{4.187}$$

$$t_{22} = 2 \int_V \sum_{i=1}^{3} \frac{\partial v_{i2}}{\partial \zeta_2} U_i^{(0)} \, dV - 2 \iint_{S_2} \sum_{i=1}^{3} U_i^{(0)\,2} \Bigg|_{\zeta_2=1} d\zeta_1 \, d\zeta_3, \tag{4.188}$$

$$t_{33} = 2 \int_V \sum_{i=1}^{3} \frac{\partial v_{i3}}{\partial \zeta_3} U_i^{(0)} \, dV - 2 \iint_{S_3} \sum_{i=1}^{3} U_i^{(0)\,2} \Bigg|_{\zeta_3=1} d\zeta_1 \, d\zeta_2, \tag{4.189}$$

$$t_{12} = t_{21} = \int_V \sum_{i=1}^{3} \left[ \frac{\partial v_{i1}}{\partial \zeta_2} + \frac{\partial v_{i2}}{\partial \zeta_1} \right] U_i^{(0)} \, dV, \tag{4.190}$$

$$t_{13} = t_{31} = \int_V \sum_{i=1}^{3} \left[ \frac{\partial v_{i1}}{\partial \zeta_3} + \frac{\partial v_{i3}}{\partial \zeta_1} \right] U_i^{(0)} \, dV, \tag{4.191}$$

$$t_{23} = t_{32} = \int_V \sum_{i=1}^{3} \left[ \frac{\partial v_{i2}}{\partial \zeta_3} + \frac{\partial v_{i3}}{\partial \zeta_2} \right] U_i^{(0)} \, dV. \tag{4.192}$$

This HFH solution extends the work of [82] by considering a vector valued electric field, lossy material, and a three dimensional domain. It reduces to the solution found by [82] by assuming a linear polarized field in two dimensions and taking $\epsilon'' \equiv 0$.

### 4.3.2 One Dimensional Example

In order to interpret any results found for the 1D photonic crystal, we first consider the problem for a homogeneous medium. Consider the Helmholtz equation of a homogeneous

lossy medium

$$y'' + (\epsilon' - i\epsilon'')y = 0, \tag{4.193}$$

where we assume the ansatz $y = ae^{i(k+i\kappa)x}$. Plugging it in, yields $-(k + i\kappa)^2 + \epsilon' - i\epsilon'' = 0$. Expanding this out and equating real and imaginary parts, yields the system

$$k^2 - \kappa^2 = \epsilon', \tag{4.194}$$

$$-2k\kappa = \epsilon'', \tag{4.195}$$

which is equivalent to those of (4.239), (4.240), (4.241), and (4.242). This system can be solved for the dielectric constants as

$$k = \pm\sqrt{\frac{|\epsilon| + \epsilon'}{2}}, \tag{4.196}$$

$$\kappa = \pm\sqrt{\frac{|\epsilon| - \epsilon'}{2}}. \tag{4.197}$$

We plot $k(\epsilon', \epsilon'')$ and $\kappa(\epsilon', \epsilon'')$ in Figure 4.4 and gain insight into how the Bloch parameter and attenuation parameter depend on the permittivity and dielectric loss.

The relationship between $k$,$\kappa$,$\epsilon'$, and $\epsilon''$ can be classified into four different cases. Case 1: all points along the positive $x$-axis where $\epsilon' > 0$, $\epsilon'' = 0$ yield non-attenuated traveling waves $k \neq 0$, $\kappa = 0$. Case 2: all points along the negative $x$-axis where $\epsilon' < 0$, $\epsilon'' = 0$ yields strongly attenuated non-propagating waves $k = 0$, $\kappa \neq 0$. Case 3: right half
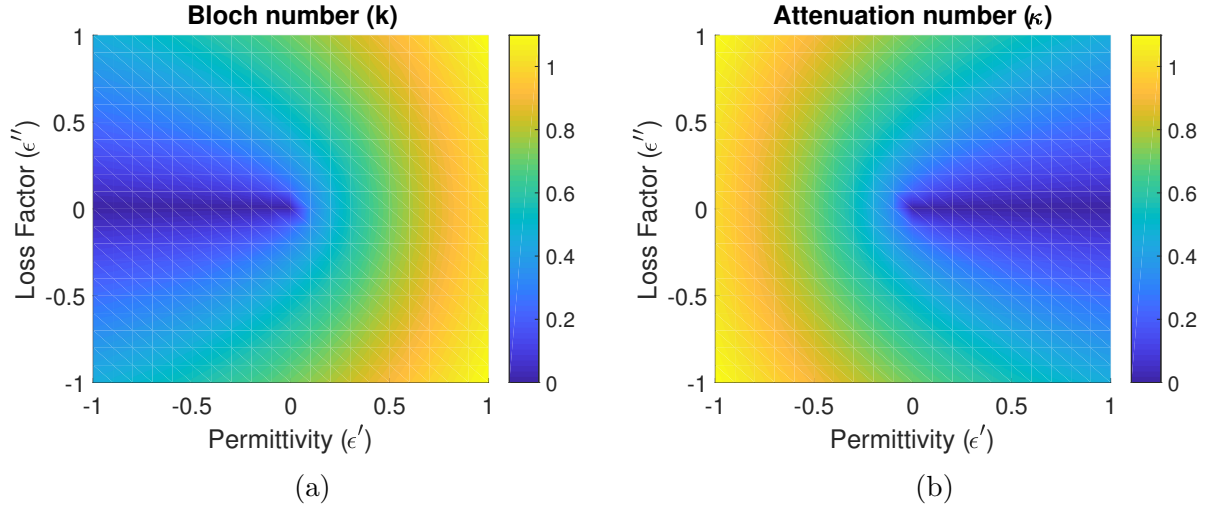
Figure 4.4: Complex wave number as a function of permittivity $\epsilon'$ and loss factor $\epsilon''$ for Bloch number $k$ (a); and attenuation number $\kappa$ (b)

plane, where $\epsilon' > 0$, $\epsilon'' \neq 0$ yields strong traveling waves with weak attenuation, $k$ large, $\kappa$ small. Case 4: left half plane $\epsilon' < 0$, $\epsilon'' \neq 0$, yields weak traveling waves with strong attenuation.

These plots show some very important consequences. There are only two ways for waves to be attenuated: by loss to the material $\epsilon'' \neq 0$ and reflection of waves $\epsilon' < 0$. Case 1 refers to the waves produced from a lossless material outside a band gap. Band gaps which are particular frequencies where waves cannot propagate through the medium only exist in Case 2 for no dielectric losses. The moment dielectric losses are introduced $k$ can no longer be zero, allowing for propagation of waves. Despite this, the negative permittivity still yields large attenuation from reflections which are known as evanescent waves. This is a characteristic feature of the 1D photonic crystal as they are also known as dielectric mirrors or

Bragg mirrors since they are non-metallic materials that produce large reflections. No purely homogeneous material is known to have a negative permittivity. The concept of negative permittivity was first hypothesized by Veselago in the 1960s [104]. Since many such materials possessing an effective negative permittivity have be made and are known as metamaterials, negative index materials, or left-handed materials [68]. It has been shown that the effective permittivity within the band gap of a photonic crystal is negative [105–107], which explains the large attenuation we see in Figure 4.5b. Once dielectric losses are introduced, there no longer exist any band gaps as shown by Figure 4.5c. Despite this, the frequencies that were associated with the band gaps still produce an effectively negative permittivity yielding large attenuation via reflections, as shown by Figure 4.5d. The same figure also shows that off these band gap frequencies (where there previously was no attenuation) now exhibits small amounts of attenuation due to the dielectric loss. The non-perturbed solution for correction $\gamma_2 = 0$ occurs when $k^2 - \kappa^2 = 0$ away from the periodic or antiperiodic cases. $k^2 - \kappa^2 > 0$ correspond to positive permittivity and posses attenuation solely from dielectric loss, and, conversely, $k^2 - \kappa^2 < 0$ corresponds to a negative permittivity residing within the band gap frequencies and possesses attenuation from dielectric losses as well as reflections. Furthermore, even within the band gap frequencies, the Bloch parameters corresponding to purely periodic (antiperiodic) solutions are no longer attainable in the presence of a lossy material.

Next, we consider the behavior of an inhomogeneous laminated material approximated by the HFH method applied to a scalar electric field. We begin by considering the

nondimensionalized Helmholtz equation

$$E_{z'z'} + \gamma^2 \epsilon E = 0, \tag{4.198}$$

where $\epsilon = \epsilon' - i\eta^2 \epsilon''$. Expanding the electric field and wavenumber in an asymptotic series $E = E^{(0)} + \eta E^{(1)} + \eta^2 E^{(2)} + \cdots$, $\gamma^2 = \gamma_0^2 + \eta \gamma_1^2 + \eta^2 \gamma_2^2 + \cdots$, and using multiple scales, the derivative becomes $\frac{\partial}{\partial z'} = \eta \frac{\partial}{\partial z} + \frac{\partial}{\partial \zeta}$. The expanded equation is

$$\eta^2 \frac{\partial^2 E}{\partial z^2} + 2\eta \frac{\partial^2 E}{\partial z \partial \zeta} + \frac{\partial^2 E}{\partial \zeta^2} + \left[ \gamma_0^2 + \eta \gamma_1^2 + \eta^2 \gamma_2^2 + \cdots \right] (\epsilon' - i\eta^2 \epsilon'') E = 0. \tag{4.199}$$

For simplicity we assume the cell problem is nondimensionalized on the lossy layer so that the cell domain is $-(\lambda - 1) \leq \zeta \leq 1$. The leading order differential equation is

$$\frac{\partial^2 E^{(0)}}{\partial \zeta^2} + \gamma_0^2 \epsilon' E^{(0)} = 0 \tag{4.200}$$

with a solution given by

$$E^{(0)}(z, \zeta) = \begin{cases} \alpha_{11}(z) \cos(\gamma_0 \sqrt{\epsilon_1'} \zeta) + \alpha_{12}(z) \sin(\gamma_0 \sqrt{\epsilon_1'} \zeta), & -(\lambda - 1) \leq \zeta \leq 0, \\ \alpha_{21}(z) \cos(\gamma_0 \sqrt{\epsilon_2'} \zeta) + \alpha_{22}(z) \sin(\gamma_0 \sqrt{\epsilon_2'} \zeta), & 0 \leq \zeta \leq 1. \end{cases} \tag{4.201}$$

In order to solve for the microscale solution we first apply the electromagnetic boundary conditions (1.23)-(1.26) of Chapter 1 at each internal interface. These conditions under the

laminate geometry include continuity and continuity of the derivative

$$E_1^{(0)}(z, 0) = E_2^{(0)}(z, 0), \tag{4.202}$$

$$\frac{\partial E_1^{(0)}}{\partial \zeta}(z, 0) = \frac{\partial E_2^{(0)}}{\partial \zeta}(z, 0). \tag{4.203}$$

Then the set of conditions on the external boundaries of the cell are given by the Floquet-Bloch conditions

$$E_2^{(0)}(z, 1) = e^{i\lambda\eta\mathcal{K}} E_1^{(0)}(z, -(\lambda - 1)), \tag{4.204}$$

$$\frac{\partial E_2^{(0)}}{\partial \zeta}(z, 1) = e^{i\lambda\eta\mathcal{K}} \frac{\partial E_1^{(0)}}{\partial \zeta}(z, -(\lambda - 1)), \tag{4.205}$$

which determine the attenuation and phase change across one cell, where $\mathcal{K} = k + i\kappa$, $k$ is the Bloch parameter, and $\kappa$ is the attenuation parameter. Applying continuity at the internal interface (4.202),

$$\alpha_{11} = \alpha_{21}. \tag{4.206}$$

Applying continuity of the derivative (4.203),

$$\gamma_0 \sqrt{\epsilon_1'} \alpha_{12} = \gamma_0 \sqrt{\epsilon_2'} \alpha_{22}. \tag{4.207}$$

136

Applying Floquet-Bloch condition (4.204),

$$\alpha_{21}\cos(\gamma_0\sqrt{\epsilon_2'}) + \alpha_{22}\sin(\gamma_0\sqrt{\epsilon_2'}) = e^{i\lambda\eta\mathcal{K}}\alpha_{11}\cos(\gamma_0\sqrt{\epsilon_1'}(\lambda-1)) - e^{i\lambda\eta\mathcal{K}}\alpha_{12}\sin(\gamma_0\sqrt{\epsilon_1'}(\lambda-1)).$$

$$(4.208)$$

Applying Floquet-Bloch condition (4.205),

$$-\gamma_0\sqrt{\epsilon_2'}\alpha_{21}\sin(\gamma_0\sqrt{\epsilon_2'}) + \gamma_0\sqrt{\epsilon_2'}\alpha_{22}\cos(\gamma_0\sqrt{\epsilon_2'})$$

$$= e^{i\lambda\eta\mathcal{K}}\gamma_0\sqrt{\epsilon_1'}\alpha_{11}\sin(\gamma_0\sqrt{\epsilon_1'}(\lambda-1)) + e^{i\lambda\eta\mathcal{K}}\gamma_0\sqrt{\epsilon_1'}\alpha_{12}\cos(\gamma_0\sqrt{\epsilon_1'}(\lambda-1)). \qquad (4.209)$$

Substitute (4.206) and (4.207) into (4.208) and (4.209), we get:

$$\alpha_{21}\cos(\gamma_0\sqrt{\epsilon_2'}) + \alpha_{22}\sin(\gamma_0\sqrt{\epsilon_2'}) = e^{i\lambda\eta\mathcal{K}}\alpha_{21}\cos(\gamma_0\sqrt{\epsilon_1'}(\lambda-1))$$

$$- e^{i\lambda\eta\mathcal{K}}\frac{\sqrt{\epsilon_2'}}{\sqrt{\epsilon_1'}}\alpha_{22}\sin(\gamma_0\sqrt{\epsilon_1'}(\lambda-1)), \qquad (4.210)$$

$$-\sqrt{\epsilon_2'}\alpha_{21}\sin(\gamma_0\sqrt{\epsilon_2'}) + \sqrt{\epsilon_2'}\alpha_{22}\cos(\gamma_0\sqrt{\epsilon_2'}) = e^{i\lambda\eta\mathcal{K}}\sqrt{\epsilon_1'}\alpha_{21}\sin(\gamma_0\sqrt{\epsilon_1'}(\lambda-1))$$

$$+ e^{i\lambda\eta\mathcal{K}}\sqrt{\epsilon_2'}\alpha_{22}\cos(\gamma_0\sqrt{\epsilon_1'}(\lambda-1)), \qquad (4.211)$$

This system can be solved to obtain a characteristic equation,

$$2\sqrt{\epsilon_1'\epsilon_2'}\left[\cos(\gamma_0\sqrt{\epsilon_1'}(\lambda-1))\cos(\gamma_0\sqrt{\epsilon_2'}) - \cos(\lambda\eta\mathcal{K})\right]$$

$$- (\epsilon_1' + \epsilon_2')\sin(\gamma_0\sqrt{\epsilon_1'}(\lambda-1))\sin(\gamma_0\sqrt{\epsilon_2'}) = 0, \qquad (4.212)$$

which is equivalent to the characteristic equation of the illustrative example of [82] by letting $\lambda = 2$, $\epsilon_1' = 1$, $\epsilon_2' = r^2$, and $\mathcal{K} \in \mathbb{R}$.

We will now find solutions for the periodic $\lambda \eta k = 0$ and antiperiodic $\lambda \eta k = \pi$ case with no attenuation $\kappa = 0$; then the first and second correction problems will define perturbation solutions away from these two states. The characteristic equation for the periodic (antiperiodic) case is

$$2\sqrt{\epsilon_1' \epsilon_2'}\left[\cos(\gamma_0\sqrt{\epsilon_1'}(\lambda - 1))\cos(\gamma_0\sqrt{\epsilon_2'}) \mp 1\right] - (\epsilon_1' + \epsilon_2')\sin(\gamma_0\sqrt{\epsilon_1'}(\lambda - 1))\sin(\gamma_0\sqrt{\epsilon_2'}) = 0,$$

(4.213)

which yields a discrete set of wavenumbers $\gamma_0$ for each case. Next, we finish solving for the microscale solution. Let $\alpha_{22} = \sqrt{\epsilon_1'}\beta_{22}$. Applying (4.206) and (4.207), we have

$$E_1 = \alpha_{21}\cos(\gamma_0\sqrt{\epsilon_1'}\zeta) + \sqrt{\epsilon_2'}\beta_{22}\sin(\gamma_0\sqrt{\epsilon_1'}\zeta),$$

(4.214)

$$E_2 = \alpha_{21}\cos(\gamma_0\sqrt{\epsilon_2'}\zeta) + \sqrt{\epsilon_1'}\beta_{22}\sin(\gamma_0\sqrt{\epsilon_2'}\zeta).$$

(4.215)

Condition (4.210) can also be written as

$$\alpha_{21}\left[\cos(\gamma_0\sqrt{\epsilon_2'}) \mp \cos(\gamma_0\sqrt{\epsilon_1'}(\lambda - 1))\right] = -\beta_{22}\left[\sqrt{\epsilon_1'}\sin(\gamma_0\sqrt{\epsilon_2'}) \pm \sqrt{\epsilon_2'}\sin(\gamma_0\sqrt{\epsilon_1'}(\lambda - 1))\right],$$

(4.216)

138

for the periodic (antiperiodic) case, which then implies that

$$\alpha_{21} = \frac{\sqrt{\epsilon_2'} \sin(\gamma_0 \sqrt{\epsilon_1'}(\lambda - 1)) + e^{-i\lambda \eta K} \sqrt{\epsilon_1'} \sin(\gamma_0 \sqrt{\epsilon_2'})}{\cos(\gamma_0 \sqrt{\epsilon_1'}(\lambda - 1)) - e^{-i\lambda \eta K} \cos(\gamma_0 \sqrt{\epsilon_2'})} \beta_{22}. \qquad (4.217)$$

We define the constant

$$p = \frac{\sqrt{\epsilon_2'} \sin(\gamma_0 \sqrt{\epsilon_1'}(\lambda - 1)) + e^{\lambda \eta \kappa} \sqrt{\epsilon_1'} \sin(\gamma_0 \sqrt{\epsilon_2'})}{\cos(\gamma_0 \sqrt{\epsilon_1'}(\lambda - 1)) - e^{\lambda \eta \kappa} \cos(\gamma_0 \sqrt{\epsilon_2'})}, \qquad (4.218)$$

which reduces to

$$p = \frac{\sqrt{\epsilon_2'} \sin(\gamma_0 \sqrt{\epsilon_1'}(\lambda - 1)) \pm \sqrt{\epsilon_1'} \sin(\gamma_0 \sqrt{\epsilon_2'})}{\cos(\gamma_0 \sqrt{\epsilon_1'}(\lambda - 1)) \mp \cos(\gamma_0 \sqrt{\epsilon_2'})}, \qquad (4.219)$$

for the periodic (antiperiodic) case. Letting $f(z) = \beta_{22}(z)$ we arrive at the solution

$$E^{(0)}(z, \zeta) = f^{(0)} U^{(0)} = f^{(0)}(z) \begin{cases} \sqrt{\epsilon_2'} \sin(\gamma_0 \sqrt{\epsilon_1'} \zeta) + p \cos(\gamma_0 \sqrt{\epsilon_1'} \zeta), & -(\lambda - 1) \leq \zeta \leq, 0 \\ \sqrt{\epsilon_1'} \sin(\gamma_0 \sqrt{\epsilon_2'} \zeta) + p \cos(\gamma_0 \sqrt{\epsilon_2'} \zeta), & 0 \leq \zeta \leq 1, \end{cases}$$

$$(4.220)$$

In the same manner as in the general solution derived above, it can be shown that applying the Fredholm Alternative to the first correction problem requires that $\gamma_1 = 0$. Hence the equation governing the first correction is

$$E_{\zeta\zeta}^{(1)} + \gamma_0^2 \epsilon' E^{(1)} = -2 f_z^{(0)} U_\zeta^{(0)}. \qquad (4.221)$$

which yields the solution

$$E^{(1)} = f^{(1)}U^{(0)} + f_z^{(0)}\left[AV + B\zeta U^{(0)}\right], \tag{4.222}$$

where the first term $f^{(1)}U^{(0)}$ is the homogeneous solution, and the second is the particular solution, where $V$ is a non-periodic (non-antiperiodic) homogeneous solution and $B$ is determined by method of undetermined coefficients. Since we require that $E^{(1)}$ is periodic (antiperiodic), the constant $A$ is chosen to satisfy this condition. Plugging (4.222) into the differential equation (4.221) shows that $B = -1$. Thus the solution is

$$E^{(1)} = f^{(1)}U^{(0)} + f_z^{(0)}\left[AV - \zeta U^{(0)}\right]. \tag{4.223}$$

To determine $A$ we apply periodicity (antiperiodicity) to the particular solution

$$\left.(AV - \zeta U^{(0)})\right|_1 = \pm \left.(AV - \zeta U^{(0)})\right|_{-(\lambda-1)} \tag{4.224}$$

and solving for $A$ and applying periodicity (antiperiodicity) of the leading order solution $\left.U^{(0)}\right|_1 = \pm \left.U^{(0)}\right|_{-(\lambda-1)}$, we have an expression for $A$:

$$A = \frac{\lambda U^{(0)}(1)}{V(1) \mp V(-(\lambda-1))}. \tag{4.225}$$

Since $\gamma_1 = 0$, we do not yet have a perturbed solution away from the two base states. Proceeding to the second correction we find the correction $\gamma_2$. The equation for the second

correction is given by

$$E_{\zeta\zeta}^{(2)} + \gamma_0^2 \epsilon' E^{(2)} = -f_{zz}^{(0)} U^{(0)} - 2E_{z\zeta}^{(1)} + \gamma_0^2 i \epsilon'' f^{(0)} U^{(0)} - \gamma_2^2 \epsilon' f^{(0)} U^{(0)}. \tag{4.226}$$

Since the Helmholtz equation is self-adjoint by applying the Fredholm Alternative Theorem the compatibility condition is found to be

$$-f_{zz}^{(0)} \int_{-(\lambda-1)}^{1} (U^{(0)})^2 \, d\zeta - 2 \int_{-(\lambda-1)}^{1} E_{z\zeta}^{(1)} U^{(0)} \, d\zeta + \gamma_0^2 i f^{(0)} \int_{-(\lambda-1)}^{1} \epsilon'' (U^{(0)})^2 \, d\zeta$$

$$-\gamma_2^2 f^{(0)} \int_{-(\lambda-1)}^{1} \epsilon' (U^{(0)})^2 \, d\zeta = 0. \tag{4.227}$$

The second integral of (4.227) is written out as

$$\int_{-(\lambda-1)}^{1} E_{z\zeta}^{(1)} U^{(0)} \, d\zeta = f_z^{(1)} \int_{-(\lambda-1)}^{1} U_\zeta^{(0)} U^{(0)} \, d\zeta + f_{zz}^{(0)} A \int_{-(\lambda-1)}^{1} V_\zeta U^{(0)} \, d\zeta$$

$$- f_{zz}^{(0)} \int_{-(\lambda-1)}^{1} (U^{(0)})^2 \, d\zeta - f_{zz}^{(0)} \int_{-(\lambda-1)}^{1} \zeta U_\zeta^{(0)} U^{(0)} \, d\zeta. \tag{4.228}$$

The first integral of (4.228) is evaluated as

$$\int_{-(\lambda-1)}^{1} U_\zeta^{(0)} U^{(0)} \, d\zeta = \frac{1}{2} \int_{-(\lambda-1)}^{1} \frac{\partial}{\partial \zeta} \left( U^{(0)} \right)^2 \, d\zeta = \frac{1}{2} \left( U^{(0)} \right)^2 \Big|_{-(\lambda-1)}^{1} = 0 \tag{4.229}$$

by periodicity. The last integral of (4.228) can be calculated to be

$$\int_{-(\lambda-1)}^{1} \zeta U_\zeta^{(0)} U^{(0)} \, d\zeta = \frac{1}{2} \int_{-(\lambda-1)}^{1} \zeta \frac{\partial}{\partial \zeta} (U^{(0)})^2 \, d\zeta = \frac{\lambda}{2} (U^{(0)})^2 \Big|_1 - \frac{1}{2} \int_{-(\lambda-1)}^{1} (U^{(0)})^2 \, d\zeta \tag{4.230}$$

141

by applying integration by parts and periodicity of the leading order solution. The integral (4.228) becomes

$$
\int_{-(\lambda-1)}^{1} E_{z\zeta}^{(1)} U^{(0)} \, d\zeta = f_{zz}^{(0)} A \int_{-(\lambda-1)}^{1} V_\zeta U^{(0)} \, d\zeta - f_{zz}^{(0)} \frac{\lambda}{2} (U^{(0)})^2 \Big|_1 - f_{zz}^{(0)} \frac{1}{2} \int_{-(\lambda-1)}^{1} (U^{(0)})^2 \, d\zeta,
$$

$$(4.231)$$

and finally the compatibility condition (4.227) reduces to

$$
f_{zz}^{(0)} \left[ \lambda(U^{(0)})^2 \big|_1 - 2A \int_{-(\lambda-1)}^{1} V_\zeta U^{(0)} \, d\zeta \right]
$$
$$
+ f^{(0)} \left[ i\gamma_0^2 \int_{-(\lambda-1)}^{1} \epsilon''(U^{(0)})^2 \, d\zeta - \gamma_2^2 \int_{-(\lambda-1)}^{1} \epsilon'(U^{(0)})^2 \, d\zeta \right] = 0, \qquad (4.232)
$$

which is the differential equation for the macroscale function $f^{(0)}(z)$. Next, we determine $f^{(0)}$ by applying the Floquet-Bloch condition on the macroscale for both left moving $u(z + \lambda\eta, \zeta)$ and right moving $u(z - \lambda\eta, \zeta)$ wave for the periodic (antiperiodic) case. The Floquet-Bloch condition

$$
E^{(0)}(z \pm \lambda\eta, \zeta) = e^{i\mathcal{K}\lambda\eta} E^{(0)}(z, \zeta), \qquad (4.233)
$$

after substituting in the leading order solution, becomes

$$
f^{(0)}(z \pm \lambda\eta) = e^{i\mathcal{K}\lambda\eta} f^{(0)}(z), \qquad (4.234)
$$

142

which implies

$$f^{(0)}(z) = e^{\pm i \mathcal{K} z} = e^{\pm (-\kappa + ik)z}. \qquad (4.235)$$

As for the antiperiodic case, the condition

$$E^{(0)}(z \pm \lambda \eta, \zeta) = -e^{i \mathcal{K} \lambda \eta} E^{(0)}(z, \zeta), \qquad (4.236)$$

yields that

$$f^{(0)}(z \pm \lambda \eta) = e^{i(\mathcal{K} - \frac{\pi}{\lambda \eta})\lambda \eta} f^{(0)}(z), \qquad (4.237)$$

which implies the macroscale dependence is

$$f^{(0)}(z) = e^{\pm i(\mathcal{K} - \frac{\pi}{\lambda \eta})z} = e^{\pm (-\kappa + i(k - \frac{\pi}{\lambda \eta}))z}. \qquad (4.238)$$

We now substitute the expressions for $f^{(0)}$ into the differential equation to get conditions relating $k$, $\kappa$ and $\gamma_2$. The conditions do not depend on the direction of the wave. The result for the periodic case is

$$k^2 - \kappa^2 = \frac{-\gamma_2^2 \int_{-(\lambda-1)}^1 \epsilon'(U^{(0)})^2 \, d\zeta}{\left[ \lambda(U^{(0)})^2|_1 - 2A \int_{-(\lambda-1)}^1 V_\zeta U^{(0)} \, d\zeta \right]} = \gamma_2^2 \epsilon'_{eff}, \qquad (4.239)$$

$$-2k\kappa = \frac{-\gamma_0^2 \int_{-(\lambda-1)}^1 \epsilon''(U^{(0)})^2 \, d\zeta}{\left[ \lambda(U^{(0)})^2|_1 - 2A \int_{-(\lambda-1)}^1 V_\zeta U^{(0)} \, d\zeta \right]} = \gamma_0^2 \epsilon''_{eff}, \qquad (4.240)$$

143

and for the antiperiodic case

$$\left(k - \frac{\pi}{\lambda\eta}\right)^2 - \kappa^2 = \frac{-\gamma_2^2 \int_{-(\lambda-1)}^1 \epsilon'(U^{(0)})^2 \, d\zeta}{\left[\lambda(U^{(0)})^2|_1 - 2A \int_{-(\lambda-1)}^1 V_\zeta U^{(0)} \, d\zeta\right]} = \gamma_2^2 \epsilon'_{eff}, \tag{4.241}$$

$$-2\left(k - \frac{\pi}{\lambda\eta}\right)\kappa = \frac{-\gamma_0^2 \int_{-(\lambda-1)}^1 \epsilon''(U^{(0)})^2 \, d\zeta}{\left[\lambda(U^{(0)})^2|_1 - 2A \int_{-(\lambda-1)}^1 V_\zeta U^{(0)} \, d\zeta\right]} = \gamma_0^2 \epsilon''_{eff}. \tag{4.242}$$

Defining the quantities above as effective permittivity and effective dielectric loss (4.239-4.240) and (4.241-4.242) closely resemble similar equations, (4.194-4.195), for a homogeneous medium. Therefore we expect the same properties associated with Figure 4.4 to hold in the homogenization solution. The perturbation equation for the eigenfrequency $\gamma \approx \gamma_0 + \frac{\eta^2}{2}\frac{\gamma_2^2}{\gamma_0}$ can be written down by applying correction (4.239)

$$\gamma \approx \gamma_0 + \eta^2 \frac{k^2 - \kappa^2}{2\gamma_0 \epsilon'_{eff}}. \tag{4.243}$$

The approximation to the wavenumber can be written in terms of the Bloch parameter, by substituting (4.240) into (4.243), found as

$$\gamma \approx \gamma_0 + \frac{(\lambda\eta k)^2}{2\lambda^2 \gamma_0 \epsilon'_{eff}} - \frac{\lambda^2 \gamma_0^3 (\eta^2 \epsilon''_{eff})^2}{8\gamma_0 \epsilon'_{eff}(\lambda\eta k)^2}, \tag{4.244}$$

where $0 \leq \lambda\eta k \leq \pi$ is the Brillouin zone of the photonic crystal. The similar approximation for the antiperiodic case is found as

$$\gamma \approx \gamma_0 + \frac{(\lambda\eta k - \pi)^2}{2\lambda^2 \gamma_0 \epsilon'_{eff}} - \frac{\lambda^2 \gamma_0^3 (\eta^2 \epsilon''_{eff})^2}{8\epsilon'_{eff}(\lambda\eta k - \pi)^2}. \tag{4.245}$$

144

Similarly, the dispersion curve for the attenuation coefficient can also be found, by solving for $k$ in 4.240) and substituting in (4.243),

$$\gamma \approx \gamma_0 - \frac{(\lambda\eta\kappa)^2}{2\lambda^2\gamma_0\epsilon'_{eff}} + \frac{\lambda^2\gamma_0^3(\eta^2\epsilon''_{eff})^2}{8\epsilon'_{eff}(\lambda\eta\kappa)^2}, \tag{4.246}$$

and it remains the same for the antiperiodic case as well. The parameter group $\eta^2\epsilon''_{eff}$ represents the unscaled or natural effective dielectric constant associated with a dielectric medium of this geometry. The Bloch number expansions (4.244) and (4.245) and the attenuation expansion (4.246) reduce to those found by [82] for the case of a lossless medium when $\epsilon'' = 0$. While the attenuation of waves was not explicitly discussed in [82], it is trivial to derive the expression. The perturbation approximations break down when $k$ or $\kappa$ are $O(\eta)$ making the third term in (4.244-4.246) $O(1)$. A similar break down of the approximation occurs when $k$ or $\kappa$ are $O(\eta^{-1})$ making the second term in (4.244-4.246) $O(1)$. The asymptotic approximations derived are only valid for $\gamma_0$ that are simple roots of the characteristic equation. The degenerate case when $\gamma_0$ has multiplicity two yields no attenuation to leading order and yields a dispersion approximation as found by [82].

The variable groups $\lambda\eta k$ and $\lambda\eta\kappa$ represent the Brillouin zone and attenuation variables. The eigenfrequency is plotted against these variables to produce the dispersion curves shown in Figure 4.5 that relate $\gamma$ to $k$ and $\kappa$. The periodic base state corresponds to $\lambda\eta k = 0$ while the antiperiodic base state corresponds to $\lambda\eta k = \pi$. The (blue) curves are asymptotic approximations to the dispersion curve perturbed away from the periodic base state, while the (red) curves are asymptotic approximations to the dispersion curve perturbed away from

the antiperiodic base state. Figures 4.5a and 4.5b plot the Brillouin zone and attenuation curves for a lossless medium. Figure 4.5a reproduces the findings of [82]. The dispersion curves for the lossless case show the existence of band gaps, frequency intervals where no wave propagation can occur. The curves show large attenuation within the band gap regions which correspond to large reflections. As mentioned previously it has been shown that band gaps possess an negative effective permittivity [105–107], corresponding to Case 2 of Figure 4.4 we expect $k = 0$ and $\kappa$ to be large. Once dielectric loss is nonzero, as shown by Figure 4.5c and Figure 4.5d the existence of band gaps cease. Waves are capable of propagating through the medium though still possess a large attenuation, which corresponds to the Case 4 of Figure 4.4. Finally as in Case 3 of Figure 4.4 outside a band gap $k$ is large while $\kappa$ is small. We compare the dispersion curves produced by the HFH to those of the associated 1D laminate acoustic problem [108]. The dispersion curves of the acoustic problem, displayed in Figure 4.6, show similar features to Figure 4.5. Existence of band gaps for lossless media which no longer exist in the presence of material losses. Small attenuation develops outside the band gap regions when losses are present.

Now that we have an understanding of the dispersion relations for a particular monochromatic wave with frequency corresponding to wavenumber $\gamma$, we can determine the $k$ and $\kappa$ that govern the macroscopic behavior and plot the solutions. We now compare the solutions generated by the HFH against the exact solutions determined by the TMM. Consider a single heterogeneous slab of material possessing $N$ two phase cells, where the first layer is freespace with $\epsilon = 1$ and the second layer is a lossy dielectric with $\epsilon = 4 - i\epsilon''$. The impinging wave is monochromatic with $\gamma = 1.91063323$ and is at normal incidence from
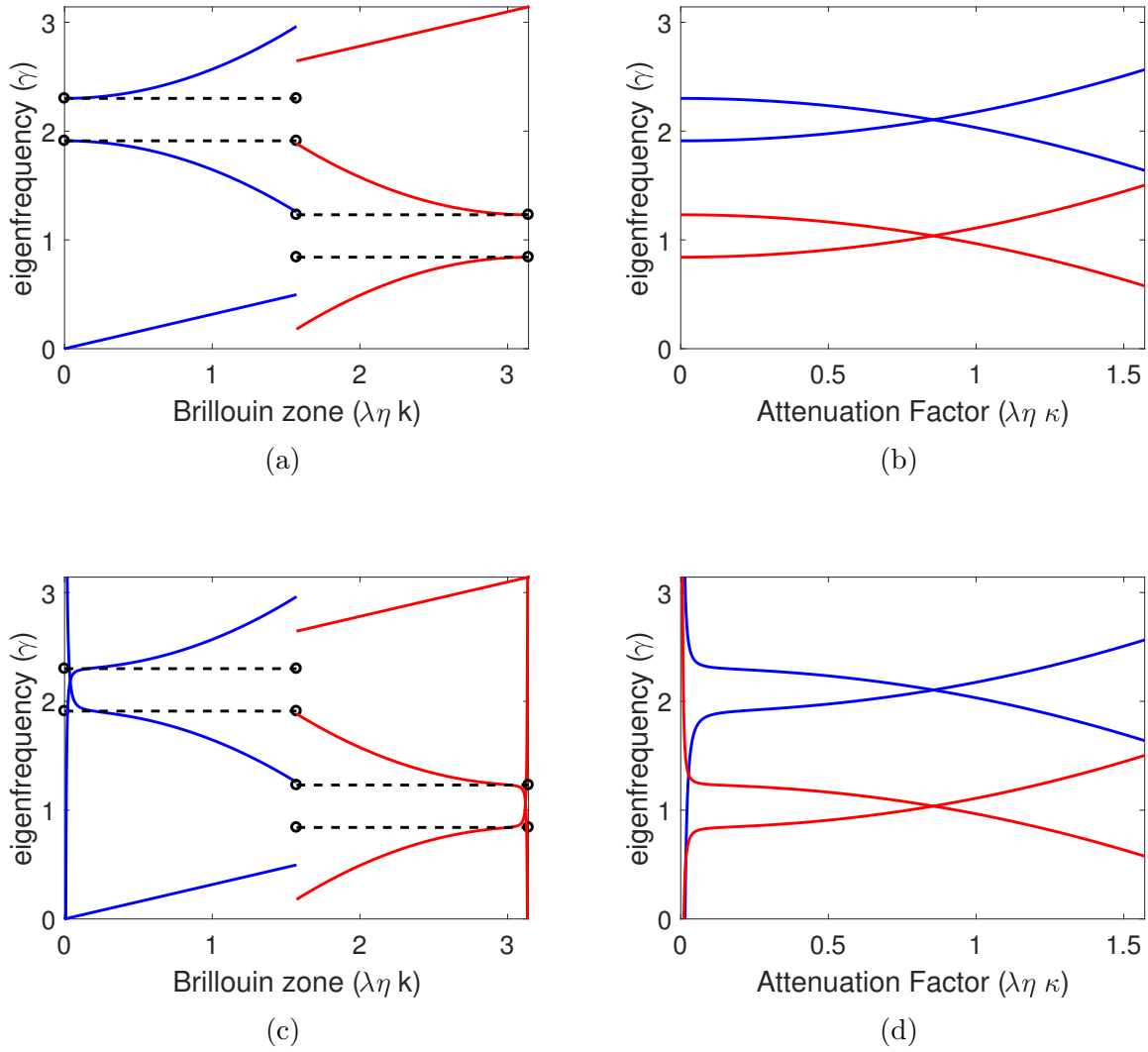
Figure 4.5: Dispersion curves relating the nondimensional wavenumber $\gamma$ with the Bloch number $k$ (a) and attenuation number $\kappa$ (b) for a lossless medium and the Bloch number $k$ (c) and attenuation number $\kappa$ (d) for a lossy medium with $\epsilon'' = 0.1$ and $\eta = 0.01$.

147
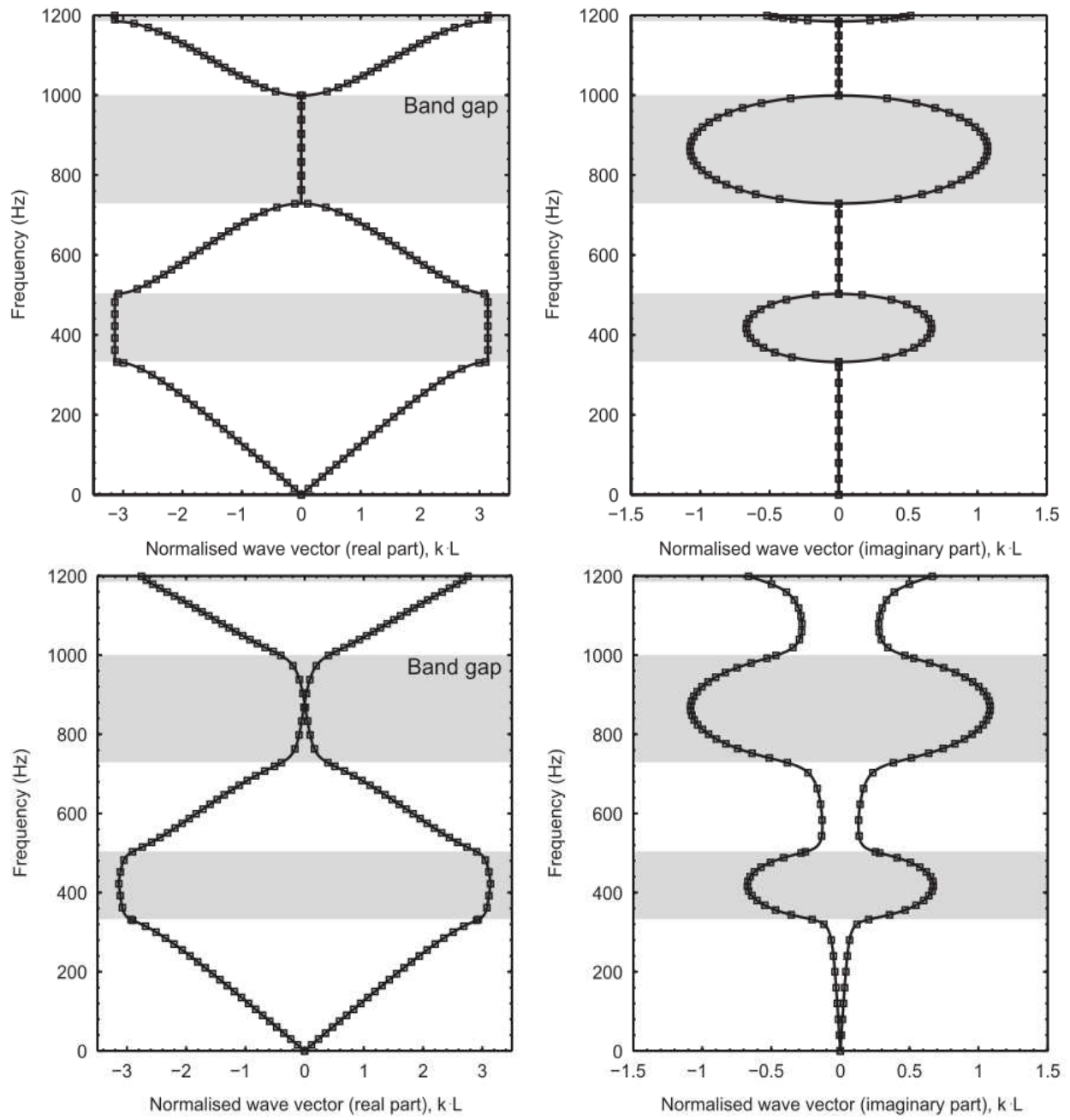
Figure 4.6: Dispersion curves of acoustic analogue of 1D photonic crystal (top) lossless media (bottom) lossy media

the left. For a characteristic microscale length $l = 1$mm, this corresponds to a frequency of 91.2 GHz. The TMM can be applied directly to this problem for different values of $N$ and $\epsilon''$. In order to apply the HFH to this problem, we need to solve the system

$$E_1(\zeta) = a_1 e^{i\gamma\zeta} + b_1 e^{-i\gamma\zeta}, \qquad\qquad -\infty < \zeta \le 0, \qquad (4.247)$$

$$E_2(\zeta) = a_2 e^{i(k+i\kappa)\eta\zeta} U(g(\zeta)) + b_2 e^{-i(k+i\kappa)\eta\zeta} U(g(\zeta)), \qquad 0 \le \zeta \le \lambda N, \qquad (4.248)$$

$$E_3(\zeta) = a_3 e^{i\gamma\zeta} + b_3 e^{-i\gamma\zeta}, \qquad\qquad \lambda N \le \zeta < \infty, \qquad (4.249)$$

subject to the conditions

$$\lim_{\zeta\to-\infty} \left( \frac{\partial}{\partial z} + i\gamma \right) (E_1 - 1) = 0, \qquad\qquad (4.250)$$

$$E_1(0) = E_2(0), \qquad\qquad (4.251)$$

$$\frac{\partial E_1}{\partial \zeta}(0) = \frac{\partial E_2}{\partial \zeta}(0), \qquad\qquad (4.252)$$

$$E_1(\lambda N) = E_2(\lambda N), \qquad\qquad (4.253)$$

$$\frac{\partial E_1}{\partial \zeta}(\lambda N) = \frac{\partial E_2}{\partial \zeta}(\lambda N), \qquad\qquad (4.254)$$

$$\lim_{\zeta\to\infty} \left( \frac{\partial}{\partial z} - i\gamma \right) E_3 = 0, \qquad\qquad (4.255)$$

where $g(\zeta) = mod(\zeta, \lambda) - (\lambda - 1)$ since the argument for $U(\zeta)$ is restricted to the cell domain

$-(\lambda - 1) \leq \zeta \leq 1$. Solving the system yields coefficients

$$a_2 = 2\frac{2i\gamma}{C \cdot Q}, \tag{4.256}$$

$$b_2 = -\frac{B}{D}e^{2i(k+i\kappa)\eta\lambda N}a_2, \tag{4.257}$$

where

$$Q = \left[1 - \frac{A \cdot B}{C \cdot D}e^{2i(k+i\kappa)\eta\lambda N}\right], \tag{4.258}$$

$$A = [i\gamma - i(k+i\kappa)\eta]U(-(\lambda - 1)) + U_\zeta(-(\lambda - 1)), \tag{4.259}$$

$$B = [i\gamma - i(k+i\kappa)\eta]U(1) - U_\zeta(1), \tag{4.260}$$

$$C = [i\gamma + i(k+i\kappa)\eta]U(-(\lambda - 1)) + U_\zeta(-(\lambda - 1)), \tag{4.261}$$

$$D = [i\gamma + i(k+i\kappa)\eta]U(1) - U_\zeta(1). \tag{4.262}$$

Figure 4.7 compares solutions found by the HFH model against the exact solutions of the TMM. The plots show solutions with very good agreement between the two methods even for $O(1)$ dielectric loss where the HFH begins to break down. Figure 4.7a has no dielectric loss which reduces our model to that of [82] which we validated against an exact solution. A plot of the absolute error as a function of the asymptotic parameter $\eta$ for several different loss factors is shown in Figure 4.8a. It shows the error is linear in $\eta$ which is what we expect from a leading order asymptotic solution. It also demonstrates that the error increases as the dielectric loss increases since the lossy solutions are perturbed away from the lossless solutions.
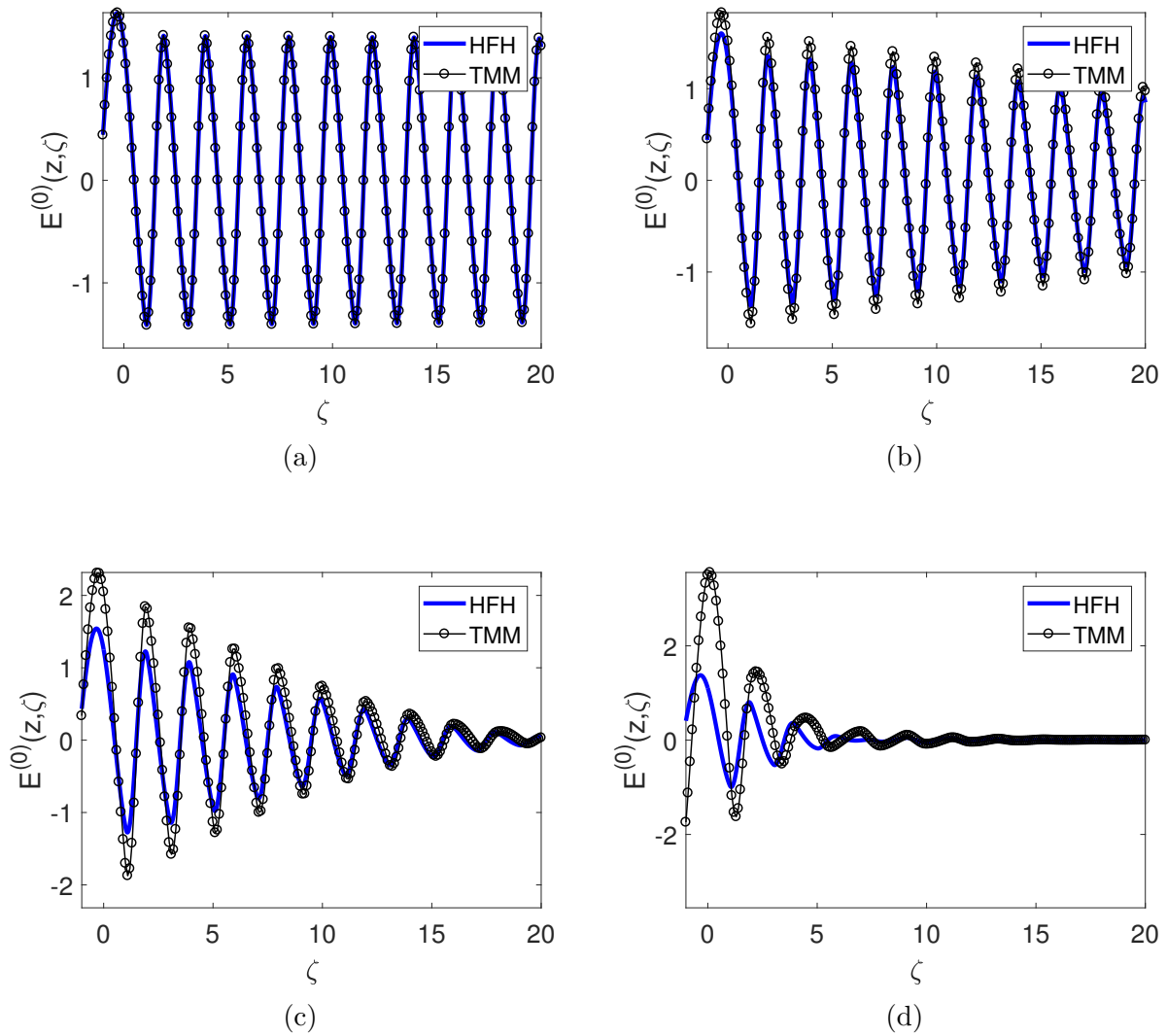
Figure 4.7: Comparison of High-frequency Homogenization solutions to those of the Transfer Matrix Method for a on sided incident wave of nondimensional wavenumber $\gamma = 1.91063323$, which for a characteristic microscale of $l = 1$mm is a frequency $f = 91.2$ GHz, impinging a single slab of a heterogeneous laminate of $2N$ layers; selected solutions include a two phase laminate with permittivity $\epsilon'_1 = 1$ and $\epsilon'_2 = 4 - i\epsilon''$; $N = 500$, $\epsilon'' = 0$ (a), $N = 500$, $\epsilon'' = 0.01$ (b), $N = 50$, $\epsilon'' = 0.1$ (c), $N = 50$, $\epsilon'' = 1$ (d).
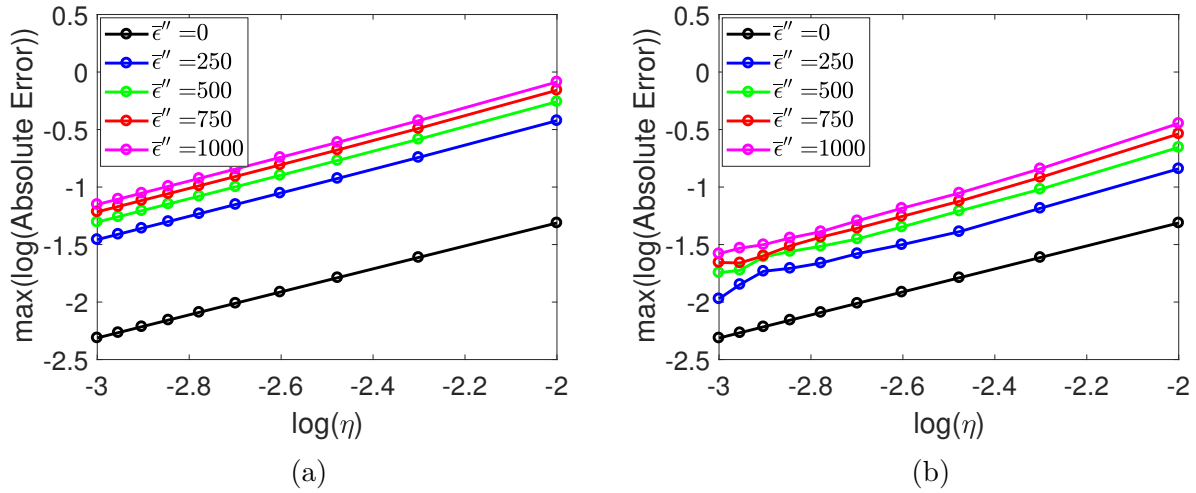
Figure 4.8: Logarithmic plot of the absolute error between the High-frequency Homogenization and the Transfer Matrix Method as a function of $\eta$ and several different values for the dielectric loss: solutions using (4.219) (a), solutions using (4.218) (b).
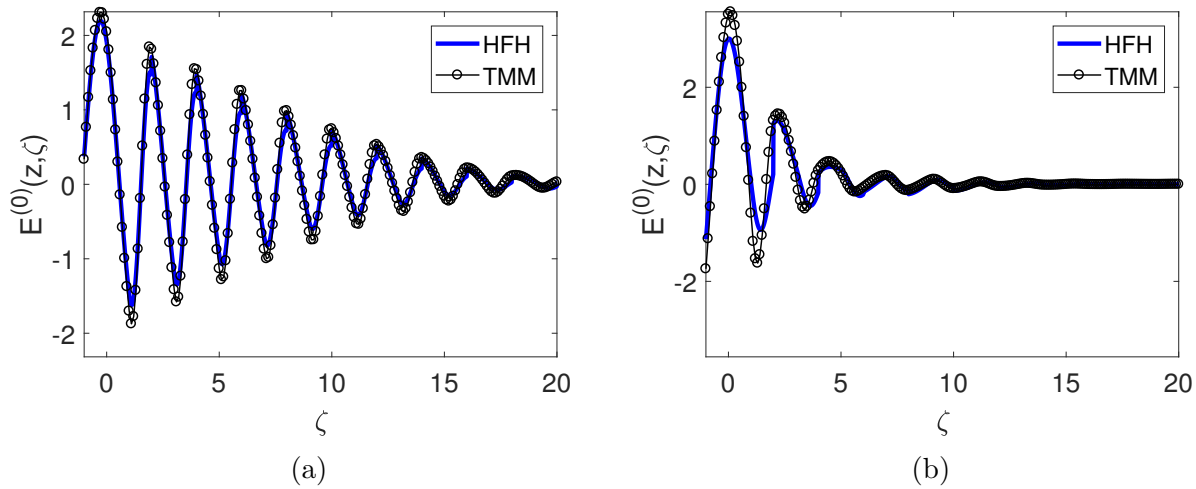


Figure 4.9: Use of (4.218) for a comparison of High-frequency Homogenization solutions to those of the Transfer Matrix Method: $N = 50$, $\epsilon'' = 0.1$ (a), $N = 50$, $\epsilon'' = 1$ (b).

One aspect to notice about the HFH solutions is that the amplitude at $\zeta = 0$ is the same for all of the solutions. Examining the equation for the leading order solution (4.220), we notice that the only dependence on the dielectric loss appears in the macroscale function $f(z) = e^{(-\kappa+ik)z}$ through the Bloch number and Attenuation number. It shows that, indeed, the amplitude at $\zeta = 0$ remains constant; however, we know that a large dielectric loss will produce large reflections at each of the layer interfaces, increasing the field at $\zeta = 0$ as seen by the TMM in Figures 4.7c and 4.7d. Up to this point we have considered solutions by using (4.220) with (4.219). In contrast, now that we have an approximation for $k$ and $\kappa$, we could instead directly use (4.218), which would then allow the solution to vary its amplitude at $\zeta = 0$. Solutions attained by applying this modification are shown in Figure 4.9. This substitution yields solutions that fail to satisfy the boundary conditions imposed on the cell problem. Though it fails to satisfy the boundary conditions exactly since (4.219) and (4.218) are asymptotic as $\eta \to 0$ it is an accurate method. This alternate method does produce solutions with significantly less error as shown by Figure 4.8b.

The HFH method has, therefore, been verified against the exact solution of the TMM. In the Conclusions we discuss how it can coupled together with the thermal homogenization and used to model a porous media heat exchanger.

It was a great step in science when men became convinced that, in order to understand the nature of things, they must begin by asking, not whether a thing is good or bad, noxious or beneficial, but of what kind it is? And how much is there of it? Quality and Quantity were then first recognized as the primary features to be observed in scientific inquiry.

James Clerk Maxwell (1831-1879)

CHAPTER V

CONCLUSIONS

In Chapter 2 we developed a model for the EM heating of a three-layer laminate with no fluid flow. EM waves in the high-frequency regime can become resonant in the presence of a defect layer accumulating EM energy. The strengthening of the electric field causes the power response curve to create stable steady solutions at medium-high temperatures which have the benefit of efficient EM heating while avoiding the dangerous effects of thermal runaway. Spatial effects were shown to be important as the application of an inlet Dirichlet condition established traveling-wave solutions at the left turning points of the SS-curve. The non-existence regions of the steady states force the heat exchanger to operate at lower temperatures making it less efficient.

Chapter 3 introduces fluid flow in the exterior layers increases the speed of the traveling wave solutions and widens the non-existence regions in the SS-curve through the use of a low-advection asymptotic model. In contrast, a large-advection model was developed and solved by a Galerkin method which was shown to have fast convergence. It was compared against a fully numerical solution using the Peaceman-Rachford ADI method.

Understanding the results for the triple-layer laminate models, the geometry of a porous laminate structure was considered in Chapter 4. The energy equation was homogenized which resulted in an anisotropic media with mixture formula for the thermal

conductivity. The dependence on the electric field requires the solution to the wave scattering problem. Classical long-wave homogenization of Maxwell's equations showed that a spatially independent dielectric reduced to the simple mixture rules; however, this simplification cannot be made once the temperature dependence is included. The wave-geometry interactions that seen in the triple-layer models occurred in the high-frequency regime. The high-frequency homogenization model of [82] was extended for the general three-dimensional two-phase periodic media to include small dielectric losses. The model was validated against for one-dimensional laminate with the exact solution by use of the Transfer Matrix Method.

A continuation of the work in the future would involve coupling the HFH of the electric field to the homogenized energy equation and solve the two-dimensional thermal problem by applying the PR-ADI scheme as we did for the three-layer laminate in Chapter 3. This type of model would be useful in running computational experiments on how different phenomena traditionally associated with photonic crystals affects the temperature profile of a EM heated porous material. Such results, as the SS-curve was in the triple-layer case, could result in better control and novel operating states in EM heat exchangers.

An additional high-frequency model to consider would be a weakly nonuniform asymptotic model. By considering temperature profiles with gradient of order $\eta$, the gradient of the dielectric would be of the same order. It would then imply that the curl-curl derivation of the electric field (1.22) would reduce to the Helmholtz equation at leading order, and thus solvable by the TMM at each order. The benefit of this, other than the ease of implementing the TMM, is that at the first correction depending on the polarization of the incident plane wave a normal component of the electric field to the laminates would be produced where

156

there was none before. This is an effect of Maxwell's equations not present in the Helmholtz models.

Natural scenarios to investigate would include understanding the power response of the inhomogeneous medium. If a defect layer were introduced and resonance applied, how would steady state solutions behave? Could a laminate be designed to produce a multiple S-shaped curve like that of Figure 2.9, ideal for thermal runaway control? Of course, the essential question in developing an EM heat exchanger is how to make it most efficient. As discussed in Chapter 3, there is an inherent optimization problem between the efficiency of EM energy absorbed and the thermal energy collected which would be of considerable interest. There are a multitude of additional questions to be asked and answered in the study of EM heat exchangers, especially on the influence of fluid dynamic effects on their operation. This work has uncovered a few characteristics of these devices from the three-layer models and it has developed a new high-frequency homogenization method that can be used to model the operation of a heat exchanger with a lossy porous media target material in future work.

... achieving a dream is about more than just what you accomplish. It's about who you become in the process!

James Clerk Maxwell (1831-1879)

PUBLICATIONS

[1] J.M. Gaone, B.S. Tilley, and V.V. Yakovlev. Permittivity-based control of thermal run-away in a triple-layer laminate. In *IEEE MTT-S Intern. Microwave Symp. Dig.*, (Honolulu, HI, June 2017), 978-1-5090-6360-4.

[2] A.A. Mohekar, J.M. Gaone, B.S. Tilley, and V.V. Yakovelev. Multiphysics simulation of temperature profiles in a triple-layer model of a microwave heat exchanger. In *IEEE MTT-S Intern. Microwave Symp. Dig.*, (Philadelphia, PA, June 2018) (accepted for publication).

# BIBLIOGRAPHY

[3] W.B. Westphal and A. Sils. Dielectric constant and loss data. Technical report, Air Force Materials Laboratory, Technical Report AFML-TR-72-39, 1972.

[4] V.V. Yakovlev, S.M. Allan, M.L. Fall, and H.S. Shulman. Computational study of thermal runaway in microwave processing of zirconia. In J. Tao, editor, *Microwave and RF Power Applications*, Cépaduès Éditions, pages 303–306, 2011.

[5] A.E. Bergles. Enhancement of convective heat transfer - Newton's legacy pursued. *Mech. Teoret. i Stos.*, 3, 1989.

[6] B.S. Tilley. On microchannel shapes in liquid-cooled electronics applications. *Inter. J. Heat Mass Transfer*, 62:163–173, 2013.

[7] I. Martinez. Heat and mass transfer, online. http://webserver.dmt.upm.es/ isidoro/bk3/c12/Heat%20exchangers.pdf.

[8] A. Jamar, Z.A.A. Majid, W.H. Azmi, M. Norhafana, and A.A. Razak. A review of water heating system for solar energy applications. *Inter. Commun. Heat and Mass Transfer*, 76:178–187, 2016.

[9] S.A. Kalogirou. Solar thermal collectors and applications. *Progress Energy Combust. Sci.*, 30:231–295, 2004.

[10] G. Zhu, T. Wendelin, M.J. Wagner, and C. Kutscher. History, current state, and future of linear Fresnel concentrating solar collectors. *Solar Energy*, 103:639–652, 2014.

[11] P. George and R. Beach. Beamed-energy propulsion (BEP) study. Technical report, NASA/TM-2012-217014, 2012.

[12] K.S. Ong. Thermal performance of solar air heaters: mathematical model and solution procedure. *Solar Energy*, 55(2):93–109, 1995.

[13] N. Pasumarthi and S.A. Sherif. Experimental and theoretical performance of a demonstration solar chimney model - part 1: mathematical model development. *Inter. J. Energy Research*, 22:277–288, 1998.

[14] H.D. Ammari. A mathematical model of thermal performance of a solar air heater with slats. *Renew. Energy*, 28:1597–1615, 2003.

[15] K.S. Ong. A mathematical model of a solar chimney. *Renew. Energy*, 28:1047–1060, 2003.

[16] M.N.A. Bakar, M. Othman, M.H. Din, N.A. Manaf, and H. Jarimi. Design concept and mathematical model of a bi-fluid photovoltaic/thermal (PV/T) solar collector. *Renew. Energy*, 67:153–164, 2014.

[17] O. A. Bég, N. Ali, A. Zaman, E.T.A. Bég, and A. Sohail. Computational modeling of heat transfer in an annular porous medium solar energy absorber with the P1-radiative differential approximation. *J. Taiwan Inst. Chem. Eng.*, 66:258–268, 2016.

[18] Y. Cengel and A. Ghajar. *Heat and Mass Transfer: Fundamentals and Applications*. McGraw-Hill, 5 edition, 2015.

[19] C.M. Sabliov, D.A. Salvi, and D. Boldor. High frequency electromagnetism, heat transfer and fluid flow coupling in ANSYS multiphysics. *J. Microwave Power Electromagnetic Energy*, 41(4):5–17, 2007.

[20] D. Salvi, D. Boldor, J. Ortego, G.M. Aita, and C.M. Sabliov. Numerical modeling of continuous flow microwave heating: a critical comparison of COMSOL and ANSYS. *J. Microwave Power Electromagnetic Energy*, 44(4):187–197, 2010.

[21] S. Demjanenko, K. Nowak, R. Northrup, S. Bogachev, E.M. Kiley, D. Bouvard, S.L. Weekes, and V.V. Yakovlev. Interpolation algorithms for interfacing FDTD and FEM meshes in multiphysics modeling of microwave sintering. In *Proc. 12th Seminar: Computer Modeling in Microwave Engineering and Applications - Advances in Modeling of Microwave Sintering*, pages 62–64, (Grenoble, France, March 2010).

[22] D. Salvi, D. Boldor, G.M. Aita, and C.M. Sabliov. COMSOL multiphysics model for continuous flow microwave heating of liquids. *J. Food Eng.*, 104:422–429, 2011.

[23] J.M. Osepchuck. A history of microwave heating applications. *IEEE Trans. Microwave Theory Techniques*, MTT-32:1200–1224, 1984.

[24] L.A. Campañone and N.E. Zaritzky. Mathematical analysis of microwave heating process. *J. Food Eng.*, 69:359–368, 2005.

[25] F. Marra, J. Lyng, V. Romano, and B. McKenna. Radio-frequency heating of foodstuff: solution and validation of a mathematical model. *J. Food Eng.*, 79:998–1006, 2007.

[26] L. Zhou, V.M. Puri, R.C. Anantheswaran, and G. Yeh. Finite element modeling of heat and mass transfer in food materials during microwave heating - model development and validation. *J. Food Eng.*, 25:509–529, 1995.

[27] M.R. Booty, J.K. Bechtold, and G.A. Kriegsmann. Microwave-induced combustion: a one-dimensional model. *Combust. Theory Modeling*, 2:57–80, 1998.

[28] B.S. Tilley and G.A. Kriegsmann. Microwave-enhanced vapor infiltration: a sharp interface model. *J. Eng. Math.*, 41:33–54, 2001.

[29] G.A. Kriegsmann. Electric discharge sintering: a mathematical model. *SIAM J. Appl. Math.*, 68(6):1503–1517, 2008.

[30] E.M. Kiley. *Reduced-dimensional coupled electromagnetic, thermal, and mechanical models of microwave sintering.* PhD thesis, Worcester Polytechnic Institute, 2016.

[31] C. Maniére, T. Zahrah, and E.A. Olevsky. Inherent heating instability of direct microwave sintering process: Sample analysis for porous 3Y-ZRO$_2$. *Scripta Materialia*, 128:49–52, 2017.

[32] D.E. Clark and W.H. Sutton. Microwave processing of materials. *Annu. Rev. Mater. Sci.*, 26:299–331, 1996.

[33] Y.V. Bykov, K.I. Rybakov, and V.E. Semenov. High-temperature microwave processing of materials. *J. Phys. D: Appl. Phys.*, 34:R55–R75, 2001.

[34] S.P. Kochhar and A.P. Singh. Developments in microwave processing of materials. *Asian J. Chem.*, 23(8):3307–3312, 2011.

[35] P. Rattanadecho and W. Klinbun. Numerical analysis of natural convection in porous media subjected to electromagnetic energy using local thermal nonequilibrium (LTNE) models. *Drying Tech.*, 30:1896–1905, 2012.

[36] R.R. Mishra and A.K. Sharma. Microwave-material interaction phenomena: heating mechanisms, challenges and opportunities in material processing. *Composites:Part A*, 81:78–97, 2016.

[37] G.A. Kriegsmann. Pattern formation in microwave heated ceramics: cylinders and slabs. *IMA J. Appl. Math.*, 66:1–32, 2001.

[38] V.V. Yakovlev. Effect of frequency alteration regimes on the heating patterns in a solid-state-fed microwave cavity. *J. Microwave Power and Electromagnetic Energy*, 52(1):31–44, 2018.

[39] G.A. Kriegsmann, M.E. Brodwin, and D.G. Watters. Microwave heating of a ceramic halfspace. *SIAM J. Appl. Math.*, 50(4):1088–1098, 1990.

[40] N. Gupta, V. Midha, V. Balakotaiah, and D.J. Economou. Bifurcation analysis of thermal runaway in microwave heating of ceramics. *J. Electrochemical Soc.*, 146(12):4659–4665, 1999.

[41] M. Willert-Porada. *Advances in Microwave and Radio Frequency Proceedings*. Springer, 2006.

[42] G. Roussy, A. Bennani, and J. Thiebaut. Temperature runaway of microwave irradiated materials. *J. Appl. Phys.*, 62:1167–1170, 1987.

[43] K.G. Ayappa, H.T. Davis, G. Crapiste, E.A. Davis, and J. Gordon. Microwave heating: an evaluation of power formulations. *Chem. Eng. Sci.*, 46(4):1005–1016, 1991.

[44] J.M. Hill and M.J. Jennings. Formulation of model equations for heating by microwave radiation. *Appl. Math. Modeling*, 17:389–379, 1993.

[45] J.A. Pelesko and G.A. Kriegsmann. Microwave heating of ceramic laminates. *J. Eng. Math.*, 32:1–18, 1997.

[46] X. Wu. *Experimental and theoretical study of microwave heating of thermal runaway materials*. PhD thesis, Virginia Polytechnic Institute, 2002.

[47] G.A. Kriegsmann. Thermal runaway and its control in microwave heated ceramics. *MRS Proc.*, 269, 1992.

[48] X. Wu, J.R. Thomas, and W.A. Davis. Control of thermal runaway in microwave resonant cavities. *J. Appl. Phys.*, 92(6):3374–3380, 2002.

[49] V.E. Semenov and N.A. Zharova. Thermal runaway and hot spots under controlled microwave heating. *Adv. Microwave Radio Frequency Processing*, pages 482–490, 2006.

[50] L. ChangJun and D. Sheen. Analysis and control of the thermal runaway of ceramic slab under microwave heating. *Sci. China Ser. E-Tech. Sci.*, 51(12):2233–2241, 2008.

[51] J.M. Hill and T.R. Marchant. Modelling microwave heating. *Appl. Math. Modeling*, 20:3–15, 1996.

[52] S. Poisson. Second mémoire sur la théorie du magnétisme. *Mem. Acad. France*, 5, 1822.

[53] J. Maxwell. *A Treatise on Electricity and Magnetism*. Clarendon Press, Oxford, 1881.

[54] A. Einstein. Eine neue bestimmung der molekuldimensionen. *Ann. Phys.*, 324(2):289–306, 1906.

[55] R.M. Bowen. *Continuum Physics, Chap. Theory of Mixtures*. New York: Academic Press, 1976.

[56] A. Sihvola. *Electromagnetic Mixing Formulas and Applications*, volume 47 of *Electromagnetic Waves*. The Institution of Electrical Engineers, 1999.

[57] Y. Davit, C.G. Bell, H.M. Byrne, L.A.C. Chapman, L.S. Kimpton, G.E. Lang, K.H.L. Leonard, J.M. Oliver, N.C. Pearson, R.J. Shipley, S.L. Waters, J.P. Whiteley, B.D. Wood, and M. Quintard. Homogenization via formal multiscale asymptotics and volume averaging: How do the two techniques compare? *Advances in Water Resources*, 62 (part B):178–206, 2013.

[58] I. Babŭska. *Homogenization and its Application. Mathematical and Computational Problems, Numerical Solution of Partial Differential Equations III*. Academic Press, 1976.

[59] F.C. Karal Jr. and J.B. Keller. Elastic, electromagnetic, and other waves in a random medium. *J. Math. Phys.*, 5(4):537–547, 1964.

[60] E. Sanchez-Palencia. Solutions périodiques par rapport aux variables d'espaces et applications. *C R Acad. Sci. Paris*, 271:A1129–32, 1970.

[61] A. Bensoussan, J.L. Lions, and G. Papanicolaou. *Asymptotic Analysis for Periodic Structures*. AMS Chelsea Publishing, 1978.

[62] F. Murat. *H-convergence*. Séminaire d'Analyse Fonctionnelle et Numérique d'Alger, 1977.

[63] L. Tartar. *Cours Peccot*. Collège de France, 1977.

164

[64] G. Nguetseng. A general convergence result for a functional related to the theory of homogenization. *SIAM J. Math. Anal.*, 20(3):608–623, 1989.

[65] G. Allaire. Homogenization and two-scale convergence. *SIAM J. Math. Anal.*, 23(6):1482–1518, 1992.

[66] E. Frénod. Two-scale convergence. *ESAIM: Proceedings*, 38:1–35, December 2012.

[67] T.F. Krauss and R.M. De La Rue. Photonic crystals in the optical regime - past, present and future. *Progress Quantum Electronics*, 23:51–96, 1999.

[68] P. Markos and C.M. Soukoulis. *Wave Propagation: From Electrons to Photonic Crystals and Left-handed Materials*. Princeton University Press, 2008.

[69] A. Kirchner, K. Busch, and C.M. Soukoulis. Transport properties of random arrays of dielectric cylinders. *Phys. Rev. B*, 57(1):277–288, 1998.

[70] P. Halevi, A.A. Krokhin, and J. Arriaga. Photonic crystal optics and homogenization of 2D periodic composites. *Phys. Rev. Lett.*, 82(4):719–722, 1999.

[71] A.A. Krokhin, P. Halevi, and J. Arriaga. Long-wavelength limit (homogenization) for two-dimensional photonic crystals. *Phys. Rev. B*, 65, 2002.

[72] G.A. Kriegsmann. Electromagnetic propagation in periodic porous structures. *Wave Motion*, 36:457–472, 2002.

[73] N. Wellander and G. Kristensson. Homogenization of the Maxwell equations at fixed frequency. *SIAM J. Appl. Math.*, 64(1):170–195, 2003.

[74] D. Sjoberg, C. Engstrom, G. Kristensson, D.J.N. Wall, and N. Wellander. A Floquet-Bloch decomposition of maxwell's equations applied to homogenization. *Multiscale Model. Simul.*, 4(1):149–171, 2005.

[75] S. Guenneau, R. Craster, T. Antonakakis, K. Cherednichenko, and S. Cooper. Homogenization techniques for periodic structures. In Evgeny Popov, editor, *Gratings: Theory and Numeric Applications*, chapter 11. Presses universitaires de Provence (PUP), 2012.

[76] E. Tuncer. Dielectric mixtures - importance and theoretical approaches. *IEEE Electrical Insulation Magazine*, 29(6):49–58, 2013.

[77] A. Sihvola. Homogenization principles and effect of mixing on dielectric behavior. *Photonics and Nanostructures - Fundamentals and Applications*, 11:364–373, 2013.

[78] A.P. Vinogradov and A.V. Merzlikin. On the problem of homogenization one-dimensional systems. *J. Exper. Theor. Phys.*, 94(3):482–488, 2002.

[79] H.T. Banks, V.A. Bokil, D. Cioranescu, N.L. Gibson, G. Griso, and B. Miara. Homogenization of periodically varying coefficients in electromagnetic materials. *J. Sci. Comp.*, 28:191–221, 2005.

[80] Y. Amirat and V. Shelukhin. Homogenization of time harmonic Maxwell equations and the frequency dispersion effect. *J. Math. Pures Appl.*, 95:420–443, 2011.

[81] J. Carbonell, F. Cervera, J. Sánchez-Dehesa, J. Arriaga, L. Gumen, and A. Krokhin. Homogenization of two-dimensional anisotropic dissipative photonic crystal. *Appl. Phys. Lett.*, 97, 2010.

[82] R.V. Craster, J. Kaplunov, and A.V. Pichugin. High-frequency homogenization for periodic media. *Proc. R. Soc. A*, 466:2341–2362, 2010.

[83] E. Cassan, J. Dellinger, X. le Roux, K. Van Do, F. de Fornel, and Benoît Cluzel. Homogenization limit in a graded photonic crystal. *Phys. Rev. B*, 88, 2013.

[84] G.L. Harris. *Properties of Silicon Carbide*. INSPEC, Institution of Electrical Engineers, 1995.

[85] D.J. Griffiths. *Introduction to Electrodynamics*. Pearson Education, 1999.

[86] J.D. Jackson. *Classical Electrodynamics*. John Wiley and Sons, 1999.

[87] G.A. Kriegsmann. Thermal runaway in microwave heated ceramics: a one-dimensional model. *J. Appl. Phys.*, 71(4):1960–1966, 1992.

[88] A.V. Kavokin, J.J. Baumberg, G. Malpuech, and F.P. Laussy. *Microcavities*. Series on semiconductor science and technology. Oxford University Press, 2011.

[89] U.S. Inan and R.A. Marshall. *Numerical Electromagnetics: The FDTD Method*. Cambridge University Press, 2011.

[90] J.H. Mathews and K.D. Fink. *Numerical Electromagnetics: The FDTD Method*. Pearson, 2004.

[91] S.J. Ruuth. Implicit-explicit methods for reaction-diffusion problems in pattern formation. *J. Math. Biology*, 34, 1994.

[92] V. Volpert. *Elliptic Partial Differential Equations, Volume 2: Reaction-Diffusion Equations*, volume 104 of *Monographs in Mathematics*. Birkhauser, 2014.

[93] Y.B. Zeldovich and D.A. Frank-Kamenetskii. *A Theory of Thermal Propagation of Flame*, volume 9. Acta Physicochim, 1938.

[94] P.K. Kundu, I.M. Cohen, and D.R. Dowling. *Fluid Mechanics*. Elsevier, 5 edition, 2012.

[95] National Institute of Standards and Technology. Nist chemistry webbook, srd 69, 2017.

[96] B.S. Tilley, V.C. Yang, J.C. Baiense, and S. Evans. Frequency-dependent thermal resistance of vertical U-tube geothermal heat exchangers. *J. Eng. Math.*, 102(1):131–150, 2017.

[97] L.C. Evans. *Partial Differential Equations*, volume 19 of *Graduate Studies in Mathematics*. American Mathematical Society, 2010.

[98] H. Ni, A.K. Datta, and K.E. Torrance. Moisture transport in intensive microwave heating of biomaterials: a multiphase porous media model. *Inter. J. Heat Mass Transfer*, 42:1501–1512, 1999.

[99] O.D. Makinde and P.Y. Mhone. Heat transfer to MHD oscillatory flow in a channel filled with porous medium. *Rom. J. Phys.*, 50(9-10):931–938, 2005.

[100] W. Klinbun, K. Vafai, and P. Rattanadecho. Electromagnetic field effects on transport through porous media. *Inter. J. Heat Mass Transfer*, 55:325–335, 2012.

[101] W. Klinbun and P. Rattanadecho. Numerical model of microwave driven convection in multilayer porous packed bed using a rectangular waveguide. *J. Heat Transfer*, 134, 2012.

[102] W. Klinbun and P. Rattanadecho. Investigation into heat transfer and fluid flow characteristics of liquid two-layer and emulsion in microwave processing. *Inter. Commun. Heat and Mass Transfer*, 70:115–126, 2016.

[103] S.D. Schampheleire, P.D. Jaeger, K.D. Kerpel, B. Ameel, H. Huisseune, and M.D. Paepe. How to study thermal applications of open-cell metal foam: Experiments and computational fluid dynamics. *Materials*, 9:1–27, 2016.

[104] V.G. Veselago. The electrodynamics of substances with simultaneously negative values of $\epsilon$ and $\mu$. *Soviet Physics Uspekhi*, 10(4):509, 1968.

[105] D. Maystre. Getting effective permittivity and permeability equal to -1 in 1d dielectric photonic crystals. *J. Modern Optics*, 53(13):1901–1917, 2006.

[106] R.A. Depine, M.L. Martínez-Ricci, J.A. Monsoriu, E. Silvestre, and P. Andrés. Zero permeability and zero permittivity band gaps in 1d metamaterial photonic crystals. *Physics Letters A*, 364:352–355, 2008.

[107] G. Ji-Yong, C. Hong, L. Hong-Qiang, and Z. Ye-Wen. Effective permittivity and permeability of one-dimensional dielectric photonic crystal within a band gap. *Chin. Phys. Soc.*, 17(7):2544–2552, 2008.

[108] L. Junyi and D.S. Balint. An inverse method to determine the dispersion curves of periodic structures based on wave superposition. *J. Sound and Vibration*, 350:41–72, 2015.

APPENDICES

# APPENDIX A

## IDENTITIES AND THEOREMS

**Vector Identities**

$$\nabla(fg) = f\nabla g + g\nabla f \tag{I.1}$$

$$\nabla \cdot (f\mathbf{v}) = f\nabla \cdot \mathbf{v} + \mathbf{v} \cdot \nabla f \tag{I.2}$$

$$\nabla \times \nabla \times \mathbf{v} = \nabla(\nabla \cdot \mathbf{v}) - \nabla^2 \mathbf{v} \tag{I.3}$$

$$\nabla(\mathbf{v} \cdot \mathbf{w}) = (\mathbf{v} \cdot \nabla)\mathbf{w} + (\mathbf{w} \cdot \nabla)\mathbf{v} + \mathbf{v} \times (\nabla \times \mathbf{w}) + \mathbf{w} \times (\nabla \times \mathbf{v}) \tag{I.4}$$

$$\mathbf{A} \cdot (\mathbf{B} \times \mathbf{C}) = \mathbf{B} \cdot (\mathbf{C} \times \mathbf{A}) \tag{I.5}$$

$$\mathbf{u} \times (\nabla \times \mathbf{v}) = \nabla_v(\mathbf{u} \cdot \mathbf{v}) - (\mathbf{u} \cdot \nabla)\mathbf{v} = \mathbf{u} \cdot \nabla\mathbf{v} - \mathbf{u} \cdot (\nabla\mathbf{v})^T \tag{I.6}$$

$\nabla_v$ is called Feynman notation and only applies derivatives to function $v$.

**Tensor Identities**

$$div(\underline{\underline{\mathbf{A}}}) = \nabla \cdot \underline{\underline{\mathbf{A}}}^T \tag{I.7}$$

$$\nabla^2 \mathbf{v} = \text{div}(\text{grad } \mathbf{v}) = \nabla \cdot (\nabla \mathbf{v})^T \tag{I.8}$$

$$\nabla \cdot (f\underline{\underline{\mathbf{A}}}) = f\nabla \cdot \underline{\underline{\mathbf{A}}} + \nabla f \cdot \underline{\underline{\mathbf{A}}} \tag{I.9}$$

$$(\mathbf{v} \cdot \nabla)\mathbf{w} = \mathbf{v} \cdot (\nabla \mathbf{w})^T \tag{I.10}$$

$$\nabla \cdot (\nabla_\xi \mathbf{v})^T = \nabla_\xi \cdot (\nabla \mathbf{v})^T \tag{I.11}$$

**Integral Identities**

$$\int_v \nabla \cdot \mathbf{v} \, dV = \int_{\partial V} \mathbf{v} \cdot \mathbf{n} \, dS \qquad \text{(Divergence Theorem)} \tag{I.12}$$

$$\int_V f\nabla \cdot \mathbf{v} \, dV + \int_V \mathbf{v} \cdot \nabla f \, dV = \int_{\partial V} f\mathbf{v} \cdot \mathbf{n} \, dS \qquad \text{(Divergence Theorem Corollary)} \tag{I.13}$$

$$\int_V \left[ f\nabla^2 g - g\nabla^2 f \right] dV = \int_{\partial V} [f\nabla g - g\nabla f] \cdot \mathbf{n} \, dS \qquad \text{(Green's 2nd Identity)} \tag{I.14}$$

$$\int_V \nabla(fg) \, dV = \int_{\partial V} fg\mathbf{n} \, dS \tag{I.15}$$

$$\int_V f\nabla f \, dV = \frac{1}{2} \int_{\partial V} f^2 \mathbf{n} \, dS \tag{I.16}$$

*Proof.* Proof of Identities (I.15) and (I.16). Apply the Divergence Theorem (I.12) with vector $\mathbf{v} = fg\mathbf{c}$ where $\mathbf{c}$ is a constant vector. By the product rule (I.2),

$$\int_V \nabla \cdot (fg\mathbf{c}) = \int_V \mathbf{c} \cdot \nabla(fg) + \int_V fg\nabla \cdot \mathbf{c}. \tag{I.17}$$

The last integral is zero since $\mathbf{c}$ is constant. Applying the Divergence Theorem gives

$$\int_V \mathbf{c} \cdot \nabla(fg) \, dV = \int_{\partial V} fg\mathbf{c} \cdot \mathbf{n} \, dS \qquad \text{(I.18)}$$

which can be rewritten as

$$\mathbf{c} \cdot \int_V \nabla(fg) \, dV = \mathbf{c} \cdot \int_{\partial V} fg\mathbf{n} \, dS. \qquad \text{(I.19)}$$

Thus the right vectors must be equivalent so we have the identity

$$\int_V \nabla(fg) \, dV = \int_{\partial V} fg\mathbf{n} \, dS. \qquad \text{(I.20)}$$

Apply product rule

$$\int_V f\nabla g \, dV + \int_V g\nabla f \, dV = \int_{\partial V} fg\mathbf{n} \, dS, \qquad \text{(I.21)}$$

and let $f = g$ then we have the identity

$$\int_V f\nabla f \, dV = \frac{1}{2} \int_{\partial V} f^2\mathbf{n} \, dS. \qquad \text{(I.22)}$$

$\square$

## Other Theorems and Proofs

**Proposition 1.** *The Helmholtz operator* $L\mathbf{u} = \nabla^2\mathbf{u} + \gamma_0^2\epsilon'\mathbf{u}$ *on $V$ with $\mathbf{u}$ and $\nabla\mathbf{u}$ periodic on $\partial V$ is self-adjoint.*

*Proof.* The inner product of the Helmholtz operator with vector $\mathbf{v}$ is

$$\langle L\mathbf{u}, \mathbf{v}\rangle = \int_V \left[\nabla^2\mathbf{u} + \gamma_0^2\epsilon'\mathbf{u}\right]\cdot\overline{\mathbf{v}}\,dV = \sum_{i=1}^{3}\int_V \overline{v}_i\nabla^2 u_i\,dV + \int_V \gamma_0^2\epsilon'\mathbf{u}\cdot\overline{\mathbf{v}}\,dV. \qquad (\text{I}.23)$$

Applying product rule (I.2) the inner product becomes,

$$\langle L\mathbf{u}, \mathbf{v}\rangle = \sum_{i=1}^{3}\int_V \nabla\cdot(\overline{v}_i\nabla u_i)\,dV - \sum_{i=1}^{3}\int_V \nabla u_i\cdot\nabla\overline{v}_i\,dV + \int_V \gamma_0^2\epsilon'\mathbf{u}\cdot\overline{\mathbf{v}}\,dV, \qquad (\text{I}.24)$$

and applying divergence theorem (I.12),

$$\langle L\mathbf{u}, \mathbf{v}\rangle = \sum_{i=1}^{3}\int_{\partial V} \overline{v}_i\nabla u_i\cdot\mathbf{n}\,dS - \sum_{i=1}^{3}\int_V \nabla u_i\cdot\nabla\overline{v}_i\,dV + \int_V \gamma_0^2\epsilon'\mathbf{u}\cdot\overline{\mathbf{v}}\,dV. \qquad (\text{I}.25)$$

Apply (I.2) again

$$\langle L\mathbf{u}, \mathbf{v}\rangle = \sum_{i=1}^{3}\int_{\partial V} \overline{v}_i\nabla u_i\cdot\mathbf{n}\,dS - \sum_{i=1}^{3}\left[\int_V \nabla\cdot(u_i\nabla\overline{v}_i)\,dV - \int_V u_i\nabla^2\overline{v}_i\,dV\right] + \int_V \gamma_0^2\epsilon'\mathbf{u}\cdot\overline{\mathbf{v}}\,dV,$$

$$(\text{I}.26)$$

Once more we apply (I.12),

$$\langle L\mathbf{u}, \mathbf{v} \rangle = \sum_{i=1}^{3} \int_{\partial V} \overline{v}_i \nabla u_i \cdot \mathbf{n} \, dS - \sum_{i=1}^{3} \int_{\partial V} u_i \nabla \overline{v}_i \cdot \mathbf{n} \, ds + \int_V u_i \nabla^2 \overline{v}_i \, dV + \int_V \gamma_0^2 \epsilon' \mathbf{u} \cdot \overline{\mathbf{v}} \, dV,$$

(I.27)

which can be rewritten as

$$\langle L\mathbf{u}, \mathbf{v} \rangle = \int_V \mathbf{u} \cdot \left[ \nabla^2 \overline{\mathbf{v}} + \gamma_0^2 \epsilon' \overline{\mathbf{v}} \right] \, dV + \int_{\partial V} \left[ \overline{\mathbf{v}} \cdot \nabla \mathbf{u} - \mathbf{u} \cdot \nabla \overline{\mathbf{v}} \right] \cdot \mathbf{n} \, dS. \qquad (I.28)$$

Finally by periodicity of $\mathbf{u}, \mathbf{v}, \nabla \mathbf{u}, \nabla \mathbf{v}$ the second integral is zero thus it is proved. $\qquad \square$

**Theorem 3.** *(Fredholm Alternative) A linear differential equation $Lu = f$ subject to linear boundary conditions $Bu = 0$ has a solution iff $\langle f, v \rangle = 0 \; \forall v$ satisfying $L^* v = 0$ subject to $B^* v = 0$.*

## APPENDIX B

## TRANSFER MATRIX METHOD

The Transfer Matrix Method (TMM) is used to find exact solutions to the Helmholtz equation on laminate domains at normal incidence. The description of the method is taken from [68]. The Helmholtz equation

$$\frac{\partial^2 E_j}{\partial z^2} + k_j^2 E_j = 0, \tag{I.1}$$

is solved for within each layer domain $j$ and with boundary conditions of continuity and continuity of the derivative. The general solution and the derivative are given by

$$E_j = c_j e^{ik_j z} + d_j e^{-ik_j z} \tag{I.2}$$

$$\frac{\partial E_j}{\partial z} = ik_j c_j e^{ik_j z} - ik_j d_j e^{-ik_j z}. \tag{I.3}$$

We first consider the interaction of the solutions at an interface, $z = z_0$, between regions 1 and 2. Applying the boundary condition give the equations

$$c_1 e^{ik_1 z_0} + d_1 e^{-ik_1 z_0} = c_2 e^{ik_2 z_0} + d_2 e^{-ik_2 z_0}, \tag{I.4}$$

$$ik_1 c_1 e^{ik_1 z_0} - ik_1 d_1 e^{-ik_1 z_0} = ik_2 c_2 e^{ik_2 z_0} - ik_2 d_2 e^{-k_2 z_0}. \tag{I.5}$$
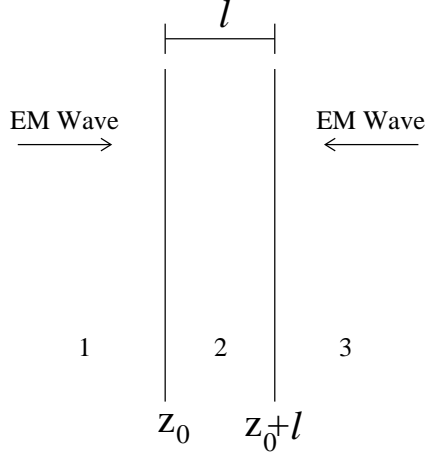
Figure B.1: Transfer Matrix Method: single layer propagation

First we obtain an equation for $d_2$ in terms of $c_1$ and $d_1$ by solving (I.4) for $c_2$ and substituting into (I.5). Next, we can solve for $c_2$ in terms of $c_1$ and $d_1$ by substituting the new equation for $d_2$ into (I.4). The resulting equations are

$$c_2 = \frac{k_2 + k_1}{2k_2} e^{i(k_1 - k_2)z_0} c_1 + \frac{k_2 - k_1}{2k_2} e^{-i(k_2 + k_1)z_0} d_1, \qquad (I.6)$$

$$d_2 = \frac{k_2 - k_1}{2k_2} e^{i(k_2 + k_1)z_0} c_1 + \frac{k_2 + k_1}{2k_2} e^{i(k_2 - k_1)z_0} d_1. \qquad (I.7)$$

This system can be written in matrix notation as

$$\begin{bmatrix} c_2 \\ d_2 \end{bmatrix} = \begin{bmatrix} \frac{k_2+k_1}{2k_2} e^{i(k_1-k_2)z_0} & \frac{k_2-k_1}{2k_2} e^{-i(k_2+k_1)z_0} \\ \frac{k_2-k_1}{2k_2} e^{i(k_2+k_1)z_0} & \frac{k_2+k_1}{2k_2} e^{i(k_2-k_1)z_0} \end{bmatrix} \begin{bmatrix} c_1 \\ d_1 \end{bmatrix}, \qquad (I.8)$$

or rather the system can be written so that the matrix is independent of the spatial location

176

$z_0$ as

$$\begin{bmatrix} c_2 e^{ik_2 z_0} \\ d_2 e^{-ik_2 z_0} \end{bmatrix} = \begin{bmatrix} \frac{k_2+k_1}{2k_2} & \frac{k_2-k_1}{2k_2} \\ \frac{k_2-k_1}{2k_2} & \frac{k_2+k_1}{2k_2} \end{bmatrix} \begin{bmatrix} c_1 e^{ik_1 z_0} \\ d_1 e^{-ik_1 z_0} \end{bmatrix}, \tag{I.9}$$

and this is known as the Transfer Matrix.

Assume now we have another interface. We now have two interfaces corresponding to a single layer of length $l$, and there are now 3 regions. We can similarly write down the transfer matrix for the interaction between regions 2 and 3 as

$$\begin{bmatrix} c_3 e^{ik_3(z_0+l)} \\ d_3 e^{-ik_3(z_0+l)} \end{bmatrix} = \begin{bmatrix} \frac{k_3+k_2}{2k_3} & \frac{k_3-k_2}{2k_3} \\ \frac{k_3-k_2}{2k_3} & \frac{k_3+k_2}{2k_3} \end{bmatrix} \begin{bmatrix} c_2 e^{ik_2(z_0+l)} \\ d_2 e^{-ik_2(z_0+l)} \end{bmatrix}. \tag{I.10}$$

Now we wish to relate the coefficients of region 1 to those of region 3. To achieve this, we first realize there is a simple transfer matrix relating how a wave changes across a homogeneous material, between $z = z_0$ and $z = z_0 + l$. This relationship is given by

$$\begin{bmatrix} c_2 e^{ik_2(z_0+l)} \\ d_2 e^{-ik_2(z_0+l)} \end{bmatrix} = \begin{bmatrix} e^{ik_2 l} & 0 \\ 0 & e^{-ik_2 l} \end{bmatrix} \begin{bmatrix} c_2 e^{ik_2 z_0} \\ d_2 e^{-ik_2 z_0} \end{bmatrix}. \tag{I.11}$$

Now the coefficients $c_3, d_3$ can be related to $c_1, d_1$ by the following matrix transformation,

$$\begin{bmatrix} c_3 e^{ik_3(z_0+l)} \\ d_3 e^{-ik_3(z_0+l)} \end{bmatrix} = \begin{bmatrix} \frac{k_3+k_2}{2k_3} & \frac{k_3-k_2}{2k_3} \\ \frac{k_3-k_2}{2k_3} & \frac{k_3+k_2}{2k_3} \end{bmatrix} \begin{bmatrix} e^{ik_2 l} & 0 \\ 0 & e^{-ik_2 l} \end{bmatrix} \begin{bmatrix} \frac{k_2+k_1}{2k_2} & \frac{k_2-k_1}{2k_2} \\ \frac{k_2-k_1}{2k_2} & \frac{k_2+k_1}{2k_2} \end{bmatrix} \begin{bmatrix} c_1 e^{ik_1 z_0} \\ d_1 e^{-ik_1 z_0} \end{bmatrix}. \tag{I.12}$$

We label we matrix appropriately such that

$$
\begin{bmatrix} c_3 e^{ik_3(z_0+l)} \\ d_3 e^{-ik_3(z_0+l)} \end{bmatrix} = M_{23} M_{22} M_{12} \begin{bmatrix} c_1 e^{ik_1 z_0} \\ d_1 e^{-ik_1 z_0} \end{bmatrix}.
\tag{I.13}
$$

Next, we generalize this to $n$ layers of length $l_j$. Now there are $n+2$ regions starting with $j = 0$ and ending with $j = n+1$. The total length of all the layers is given by $L$. The matrix transformation that relates the coefficients is

$$
\begin{bmatrix} c_{n+1} e^{ik_{n+1}(z_0+L)} \\ d_{n+1} e^{-ik_{n+1}(z_0+L)} \end{bmatrix} = \underbrace{M_{n,n+1} \prod_{i=1}^{n} M_{i,i} M_{i-1,i}}_{M_n} \begin{bmatrix} c_0 e^{ik_0 z_0} \\ d_0 e^{-ik_0 z_0} \end{bmatrix},
\tag{I.14}
$$

where $M_n$ is the transfer matrix. Next, to close the system we introduce incident waves, so $c_0 = E_L$ and $d_{n+1} = E_R$ are known. The system becomes

$$
\begin{bmatrix} c_{n+1} e^{ik_{n+1}(z_0+L)} \\ E_R e^{-ik_{n+1}(z_0+L)} \end{bmatrix} = \begin{bmatrix} M_n^{11} & M_n^{12} \\ M_n^{21} & M_n^{22} \end{bmatrix} \begin{bmatrix} E_L e^{ik_0 z_0} \\ d_0 e^{-ik_0 z_0} \end{bmatrix}.
\tag{I.15}
$$

This 2x2 system can be solved for $c_{n+1}$ and $d_0$ with solutions

$$
d_0 = \frac{1}{M_n^{22} e^{-ik_0 z_0}} \left[ E_R e^{-ik_{n+1}(z_0+L)} - M_n^{21} E_L e^{ik_0 z_0} \right],
\tag{I.16}
$$

$$
c_{n+1} = \frac{1}{e^{ik_{n+1}(z_0+L)}} \left[ M_n^{11} E_L e^{ik_0 z_0} + M_n^{12} d_0 e^{-ik_0 z_0} \right].
\tag{I.17}
$$

Finally, now that both $c_0$ and $d_0$ are known, the rest of the coefficients for all the layers can
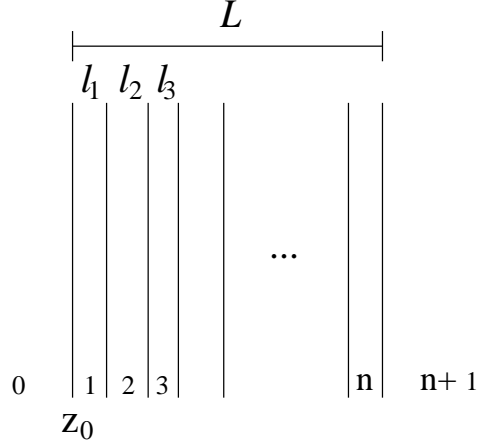
Figure B.2: Transfer Matrix Method: multiple layer propagation

be found using the transfer matrix method,

$$
\begin{bmatrix} c_{j+1}e^{ik_{j+1}\left(z_0+\sum_{i=1}^{j}l_i\right)} \\ d_{j+1}e^{-ik_{j+1}\left(z_0+\sum_{i=1}^{j}l_i\right)} \end{bmatrix} = M_j \begin{bmatrix} c_0 e^{ik_0 z_0} \\ d_0 e^{-ik_0 z_0} \end{bmatrix},
\tag{I.18}
$$

where $M_j = M_{j,j+1} \prod_{i=1}^{j-1} M_{i,i} M_{i-1,i}$.

Consider the example of having an laminate with an odd number of alternating layers. Let the number of layers be $2n+1$ and let the lengths of each layers be given by $l_1$, $l_2$ and wavenumber $k_1$, $k_2$ corresponding to either material 1 or material 2. Let the semi-infinite region be free space with wavenumber $k_0$ and let the position of the first interface be given by $z_0$. This problem requires two transfer matrices with free space, two transfer matrices

between material 1 to 2 or material 2 to 1, and two homogeneous transfer matrices,

$$M_{01} = \begin{bmatrix} \frac{k_1+k_0}{2k_1} & \frac{k_1-k_0}{2k_1} \\ \frac{k_1-k_0}{2k_1} & \frac{k_1+k_0}{2k_1} \end{bmatrix}, \qquad M_{10} = \begin{bmatrix} \frac{k_0+k_1}{2k_0} & \frac{k_0-k_1}{2k_0} \\ \frac{k_0-k_1}{2k_0} & \frac{k_0+k_1}{2k_0} \end{bmatrix}, \qquad (\text{I.19})$$

$$M_{12} = \begin{bmatrix} \frac{k_2+k_1}{2k_2} & \frac{k_2-k_1}{2k_2} \\ \frac{k_2-k_1}{2k_2} & \frac{k_2+k_1}{2k_2} \end{bmatrix}, \qquad M_{21} = \begin{bmatrix} \frac{k_1+k_2}{2k_1} & \frac{k_1-k_2}{2k_1} \\ \frac{k_1-k_2}{2k_1} & \frac{k_1+k_2}{2k_1} \end{bmatrix}, \qquad (\text{I.20})$$

$$M_{11} = \begin{bmatrix} e^{ik_1 l_1} & 0 \\ 0 & e^{-ik_1 l_1} \end{bmatrix}, \qquad M_{22} = \begin{bmatrix} e^{ik_2 l_2} & 0 \\ 0 & e^{-ik_2 l_2} \end{bmatrix}. \qquad (\text{I.21})$$

The total length of the laminate is $L = (n+1)l_1 + nl_2$. The transfer matrix method then gives the relationship between outer free space coefficients as

$$\begin{bmatrix} c_{n+1}e^{ik_0(z_0+L)} \\ d_{n+1}e^{-ik_0(z_0+L)} \end{bmatrix} = M_{10}M_{11} \left( \prod_{i=1}^{n} M_{21}M_{22}M_{12}M_{11} \right) M_{01} \begin{bmatrix} c_0 e^{ik_0 z_0} \\ d_0 e^{-ik_0 z_0} \end{bmatrix}. \qquad (\text{I.22})$$

Then, once $c_0$ and $d_0$ are known, the rest of the coefficients can be found.

For $j+1$ odd

$$\begin{bmatrix} c_{j+1}e^{ik_1\left(z_0+\frac{j}{2}(l_1+l_2)\right)} \\ d_{j+1}e^{-ik_1\left(z_0+\frac{j}{2}(l_1+l_2)\right)} \end{bmatrix} = \left( \prod_{i=1}^{\frac{j}{2}} M_{21}M_{22}M_{12}M_{11} \right) M_{01} \begin{bmatrix} c_0 e^{ik_0 z_0} \\ d_0 e^{-ik_0 z_0} \end{bmatrix}. \qquad (\text{I.23})$$

For $j+1$ even the coefficients are found by

$$\begin{bmatrix} c_{j+1}e^{ik_2\left(z_0+l_1+\frac{j-1}{2}(l_1+l_2)\right)} \\ d_{j+1}e^{-ik_2\left(z_0+l_1+\frac{j-1}{2}(l_1+l_2)\right)} \end{bmatrix} = M_{12}M_{11} \left( \prod_{i=1}^{\frac{j-1}{2}} M_{21}M_{22}M_{12}M_{11} \right) M_{01} \begin{bmatrix} c_0 e^{ik_0 z_0} \\ d_0 e^{-ik_0 z_0} \end{bmatrix}. \qquad (\text{I.24})$$

APPENDIX C

MATLAB CODE

Numerical solutions and simulations are implemented using MATLAB code compiled and executed on MATLAB version 9.2.0.556344 (R2017a)

C.1  main files

```
%PROGRAM: PowerResponse.m
%FUNCTION CALLS: ParamDeclare.m, Emag3.m
%DESCRIPTION: Generates power response curve for a triple layer laminate
%using a volumetric averaging to find an analytical solution for the curve.
%Determines turning points (TP) and plots solid lines for positive sloped
%branches (stable) and dashed lines for negative sloped branches (unstable)

clear; %Clears all declared parameters and variables

%%%%%%%%%%%%%%%%%%%%%%%%%%%%%%%%%%%%%%%%%%%%%%%%%%%%%%%%%%%%%%%%%%%%%%%%%%%%
%%%%%%%%%%%%%%%%%%%%%%%%%%% DECLARE MODEL PARAMETERS %%%%%%%%%%%%%%%%%%%%%%%%%
%%%%%%%%%%%%%%%%%%%%%%%%%%%%%%%%%%%%%%%%%%%%%%%%%%%%%%%%%%%%%%%%%%%%%%%%%%%%

[Param,Fcn] = ParamDeclare; %Retrieves parameters from master list

%Initiliaze parameters
for j=1:length(Param)
    evalc([Param{j,1},'=',Param{j,2}]);
end
for j=1:length(Fcn)
    evalc(Fcn{j});
end

L =@(T) 2.*K.*Bi.*T+2.*K.*Q.*((T+1).^4-1); %External Losses
Pow =@(T) L(T)./(lossm(T).*Emag3(T,Param,Fcn)); %Power Response Curve

%Temperature Range for Plotting Power Response Curve
T0 = 0;
```

181

```
Tf = 7;
T = T0:1e-3:Tf;

%%%%%%%%%%%%%%%%%%%%%%%%%%%%%%%%%%%%%%%%%%%%%%%%%%%%%%%%%%%%%%%%%%%%%%%%%%%
%%%%%%%%%%%%%%%%%%%%%%% Plots Power Response Curve %%%%%%%%%%%%%%%%%%%%%%%%
%%%%%%%%%%%%%%%%%%%%%%%%%%%%%%%%%%%%%%%%%%%%%%%%%%%%%%%%%%%%%%%%%%%%%%%%%%%
figure(1) %open figure

UniformPwrRes(:,1)=Pow(T); %Create vector of power values
UniformPwrRes(:,2)=T; %Create vector of temperature calues
SSlength=length(T); %Number of points in the curve

TPcount = 1; %Initilize TP counter
TPindexOLD = 1; %Initilize TP counter for previous TP

%LOOP: Loops over the points in the curve and determines the TP location by
%finding when the numerical derivative changes sign
for i=2:SSlength-1
    %First order Forward Difference
    Diff1 = (UniformPwrRes(i+1,1)-UniformPwrRes(i,1))/(UniformPwrRes(i+1,2)...
-UniformPwrRes(i,2));
    %First order Backward Difference
    Diff2 = (UniformPwrRes(i,1)-UniformPwrRes(i-1,1))/(UniformPwrRes(i,2)...
-UniformPwrRes(i-1,2));

    if Diff1 >=0 && Diff2 <= 0
        %Derivative changes from negative to positive. Plots the previous
        %branch of negative slope with a dahsed line (unstable branch)
        TPindex(TPcount) = i; %Assigns index i as a TP
        plot(UniformPwrRes(TPindexOLD:TPindex(TPcount),1)...
        ,UniformPwrRes(TPindexOLD:TPindex(TPcount),2)*300+300...
        ,'--k','LineWidth',2);
        hold on
        TPindexOLD = TPindex(TPcount); %Assigns index i as the OLD index
        TPcount = TPcount + 1; %Increases count of the TPs
    elseif Diff1 <=0 && Diff2 >=0
        %Derivative changes from positive to negative. Plots the previous
        %branch of positive slope with a solid line (stable branch)
        TPindex(TPcount) = i;%Assigns index i as a TP
        plot(UniformPwrRes(TPindexOLD:TPindex(TPcount),1)...
        ,UniformPwrRes(TPindexOLD:TPindex(TPcount),2)*300+300...
        ,'-k','LineWidth',2);
        hold on
```

```
        TPindexOLD = TPindex(TPcount); %Assigns index i as the OLD index
        TPcount = TPcount + 1; %Increases count of the TPs
    end
end
%Plots the last branch of the cure
plot(UniformPwrRes(TPindexOLD:SSlength,1)...
,UniformPwrRes(TPindexOLD:SSlength,2)*300+300,'-k','LineWidth',2);
xlabel('Power (P)')
ylabel('Temperature (K)')
set(gca,'FontSize',18)
```

```
%PROGRAM: Solution_LowPeclet.m
%FUNCTION CALLS: ParamDeclare.m, Emag3.m, tridiag.m
%DESCRIPTION: Solves the leading order advection-diffusion equation governing
%lossy plate placed between two fluid channels exhibiting Poiseuille flow
%calculated by an asymptotic volumetric average of the 1D advection-diffusion
%equation with Electromagnetic heating.  An Implicit-Explicit method is used
%to find a temporal solution. The Crank-Nicolson method is used on linear
%terms, the Upwinding method for the advection term and the Adams-Bashforth
%method on the nonlinear terms. This code has a lot of options. Setting
%options c1 through c5 between 0 or 1 we can turn on and off particular
%features of the problem quickly and easily without altering parameters.
%Changing c6 between 0,1, or 2 we can switch boundary conditions easily. We
%also have the feature of restricting the application of the source to a
%subinterval of the overall domain. This is done by modifying the variables
%xLow and xHigh to the desired subdomain of the overall domain [0,xLength].
%If this feature is used then c7 is used to determine the criterion at
%which the relative error is sufficiently small to stop the code, either
%when the error over the whole domain is small enough or just the error
%over the subdomain is small enough. The red dashed lines in the solution
%plot shows the subdomain on which the source is being applied. Later in
%the code there is a section that can be uncommented that will numerically
%determine the wave velocity of a traveling wave solution but is only
%useful if the user sets up conditions for existence of a traveling wave
%solution. Additionally the program plots the uniform heating power
%response curve as well as the solution in the phase plane.

clear; %Resets all parameters and declarations

%%%%%%%%%%%%%%%%%%%%%%%%%%%%%%%%%%%%%%%%%%%%%%%%%%%%%%%%%%%%%%%%%%%%%%%%%%%%%
%%%%%%%%%%%%%%%%%%%%%%%%%% DECLARE MODEL PARAMETERS %%%%%%%%%%%%%%%%%%%%%%%%%
%%%%%%%%%%%%%%%%%%%%%%%%%%%%%%%%%%%%%%%%%%%%%%%%%%%%%%%%%%%%%%%%%%%%%%%%%%%%%

[Param,Fcn] = ParamDeclare; %Retrieves parameters from master list

%INITIALIZE PARAMETERS FROM Param AND Fcn FOR USE IN PROGRAM
for j=1:length(Param)
    evalc([Param{j,1},'=',Param{j,2}]);
end
for j=1:length(Fcn)
    evalc(Fcn{j});
end

%%%%%%%%%%%%%%%%%%%%%%%%%%%%%%%%%%%%%%%%%%%%%%%%%%%%%%%%%%%%%%%%%%%%%%%%%%%%%
```

```
%%%%%%%%%%%%%%%%%%%% PROGRAM INITIALIZATIONS %%%%%%%%%%%%%%%%%%%%%%%%%%%
%%%%%%%%%%%%%%%%%%%%%%%%%%%%%%%%%%%%%%%%%%%%%%%%%%%%%%%%%%%%%%%%%%%%%%%%%
dx = 1e-2; %Spatial Step Size
dt = dx.^2/2; %Temporal Step Size
dt = 0.005;

NMAX = 1e5; %Maximum number of time steps
tol = 1e-6; %Exit relative error tolerance for Steady State
xLength = 10; %length of truncated channel
tPrint = 500; %Number of time steps between solution plots

%PHYSICAL PROCESS ACTIVATION (0=off, 1=on)
%By setting values to 0 or 1 we can turn specific physical processes on or
%off to easily examine simple cases or the full model
c1 = 1; %Diffusion
c2 = 1; %Advection
c3 = 1; %Source Power
c4 = 1; %Boundary Conducttion
c5 = 0; %Boundary Radiaton
c6 = 1; %Inlet/Outlet Condition (c6=0,1,2 Insulating, Dirichlet, Flux)
c7 = 1; %Time Loop Exit Consition (c7=0 max err whole domain, ...
        %c7=1 max err subdomain)

%SOURCE SEGMENTATION
%[xLow xHigh] = interval of applied sources
%H1 = heaviside for EM source, H2 = heaviside for Thermal loss
xLow = 0;
xHigh = xLength; %xLength; %Use xLength for the full domain;
H1 =@(x) heaviside(x-xLow).*heaviside(-x+xHigh);
H2 =@(x) heaviside(x-xLow).*heaviside(-x+xHigh);

%%%%%%%%%%%%%%%%%%%%%%%%%%%%%%%%%%%%%%%%%%%%%%%%%%%%%%%%%%%%%%%%%%%%%%%%%
%%%%%%%%%%%%%%%%%%%% DO NOT CHANGE BEYOND THIS POINT %%%%%%%%%%%%%%%%%%%%
%%%%%%%%%%%%%%%%%%%%%%%%%%%%%%%%%%%%%%%%%%%%%%%%%%%%%%%%%%%%%%%%%%%%%%%%%

%NUMERICAL INITIALIZATIONS
%X-DOMAIN
xi = 0;
xf = xLength;
x = xi:dx:xf; %Discretized nondimensional domain
IMAX = length(x);
ILow = (xLow-xi)./dx+1;
IHigh = (xHigh-xi)./dx+1;
```

```matlab
Idom = ILow:IHigh;
T = zeros(IMAX,2); %Next Time Temperature Solution (to be found)

%Z-DOMAIN
lam0SCALED = lam0/l; %Nondimensional wavelength
dz = (lam0SCALED)/100;
z1 = -2*(lam-1):dz:-(lam-1);
z2 = -(lam-1):dz:0;
z3 = 0:dz:1;
z4 = 1:dz:lam;
z5 = lam:dz:2*lam-1;

%Determines locates of steady states in power response for given power P
Temp = 0:.01:7.2;
PowRoot = (2*K*Bi*Temp+2*K*Q*((Temp+1).^4-1))./(lossm(Temp)...
.*Emag3(Temp,Param,Fcn))-P;
Pcount = 1;
for i=1:length(Temp)-1
   if PowRoot(i+1)*PowRoot(i)<=0
       Troot(Pcount) = 0.5*(Temp(i+1)+Temp(i));
       PTroot(Pcount) = (PowRoot(i+1)-PowRoot(i))./(Temp(i+1)-Temp(i));
       Pcount = Pcount+1;
   end
end

%%%%%%%%%%%%%%%%%%%%%%%%%%%%%%%%%%%%%%%%%%%%%%%%%%%%%%%%%%%%%%%%%%%%%%%%%
%%%%%%%%%%%%%%%%%%%%%%%%%%%% Initial conditions %%%%%%%%%%%%%%%%%%%%%%%%%
%%%%%%%%%%%%%%%%%%%%%%%%%%%%%%%%%%%%%%%%%%%%%%%%%%%%%%%%%%%%%%%%%%%%%%%%%
Tinit = Troot(length(Troot)); %Initital temperature


%%%%%%%%%%%%%%%%%%%%%%%%%%%%%%%%%%%%%%%%%%%%%%%%%%%%%%%%%%%%%%%%%%%%%%%%%
%%%%%%%%%%%%%%%%%%%%%%%%%%%% Boundary conditions %%%%%%%%%%%%%%%%%%%%%%%%
%%%%%%%%%%%%%%%%%%%%%%%%%%%%%%%%%%%%%%%%%%%%%%%%%%%%%%%%%%%%%%%%%%%%%%%%%
Uplus = max(Ue,0);
Uminus = min(Ue,0);

if c6 == 0
    %%%%%%%%%%%%%%%%%%%%%%%%%% Insulating Condition %%%%%%%%%%%%%%%%%%%%%%%%%%
    %sets insulating boundary conditions on both sides

    %Left Condition
    aL = 1;
```

```matlab
    bL = 0;
    cL = 0;
    %Right Condition
    aR = 1;
    bR = 0;
    cR = 0;
elseif c6 == 1
    %%%%%%%%%%%%%%%%%%%%%%% Dirichlet Condition %%%%%%%%%%%%%%%%%%%%%%%%%%
    %sets inlet temperature to ambient temperature

    %Left Condition
    aL = 0;
    bL = 1;
    cL = 0; %Troot(length(Troot)-2); %Uncomment for exact traveling wave
    %Right Condition
    aR = Uplus./Ue;
    bR = -Uminus./Ue;
    cR = 0;
elseif c6 == 2
    %%%%%%%%%%%%%%%%%%%%%%%%% Robin Condition %%%%%%%%%%%%%%%%%%%%%%%%%%%
    %set up so upstream condition is continuity of flux and downstream
    %condition is insulated no matter what direction the fluid is flowing

    %Left Condition
    aL = 1+2*(lam-1);
    bL = -Pe*Uplus;
    bL = -Pe*Uplus+Pe*Uminus;
    cL = 0;
    %Right Condition
    aR = 1+2*(lam-1);
    bR = -Pe*Uminus;
    bR = -Pe*Uminus+Pe*Uplus;
    bR = 0;
    cR = 0;
end

%%%%%%%%%%%%%%%%%%%%%%%%%%%%%%%%%%%%%%%%%%%%%%%%%%%%%%%%%%%%%%%%%%%%%%%%%%
%%%%%%%%%%%%%%%%%%%%%%%%%%% THERMAL SOLUTION %%%%%%%%%%%%%%%%%%%%%%%%%%%%%
%%%%%%%%%%%%%%%%%%%%%%%%%%%%%%%%%%%%%%%%%%%%%%%%%%%%%%%%%%%%%%%%%%%%%%%%%%

%MATRIX COEFFICIENT GROUPS
s1 = c1.*(B.*dt)./(2.*A.*dx.^2);
s2plus = c2.*(K.*Pe.*Uplus.*dt)./(A.*dx);
```

```
s2minus = c2.*(K.*Pe.*Uminus.*dt)./(A.*dx);
s3 = c4.*(K.*Bi.*dt./A).*H2(x');


%MATRIX EQUATION INILIATIZATIONS
L = ones(1,IMAX); %left diagonal
M = ones(1,IMAX); %middle diagonal
R = ones(1,IMAX); %right diagonal
RHS = zeros(1,IMAX); %right hand side


%INITIAL CONDITON
T(:,1) = Tinit;


%NONLINEAR TERMS FOR INITIAL CONDITION
sig = lossm(T(:,1));
E = Emag3(T(:,1),Param,Fcn).*H1(x');
N1 = c3.*(P./A).*sig.*E-c5.*(2.*K.*Q./A).*((T(:,1)+1).^4-1).*H2(x');


%%%%%%%%%%%%%%%%%%%% TIME STEP 1 SOLUTION %%%%%%%%%%%%%%%%%%%%%%%%%%%%
%Uses Crank-Nicolson on linear terms and uses Euler's Method on
%nonlinear terms. This is necessary since the Adams-Bashforth method
%used hearafter requires solutions from two previoius time steps


%FIRST ROW OF MATRIX
M(1) = bL-aL./dx;
R(1) = aL./dx;
RHS(1) = cL;
%MAIN BLOCK OF MATRIX
for i=2:IMAX-1
    L(i) = -s1;
    M(i) = 1+2.*s1+s3(i);
    R(i) = -s1;
    RHS(i) = (s1+s2plus).*T(i-1,1)+(1-2.*s1-s3(i)-s2plus+s2minus)...
.*T(i,1)+(s1-s2minus).*T(i+1,1)+dt*N1(i);
end
%LAST ROW OF MATRIX
L(IMAX) = -aR./dx;
M(IMAX) = aR./dx+bR;
RHS(IMAX) = cR;


%NEXT TIME STEP SOLUTION
T(:,2)= tridiag(L,M,R,RHS);


%UPDATE TEMPERATURE SOLUTIONS
```

```matlab
T(:,1)=T(:,2);
sig = lossm(T(:,2));
E = Emag3(T(:,2),Param,Fcn).*H1(x');
N2 = N1;
N1 = c3.*(P./A).*sig.*E-c5.*(2.*K.*Q./A).*((T(:,2)+1).^4-1).*H2(x');


%%%%%%%%%%%%%%%%%%%%%%%%% TIME LOOP %%%%%%%%%%%%%%%%%%%%%%%%%%%%%%%%%%
relerr = 1; %Initialization of relative error
tcount = 2; %Time Step Counter

%LOOP: Loops over time until tolerance is met or max time step is reached
while relerr > tol && tcount < NMAX
    tcount = tcount + 1; %Update time step

    %FIRST ROW OF MATRIX
    M(1) = bL-aL./dx;
    R(1) = aL./dx;
    RHS(1) = cL;
    %MAIN BLOCK OF MATRIX
    for i=2:IMAX-1
        L(i) = -s1;
        M(i) = 1+2.*s1+s3(i);
        R(i) = -s1;
        RHS(i) = (s1+s2plus).*T(i-1,1)+(1-2.*s1-s3(i)-s2plus+s2minus)...
.*T(i,1)+(s1-s2minus).*T(i+1,1)+(dt./2).*(3*N1(i)-N2(i));
    end
    %LAST ROW OF MATRIX
    L(IMAX) = -aR./dx;
    M(IMAX) = aR./dx+bR;
    RHS(IMAX) = cR;

    %NEXT TIME STEP SOLUTION
    T(:,2)= tridiag(L,M,R,RHS);

        %use with no diffusion
        if c1 == 0
            T(1,2) = T(2,2);
        end

    %CALCULATE RELATIVE ERROR FOR STEADY STATE CONVERGENCE
    if c7 == 0
        relerr = max(abs(T(:,2)-T(:,1)))./max(abs(T(:,2)));
    elseif c7 == 1
```

```
        relerr = max(abs(T(Idom,2)-T(Idom,1))))./max(abs(T(Idom,2)));
end

%UPDATE TEMPERATURE SOLUTIONS
T(:,1)=T(:,2);
N2 = N1;
sig = lossm(T(:,2));
E = Emag3(T(:,2),Param,Fcn).*H1(x');
N1 = c3.*(P./A).*sig.*E-c5.*(2.*K.*Q./A).*((T(:,2)+1).^4-1).*H2(x');

%EVOLUTION OF TEMPERATURE PROFILE IN TIME
if mod(tcount,tPrint) == 0

    figure(1)
    set(gca,'fontsize',18)
    title(['Time elapse: ' num2str(dt*tcount) ' nondim']);
    xlabel('Streamwise Length (x)')
    ylabel('Temperature (T)')
    plot(x,T(:,2)*300+300,'b','LineWidth',2)
    hold on
    plot([xLow xLow],[0 max(T(:,2)*300+300)],'--r',[xHigh xHigh]...
    ,[0 max(T(:,2)*300+300)],'--r','Linewidth',2);
    hold on

    %Power Response Calculation
    Temp = 0:.01:6.5;
    PowRes = (2*K*Bi*Temp+2*K*Q*((Temp+1).^4-1))./(lossm(Temp)...
    .*Emag3(Temp,Param,Fcn));
    %
    if psign == -1
        IEXIT = xHigh/dx+1;
        PowResDiff = (2*K*Bi*Temp+2*K*Q*((Temp+1).^4-1)+K*Pe*Ue...
        .*((25*T(IEXIT,2)-48*T(IEXIT-1,2)+36*T(IEXIT-2,2)...
        -16*T(IEXIT-3,2)+3*T(IEXIT-4,2))./(12*dx))-B.*(35*T(IEXIT,2)...
        -104*T(IEXIT-1,2)+114*T(IEXIT-2,2)-56*T(IEXIT-3,2)...
        +11*T(IEXIT-4,2))./(12*dx^2))./(lossm(Temp).*Emag3(Temp,Param,Fcn));
        figure(2)
        set(gca,'fontsize',18)
        plot(PowRes,Temp,'-b',P,T(IEXIT,2),'k*',P,T(1,2),'g*','LineWidth',2);
        axis([0 max(PowRes)+2 0 Temp(length(Temp))])
    elseif psign == 1
        IEXIT = xLow/dx+1;
        PowResDiff = (2*K*Bi*Temp+2*K*Q*((Temp+1).^4-1)+K*Pe*Ue...
```

```matlab
      .*((-25*T(IEXIT,2)+48*T(IEXIT+1,2)-36*T(IEXIT+2,2)...
      +16*T(IEXIT+3,2)-3*T(IEXIT+4,2))./(12*dx))-B.*(35*T(IEXIT,1)...
      -104*T(IEXIT+1,1)+114*T(IEXIT+2,1)-56*T(IEXIT+3,1)...
      +11*T(IEXIT+4,1))./(12*dx^2))./(lossm(Temp).*Emag3(Temp,Param,Fcn)));
      PowResInlet = (2*K*Bi*Temp+2*K*Q*((Temp+1).^4-1)+K*Pe*Ue...
      .*((-25*T(IEXIT,2)+48*T(IEXIT+1,2)-36*T(IEXIT+2,2)...
      +16*T(IEXIT+3,2)-3*T(IEXIT+4,2))./(12*dx))-B.*(35*T(1,2)...
      -104*T(2,2)+114*T(3,2)-56*T(4,2)+11*T(5,2))./(12*dx^2))...
      ./(lossm(Temp).*Emag3(Temp,Param,Fcn));
      figure(2)
      set(gca,'fontsize',18)
      plot(PowRes,Temp,'-b',P,T(IEXIT,2),'k*',P,T(1,2),'g*','LineWidth',2);
      axis([0 max(PowRes)+2 0 Temp(length(Temp))])
end
%}

%Phase Plane Plot
[x1, x2] = meshgrid(0:.5:10,-10:1:10);
x1dot = (K.*Pe.*Ue./B).*x1-(1./B).*x2;
x2dot = P.*lossm(x1).*Emag3(x1,Param,Fcn)-2.*K.*(Bi.*x1);
figure(5)
set(gca,'fontsize',18)
quiver(x1,x2,x1dot,x2dot,'b','AutoScaleFactor',3,'MaxHeadSize'...
,0.05,'LineWidth',1)
xlabel('Temp')
ylabel('Flux')
axis([0 10 -4 10])
hold on
plot(T(1,2),K.*Pe.*Ue.*T(1,2)-B.*(T(2,2)-T(1,2))./dx,'mo')
hold on
plot(T(IMAX-1,2),K.*Pe.*Ue.*T(IMAX-1,2)-B...
.*(T(IMAX,2)-T(IMAX-2,2))./(2.*dx),'rx')
hold on
plot(T(1:IMAX-1,2),K.*Pe.*Ue.*T(1:IMAX-1,2)...
-B.*(T(2:IMAX,2)-T(1:IMAX-1,2))./dx,'r')
hold on
for i=1:Pcount-1
   plot(Troot(i),K*Pe*Ue*Troot(i),'ro',[Troot(i) Troot(i)],[-10 10],'--r')
   hold on
   eigvalPLUS(i) = 0.5*K*Pe*Ue./B+0.5*sqrt((K*Pe*Ue./B)^2...
   +4*lossm(Troot(i))*Emag3(Troot(i),Param,Fcn)*PTroot(i)/B);
   eigvalMINUS(i) = 0.5*K*Pe*Ue./B-0.5*sqrt((K*Pe*Ue./B)^2...
   +4*lossm(Troot(i))*Emag3(Troot(i),Param,Fcn)*PTroot(i)/B);
```

```matlab
                Peclet = 0:.01:20;
                PT(:,i) = -(K^2*Ue^2./(4*B*lossm(Troot(i))*Emag3(Troot(i)...
                ,Param,Fcn))).*Peclet.^2;
            end
            plot([0 10],[0 K*Pe*Ue*10],'--k')
            hold off


            %{
            %UNCOMMENT: Determines and plots wave velocity over time. Does not
            %have any meaning if a traveling wave solution is not made
            for k=1:length(T(:,2))-1
                if (T(k,2)-Troot(length(Troot)-1)).*(T(k+1,2)...
                -Troot(length(Troot)-1)) <= 0
                    xnew = (x(k)+x(k+1))/2;
                    disp(T(k,2))
                    disp(xnew)
                end
            end
            if tcount > tPrint
                Ttime(round((tcount-1)/tPrint)) = tcount*dt;
                Vtime(round((tcount-1)/tPrint)) = (xnew-xold)./(tPrint*dt);
                figure(777)
                plot(Ttime,Vtime,'-o')
                xlabel('Nondimensional Time (t)')
                ylabel('Wave Velocity (x/t)')
            end
            xold = xnew;
            %}

            pause(.1)
        end

        %TERMIINATES PROGRAM AND NOTIFIES USER LOOP EXCEEDED MAX ITERATIONS
        if tcount == NMAX
            error('Temperature Solution Did Not Reach Steady State');
        end

end %End of Time Loop


%PLOT OF STEADY STATE TEMPERATURE PROFILE
figure(1)
```

```
plot(x,T(:,2)*300+300,'g','LineWidth',2);
xlabel('Streamwise Length')
ylabel('Temperature (K)')
hold on

%STEADY STATE PLOT OF PHASE PLANE
[x1, x2] = meshgrid(0:.5:10,-10:1:10);
x1 = x1;
x2 = x2;
x1dot = (K.*Pe.*Ue./B).*x1-(1./B).*x2;
x2dot = P.*lossm(x1).*Emag3(x1,Param,Fcn)-2.*K.*(Bi.*x1);
figure(5)
quiver(x1*300+300,x2*300+300*K*Pe*Ue,x1dot*300,x2dot*300,'b'...
,'AutoScaleFactor',3,'MaxHeadSize',0.05,'LineWidth',1)
xlabel('Temperature (K)')
ylabel('Flux (K/m)')
axis([300 10*300+300 -6*300+300*K*Pe*Ue 10*300+300*K*Pe*Ue])
hold on
plot(T(1,2)*300+300,K.*Pe.*Ue.*(T(1,2)*300+300)-B.*(T(2,2)-T(1,2))...
*300./dx,'go')
hold on
plot(T(1:IMAX-1,2)*300+300,K.*Pe.*Ue.*(T(1:IMAX-1,2)*300+300)...
-B.*(T(2:IMAX,2)-T(1:IMAX-1,2))*300./dx,'g','LineWidth',2)
hold on
for i=1:Pcount-1
    plot(Troot(i)*300+300,K*Pe*Ue*(Troot(i)*300+300),'ro',...
    [Troot(i)*300+300 Troot(i)*300+300],[-10*300+300 10*300+300],'--r')
    hold on
    eigvalPLUS(i) = 0.5*K*Pe*Ue./B+0.5*sqrt((K*Pe*Ue./B)^2...
+4*lossm(Troot(i))*Emag3(Troot(i),Param,Fcn)*PTroot(i)/B);
    eigvalMINUS(i) = 0.5*K*Pe*Ue./B-0.5*sqrt((K*Pe*Ue./B)^2...
+4*lossm(Troot(i))*Emag3(Troot(i),Param,Fcn)*PTroot(i)/B);
end
plot([300 10*300+300],[300*K*Pe*Ue K*Pe*Ue*(10*300+300)],'--k')
set(gca,'fontsize',18)
```

```
%PROGRAM: Solution_LowPeclet_PwrRes.m
%FUNCTION CALLS: ParamDeclare.m, Emag3.m, tridiag.m
%DESCRIPTION: Uses a parfor loop to solve the IMEX method for steady states
%looping over power and initial temperature to find the power response
%curves in the presence of diffusive and advective effects. See PROGRAM:
%Solution_LowPeclet.m for a more detailed description of the program
%methods itself

clear; %Clears all declared parameters and variables

parpool %Begins pool of parallel processors

%%%%%%%%%%%%%%%%%%%%%%%%%%%%%%%%%%%%%%%%%%%%%%%%%%%%%%%%%%%%%%%%%%%%%%%%%%%%%
%%%%%%%%%%%%%%%%%%%%%%%%%%% DECLARE MODEL PARAMETERS %%%%%%%%%%%%%%%%%%%%%%%%%
%%%%%%%%%%%%%%%%%%%%%%%%%%%%%%%%%%%%%%%%%%%%%%%%%%%%%%%%%%%%%%%%%%%%%%%%%%%%%%

[Param,Fcn] = ParamDeclare; %Retrieves parameters from master list

%INITIALIZE PARAMETERS FROM Param AND Fcn FOR USE IN PROGRAM
for j=1:length(Param)
    evalc([Param{j,1},'=',Param{j,2}]);
end
for j=1:length(Fcn)
    evalc(Fcn{j});
end

%Initilization of parameter set to sweep over
Pdomain = .1:.1:8;
T0domain = 0:2:6;
Pnum = length(Pdomain);
T0num = length(T0domain);
Nlength = Pnum*T0num

%Declare meshgrid for testing
[X,Y] = meshgrid(T0domain,Pdomain);
Ptest = Y(:);
T0test = X(:);

tic %Start Timer
%LOOP: parfor loops over parameter set
parfor m = 1:Nlength
ConvErr = 0; %Initilize error
```

```matlab
P = Ptest(m); %Declares power value
Tinit = T0test(m); %Declares temperature value
%%%%%%%%%%%%%%%%%%%%%%%%%%%%%%%%%%%%%%%%%%%%%%%%%%%%%%%%%%%%%%%%%%%%%%%%%
%%%%%%%%%%%%%%%%%%%%%% PROGRAM INITIALIZATIONS %%%%%%%%%%%%%%%%%%%%%%%%%%%
%%%%%%%%%%%%%%%%%%%%%%%%%%%%%%%%%%%%%%%%%%%%%%%%%%%%%%%%%%%%%%%%%%%%%%%%%

dx = 1e-1; %Spatial Step Size
dt = dx.^2/2; %Temporal Step Size
%dt = dx./2;

NMAX = 1e5; %Maximum number of time steps
tol = 1e-8; %Exit relative error tolerance for Steady State
xLength = 10; %length of truncated channel
tPrint = 500; %Number of time steps between solution plots

%PHYSICAL PROCESS ACTIVATION (0=off, 1=on)
%By setting values to 0 or 1 we can turn specific physical processes on or
%off to easily examine simple cases or the full model
c1 = 1; %Diffusion
c2 = 1; %Advection
c3 = 1; %Source Power
c4 = 1; %Boundary Conducttion
c5 = 0; %Boundary Radiaton
c6 = 1; %Inlet/Outlet Condition (c6=0,1,2 Insulating, Dirichlet, Flux)
c7 = 1; %Time Loop Exit Consition (c7=0 max err large domain, c7=1
        %max err small domain)

%SOURCE SEGMENTATION
%[xLow xHigh] = interval of applied sources
%H1 = heaviside for EM source, H2 = heaviside for Thermal loss
xLow = 0;
xHigh = 10;
H1 =@(x) heaviside(x-xLow).*heaviside(-x+xHigh);
H2 =@(x) heaviside(x-xLow).*heaviside(-x+xHigh);

%%%%%%%%%%%%%%%%%%%%%%%%%%%%%%%%%%%%%%%%%%%%%%%%%%%%%%%%%%%%%%%%%%%%%%%%%
%%%%%%%%%%%%%%%%%%% DO NOT CHANGE BEYOND THIS POINT %%%%%%%%%%%%%%%%%%%%%%
%%%%%%%%%%%%%%%%%%%%%%%%%%%%%%%%%%%%%%%%%%%%%%%%%%%%%%%%%%%%%%%%%%%%%%%%%

%NUMERICAL INITIALIZATIONS
%X-DOMAIN
xi = 0;
xf = xLength;
```

```matlab
x = xi:dx:xf; %Discretized nondimensional domain
IMAX = length(x);
ILow = (xLow-xi)./dx+1;
IHigh = (xHigh-xi)./dx+1;
Idom = ILow:IHigh;
T = zeros(IMAX,2); %Next Time Temperature Solution

%Z-DOMAIN
lam0SCALED = lam0/l; %Nondimensional wavelength
dz = (lam0SCALED)/100;
z1 = -2*(lam-1):dz:-(lam-1);
z2 = -(lam-1):dz:0;
z3 = 0:dz:1;
z4 = 1:dz:lam;
z5 = lam:dz:2*lam-1;



%%%%%%%%%%%%%%%%%%%%%%%%%%%%%%%%%%%%%%%%%%%%%%%%%%%%%%%%%%%%%%%%%%%%%%%%%%
%%%%%%%%%%%%%%%%%%%%%%%%%%%%%% Boundary conditions %%%%%%%%%%%%%%%%%%%%%%%%%
%%%%%%%%%%%%%%%%%%%%%%%%%%%%%%%%%%%%%%%%%%%%%%%%%%%%%%%%%%%%%%%%%%%%%%%%%%
Uplus = max(Ue,0);
Uminus = min(Ue,0);

if c6 == 0
    %%%%%%%%%%%%%%%%%%%%%%%%% Insulating Condition %%%%%%%%%%%%%%%%%%%%%%%%%
    %sets insulating boundary conditions on both sides

    %Left Condition
    aL = 1;
    bL = 0;
    cL = 0;
    %Right Condition
    aR = 1;
    bR = 0;
    cR = 0;
elseif c6 == 1
    %%%%%%%%%%%%%%%%%%%%%%%%% Dirichlet Condition %%%%%%%%%%%%%%%%%%%%%%%%%
    %sets inlet temperature to ambient temperature
    %{
    %Left Condition
    aL = -Uminus./Ue;
    bL = Uplus./Ue;
    cL = 0;
```

196

```
    %Right Condition
    aR = Uplus./Ue;
    bR = -Uminus./Ue;
    cR = 0;
    %}
    aL = 0;
    bL = 1;
    cL = 0;
    aR = 1;
    bR = 0;
    cR = 0;
elseif c6 == 2
    %%%%%%%%%%%%%%%%%%%%%% Robin Condition %%%%%%%%%%%%%%%%%%%%%%
    %set up so upstream condition is continuity of flux and downstream
    %condition is insulated no matter what direction the fluid is flowing

    %Left Condition
    aL = 1+2*(lam-1);
    bL = -Pe*Uplus;
    bL = -Pe*Uplus+Pe*Uminus;
    cL = 0;
    %Right Condition
    aR = 1+2*(lam-1);
    bR = -Pe*Uminus;
    bR = -Pe*Uminus+Pe*Uplus;
    bR = 0;
    cR = 0;
end


%%%%%%%%%%%%%%%%%%%%%%%%%%%%%%%%%%%%%%%%%%%%%%%%%%%%%%%%%%%%%%%%%%%%%%%
%%%%%%%%%%%%%%%%%%%%%%%%%%% THERMAL SOLUTION %%%%%%%%%%%%%%%%%%%%%%%%%%
%%%%%%%%%%%%%%%%%%%%%%%%%%%%%%%%%%%%%%%%%%%%%%%%%%%%%%%%%%%%%%%%%%%%%%%

%MATRIX COEFFICIENT GROUPS
s1 = c1.*(B.*dt)./(2.*A.*dx.^2);
s2plus = c2.*(K.*Pe.*Uplus.*dt)./(A.*dx);
s2minus = c2.*(K.*Pe.*Uminus.*dt)./(A.*dx);
s3 = c4.*(K.*Bi.*dt./A).*H2(x');

%MATRIX EQUATION INILIATIZATIONS
L = ones(1,IMAX); %left diagonal
M = ones(1,IMAX); %middle diagonal
R = ones(1,IMAX); %right diagonal
```

```matlab
RHS = zeros(1,IMAX); %right hand side

%INITIAL CONDITON
T(:,1) = Tinit;

%NONLINEAR TERMS FOR INITIAL CONDITION
sig = lossm(T(:,1));
E = Emag3(T(:,1),Param,Fcn).*H1(x');
N1 = c3.*(P./A).*sig.*E-c5.*(2.*K.*Q./A).*((T(:,1)+1).^4-1).*H2(x');



%%%%%%%%%%%%%%%%%% TIME STEP 1 SOLUTION %%%%%%%%%%%%%%%%%%%%%%%%%%%
%Uses Crank-Nicolson on linear terms and uses Euler's Method on
%nonlinear terms. This is necessary since the Adams-Bashforth method
%used hearafter requires solutions from two previoius time steps

%FIRST ROW OF MATRIX
M(1) = bL-aL./dx;
R(1) = aL./dx;
RHS(1) = cL;
%MAIN BLOCK OF MATRIX
for i=2:IMAX-1
    L(i) = -s1;
    M(i) = 1+2.*s1+s3(i);
    R(i) = -s1;
    RHS(i) = (s1+s2plus).*T(i-1,1)+(1-2.*s1-s3(i)-s2plus+s2minus)...
    .*T(i,1)+(s1-s2minus).*T(i+1,1)+dt*N1(i);
end
%LAST ROW OF MATRIX
L(IMAX) = -aR./dx;
M(IMAX) = aR./dx+bR;
RHS(IMAX) = cR;

%NEXT TIME STEP SOLUTION
T(:,2)= tridiag(L,M,R,RHS);

%UPDATE TEMPERATURE SOLUTIONS
T(:,1)=T(:,2);
sig = lossm(T(:,2));
E = Emag3(T(:,2),Param,Fcn).*H1(x');
N2 = N1;
N1 = c3.*(P./A).*sig.*E-c5.*(2.*K.*Q./A).*((T(:,2)+1).^4-1).*H2(x');
```

```matlab
%%%%%%%%%%%%%%%%%%%%%%%%%%% TIME LOOP %%%%%%%%%%%%%%%%%%%%%%%%%%%%%%%%%%%%
relerr = 1; %Initialization of relative error
tcount = 2; %Time Step Counter

%LOOP: Loops until the relative error is below tollerance or until the
%maximum number of time steps is exceeded
while relerr > tol && tcount < NMAX
    tcount = tcount + 1; %Update time step

    %%%%%%%%%%%%%%%%%%%% BUILD IMPLICIT SOLVER MATRIX %%%%%%%%%%%%%%%%%%%%
    %FIRST ROW OF MATRIX
    M(1) = bL-aL./dx;
    R(1) = aL./dx;
    RHS(1) = cL;
    %MAIN BLOCK OF MATRIX
    for i=2:IMAX-1
        L(i) = -s1;
        M(i) = 1+2.*s1+s3(i);
        R(i) = -s1;
        RHS(i) = (s1+s2plus).*T(i-1,1)+(1-2.*s1-s3(i)-s2plus+s2minus)...
        .*T(i,1)+(s1-s2minus).*T(i+1,1)+(dt./2).*(3*N1(i)-N2(i));
    end
    %LAST ROW OF MATRIX
    L(IMAX) = -aR./dx;
    M(IMAX) = aR./dx+bR;
    RHS(IMAX) = cR;

    %NEXT TIME STEP SOLUTION
    T(:,2)= tridiag(L,M,R,RHS);

        %use with no diffusion
        if c1 == 0
            T(1,2) = T(2,2);
        end

    %CALCULATE RELATIVE ERROR FOR STEADY STATE CONVERGENCE
    if c7 == 0
        relerr = max(abs(T(:,2)-T(:,1)))./max(abs(T(:,2)));
    elseif c7 == 1
        relerr = max(abs(T(Idom,2)-T(Idom,1)))./max(abs(T(Idom,2)));
    end

    %UPDATE TEMPERATURE SOLUTIONS
```

```matlab
    T(:,1)=T(:,2);
    N2 = N1;
    sig = lossm(T(:,2));
    E = Emag3(T(:,2),Param,Fcn).*H1(x');
    N1 = c3.*(P./A).*sig.*E-c5.*(2.*K.*Q./A).*((T(:,2)+1).^4-1).*H2(x');

    %TERMIINATES PROGRAM AND NOTIFIES USER LOOP EXCEEDED MAX ITERATIONS
    if tcount == NMAX
        ConvErr = 1;
    end

end %Time Loop

if ConvErr == 0
    Pplot(m) = P;
    Tplot(m) = T(IMAX,2);
else
    Pplot(m) = -1;
    Tplot(m) = -1;
end


end
delete(gcp)
for m=1:Nlength
    if Pplot(m) == -1
        Pplot(m)=Pplot(m-1);
        Tplot(m)=Tplot(m-1);
    end
end

TempArray = zeros(Pnum,T0num);
TempArrayzero = zeros(Pnum,T0num);
for i = 1:T0num
    for j = 1:Pnum
        TempArray(j,i) = Tplot(j+(i-1)*Pnum);
        TempArrayzero(j,i) = Tplot(j+(i-1)*Pnum);
        if i > 1 && round(TempArray(j,i)*1000)==round(TempArray(j,i-1)*1000)
            TempArrayzero(j,i) = 0;
        end
    end
end
for i = 1:length(TempArrayzero(:,1))
```

200

```matlab
        TempArrayzero(i,:) = sort(TempArrayzero(i,:),'descend');
end
Temp = TempArrayzero(:,1:3);

UScount = 1;
for i = 1:length(Temp(:,1))
    if Temp(i,2) == 0

    elseif Temp(i,3) == 0
        UStest(UScount,1) = Temp(i,1);
        UStest(UScount,2) = Temp(i,2);
        USPplot(UScount) = Pdomain(i);
        UScount = UScount+1;
    else
        UStest(UScount,1) = Temp(i,1);
        UStest(UScount,2) = Temp(i,2);
        USPplot(UScount) = Pdomain(i);
        UScount = UScount+1;
        UStest(UScount,1) = Temp(i,2);
        UStest(UScount,2) = Temp(i,3);
        USPplot(UScount) = Pdomain(i);
        UScount = UScount+1;
    end
end

USTemp = zeros(length(UStest(:,1)),1);
for j = 1:length(UStest(:,1))

P = USPplot(j);
Tinit = 0.5*(UStest(j,1)+UStest(j,2));
Ttop = UStest(j,1);
Tbot = UStest(j,2);
error = 1;

while error > 1e-3
%%%%%%%%%%%%%%%%%%%%%%%%%%%%%%%%%%%%%%%%%%%%%%%%%%%%%%%%%%%%%%%%%%%%%%%%%%%%%%
%%%%%%%%%%%%%%%%%%%%% PROGRAM INITIALIZATIONS %%%%%%%%%%%%%%%%%%%%%%%%%%%%%%%
%%%%%%%%%%%%%%%%%%%%%%%%%%%%%%%%%%%%%%%%%%%%%%%%%%%%%%%%%%%%%%%%%%%%%%%%%%%%%%


dx = 1e-1; %Spatial Step Size
dt = dx.^2/2; %Temporal Step Size
%dt = dx./2;
```

```
NMAX = 1e5; %Maximum number of time steps
tol = 1e-8; %Exit relative error tolerance for Steady State
xLength = 10; %length of truncated channel
tPrint = 500; %Number of time steps between solution plots

%PHYSICAL PROCESS ACTIVATION (0=off, 1=on)
%By setting values to 0 or 1 we can turn specific physical processes on or
%off to easily examine simple cases or the full model
c1 = 1; %Diffusion
c2 = 1; %Advection
c3 = 1; %Source Power
c4 = 1; %Boundary Conducttion
c5 = 0; %Boundary Radiaton
c6 = 2; %Inlet/Outlet Condition (c6=0,1,2 Insulating, Dirichlet, Flux)
c7 = 1; %Time Loop Exit Consition (c7=0 max err large domain, c7=1
        %max err small domain)

%SOURCE SEGMENTATION
%[xLow xHigh] = interval of applied sources
%H1 = heaviside for EM source, H2 = heaviside for Thermal loss
xLow = 0;
xHigh = 10;
H1 =@(x) heaviside(x-xLow).*heaviside(-x+xHigh);
H2 =@(x) heaviside(x-xLow).*heaviside(-x+xHigh);

%%%%%%%%%%%%%%%%%%%%%%%%%%%%%%%%%%%%%%%%%%%%%%%%%%%%%%%%%%%%%%%%%%%%%%%%%%%
%%%%%%%%%%%%%%%%%%%% DO NOT CHANGE BEYOND THIS POINT %%%%%%%%%%%%%%%%%%%%%%%
%%%%%%%%%%%%%%%%%%%%%%%%%%%%%%%%%%%%%%%%%%%%%%%%%%%%%%%%%%%%%%%%%%%%%%%%%%%%

%NUMERICAL INITIALIZATIONS
%X-DOMAIN
xi = 0;
xf = xLength;
x = xi:dx:xf; %Discretized nondimensional domain
IMAX = length(x);
ILow = (xLow-xi)./dx+1;
IHigh = (xHigh-xi)./dx+1;
Idom = ILow:IHigh;
T = zeros(IMAX,2); %Next Time Temperature Solution (to be found)

%Z-DOMAIN
lam0SCALED = lam0/l; %Nondimensional wavelength
```

```matlab
dz = (lam0SCALED)/100;
z1 = -2*(lam-1):dz:-(lam-1);
z2 = -(lam-1):dz:0;
z3 = 0:dz:1;
z4 = 1:dz:lam;
z5 = lam:dz:2*lam-1;

%%%%%%%%%%%%%%%%%%%%%%%%%%%%%%%%%%%%%%%%%%%%%%%%%%%%%%%%%%%%%%%%%%%%%%%%%%%
%%%%%%%%%%%%%%%%%%%%%%%%%%% Boundary conditions %%%%%%%%%%%%%%%%%%%%%%%%%
%%%%%%%%%%%%%%%%%%%%%%%%%%%%%%%%%%%%%%%%%%%%%%%%%%%%%%%%%%%%%%%%%%%%%%%%%%%
Uplus = max(-Ue,0);
Uminus = min(-Ue,0);

if c6 == 0
    %%%%%%%%%%%%%%%%%%%%%%%%% Insulating Condition %%%%%%%%%%%%%%%%%%%%%%%%%%%%%
    %sets insulating boundary conditions on both sides

    %Left Condition
    aL = 1;
    bL = 0;
    cL = 0;
    %Right Condition
    aR = 1;
    bR = 0;
    cR = 0;
elseif c6 == 1
    %%%%%%%%%%%%%%%%%%%%%%%%% Dirichlet Condition %%%%%%%%%%%%%%%%%%%%%%%%%%%%%
    %sets inlet temperature to ambient temperature

    %Left Condition
    aL = -Uminus./Ue;
    bL = Uplus./Ue;
    cL = 0;
    %Right Condition
    aR = Uplus./Ue;
    bR = -Uminus./Ue;
    cR = 0;
elseif c6 == 2
    %%%%%%%%%%%%%%%%%%%%%%%%%% Robin Condition %%%%%%%%%%%%%%%%%%%%%%%%%%%%%%
    %set up so upstream condition is continuity of flux and downstream
    %condition is insulated no matter what direction the fluid is flowing

    %Left Condition
```

```matlab
    aL = 1+2*(lam-1);
    bL = -Pe*Uplus;
    bL = -Pe*Uplus+Pe*Uminus;
    cL = 0;
    %Right Condition
    aR = 1+2*(lam-1);
    bR = -Pe*Uminus;
    bR = -Pe*Uminus+Pe*Uplus;
    bR = 0;
    cR = 0;
end


%%%%%%%%%%%%%%%%%%%%%%%%%%%%%%%%%%%%%%%%%%%%%%%%%%%%%%%%%%%%%%%%%%%%
%%%%%%%%%%%%%%%%%%%%%%%%%% THERMAL SOLUTION %%%%%%%%%%%%%%%%%%%%%%%%
%%%%%%%%%%%%%%%%%%%%%%%%%%%%%%%%%%%%%%%%%%%%%%%%%%%%%%%%%%%%%%%%%%%%

%MATRIX COEFFICIENT GROUPS
s1 = c1.*(B.*dt)./(2.*A.*dx.^2);
s2plus = c2.*(K.*Pe.*Uplus.*dt)./(A.*dx);
s2minus = c2.*(K.*Pe.*Uminus.*dt)./(A.*dx);
s3 = c4.*(K.*Bi.*dt./A).*H2(x');

%MATRIX EQUATION INILIATIZATIONS
L = ones(1,IMAX); %left diagonal
M = ones(1,IMAX); %middle diagonal
R = ones(1,IMAX); %right diagonal
RHS = zeros(1,IMAX); %right hand side

%INITIAL CONDITON
T(:,1) = Tinit;

%NONLINEAR TERMS FOR INITIAL CONDITION
sig = lossm(T(:,1));
E = Emag3(T(:,1),Param,Fcn).*H1(x');
N1 = c3.*(P./A).*sig.*E-c5.*(2.*K.*Q./A).*((T(:,1)+1).^4-1).*H2(x');

%%%%%%%%%%%%%%%%%%%%%% TIME STEP 1 SOLUTION %%%%%%%%%%%%%%%%%%%%%%%%
%Uses Crank-Nicolson on linear terms and uses Euler's Method on
%nonlinear terms. This is necessary since the Adams-Bashforth method
%used hearafter requires solutions from two previoius time steps

%FIRST ROW OF MATRIX
M(1) = bL-aL./dx;
```

```
R(1) = aL./dx;
RHS(1) = cL;
%MAIN BLOCK OF MATRIX
for i=2:IMAX-1
    L(i) = -s1;
    M(i) = 1+2.*s1+s3(i);
    R(i) = -s1;
    RHS(i) = (s1+s2plus).*T(i-1,1)+(1-2.*s1-s3(i)-s2plus+s2minus)...
    .*T(i,1)+(s1-s2minus).*T(i+1,1)+dt*N1(i);
end
%LAST ROW OF MATRIX
L(IMAX) = -aR./dx;
M(IMAX) = aR./dx+bR;
RHS(IMAX) = cR;

%NEXT TIME STEP SOLUTION
T(:,2)= tridiag(L,M,R,RHS);

%UPDATE TEMPERATURE SOLUTIONS
T(:,1)=T(:,2);
sig = lossm(T(:,2));
E = Emag3(T(:,2),Param,Fcn).*H1(x');
N2 = N1;
N1 = c3.*(P./A).*sig.*E-c5.*(2.*K.*Q./A).*((T(:,2)+1).^4-1).*H2(x');

TinitOLD = Tinit;
if T(IMAX,2) < Tinit
    Tbot = Tinit;
    Tinit = 0.5*(Ttop+Tinit);
elseif T(IMAX,2) > Tinit
    Ttop = Tinit;
    Tinit = 0.5*(Tbot+Tinit);
end
error = abs(Tinit-TinitOLD);


end %Unstable Loop

USTemp(j) = 0.5*(Tinit+TinitOLD);

end %Test Points Loop
```

```
%%%%%%%%%%%%%%%%%%%%%%%%%%%%%%%%%%%%%%%%%%%%%%%%%%%%%%%%%%%%%%%
%%%%%%%%%%%%%%%%%%%%% Plot Solution Curve %%%%%%%%%%%%%%%%%%%%%
%%%%%%%%%%%%%%%%%%%%%%%%%%%%%%%%%%%%%%%%%%%%%%%%%%%%%%%%%%%%%%%

%Put Stable\Unstable Solutions together
Solution = [Tplot' Pplot'; USTemp USPplot'];
Solution = sortrows(Solution); %Sort according to temperature

figure(1)
plot(Pplot,Tplot,'o',USPplot,USTemp,'ro') %Plot Data
hold on
plot(Solution(:,2),Solution(:,1),'k') %Plot curve

%Traditional Power Response Calculation
        Temp = 0:.01:7.2;
        PowRes = (2*K*Bi*Temp+2*K*Q*((Temp+1).^4-1))./(lossm(Temp)...
        .*Emag3(Temp,Param,Fcn));

        if psign == -1
            figure(1)
            set(gca,'fontsize',18)
            plot(PowRes,Temp,'-b','LineWidth',2);
            axis([0 max(PowRes)+2 0 Temp(length(Temp))])
        elseif psign == 1
            figure(1)
            set(gca,'fontsize',18)
            plot(PowRes,Temp,'-b','LineWidth',2);
            axis([0 max(PowRes)+2 0 Temp(length(Temp))])
        end

%Save Figure
saveas(gcf,['PwrRes_Pe' num2str(Pe) '.fig'])

toc %End Timer
```

```
%PROGRAM: Solution_LargePeclet.m
%FUNCTIONS: ParamDeclare.m, secant.m
%DESCRIPTION: Solves the Large advection (Pe=O(1)) problem for the
%triple-layer laminate problem at low power (P=O(\eta)) by employing the
%Galerkin method

clear; %Clears all declared parameters and variables

%%%%%%%%%%%%%%%%%%%%%%%%%%%%%%%%%%%%%%%%%%%%%%%%%%%%%%%%%%%%%%%%%%%%%%%%%%
%%%%%%%%%%%%%%%%%%%%%%%%% DECLARE MODEL PARAMETERS %%%%%%%%%%%%%%%%%%%%%%%%
%%%%%%%%%%%%%%%%%%%%%%%%%%%%%%%%%%%%%%%%%%%%%%%%%%%%%%%%%%%%%%%%%%%%%%%%%%

[Param,Fcn] = ParamDeclare; %Retrieves parameters from master list

%INITIALIZE PARAMETERS FROM Param AND Fcn FOR USE IN PROGRAM
for j=1:length(Param)
    evalc([Param{j,1},'=',Param{j,2}]);
end
for j=1:length(Fcn)
    evalc(Fcn{j});
end

Pe = Pe*(lam-1)^4; %Redefining for scaled Peclet number

%%%%%%%%%%%%%%%%%%%%%%%%%%%%%%%%%%%%%%%%%%%%%%%%%%%%%%%%%%%%%%%%%%%%%%%%%%
%%%%%%%%%%%%%%%%%%%%%%% PROGRAM INITIALIZATIONS %%%%%%%%%%%%%%%%%%%%%%%%%%
%%%%%%%%%%%%%%%%%%%%%%%%%%%%%%%%%%%%%%%%%%%%%%%%%%%%%%%%%%%%%%%%%%%%%%%%%%
xlength = 1;
eta = 1e-1; %Asymptotic parameter, chosen by geometry
mu = 0:1:1e6; %range of values over which to search for roots
eigtol = 1e-6; %error tolerance for finding roots
zeta = 0:.01:1; %microscale domain discretization
x = 0:.01:xlength; %macroscale domain discretization
f =@(x) zeros(length(x),1); %Initilization of T2 temperature at inlet
g =@(x) zeros(length(x),1); %Initilization of T4 temperature at inlet

%%%%%%%%%%%%%%%%%%%%%%%%%%%%%%%%%%%%%%%%%%%%%%%%%%%%%%%%%%%%%%%%%%%%%%%%
%%%%%%%%%%%%%%%%%%%%%%%%%% Find Eigenvalues %%%%%%%%%%%%%%%%%%%%%%%%%%%%
%%%%%%%%%%%%%%%%%%%%%%%%%%%%%%%%%%%%%%%%%%%%%%%%%%%%%%%%%%%%%%%%%%%%%%%%
a = 2*(lam-1)./K; %new constant defined

%Characteristic Equations for the two eigenvalues
CharEq1 =@(x) sqrt(x).*sin(sqrt(x))-(lam-1)*Bi*cos(sqrt(x));
```

```
CharEq2 =@(x) [K*x-2*(lam-1)^2*Bi].*sin(sqrt(x))-[K*Bi+2]*sqrt(x).*cos(sqrt(x));

%Determines initial guesses for root finding the eigenvalues
count1 = 1; %counter for number of eigenvalues in the first set
count2 = 1; %counter for number of eigenvalues in the second set

%LOOP: Loops over range where we search for eigenvalues. Assuming by
%inspection that all of the roots are simple we find where the
%characterisitic function changes sign and use the gridpoints are either
%side as the initial values in the secant root finding method
for i=1:length(mu)-1
    if CharEq1(mu(i+1))*CharEq1(mu(i))<0
        MU1(1,count1) = mu(i);
        MU1(2,count1) = mu(i+1);
        count1 = count1 + 1;
    end
    if CharEq2(mu(i+1))*CharEq2(mu(i))<0
        MU2(1,count2) = mu(i);
        MU2(2,count2) = mu(i+1);
        count2 = count2 + 1;
    end
end

z1 = zeros(1,count1-1); %Initialize vector for first set of eigenvalues
z2 = zeros(1,count2-1); %Initialize vector for second set of eigenvalues

%LOOP: Loop over number of times characteristic equation changed sign by
%using the counters. Apply the secant root finding method to determine
%roots with the error tolerance specified by eigtol
for i=1:count1-1
    z1(i) = secant(CharEq1,MU1(1,i),MU1(2,i),eigtol);
    z2(i) = secant(CharEq2,MU2(1,i),MU2(2,i),eigtol);
end
for i=1:count2-1
    z2(i) = secant(CharEq2,MU2(1,i),MU2(2,i),eigtol);
end

%{
%Plot of the Characterisitc Function
figure(1)
plot([mu(1) mu(length(mu))],[0 0],'k',mu,CharEq1(mu),'b')
axis([mu(1) mu(length(mu)) min(CharEq1(mu)) max(CharEq1(mu))])
title('Characterisitc Function')
```

```
hold on

%Plots found roots of the Characterisitc Function
for i=1:length(z1)
    plot(z1(i),0,'ro');
    hold on
end

%Plot of the Characterisitc Function
figure(2)
plot([mu(1) mu(length(mu))],[0 0],'k',mu,CharEq2(mu),'b')
axis([mu(1) mu(length(mu)) min(CharEq2(mu)) max(CharEq2(mu))])
title('Characterisitc Function')
hold on

%Plots found roots of the Characterisitc Function
for i=1:length(z2)
    plot(z2(i),0,'ro');
    hold on
end
%}

%Define truncation for the number of eigenvalues found
N = min(length(z1),length(z2));

%%%%%%%%%%%%%%%%%%%%%%%%%%%%%%%%%%%%%%%%%%%%%%%%%%%%%%%%%%%%%%%%%%%%%%%%%%
%%%%%%%%%%%%%%%%% Define Plug Flow Eigenfunctions %%%%%%%%%%%%%%%%%%%%%
%%%%%%%%%%%%%%%%%%%%%%%%%%%%%%%%%%%%%%%%%%%%%%%%%%%%%%%%%%%%%%%%%%%%%%%%%%

Psi1 = zeros(length(zeta),N); %Initialize First Plug Flow Eigenfunction
Psi2 = zeros(length(zeta),N); %Initialize Second Plug Flow Eigenfunction
%Defines first N Plug Flow Eigenfunctions
for i=1:N
    for j=1:length(zeta)
        Psi1(j,i) = cos(sqrt(z1(i))*zeta(j));
        Psi2(j,i) = (sqrt(z2(i))/a)*cos(sqrt(z2(i))*zeta(j))...
        +sin(sqrt(z2(i))*zeta(j));
    end
end

%{
%%%%%%%%%%%%% Plots the N Plug Flow eigenfunctions %%%%%%%%%%%%%
rem = mod(N,4);
```

209

```
for j=1:floor(N/4)
    figure(j+2)
    subplot(4,2,1)
    plot(zeta,Psi1(:,1+(j-1)*4))
    title('\Psi_1')
    ylabel(['n = ' num2str(1+(j-1)*4)])
    subplot(4,2,2)
    plot(zeta,Psi2(:,1+(j-1)*4))
    title('\Psi_2')
    for i=2:4
        subplot(4,2,2*i-1)
        plot(zeta,Psi1(:,i+(j-1)*4))
        ylabel(['n = ' num2str(i+(j-1)*4)])
        subplot(4,2,2*i)
        plot(zeta,Psi2(:,i+(j-1)*4))
    end
end
if rem == 1
    figure(ceil(N/4)+1)
    subplot(4,2,1)
    plot(zeta,Psi1(:,1+(ceil(N/4)-1)*4))
    title('\Psi_1')
    ylabel(['n = ' num2str(1+(ceil(N/4)-1)*4)])
    subplot(4,2,2)
    plot(zeta,Psi2(:,1+(ceil(N/4)-1)*4))
    title('\Psi_2')
elseif rem > 1
    figure(ceil(N/4)+1)
    subplot(4,2,1)
    plot(zeta,Psi1(:,1+(ceil(N/4)-1)*4))
    title('\Psi_1')
    ylabel(['n = ' num2str(1+(ceil(N/4)-1)*4)])
    subplot(4,2,2)
    plot(zeta,Psi2(:,1+(ceil(N/4)-1)*4))
    title('\Psi_2')
    for i=2:rem
        subplot(4,2,2*i-1)
        plot(zeta,Psi1(:,i+(ceil(N/4)-1)*4))
        ylabel(['n = ' num2str(i+(ceil(N/4)-1)*4)])
        subplot(4,2,2*i)
        plot(zeta,Psi2(:,i+(ceil(N/4)-1)*4))
    end
end
```

```
pause
%}


%%%%%%%%%%%%%%%%%%%%%%%%%%%%%%%%%%%%%%%%%%%%%%%%%%%%%%%%%%%%%%%%%%%%%%%
%%%%%%%%%%%% Determine Poiseulle Flow Eigenfunctions %%%%%%%%%%%%%%%
%%%%%%%%%%%%%%%%%%%%%%%%%%%%%%%%%%%%%%%%%%%%%%%%%%%%%%%%%%%%%%%%%%%%%%%
w =@(x) -x.*(x-1); %Scaled Poiseulle Fluid Velocity
lambdaN = 10; %Number of Galerkin modes used in solution (max=N)

%%%%%%%%% Solve Generalized Eigenvalue Problem Mv=lambda*Bv %%%%%%%%%%
M1 = zeros(lambdaN,lambdaN); %Initialize Diagonal Matrix
M2 = zeros(lambdaN,lambdaN); %Initialize Diagonal Matrix
B1 = zeros(lambdaN,lambdaN); %Initialize Full Matrix
B2 = zeros(lambdaN,lambdaN); %Initialize Full Matrix

%Construct Matricies M and B
for i = 1:lambdaN
    M1(i,i) = z1(i);
    M2(i,i) = z2(i);
    for j = 1:lambdaN
        B1(i,j) = trapz(zeta,(Psi1(:,j).*Psi1(:,i)).*w(zeta'))...
        ./trapz(zeta,Psi1(:,i).^2);
        B2(i,j) = trapz(zeta,(Psi2(:,j).*Psi2(:,i)).*w(zeta'))...
        ./trapz(zeta,Psi2(:,i).^2);
    end
end

%Solve Generalized eigenvalue problems
[V1,D1] = eig(full(B1),full(M1)); %MATLAB recommended command (lambdaN=N)
[V2,D2] = eig(full(B2),full(M2)); %MATLAB recommended command (lambdaN=N)
%NOTE: eigenvalues found in diagonals of D1 and D2 are recipricals of the
%eigenvalues (lambda) which we are after

lambda1 = zeros(1,lambdaN); %Initialize vector of Poiseulle eigenvalues
lambda2 = zeros(1,lambdaN); %Initialize vector of Poiseulle eigenvalues
for i=1:lambdaN %Define Poiseulle eigenvalues
    lambda1(i)=1./D1(i,i);
    lambda2(i)=1./D2(i,i);
end

%%%%%%%%%%%%%%%%%%%%%%%%%%%%%%%%%%%%%%%%%%%%%%%%%%%%%%%%%%%%%%%%%%%%%%%
%%%%%%%%%%%%%% Define Poiseulle Flow Eigenfunctions %%%%%%%%%%%%%%%%%
```

```
%%%%%%%%%%%%%%%%%%%%%%%%%%%%%%%%%%%%%%%%%%%%%%%%%%%%%%%%%%%%%%%%%%%%%%

Phi1 = zeros(length(zeta),lambdaN); %Initialize First Eigenfunction
Phi2 = zeros(length(zeta),lambdaN); %Initialize Second Eigenfunction
%Define Poiseulle Flow Eigenfunctions
for j = 1:lambdaN
    for i = 1:lambdaN
        Phi1(:,j) = Phi1(:,j) + V1(i,j).*Psi1(:,i);
        Phi2(:,j) = Phi2(:,j) + V2(i,j).*Psi2(:,i);
    end
end

%{
%%%%%%%%% Plots the lambdaN Poisuelle Flow eigenfunctions %%%%%%%%%%%
rem = mod(lambdaN,4);
for j=1:floor(lambdaN/4)
    figure(ceil(lambdaN/4)+j+1)
    subplot(4,2,1)
    plot(zeta,Phi1(:,1+(j-1)*4))
    title('\Phi_1')
    ylabel(['n = ' num2str(1+(j-1)*4)])
    subplot(4,2,2)
    plot(zeta,Phi2(:,1+(j-1)*4))
    title('\Phi_2')
    for i=2:4
        subplot(4,2,2*i-1)
        plot(zeta,Phi1(:,i+(j-1)*4))
        ylabel(['n = ' num2str(i+(j-1)*4)])
        subplot(4,2,2*i)
        plot(zeta,Phi2(:,i+(j-1)*4))
    end
end
if rem == 1
    figure(2*ceil(lambdaN/4)+1)
    subplot(4,2,1)
    plot(zeta,Phi1(:,1+(ceil(lambdaN/4)-1)*4))
    title('\Phi_1')
    ylabel(['n = ' num2str(1+(ceil(lambdaN/4)-1)*4)])
    subplot(4,2,2)
    plot(zeta,Phi2(:,1+(ceil(lambdaN/4)-1)*4))
    title('\Phi_2')
elseif rem > 1
    figure(2*ceil(lambdaN/4)+1)
```

```matlab
    subplot(4,2,1)
    plot(zeta,Phi1(:,1+(ceil(lambdaN/4)-1)*4))
    title('\Phi_1')
    ylabel(['n = ' num2str(1+(ceil(lambdaN/4)-1)*4)])
    subplot(4,2,2)
    plot(zeta,Phi2(:,1+(ceil(lambdaN/4)-1)*4))
    title('\Phi_2')
    for i=2:rem
        subplot(4,2,2*i-1)
        plot(zeta,Phi1(:,i+(ceil(lambdaN/4)-1)*4))
        ylabel(['n = ' num2str(i+(ceil(lambdaN/4)-1)*4)])
        subplot(4,2,2*i)
        plot(zeta,Phi2(:,i+(ceil(lambdaN/4)-1)*4))
    end
end
%}


%%%%%%%%%%%%%%%%%%%%%%%%%%%%%%%%%%%%%%%%%%%%%%%%%%%%%%%%%%%%%%%%%%%%%%%%%%
%%%%%%%%%%%%%%%%%%%% Leading Order Solution O(\eta) %%%%%%%%%%%%%%%%%%
%%%%%%%%%%%%%%%%%%%%%%%%%%%%%%%%%%%%%%%%%%%%%%%%%%%%%%%%%%%%%%%%%%%%%%%%%%

c1 = zeros(1,lambdaN); %Initialize Eigenfunction Expansion Coefficient
c2 = zeros(1,lambdaN); %Initialize Eigenfunction Expansion Coefficient
Theta = zeros(length(zeta),length(x)); %Initialize Average Temperature
Delta = zeros(length(zeta),length(x)); %Initialize Difference Temperature
T2 = zeros(length(zeta),length(x)); %Initialize Region 2 Temperature
T4 = zeros(length(zeta),length(x)); %Initialize Region 4 Temperature

%LOOP: Loops over first lambdaN Galerkin modes to find the solution
for j = 1:lambdaN
    c1(j) = trapz(zeta,0.5.*(f(zeta')+g(zeta')).*Phi1(:,j).*w(zeta'))...
    ./trapz(zeta,Phi1(:,j).^2.*w(zeta'));
    c2(j) = trapz(zeta,0.5.*(f(zeta')-g(zeta')).*Phi2(:,j).*w(zeta'))...
    ./trapz(zeta,Phi2(:,j).^2.*w(zeta'));

    for k = 1:length(x)
        for i = 1:length(zeta)
            Theta(i,k) = Theta(i,k) + c1(j).*exp(-lambda1(j).*x(k)./Pe)...
            .*Phi1(i,j);
            Delta(i,k) = Delta(i,k) + c2(j).*exp(-lambda2(j).*x(k)./Pe)...
            .*Phi2(i,j);
        end
```

```
    end
end
T2 = Theta+Delta;
T4 = Theta-Delta;

%{
%Plot Region 2 Temperature in \xi and x
figure(100)
mesh(zeta,x,T2')
xlabel('\xi')
ylabel('x')
%axis([0 1 0 1 0 1.5])
title('Region 2 Temperature')
view(0,0)

%Plot inlet temperature with its eigenfunction approximation
figure(101)
plot(zeta,0.5*(f(zeta)+g(zeta)),'k',zeta,T2(:,1))
title('Inlet Temperature')
pause
%}

%%%%%%%%%%%%%%%%%%%%%%%%%%%%%%%%%%%%%%%%%%%%%%%%%%%%%%%%%%%%%%%%%%%%%%%%
%%%%%%%%%%%%%%%%% First Correction Solution O(\eta) %%%%%%%%%%%%%%%%%
%%%%%%%%%%%%%%%%%%%%%%%%%%%%%%%%%%%%%%%%%%%%%%%%%%%%%%%%%%%%%%%%%%%%%%%%

im = sqrt(-1); %imaginary unit
r2 = gam.*sqrt(epf(0)); %Complex wavenumber for region 2
r3 = gam.*sqrt(epm(0)); %Complec wavenumber for region 3
r4 = gam.*sqrt(epf(0)); %Complex wavenumber for region 4

%Construction of a3, b3, coefficients of EM wave in lossy material
Q1 = (1+((gam-r2)./(gam+r2)).*exp(-2.*im.*r2.*(lam-1)))./(1-((gam-r2)...
./(gam+r2)).*exp(-2.*im.*r2.*(lam-1)));
Q2 = (exp(-im.*r4)+((gam-r4)./(gam+r4)).*exp(im.*(r4-2.*r4.*lam)))...
./(exp(-im.*r4)-((gam-r4)./(gam+r4)).*exp(im.*(r4-2.*r4.*lam)));
den = (r2.*r4.*Q1.*Q2+r2.*r3.*Q1+r3.*r4.*Q2+r3.^2).*exp(im.*r3)...
-(r2.*r4.*Q1.*Q2-r2.*r3.*Q1-r3.*r4.*Q2+r3.^2).*exp(-im.*r3);
a3num = (im.*r4.*Q2-im.*r3).*exp(-im.*r3).*(Q1+1).*im.*r2...
.*(2.*gam./(gam+r2)).*exp(im.*(gam-r2).*(lam-1)).*EL-(im.*r2.*Q1+im.*r3)...
.*(Q2+1).*im.*r4.*(2.*gam./(gam+r4)).*exp(im.*(gam.*lam+(1-lam).*r4)-im*gam).*ER;
b3num = -(im.*r4.*Q2+im.*r3).*exp(im.*r3).*(Q1+1).*im.*r2...
.*(2.*gam./(gam+r2)).*exp(im.*(gam-r2).*(lam-1)).*EL+(im.*r2.*Q1-im.*r3)...
```

```matlab
.*(Q2+1).*im.*r4.*(2.*gam./(gam+r4)).*exp(im.*(gam.*lam+(1-lam).*r4)-im*gam).*ER;
a3 = a3num./den;
b3 = b3num./den;

%Electric field in region 3
E3 =@(z) a3*exp(i*r3*z)+b3*exp(-i*r3*z);
%Modulus of electric field in region 3
modE3 =@(z) a3*conj(a3)*exp(im*(r3-conj(r3))*z)+b3*conj(b3)...
*exp(-im*(r3-conj(r3))*z)+a3*conj(b3)*exp(im*(r3+conj(r3))*z)...
+b3*conj(a3)*exp(-im*(r3+conj(r3))*z);
%Integral of the modulus of E3
intE3 =@(z) (a3*conj(a3)./(im*(r3-conj(r3)))).*exp(im.*(r3-conj(r3)).*z)...
-(b3*conj(b3)./(im*(r3-conj(r3)))).*exp(-im*(r3-conj(r3)).*z)+(a3*conj(b3)...
./(im*(r3+conj(r3))))*exp(im*(r3+conj(r3)).*z)-(b3*conj(a3)...
./(im*(r3+conj(r3))))*exp(-im*(r3+conj(r3)).*z)...
-((a3*conj(a3)./(im*(r3-conj(r3))))-(b3*conj(b3)./(im*(r3-conj(r3))))...
+(a3*conj(b3)./(im*(r3+conj(r3))))-(b3*conj(a3)./(im*(r3+conj(r3)))));
%Two integrals of the modulus of E3
intintE3 =@(z) -(a3*conj(a3)./(r3-conj(r3)).^2).*exp(im.*(r3-conj(r3)).*z)...
-(b3*conj(b3)./(r3-conj(r3)).^2).*exp(-im*(r3-conj(r3)).*z)-(a3*conj(b3)...
./(r3+conj(r3)).^2)*exp(im*(r3+conj(r3)).*z)-(b3*conj(a3)./(r3+conj(r3)).^2)...
*exp(-im*(r3+conj(r3)).*z)-((a3*conj(a3)./(im*(r3-conj(r3))))-(b3*conj(b3)...
./(im*(r3-conj(r3))))+(a3*conj(b3)./(im*(r3+conj(r3))))-(b3*conj(a3)./(im...
*(r3+conj(r3))))).*z-(-(a3*conj(a3)./(r3-conj(r3)).^2)-(b3*conj(b3)...
./(r3-conj(r3)).^2)-(a3*conj(b3)./(r3+conj(r3)).^2)-(b3*conj(a3)...
./(r3+conj(r3)).^2));



%Define Sources at the Internal Boundary from Leading Order Electric Field
C = ((lam-1)./(2*K))*P*lossm(0).*(intE3(0)-intE3(1));
D = ((lam-1)./(2*K))*P*lossm(0).*(intE3(0)+intE3(1))+((lam-1)./K)...
*P*lossm(0).*(intintE3(0)-intintE3(1));
%Define volumetric source in regions 2 and 4
F =@(z) 0;
G =@(z) 0;

%Initilize parameters for first correction solution
c1 = zeros(1,lambdaN);
c2 = zeros(1,lambdaN);
S1 = zeros(1,lambdaN);
S2 = zeros(1,lambdaN);
Theta = zeros(length(zeta),length(x));
Delta = zeros(length(zeta),length(x));
```

```
T2 = zeros(length(zeta),length(x));
T4 = zeros(length(zeta),length(x));

%LOOP: Loop over number of Galerkin modes to construct solution
for j = 1:lambdaN
    S1(j) = (-C*Phi1(1,j))./(Pe*trapz(zeta,Phi1(:,j).^2.*w(zeta')))...
    -trapz(zeta,F(zeta').*Phi1(:,j))./(Pe*trapz(zeta,Phi1(:,j).^2.*w(zeta')));
    S2(j) = (-D*Phi2(1,j))./(Pe*trapz(zeta,Phi2(:,j).^2.*w(zeta')))...
    -trapz(zeta,G(zeta').*Phi2(:,j))./(Pe*trapz(zeta,Phi2(:,j).^2.*w(zeta')));
    c1(j) = trapz(zeta,0.5.*(f(zeta')+g(zeta')).*Phi1(:,j).*w(zeta'))...
    ./(trapz(zeta,Phi1(:,j).^2.*w(zeta')))-Pe*S1(j)/lambda1(j);
    c2(j) = trapz(zeta,0.5.*(f(zeta')-g(zeta')).*Phi2(:,j).*w(zeta'))...
    ./(trapz(zeta,Phi2(:,j).^2.*w(zeta')))-Pe*S2(j)/lambda2(j);

    for k = 1:length(x)
        for i = 1:length(zeta)
            Theta(i,k) = Theta(i,k) + (c1(j).*exp(-lambda1(j).*x(k)./Pe)...
            +Pe.*S1(j)./lambda1(j)).*Phi1(i,j);
            Delta(i,k) = Delta(i,k) + (c2(j).*exp(-lambda2(j).*x(k)./Pe)...
            +Pe.*S2(j)./lambda2(j)).*Phi2(i,j);
        end
    end
end
%Define solutions in regions 2 and 4 from solutions of average and
%difference fucntions Theta and Delta
T2 = Theta+Delta;
T4 = Theta-Delta;

%Define microscale domain of each layer
zed2 = -(lam-1)*zeta;
zed3 = zeta;
zed4 = (lam-1)*zeta+1;

%Calculate solution in region 3 from the solutions in regions 2 and 4
T3 = zeros(length(zed3),length(x));
    for k = 1:length(x)
        for i = 1:length(zed3)
            T3(i,k) = -P*lossm(0)*intintE3(zed3(i))+(T4(1,k)-T2(1,k)...
            +P*lossm(0)*intintE3(1)-P*lossm(0)*intintE3(0))*zed3(i)...
            +T2(1,k)+P*lossm(0)*intintE3(0);
        end
    end
```

```
%Define grid for surface plot
zgrid = 1:10:length(zeta); %plots every 10 grid points in z
xgrid = 1:10:length(x);

%Interpolated surface plot with colorbar
figure(324)
surf(zed2(zgrid),x(xgrid)/eta,eta*T2(zgrid,xgrid)'*300+300)
hold on
surf(zed3(zgrid),x(xgrid)/eta,eta*T3(zgrid,xgrid)'*300+300)
hold on
surf(zed4(zgrid),x(xgrid)/eta,eta*T4(zgrid,xgrid)'*300+300)
shading interp
view(0,90)
colorbar
hold on
%Plots location of layer interfaces as solid black lines
MAXVAL = max([max(max(eta*T2'*300+300)) max(max(eta*T3'*300+300))...
 max(max(eta*T4'*300+300))]);
surf([0 0],[0 10],MAXVAL*ones(2),'LineWidth',2)
surf([1 1],[0 10],MAXVAL*ones(2),'LineWidth',2)
xlabel('Spanwise Length (z)')
ylabel('Streamwise Length (x)')
title('Temperature (K)')
set(gca,'Fontsize',16)
hold off

%Interpolated 3D solution plot
figure(202)
surf(zed2(zgrid),x(xgrid)/eta,eta*T2(zgrid,xgrid)'*300+300)
hold on
surf(zed3(zgrid),x(xgrid)/eta,eta*T3(zgrid,xgrid)'*300+300)
hold on
surf(zed4(zgrid),x(xgrid)/eta,eta*T4(zgrid,xgrid)'*300+300)
shading interp
xlabel('Spanwise Length (z)')
ylabel('Streamwise Length (x)')
zlabel('Temperature (K)')
set(gca,'Fontsize',16)

xh = get(gca,'XLabel');
set(xh, 'Units', 'Normalized')
pos = get(xh, 'Position');
```

```
set(xh, 'Position', pos.*[0.75,0.75,1],'Rotation',14)

yh = get(gca,'YLabel');
set(yh, 'Units', 'Normalized')
pos = get(yh, 'Position');
set(yh, 'Position', pos.*[0.65,-0.4,1],'Rotation',-26)
```

```
%PROGRAM: Solution_LargePeclet_EvalConv.m
%FUNCTIONS: ParamDeclare.m, secant.m
%DESCRIPTION: Plots the convergence of the first five eigenvalues against
%the number of Galerkin modes used to approximate them

clear; %Clears all declared parameters and variables

%%%%%%%%%%%%%%%%%%%%%%%%%%%%%%%%%%%%%%%%%%%%%%%%%%%%%%%%%%%%%%%%%%%%%%%%%%%%
%%%%%%%%%%%%%%%%%%%%%%%%%% DECLARE MODEL PARAMETERS %%%%%%%%%%%%%%%%%%%%%%%%%%
%%%%%%%%%%%%%%%%%%%%%%%%%%%%%%%%%%%%%%%%%%%%%%%%%%%%%%%%%%%%%%%%%%%%%%%%%%%%%

[Param,Fcn] = ParamDeclare; %Retrieves parameters from master list

%INITIALIZE PARAMETERS FROM Param AND Fcn FOR USE IN PROGRAM
for j=1:length(Param)
    evalc([Param{j,1},'=',Param{j,2}]);
end
for j=1:length(Fcn)
    evalc(Fcn{j});
end

Pe = Pe*(lam-1)^4; %Redefining for scaled Peclet number

%%%%%%%%%%%%%%%%%%%%%%%%%%%%%%%%%%%%%%%%%%%%%%%%%%%%%%%%%%%%%%%%%%%%%%%%%%%%
%%%%%%%%%%%%%%%%%%%%%%%%% PROGRAM INITIALIZATIONS %%%%%%%%%%%%%%%%%%%%%%%%%%
%%%%%%%%%%%%%%%%%%%%%%%%%%%%%%%%%%%%%%%%%%%%%%%%%%%%%%%%%%%%%%%%%%%%%%%%%%%%
xlength = 1;
eta = 1e-1; %Asymptotic parameter, chosen by geometry
mu = 0:1:1e6; %range of values over which to search for roots
eigtol = 1e-6; %error tolerance for finding roots
zeta = 0:.01:1; %microscale domain discretization
x = 0:.01:xlength; %macroscale domain discretization
f =@(x) zeros(length(x),1); %Initilization of T2 temperature at inlet
g =@(x) zeros(length(x),1); %Initilization of T4 temperature at inlet

%%%%%%%%%%%%%%%%%%%%%%%%%%%%%%%%%%%%%%%%%%%%%%%%%%%%%%%%%%%%%%%%%%%%%%%%%%%
%%%%%%%%%%%%%%%%%%%%%%%%%% Find Eigenvalues %%%%%%%%%%%%%%%%%%%%%%%%%%%%%%%%
%%%%%%%%%%%%%%%%%%%%%%%%%%%%%%%%%%%%%%%%%%%%%%%%%%%%%%%%%%%%%%%%%%%%%%%%%%%
a = 2*(lam-1)./K; %new constant defined

%Characteristic Equations for the two eigenvalues
CharEq1 =@(x) sqrt(x).*sin(sqrt(x))-(lam-1)*Bi*cos(sqrt(x));
CharEq2 =@(x) [K*x-2*(lam-1)^2*Bi].*sin(sqrt(x))-[K*Bi+2]*sqrt(x).*cos(sqrt(x));
```

```
%Determines initial guesses for root finding the eigenvalues
count1 = 1; %counter for number of eigenvalues in the first set
count2 = 1; %counter for number of eigenvalues in the second set

%LOOP: Loops over range where we search for eigenvalues. Assuming by
%inspection that all of the roots are simple we find where the
%characterisitic function changes sign and use the gridpoints are either
%side as the initial values in the secant root finding method
for i=1:length(mu)-1
    if CharEq1(mu(i+1))*CharEq1(mu(i))<0
        MU1(1,count1) = mu(i);
        MU1(2,count1) = mu(i+1);
        count1 = count1 + 1;
    end
    if CharEq2(mu(i+1))*CharEq2(mu(i))<0
        MU2(1,count2) = mu(i);
        MU2(2,count2) = mu(i+1);
        count2 = count2 + 1;
    end
end

z1 = zeros(1,count1-1); %Initialize vector for first set of eigenvalues
z2 = zeros(1,count2-1); %Initialize vector for second set of eigenvalues

%LOOP: Loop over number of times characteristic equation changed sign by
%using the counters. Apply the secant root finding method to determine
%roots with the error tolerance specified by eigtol
for i=1:count1-1
    z1(i) = secant(CharEq1,MU1(1,i),MU1(2,i),eigtol);
    z2(i) = secant(CharEq2,MU2(1,i),MU2(2,i),eigtol);
end
for i=1:count2-1
    z2(i) = secant(CharEq2,MU2(1,i),MU2(2,i),eigtol);
end

%Define truncation for the number of eigenvalues found
N = min(length(z1),length(z2));

N = 10:5:100;
lam1 = zeros(5,length(N));
lam2 = zeros(5,length(N));
for k = 1:length(N)
```

```matlab
%%%%%%%%%%%%%%%%%%%%%%%%%%%%%%%%%%%%%%%%%%%%%%%%%%%%%%%%%%%%%%%%%%%%%%%%%%%%
%%%%%%%%%%%%%%% Define Plug Flow Eigenfunctions %%%%%%%%%%%%%%%%%%%%
%%%%%%%%%%%%%%%%%%%%%%%%%%%%%%%%%%%%%%%%%%%%%%%%%%%%%%%%%%%%%%%%%%%%%%%%%%%%

Psi1 = zeros(length(zeta),N(k)); %Initialize First Plug Flow Eigenfunction
Psi2 = zeros(length(zeta),N(k)); %Initialize Second Plug Flow Eigenfunction
%Defines first N Plug Flow Eigenfunctions
for i=1:N(k)
    for j=1:length(zeta)
        Psi1(j,i) = cos(sqrt(z1(i))*zeta(j));
        Psi2(j,i) = (sqrt(z2(i))/a)*cos(sqrt(z2(i))*zeta(j))...
        +sin(sqrt(z2(i))*zeta(j));
    end
end


%%%%%%%%%%%%%%%%%%%%%%%%%%%%%%%%%%%%%%%%%%%%%%%%%%%%%%%%%%%%%%%%%%%%%%%%%%%%
%%%%%%%%%%%%%%% Determine Poiseulle Flow Eigenfunctions %%%%%%%%%%%%%%%%
%%%%%%%%%%%%%%%%%%%%%%%%%%%%%%%%%%%%%%%%%%%%%%%%%%%%%%%%%%%%%%%%%%%%%%%%%%%%
w =@(x) -x.*(x-1); %Scaled Poiseulle Fluid Velocity
lambdaN = N(k); %Number of Poiseulle Flow Eigenvalues to use (max=N)


%%%%%%%%% Solve Generalized Eigenvalue Problem Mv=lambda*Bv %%%%%%%%%
M1 = zeros(lambdaN,lambdaN); %Initialize Diagonal Matrix
M2 = zeros(lambdaN,lambdaN); %Initialize Diagonal Matrix
B1 = zeros(lambdaN,lambdaN); %Initialize Full Matrix
B2 = zeros(lambdaN,lambdaN); %Initialize Full Matrix

%Construct Matricies M and B
for i = 1:lambdaN
    M1(i,i) = z1(i);
    M2(i,i) = z2(i);
    for j = 1:lambdaN
        B1(i,j) = trapz(zeta,(Psi1(:,j).*Psi1(:,i)).*w(zeta'))...
        ./trapz(zeta,Psi1(:,i).^2);
        B2(i,j) = trapz(zeta,(Psi2(:,j).*Psi2(:,i)).*w(zeta'))...
        ./trapz(zeta,Psi2(:,i).^2);
    end
end

%Solve Generalized eigenvalue problems
```

```matlab
[V1,D1] = eig(full(B1),full(M1)); %MATLAB recommended command (lambdaN=N)
[V2,D2] = eig(full(B2),full(M2)); %MATLAB recommended command (lambdaN=N)
%NOTE: eigenvalues found in diagonals of D1 and D2 are recipricals of the
%eigenvalues (lambda) which we are after

lambda1 = zeros(1,lambdaN); %Initialize vector of Poiseulle eigenvalues
lambda2 = zeros(1,lambdaN); %Initialize vector of Poiseulle eigenvalues
for i=1:lambdaN %Define Poiseulle eigenvalues
    lambda1(i)=1./D1(i,i);
    lambda2(i)=1./D2(i,i);
end

%Record each of the first five eigenvalues as we loop over k
lam1(1,k) = lambda1(1);
lam1(2,k) = lambda1(2);
lam1(3,k) = lambda1(3);
lam1(4,k) = lambda1(4);
lam1(5,k) = lambda1(5);


lam2(1,k) = lambda2(1);
lam2(2,k) = lambda2(2);
lam2(3,k) = lambda2(3);
lam2(4,k) = lambda2(4);
lam2(5,k) = lambda2(5);

end

%Plot error of eigenvalues against the eigenvalue approximation using 100
%Galerkin modes as the exact solution
figure(1)
plot(log(N(length(N))-N(1:length(N)-1))/log(10),log(abs(lam1(1,length(N))...
-lam1(1,1:length(N)-1)))/log(10),'-o','LineWidth',2)
hold on
plot(log(N(length(N))-N(1:length(N)-1))/log(10),log(abs(lam1(2,length(N))...
-lam1(2,1:length(N)-1)))/log(10),'-o','LineWidth',2)
hold on
plot(log(N(length(N))-N(1:length(N)-1))/log(10),log(abs(lam1(3,length(N))...
-lam1(3,1:length(N)-1)))/log(10),'-o','LineWidth',2)
hold on
plot(log(N(length(N))-N(1:length(N)-1))/log(10),log(abs(lam1(4,length(N))...
-lam1(4,1:length(N)-1)))/log(10),'-o','LineWidth',2)
hold on
plot(log(N(length(N))-N(1:length(N)-1))/log(10),log(abs(lam1(5,length(N))...
```

```matlab
-lam1(5,1:length(N)-1)))/log(10),'-o','Linewidth',2)
title('Convergence of First Five Eigenvalues for \Theta')
xlabel(['log(|' num2str(N(length(N))) '-N|)'])
ylabel(['log(|\lambda_{' num2str(N(length(N))) '}-\lambda_N|)'])
legend('\lambda_1','\lambda_2','\lambda_3','\lambda_4','\lambda_5')
set(gca,'fontsize',18)

figure(2)
plot(log(N(length(N))-N(1:length(N)-1))/log(10),log(abs(lam2(1,length(N))...
-lam2(1,1:length(N)-1)))/log(10),'-o','LineWidth',2)
hold on
plot(log(N(length(N))-N(1:length(N)-1))/log(10),log(abs(lam2(2,length(N))...
-lam2(2,1:length(N)-1)))/log(10),'-o','LineWidth',2)
hold on
plot(log(N(length(N))-N(1:length(N)-1))/log(10),log(abs(lam2(3,length(N))...
-lam2(3,1:length(N)-1)))/log(10),'-o','LineWidth',2)
hold on
plot(log(N(length(N))-N(1:length(N)-1))/log(10),log(abs(lam2(4,length(N))...
-lam2(4,1:length(N)-1)))/log(10),'-o','LineWidth',2)
hold on
plot(log(N(length(N))-N(1:length(N)-1))/log(10),log(abs(lam2(5,length(N))...
-lam2(5,1:length(N)-1)))/log(10),'-o','Linewidth',2)
title('Convergence of First Five Eigenvalues for \Delta')
xlabel(['log(|' num2str(N(length(N))) '-N|)'])
ylabel(['log(|\lambda_{' num2str(N(length(N))) '}-\lambda_N|)'])
legend('\lambda_1','\lambda_2','\lambda_3','\lambda_4','\lambda_5')
set(gca,'fontsize',18)
```

```
%PROGRAM: PeacmanRachfordADI.m
%FUNCTION CALLS: ParamDeclare.m, Efield3.m, tridiag.m
%DESCRIPTION: Solves the Parabolic Differential Equation
%u_t = Kx*u_xx + Ky*u_yy + A*u_x + B(x,y)*u_y + C*u + S where the advective
%term is allowed to be spatially dependent. The Peaceman-Rachford
%Alternating Direction Implicit method is used to find solutions

clear; %Clears all declared parameters and variables

%%%%%%%%%%%%%%%%%%%%%%%%%%%%%%%%%%%%%%%%%%%%%%%%%%%%%%%%%%%%%%%%%%%%%%%%%%%%
%%%%%%%%%%%%%%%%%%%%%%%%%%% DECLARE MODEL PARAMETERS %%%%%%%%%%%%%%%%%%%%%%%%%
%%%%%%%%%%%%%%%%%%%%%%%%%%%%%%%%%%%%%%%%%%%%%%%%%%%%%%%%%%%%%%%%%%%%%%%%%%%%%

[Param,Fcn] = ParamDeclare; %Retrieves parameters from master list

%INITIALIZE PARAMETERS FROM Param AND Fcn FOR USE IN PROGRAM
for j=1:length(Param)
    evalc([Param{j,1},'=',Param{j,2}]);
end
for j=1:length(Fcn)
    evalc(Fcn{j});
end

%%%%%%%%%%%%%%%%%%%%%%%%%%%% Subdomain 1 %%%%%%%%%%%%%%%%%%%%%%%%%%%%%%%%%%%
%Input Parameters
Kx1 = .5;
Ky1 = .5;
A1 = 0; %Advection x-direction
B1 =@(x,y) x.*(x+(lam-1))*.5*Pe; %Advection y-direction
C1 = 0; %Linear Coefficient
S1 =@(u,x,y,t) 0; %Source

Lx1 = lam-1; %Length x-direction
dx1 = 5e-2; %Grid spacing
Xmax1 = Lx1/dx1 + 1; %Number of grid points

%%%%%%%%%%%%%%%%%%%%%%%%%%%% Subdomain 2 %%%%%%%%%%%%%%%%%%%%%%%%%%%%%%%%%%%
%Input Parameters
Kx2 = 1;
Ky2 = 1;
A2 = 0; %Advection x-direction
B2 = 0;
C2 = 0; %Linear Coefficient
```

```
S2 =@(u,x,y,t) P.*lossm(u).*Efield3(u,x,Param,Fcn); %Source


Lx2 = 1; %Length x-direction
dx2 = 5e-2; %Grid spacing
Xmax2 = Lx2/dx2 + 1; %Number of grid points


%%%%%%%%%%%%%%%%%%%%%%%%% Subdomain 3 %%%%%%%%%%%%%%%%%%%%%%%%%%%%%
%Input Parameters
Kx3 = .5;
Ky3 = .5;
A3 = 0; %Advection x-direction
B3 =@(x,y) -(x-1).*(lam-x)*.5*Pe; %Advection y-direction
C3 = 0; %Linear Coefficient
S3 =@(u,x,y,t) 0; %Source


Lx3 = lam-1; %Length x-direction
dx3 = 5e-2; %Grid spacing
Xmax3 = Lx3/dx3 + 1; %Number of grid points


%%%%%%%%%%%%%%%%%%%%%%%% End Subdomain Declarations %%%%%%%%%%%%%%%%%%%%%%%


%Input Parameters
Ly = 10; %Length of layers
dy = .1; %y grid spacing
Xmax = Xmax1+Xmax2+Xmax3-2; %Total number of grid points in x-direction
Ymax = Ly/dy + 1; %Number of grid points in y-direction
%Time step: use smaller step 1e-2 or 1e-3 for high power where thermal
%runaway events occur where numerical instabilities can occur with such a
%rapid change in the temperature
dt = 1e-1;
Tmax = 100001; %Maximum number of time steps


%Initializations
x = [-Lx1:dx1:0 dx2:dx2:Lx2 Lx2+dx3:dx3:Lx2+Lx3]'; %x-domain
y = 0:dy:Ly; %y-domain
%Grid points used in plotting
xgrid = [1:2:length(-Lx1:dx1:0) length(-Lx1:dx1:0)+2:2:...
length([-Lx1:dx1:0 dx2:dx2:Lx2]) length([-Lx1:dx1:0 dx2:dx2:Lx2])...
+2:2:length(x)]; %Grid points used in plotting
ygrid = 1:10:length(y);
u = zeros(Xmax,Ymax,2); %Temperature solution
L1 = zeros(Xmax,1); %subdiagonal of first tridiagonal system in ADI
M1 = zeros(Xmax,1); %main diagonal of first tridiagonal system in ADI
```

```
R1 = zeros(Xmax,1); %superdiagonal of first tridiagonal system in ADI
RHS1 = zeros(Xmax,1); %right hand side of first tridiagonal system in ADI
L2 = zeros(1,Ymax); %subdiagonal of second tridiagonal system in ADI
M2 = zeros(1,Ymax); %main diagonal of second tridiagonal system in ADI
R2 = zeros(1,Ymax); %superdiagonal of second tridiagonal system in ADI
RHS2 = zeros(1,Ymax); %right hand side of second tridiagonal system in ADI

%Boundary Conditions a*u_x + b*u = c
%Top Boundary
aT = 1;
bT = 0;
cT =@(x,t) 0;
%Bottom Boundary
aB = 0;
bB = 1;
cB =@(x,t) 0;
%Left Boundary
aL = 1;
bL = -Bi;
cL =@(y,t) 0;
%Right Boundary
aR = 1;
bR = 1;
cR =@(y,t) 0;

%Initial Condition
u0 =@(x,y) 0;

%Coefficient Groups
rx1 = Kx1*dt/(2*dx1^2);
sx1 = A1*dt/(4*dx1);
ry1 = Ky1*dt/(2*dy^2);
sy1 =@(x,y) B1(x,y)*dt/(4*dy);
ss1 = C1*dt/4;

rx2 = Kx2*dt/(2*dx2^2);
sx2 = A2*dt/(4*dx2);
ry2 = Ky2*dt/(2*dy^2);
sy2 = B2*dt/(4*dy);
ss2 = C2*dt/4;

rx3 = Kx3*dt/(2*dx3^2);
sx3 = A3*dt/(4*dx3);
```

```
ry3 = Ky3*dt/(2*dy^2);
sy3 =@(x,y) B3(x,y)*dt/(4*dy);
ss3 = C3*dt/4;

XL1 = -rx1+sx1;
XM1 = 1+2*rx1-ss1;
XR1 = -rx1-sx1;

XL2 = -rx2+sx2;
XM2 = 1+2*rx2-ss2;
XR2 = -rx2-sx2;

XL3 = -rx3+sx3;
XM3 = 1+2*rx3-ss3;
XR3 = -rx3-sx3;

YL1 =@(x,y) -ry1+sy1(x,y);
YM1 = 1+2*ry1-ss1;
YR1 =@(x,y) -ry1-sy1(x,y);

YL2 = -ry2+sy2;
YM2 = 1+2*ry2-ss2;
YR2 = -ry2-sy2;

YL3 =@(x,y) -ry3+sy3(x,y);
YM3 = 1+2*ry3-ss3;
YR3 =@(x,y) -ry3-sy3(x,y);

%%%%%%%%%%%%%%%%%%%%%%%%%%%%%%%%%%%%%%%%%%%%%%%%%%%%%%%%%%%%%%%%%%%%%%%%%%%%%
%%%%%%%%%%%%%%%%%%%%%%%%%%%%%%% Main Body %%%%%%%%%%%%%%%%%%%%%%%%%%%%%%%%%%%%
%%%%%%%%%%%%%%%%%%%%%%%%%%%%%%%%%%%%%%%%%%%%%%%%%%%%%%%%%%%%%%%%%%%%%%%%%%%%%

%Calculate Temperature from Initial Condition
for j = 1:Ymax
    for i = 1:Xmax
        u(i,j,1) = u0(x(i),y(j));
    end
end

%LOOP: Loops over time, every time step a new temperture and EM solution
%are solved for.
for n = 1:Tmax
t = n*dt; %Nondimensional time
```

```
%%%%%%%%%%%%%%%% Begin First Half of ADI Method %%%%%%%%%%%%%%%%%%%%
% LOOP: Loops over Interior Rows j=2:Ymax-1 solving system in x-direction
for j = 2:Ymax-1
    %i=1 (left boundary)
    if aL == 0
        %Dirichlet BC
        M1(1) = 1;
        RHS1(1) = cL(y(j),t)/bL;
    else
        %Robin BC
        M1(1) = bL-aL/dx1;
        R1(1) = aL/dx1;
        RHS1(1) = cL(y(j),t);
    end
    %i=2:Xmax1-1 (interior of 1st subdomain)
    L1(2:Xmax1-1) = XL1;
    M1(2:Xmax1-1) = XM1;
    R1(2:Xmax1-1) = XR1;
    RHS1(2:Xmax1-1) = (ry1-sy1(x(2:Xmax1-1),y(j))).*u(2:Xmax1-1,j-1,1)...
     + (1-2*ry1+ss1)*u(2:Xmax1-1,j,1) + (ry1+sy1(x(2:Xmax1-1),y(j)))...
     .*u(2:Xmax1-1,j+1,1) + (dt/2)*S1(u(2:Xmax1-1,j,1),x(2:Xmax1-1),y(j),t);

    %i=Xmax1 (1st subdomain connection)
    L1(Xmax1) = Kx1/dx1;
    M1(Xmax1) = -(Kx1/dx1+Kx2/dx2);
    R1(Xmax1) = Kx2/dx2;
    RHS1(Xmax1) = 0;

    %i=Xmax1+1:Xmax1+Xmax2-2 (interior of 2nd subdomain)
    L1(Xmax1+1:Xmax1+Xmax2-2) = XL2;
    M1(Xmax1+1:Xmax1+Xmax2-2) = XM2;
    R1(Xmax1+1:Xmax1+Xmax2-2) = XR2;
    RHS1(Xmax1+1:Xmax1+Xmax2-2) = (ry2-sy2)*u(Xmax1+1:Xmax1+Xmax2-2,j-1,1)...
    + (1-2*ry2+ss2)*u(Xmax1+1:Xmax1+Xmax2-2,j,1)...
    + (ry2+sy2)*u(Xmax1+1:Xmax1+Xmax2-2,j+1,1) ...
    + (dt/2)*S2(u(Xmax1+1:Xmax1+Xmax2-2,j,1),x(Xmax1+1:Xmax1+Xmax2-2),y(j),t);

    %i=Xmax1+Xmax2-1 (2nd subdomain connection)
    L1(Xmax1+Xmax2-1) = Kx2/dx2;
    M1(Xmax1+Xmax2-1) = -(Kx2/dx2+Kx3/dx3);
    R1(Xmax1+Xmax2-1) = Kx3/dx3;
    RHS1(Xmax1+Xmax2-1) = 0;
```

```
    %i=Xmax1+Xmax2:Xmax1+Xmax2+Xmax3-3 (interior of 3rd subdomain)
    L1(Xmax1+Xmax2:Xmax-1) = XL3;
    M1(Xmax1+Xmax2:Xmax-1) = XM3;
    R1(Xmax1+Xmax2:Xmax-1) = XR3;
    RHS1(Xmax1+Xmax2:Xmax-1) = (ry3-sy3(x(Xmax1+Xmax2:Xmax-1),y(j)))...
    .*u(Xmax1+Xmax2:Xmax-1,j-1,1) + (1-2*ry3+ss3)*u(Xmax1+Xmax2:Xmax-1,j,1)...
    + (ry3+sy3(x(Xmax1+Xmax2:Xmax-1),y(j))).*u(Xmax1+Xmax2:Xmax-1,j+1,1)...
    + (dt/2)*S3(u(Xmax1+Xmax2:Xmax-1,j,1),x(Xmax1+Xmax2:Xmax-1),y(j),t);

    %i=Xmax1+Xmax2+Xmax3-2 (right boundary)
    if aR == 0
        %Dirichlet BC
        M1(Xmax) = 1;
        RHS1(Xmax) = cR(y(j),t)/bR;
    else
        %Robin BC
        L1(Xmax) = -aR/dx3;
        M1(Xmax) = bR+aR/dx3;
        RHS1(Xmax) = cR(y(j),t);
    end

    %Solve Matrix System
    u(:,j,2) = tridiag(L1,M1,R1,RHS1);
end
% Note: Interior is needed to solve for top/bottom boundaries if Neumann BCs


% First Row j = 1 (Boundary Condition implemented explicitly)
if aB == 0
    %Dirichlet
    u(:,1,2) = cB(x(:),t)/bB;
else
    %Robin
    u(:,1,2) = (cB(x(:),t)-aB*u(:,2,2)/dy)/(bB-aB/dy);
end
% Last Row j = Ymax (Boundary Condition implemented explicitly)
if aT == 0
    %Dirichlet
    u(:,Ymax,2) = cT(x(:),t)/bT;
else
    %Robin
    u(:,Ymax,2) = (cT(x(:),t)+aT/dy)/(bT+aT/dy);
```

```
end

%%%%%%%%%%%%%%%%%%%%%%% End First Half %%%%%%%%%%%%%%%%%%%%%%%%%%%%

%Update Solution
u(:,:,1) = u(:,:,2);

%%%%%%%%%%%%%%%%%%%%%%% Begin Second Half %%%%%%%%%%%%%%%%%%%%%%%%%%
% Solve Interior Columns in each subdomain
%LOOP: Loops over First Subdomain i=2:Xmax1-1 solving system in y-direction
for i = 2:Xmax1-1
    %j=1 BC
    if aB == 0
        %Dirichlet BC
        M2(1) = 1;
        RHS2(1) = cB(x(i),t)/bB;
    else
        %Robin BC
        M2(1) = (bB-aB/dy);
        R2(1) = aB/dy;
        RHS2(1) = cB(x(i),t);
    end
    %j=2:Ymax-1
    L2(2:Ymax-1) = YL1(x(i),y(2:Ymax-1));
    M2(2:Ymax-1) = YM1;
    R2(2:Ymax-1) = YR1(x(i),y(2:Ymax-1));
    RHS2(2:Ymax-1) = (rx1-sx1)*u(i-1,2:Ymax-1,1) ...
    + (1-2*rx1+ss1)*u(i,2:Ymax-1,1) + (rx1+sx1)*u(i+1,2:Ymax-1,1) ...
    + (dt/2)*S1(u(i,2:Ymax-1,1),x(i),y(2:Ymax-1),t);
    %j=Ymax
    if aT == 0
        %Dirichlet BC
        M2(Ymax) = 1;
        RHS2(Ymax) = cT(x(i),t)/bT;
    else
        %Robin BC
        L2(Ymax) = -aT/dy;
        M2(Ymax) = bT+aT/dy;
        RHS2(Ymax) = cT(x(i),t);
    end

    %Solve Matrix System
    u(i,:,2) = tridiag(L2,M2,R2,RHS2);
```

```
end

%LOOP: Loops over Second Subdomain i=Xmax1+1:Xmax1+Xmax2-2 solving system
%in y-direction
for i = Xmax1+1:Xmax1+Xmax2-2
    %j=1 BC
    if aB == 0
        %Dirichlet BC
        M2(1) = 1;
        RHS2(1) = cB(x(i),t)/bB;
    else
        %Robin BC
        M2(1) = (bB-aB/dy);
        R2(1) = aB/dy;
        RHS2(1) = cB(x(i),t);
    end
    %j=2:Ymax-1
    L2(2:Ymax-1) = YL2;
    M2(2:Ymax-1) = YM2;
    R2(2:Ymax-1) = YR2;
    RHS2(2:Ymax-1) = (rx2-sx2)*u(i-1,2:Ymax-1,1) ...
    + (1-2*rx2+ss2)*u(i,2:Ymax-1,1) + (rx2+sx2)*u(i+1,2:Ymax-1,1) ...
    + (dt/2)*S2(u(i,2:Ymax-1,1),x(i),y(2:Ymax-1),t);
    %j=Ymax
    if aT == 0
        %Dirichlet BC
        M2(Ymax) = 1;
        RHS2(Ymax) = cT(x(i),t)/bT;
    else
        %Robin BC
        L2(Ymax) = -aT/dy;
        M2(Ymax) = bT+aT/dy;
        RHS2(Ymax) = cT(x(i),t);
    end

    %Solve Matrix System
    u(i,:,2) = tridiag(L2,M2,R2,RHS2);
end

%LOOP: Loops over Third Subdomain i=Xmax1+Xmax2:Xmax-1 solving system
%in y-direction
for i = Xmax1+Xmax2:Xmax-1
    %j=1 BC
```

```
    if aB == 0
        %Dirichlet BC
        M2(1) = 1;
        RHS2(1) = cB(x(i),t)/bB;
    else
        %Robin BC
        M2(1) = (bB-aB/dy);
        R2(1) = aB/dy;
        RHS2(1) = cB(x(i),t);
    end
    %j=2:Ymax-1
    L2(2:Ymax-1) = YL3(x(i),y(2:Ymax-1));
    M2(2:Ymax-1) = YM3;
    R2(2:Ymax-1) = YR3(x(i),y(2:Ymax-1));
    RHS2(2:Ymax-1) = (rx3-sx3)*u(i-1,2:Ymax-1,1) ...
    + (1-2*rx3+ss3)*u(i,2:Ymax-1,1) + (rx3+sx3)*u(i+1,2:Ymax-1,1) ...
    + (dt/2)*S3(u(i,2:Ymax-1,1),x(i),y(2:Ymax-1),t);
    %j=Ymax
    if aT == 0
        %Dirichlet BC
        M2(Ymax) = 1;
        RHS2(Ymax) = cT(x(i),t)/bT;
    else
        %Robin BC
        L2(Ymax) = -aT/dy;
        M2(Ymax) = bT+aT/dy;
        RHS2(Ymax) = cT(x(i),t);
    end

    %Solve Matrix System
    u(i,:,2) = tridiag(L2,M2,R2,RHS2);
end
% Note: Interior is needed to solve for top/bottom/connecting boundaries
%if Neumann BCs


% First Column i = 1 (Boundary Condition implemented explicitly)
if aL == 0
    %Dirichlet
    u(1,:,2) = cL(y(:),t)/bL;
else
    %Robin
    u(1,:,2) = (cL(y(:),t)-aL*u(2,:,2)/dx1)/(bL-aL/dx1);
```

```
end

%Connecting Boundary i = Xmax1 (Boundary condition implemented explicitly)
u(Xmax1,:,2) = (Kx1*u(Xmax1-1,:,2)/dx1+Kx2*u(Xmax1+1,:,2)/dx2)...
/(Kx1/dx1+Kx2/dx2);

%Connecting Boundary i = Xmax1+Xmax2-1 (Boundary condition implemented
% explicitly)
u(Xmax1+Xmax2-1,:,2) = (Kx2*u(Xmax1+Xmax2-2,:,2)/dx2...
+Kx3*u(Xmax1+Xmax2,:,2)/dx3)/(Kx2/dx2+Kx3/dx3);

% Last Column i = Xmax (Boundary condition implemented explicitly)
if aR == 0
    %Dirichlet
    u(Xmax,:,2) = cR(y(:),t)/bR;
else
    %Robin
    u(Xmax,:,2) = (cR(y(:),t)+aR*u(Xmax-1,:,2)/dx3)/(bR+aR/dx3);
end

%%%%%%%%%%%%%%%%%%%%%% End of Second Half %%%%%%%%%%%%%%%%%%%%%%%%%%

    n %Displays current time step
    %Prints error at each time step to command line
    if n > 1
        newSln=abs(u(:,1:length(y)-1,2)*300+300);
        newDiff=abs(u(:,1:length(y)-1,2)-u(:,1:length(y)-1,1))*300;
        newmax = max(newSln(:));
        fprintf('%10.10f\n',max(newDiff(:))/newmax);
        pause(.01)
    end
    oldSln = u(:,:,2); %redefine old solution
    oldmax = max(oldSln(:)); %redefine maximum of old solution

%Update Solution
u(:,:,1) = u(:,:,2);

%%%%%%%%%%%%%%%%%%%%%%%%% Plot Solution %%%%%%%%%%%%%%%%%%%%%%%%%%%%

nPlot = 1; %Number of time steps that the solution is plotted
if mod(n,nPlot) == 0

    %Interpolated 2D surface plot with colorbar
```

```
figure(1)
surf(x(xgrid),y(ygrid),u(xgrid,ygrid,2)'.*300+300)
shading interp
view(0,90)
colorbar
hold on
MAXVAL = max(max(u(:,:,2)'*300+300));
surf([0 0],[0 10],MAXVAL*ones(2),'LineWidth',2)
surf([1 1],[0 10],MAXVAL*ones(2),'LineWidth',2)
xlabel('Spanwise Length (z)')
ylabel('Streamwise Length (x)')
title('Temperature (K)')
set(gca,'Fontsize',16)
hold off

%Interpolated 3D surface plot
figure(2)
surf(x(xgrid),y(ygrid),u(xgrid,ygrid,2)'.*300+300) %Mesh Temperature Profile
shading interp
title(['Thermal Solution at t=' num2str(n*dt)])
xlabel('Spanwise Length (z)')
ylabel('Streamwise Length (x)')
zlabel('Temperature (K)')
axis([-1 2 0 10 300 320])
set(gca,'Fontsize',16)

xh = get(gca,'XLabel');
set(xh, 'Units', 'Normalized')
pos = get(xh, 'Position');
set(xh, 'Position', pos.*[0.75,0.75,1],'Rotation',14)

yh = get(gca,'YLabel');
set(yh, 'Units', 'Normalized')
pos = get(yh, 'Position');
set(yh, 'Position', pos.*[0.65,-0.4,1],'Rotation',-26)

%Mesh plot of electric field over the 2D domain
figure(3)
mesh(x(Xmax1:Xmax1+Xmax2-1),y,Efield3(u(Xmax1:Xmax1+Xmax2-1,:,2)...
,x(Xmax1:Xmax1+Xmax2-1),Param,Fcn)')
title('Electric Field')
xlabel('Spanwise Length (z)')
ylabel('Streamwise Length (x)')
```

```
    zlabel('Electric Field')
    set(gca,'Fontsize',16)

    xh = get(gca,'XLabel');
    set(xh, 'Units', 'Normalized')
    pos = get(xh, 'Position');
    set(xh, 'Position', pos.*[0.75,0.75,1],'Rotation',14)

    yh = get(gca,'YLabel');
    set(yh, 'Units', 'Normalized')
    pos = get(yh, 'Position');
    set(yh, 'Position', pos.*[0.65,-0.4,1],'Rotation',-26)

end


end
```

```
%PROGRAM: PeacmanRachfordADI_PowLoop.m
%FUNCTION CALLS: ParamDeclare.m, Efield3.m, tridiag.m
%DESCRIPTION: Solves the Parabolic Differential Equation
%u_t = Kx*u_xx + Ky*u_yy + A*u_x + B(x,y)*u_y + C*u + S where the advective
%term is allowed to be spatially dependent. The Peaceman-Rachford
%Alternating Direction Implicit method is used to find solutions. Loops
%over power and output temperature and power to text files for construction
%of power response curves later. Makes use of MATLAB Parallel Toolbox.

clear; %Clears all declared parameters and variables

%Open new text files or clear old text files
fileID01 = fopen('MaxTemp.txt','w');
fileID02 = fopen('MinTemp.txt','w');
fileID03 = fopen('MaxTempCer.txt','w');
fileID04 = fopen('MinTempCer.txt','w');
fileID05 = fopen('AveTemp.txt','w');
fileID06 = fopen('AveTempCer.txt','w');
fileID07 = fopen('Power.txt','w');
fileID08 = fopen('PowerCalc.txt','w');

%Close text files
fclose(fileID01);
fclose(fileID02);
fclose(fileID03);
fclose(fileID04);
fclose(fileID05);
fclose(fileID06);
fclose(fileID07);
fclose(fileID08);

%%%%%%%%%%%%%%%%%%%%%%%%%%%%%%%%%%%%%%%%%%%%%%%%%%%%%%%%%%%%%%%%%%%%%%%%%%%%%
%%%%%%%%%%%%%%%%%%%%%%%%%%%%% DECLARE MODEL PARAMETERS %%%%%%%%%%%%%%%%%%%%%%%%
%%%%%%%%%%%%%%%%%%%%%%%%%%%%%%%%%%%%%%%%%%%%%%%%%%%%%%%%%%%%%%%%%%%%%%%%%%%%%%

[Param,Fcn] = ParamDeclare; %Retrieves parameters from master list

%INITIALIZE PARAMETERS FROM Param AND Fcn FOR USE IN PROGRAM
for j=1:length(Param)
    evalc([Param{j,1},'=',Param{j,2}]);
end
for j=1:length(Fcn)
    evalc(Fcn{j});
```

```
end

%Power list to loop over. In practice there need to be multiple lists for
%both forward and backward hysteresis at every thermal runaway event.
PowList = 3800:50:3900;

%LOOP: parfor loop over Power List
parfor m=1:length(PowList)
Pow = PowList(m);
E0 = sqrt(2*377*Pow);
P = ((ls.^2.*E0.^2)./(2.*km.*TA));

%%%%%%%%%%%%%%%%%%%%%%%%% Subdomain 1 %%%%%%%%%%%%%%%%%%%%%%%%%%%%%
%Input Parameters
Kx1 = alpha; %Diffusivity x-direction
Ky1 = alpha; %Diffusivity y-direction
A1 = 0; %Advection x-direction
B1 =@(x,y) 0; %Advection y-direction
C1 = 0; %Linear Coefficient
S1 =@(u,x,y,t) 0; %Source

Lx1 = lam-1; %Length x-direction
dx1 = (5e-2)*Lx1; %Grid spacing
Xmax1 = round(Lx1/dx1) + 1; %Number of grid points

%%%%%%%%%%%%%%%%%%%%%%%%% Subdomain 2 %%%%%%%%%%%%%%%%%%%%%%%%%%%%%
%Input Parameters
Kx2 = 1; %Diffusivity x-direction
Ky2 = 1; %Diffusivity y-direction
A2 = 0; %Advection x-direction
B2 = 0; %Advection y-direction
C2 = 0; %Linear Coefficient
S2 =@(u,x,y,t) P.*sigm(u).*Efield3(u,x,Param,Fcn); %Source

Lx2 = 1; %Length x-direction
dx2 = (5e-2)*Lx2; %Grid spacing
Xmax2 = round(Lx2/dx2) + 1; %Number of grid points

%%%%%%%%%%%%%%%%%%%%%%%%% Subdomain 3 %%%%%%%%%%%%%%%%%%%%%%%%%%%%%
%Input Parameters
Kx3 = alpha; %Diffusivity x-direction
Ky3 = alpha; %Diffusivity y-direction
A3 = 0; %Advection x-direction
```

```matlab
%B3 =@(x,y) -alpha*Pe*psign*(x-1).*(x-lam); %Advection y-direction
B3 =@(x,y) 0;
C3 = 0; %Linear Coefficient
S3 =@(u,x,y,t) 0; %Source

Lx3 = lam-1; %Length x-direction
dx3 = (5e-2)*Lx3; %Grid spacing
Xmax3 = round(Lx3/dx3) + 1; %Number of grid points

%%%%%%%%%%%%%%%%%%% End Subdomain Declarations %%%%%%%%%%%%%%%%%%%%%

%Input Parameters
Ly = 1/eta; %Length of layers
dy = Ly/100; %y grid spacing
Xmax = Xmax1+Xmax2+Xmax3-2; %Total number of grid points in x-direction
Ymax = Ly/dy + 1; %Number of grid points in y-direction
%Time step: use smaller step 1e-2 or 1e-3 for high power where thermal
%runaway events occur where numerical instabilities can occur with such a
%rapid change in the temperature
dt = 1e-1;
Tmax = 100001; %Maximum number of time steps
tol = 1e-5; %Error tolerance
relerr = 1; %Initilize relative error

%Initializations
x = [-Lx1:dx1:0 dx2:dx2:Lx2 Lx2+dx3:dx3:Lx2+Lx3]';   %x-domain
y = 0:dy:Ly; %y-domain
%Grid points used in plotting
xgrid = [1:2:length(-Lx1:dx1:0) length(-Lx1:dx1:0)+2:2:...
length([-Lx1:dx1:0 dx2:dx2:Lx2]) length([-Lx1:dx1:0 dx2:dx2:Lx2])+2:2:...
length(x)]; %Grid points used in plotting
ygrid = 1:10:length(y);
u = zeros(Xmax,Ymax,2); %Temperature solution
L1 = zeros(Xmax,1); %subdiagonal of first tridiagonal system in ADI
M1 = zeros(Xmax,1); %main diagonal of first tridiagonal system in ADI
R1 = zeros(Xmax,1); %superdiagonal of first tridiagonal system in ADI
RHS1 = zeros(Xmax,1); %right hand side of first tridiagonal system in ADI
L2 = zeros(1,Ymax); %subdiagonal of second tridiagonal system in ADI
M2 = zeros(1,Ymax); %main diagonal of second tridiagonal system in ADI
R2 = zeros(1,Ymax); %superdiagonal of second tridiagonal system in ADI
RHS2 = zeros(1,Ymax); %right hand side of second tridiagonal system in ADI

%Boundary Conditions a*u_x + b*u = c
```

```
%Top Boundary
aT = 1;
bT = 0;
cT =@(x,t) 0;
%Bottom Boundary
aB = 1;
bB = 0;
cB =@(x,t) 0;
%Left Boundary
aL = 1;
bL = -Bi;
cL =@(y,t) 0;
%Right Boundary
aR = 1;
bR = Bi;
cR =@(y,t) 0;

%Initial Condition
u0 =@(x,y) 0;

%Coefficient Groups
rx1 = Kx1*dt/(2*dx1^2);
sx1 = A1*dt/(4*dx1);
ry1 = Ky1*dt/(2*dy^2);
sy1 =@(x,y) B1(x,y)*dt/(4*dy);
ss1 = C1*dt/4;

rx2 = Kx2*dt/(2*dx2^2);
sx2 = A2*dt/(4*dx2);
ry2 = Ky2*dt/(2*dy^2);
sy2 = B2*dt/(4*dy);
ss2 = C2*dt/4;

rx3 = Kx3*dt/(2*dx3^2);
sx3 = A3*dt/(4*dx3);
ry3 = Ky3*dt/(2*dy^2);
sy3 =@(x,y) B3(x,y)*dt/(4*dy);
ss3 = C3*dt/4;

XL1 = -rx1+sx1;
XM1 = 1+2*rx1-ss1;
XR1 = -rx1-sx1;
```

```matlab
XL2 = -rx2+sx2;
XM2 = 1+2*rx2-ss2;
XR2 = -rx2-sx2;

XL3 = -rx3+sx3;
XM3 = 1+2*rx3-ss3;
XR3 = -rx3-sx3;

YL1 =@(x,y) -ry1+sy1(x,y);
YM1 = 1+2*ry1-ss1;
YR1 =@(x,y) -ry1-sy1(x,y);

YL2 = -ry2+sy2;
YM2 = 1+2*ry2-ss2;
YR2 = -ry2-sy2;

YL3 =@(x,y) -ry3+sy3(x,y);
YM3 = 1+2*ry3-ss3;
YR3 =@(x,y) -ry3-sy3(x,y);

%%%%%%%%%%%%%%%%%%%%%%%%%%%%%%%%%%%%%%%%%%%%%%%%%%%%%%%%%%%%%%%%%%%%%%%%%%%%%%%%
%%%%%%%%%%%%%%%%%%%%%%%%%%%%%%%%% Main Body %%%%%%%%%%%%%%%%%%%%%%%%%%%%%%%%%%%%
%%%%%%%%%%%%%%%%%%%%%%%%%%%%%%%%%%%%%%%%%%%%%%%%%%%%%%%%%%%%%%%%%%%%%%%%%%%%%%%%

%Initialize Initial Condition
for j = 1:Ymax
    for i = 1:Xmax
        u(i,j,1) = u0(x(i),y(j));
    end
end

%LOOP: Loops over time, every time step a new temperture and EM solution
%are solved for.
n = 1;
while relerr > tol
t = n*dt; %Nondimensional time

%%%%%%%%%%%%%%%%%%%%% Begin First Half of ADI Method %%%%%%%%%%%%%%%%%%%%%
% LOOP: Loops over Interior Rows j=2:Ymax-1 solving system in x-direction
for j = 2:Ymax-1
   %i=1 (left boundary)
   if aL == 0
       %Dirichlet BC
```

```
        M1(1) = 1;
        RHS1(1) = cL(y(j),t)/bL;
    else
        %Robin BC
        M1(1) = bL-aL/dx1;
        R1(1) = aL/dx1;
        RHS1(1) = cL(y(j),t);
    end
    %i=2:Xmax1-1 (interior of 1st subdomain)
    L1(2:Xmax1-1) = XL1;
    M1(2:Xmax1-1) = XM1;
    R1(2:Xmax1-1) = XR1;
    RHS1(2:Xmax1-1) = (ry1-sy1(x(2:Xmax1-1),y(j))).*u(2:Xmax1-1,j-1,1)...
    + (1-2*ry1+ss1)*u(2:Xmax1-1,j,1) + (ry1+sy1(x(2:Xmax1-1),y(j)))...
    .*u(2:Xmax1-1,j+1,1) + (dt/2)*S1(u(2:Xmax1-1,j,1),x(2:Xmax1-1),y(j),t);

    %i=Xmax1 (1st subdomain connection)
    L1(Xmax1) = Kx1/dx1;
    M1(Xmax1) = -(Kx1/dx1+Kx2/dx2);
    R1(Xmax1) = Kx2/dx2;
    RHS1(Xmax1) = 0;

    %i=Xmax1+1:Xmax1+Xmax2-2 (interior of 2nd subdomain)
    L1(Xmax1+1:Xmax1+Xmax2-2) = XL2;
    M1(Xmax1+1:Xmax1+Xmax2-2) = XM2;
    R1(Xmax1+1:Xmax1+Xmax2-2) = XR2;
    RHS1(Xmax1+1:Xmax1+Xmax2-2) = (ry2-sy2)*u(Xmax1+1:Xmax1+Xmax2-2,j-1,1)...
    + (1-2*ry2+ss2)*u(Xmax1+1:Xmax1+Xmax2-2,j,1) + (ry2+sy2)...
    *u(Xmax1+1:Xmax1+Xmax2-2,j+1,1) ...
    + (dt/2)*S2(u(Xmax1+1:Xmax1+Xmax2-2,j,1),x(Xmax1+1:Xmax1+Xmax2-2),y(j),t);

    %i=Xmax1+Xmax2-1 (2nd subdomain connection)
    L1(Xmax1+Xmax2-1) = Kx2/dx2;
    M1(Xmax1+Xmax2-1) = -(Kx2/dx2+Kx3/dx3);
    R1(Xmax1+Xmax2-1) = Kx3/dx3;
    RHS1(Xmax1+Xmax2-1) = 0;

    %i=Xmax1+Xmax2:Xmax1+Xmax2+Xmax3-3 (interior of 3rd subdomain)
    L1(Xmax1+Xmax2:Xmax-1) = XL3;
    M1(Xmax1+Xmax2:Xmax-1) = XM3;
    R1(Xmax1+Xmax2:Xmax-1) = XR3;
    RHS1(Xmax1+Xmax2:Xmax-1) = (ry3-sy3(x(Xmax1+Xmax2:Xmax-1),y(j)))...
    .*u(Xmax1+Xmax2:Xmax-1,j-1,1) + (1-2*ry3+ss3)*u(Xmax1+Xmax2:Xmax-1,j,1) ...
```

241

```matlab
            + (ry3+sy3(x(Xmax1+Xmax2:Xmax-1),y(j))).*u(Xmax1+Xmax2:Xmax-1,j+1,1) ...
            + (dt/2)*S3(u(Xmax1+Xmax2:Xmax-1,j,1),x(Xmax1+Xmax2:Xmax-1),y(j),t);

        %i=Xmax1+Xmax2+Xmax3-2 (right boundary)
        if aR == 0
            %Dirichlet BC
            M1(Xmax) = 1;
            RHS1(Xmax) = cR(y(j),t)/bR;
        else
            %Robin BC
            L1(Xmax) = -aR/dx3;
            M1(Xmax) = bR+aR/dx3;
            RHS1(Xmax) = cR(y(j),t);
        end

        %Solve Matrix System
        u(:,j,2) = tridiag(L1,M1,R1,RHS1);
end
% Note: Interior is needed to solve for top/bottom boundaries if Neumann BCs


% First Row j = 1 (Boundary Condition implemented explicitly)
if aB == 0
    %Dirichlet
    u(:,1,2) = cB(x(:),t)/bB;
else
    %Robin
    u(:,1,2) = (cB(x(:),t)-aB*u(:,2,2)/dy)/(bB-aB/dy);
end
% Last Row j = Ymax (Boundary Condition implemented explicitly)
if aT == 0
    %Dirichlet
    u(:,Ymax,2) = cT(x(:),t)/bT;
else
    %Robin
    u(:,Ymax,2) = (cT(x(:),t)+aT/dy)/(bT+aT/dy);
end

%%%%%%%%%%%%%%%%%%%%%% End First Half %%%%%%%%%%%%%%%%%%%%%%%%%%%%%%

%Update Solution
u(:,:,1) = u(:,:,2);
```

```
%%%%%%%%%%%%%%%%%%%%%% Begin Second Half %%%%%%%%%%%%%%%%%%%%%%%%%%%
% Solve Interior Columns in each subdomain
%LOOP: Loops over First Subdomain i=2:Xmax1-1 solving system in y-direction
for i = 2:Xmax1-1
    %j=1 BC
    if aB == 0
        %Dirichlet BC
        M2(1) = 1;
        RHS2(1) = cB(x(i),t)/bB;
    else
        %Robin BC
        M2(1) = (bB-aB/dy);
        R2(1) = aB/dy;
        RHS2(1) = cB(x(i),t);
    end
    %j=2:Ymax-1
    L2(2:Ymax-1) = YL1(x(i),y(2:Ymax-1));
    M2(2:Ymax-1) = YM1;
    R2(2:Ymax-1) = YR1(x(i),y(2:Ymax-1));
    RHS2(2:Ymax-1) = (rx1-sx1)*u(i-1,2:Ymax-1,1) ...
    + (1-2*rx1+ss1)*u(i,2:Ymax-1,1) + (rx1+sx1)*u(i+1,2:Ymax-1,1) ...
    + (dt/2)*S1(u(i,2:Ymax-1,1),x(i),y(2:Ymax-1),t);
    %j=Ymax
    if aT == 0
        %Dirichlet BC
        M2(Ymax) = 1;
        RHS2(Ymax) = cT(x(i),t)/bT;
    else
        %Robin BC
        L2(Ymax) = -aT/dy;
        M2(Ymax) = bT+aT/dy;
        RHS2(Ymax) = cT(x(i),t);
    end

    %Solve Matrix System
    u(i,:,2) = tridiag(L2,M2,R2,RHS2);
end

%LOOP: Loops over Second Subdomain i=Xmax1+1:Xmax1+Xmax2-2 solving system
%in y-direction
for i = Xmax1+1:Xmax1+Xmax2-2
    %j=1 BC
    if aB == 0
```

```
        %Dirichlet BC
        M2(1) = 1;
        RHS2(1) = cB(x(i),t)/bB;
    else
        %Robin BC
        M2(1) = (bB-aB/dy);
        R2(1) = aB/dy;
        RHS2(1) = cB(x(i),t);
    end
    %j=2:Ymax-1
    L2(2:Ymax-1) = YL2;
    M2(2:Ymax-1) = YM2;
    R2(2:Ymax-1) = YR2;
    RHS2(2:Ymax-1) = (rx2-sx2)*u(i-1,2:Ymax-1,1) ...
    + (1-2*rx2+ss2)*u(i,2:Ymax-1,1) + (rx2+sx2)*u(i+1,2:Ymax-1,1) ...
    + (dt/2)*S2(u(i,2:Ymax-1,1),x(i),y(2:Ymax-1),t);
    %j=Ymax
    if aT == 0
        %Dirichlet BC
        M2(Ymax) = 1;
        RHS2(Ymax) = cT(x(i),t)/bT;
    else
        %Robin BC
        L2(Ymax) = -aT/dy;
        M2(Ymax) = bT+aT/dy;
        RHS2(Ymax) = cT(x(i),t);
    end

    %Solve Matrix System
    u(i,:,2) = tridiag(L2,M2,R2,RHS2);
end

%LOOP: Loops over Third Subdomain i=Xmax1+Xmax2:Xmax-1 solving system
%in y-direction
for i = Xmax1+Xmax2:Xmax-1
    %j=1 BC
    if aB == 0
        %Dirichlet BC
        M2(1) = 1;
        RHS2(1) = cB(x(i),t)/bB;
    else
        %Robin BC
        M2(1) = (bB-aB/dy);
```

```
        R2(1) = aB/dy;
        RHS2(1) = cB(x(i),t);
    end
    %j=2:Ymax-1
    L2(2:Ymax-1) = YL3(x(i),y(2:Ymax-1));
    M2(2:Ymax-1) = YM3;
    R2(2:Ymax-1) = YR3(x(i),y(2:Ymax-1));
    RHS2(2:Ymax-1) = (rx3-sx3)*u(i-1,2:Ymax-1,1) ...
    + (1-2*rx3+ss3)*u(i,2:Ymax-1,1) + (rx3+sx3)*u(i+1,2:Ymax-1,1) ...
    + (dt/2)*S3(u(i,2:Ymax-1,1),x(i),y(2:Ymax-1),t);
    %j=Ymax
    if aT == 0
        %Dirichlet BC
        M2(Ymax) = 1;
        RHS2(Ymax) = cT(x(i),t)/bT;
    else
        %Robin BC
        L2(Ymax) = -aT/dy;
        M2(Ymax) = bT+aT/dy;
        RHS2(Ymax) = cT(x(i),t);
    end

    %Solve Matrix System
    u(i,:,2) = tridiag(L2,M2,R2,RHS2);
end
% Note: Interior is needed to solve for top/bottom/connecting boundaries if Neumann BCs


% First Column i = 1 (Boundary Condition implemented explicitly)
if aL == 0
    %Dirichlet
    u(1,:,2) = cL(y(:),t)/bL;
else
    %Robin
    u(1,:,2) = (cL(y(:),t)-aL*u(2,:,2)/dx1)/(bL-aL/dx1);
end

%Connecting Boundary i = Xmax1 (Boundary condition implemented explicitly)
u(Xmax1,:,2) = (Kx1*u(Xmax1-1,:,2)/dx1+Kx2*u(Xmax1+1,:,2)/dx2)...
/(Kx1/dx1+Kx2/dx2);

%Connecting Boundary i = Xmax1+Xmax2-1 (Boundary condition implemented explicitly)
u(Xmax1+Xmax2-1,:,2) = (Kx2*u(Xmax1+Xmax2-2,:,2)/dx2...
```

```
+Kx3*u(Xmax1+Xmax2,:,2)/dx3)/(Kx2/dx2+Kx3/dx3);

% Last Column i = Xmax (Boundary condition implemented explicitly)
if aR == 0
    %Dirichlet
    u(Xmax,:,2) = cR(y(:),t)/bR;
else
    %Robin
    u(Xmax,:,2) = (cR(y(:),t)+aR*u(Xmax-1,:,2)/dx3)/(bR+aR/dx3);
end

%%%%%%%%%%%%%%%%%%%%%%%%% End of Second Half %%%%%%%%%%%%%%%%%%%%%%%%%%%%

    %n
    if n > 1
        newSln=abs(u(:,1:length(y)-1,2)*300+300);
        newDiff=abs(u(:,1:length(y)-1,2)-u(:,1:length(y)-1,1))*300;
        newmax = max(newSln(:));
        relerr = max(newDiff(:))/newmax;
        pause(.01)
    end
    oldSln = u(:,:,2);
    oldmax = max(oldSln(:));

    %Update Solution
    u(:,:,1) = u(:,:,2);


    if n > Tmax
        error('Exceeded maximum number of timesteps')
    end
    n = n+1;

end

%Calculation over Total Domain
DomainArea = (x(length(x))-x(1))*(y(length(y))-y(1));
maxTemp = max(max(u(:,:,2)))*300+300;
minTemp = min(min(u(:,:,2)))*300+300;
uu = u(:,:,2);
int = trapz(x,uu,1);
AveT = trapz(y,int)/DomainArea;
AveT = AveT*300+300;
```

```
%Calculations over Ceramic Only
CeramicArea = (x(41)-x(21))*(y(length(y))-y(1));
maxTemp3 = max(max(u(21:41,:,2)))*300+300;
minTemp3 = min(min(u(21:41,:,2)))*300+300;
intc = trapz(x(21:41),uu(21:41,:),1);
AveTc = trapz(y,intc)/CeramicArea;
AveTc = AveTc*300+300;

%Power Response Calulation
intp = trapz(x(Xmax1+1:Xmax1+Xmax2-2),(P/Pow)...
*sigm(uu(Xmax1+1:Xmax1+Xmax2-2,:)).*Efield3(uu(Xmax1+1:Xmax1+Xmax2-2,:)...
,x(Xmax1+1:Xmax1+Xmax2-2),Param,Fcn),1);
intPow = trapz(y,intp);
Pave = Kx2*Bi*(trapz(y,u(1,:,2))+trapz(y,u(length(x),:,2)))/intPow;

MAXTEMP(m) = maxTemp;
MINTEMP(m) = minTemp;
MAXTEMP3(m) = maxTemp3;
MINTEMP3(m) = minTemp3;
AVETEMP(m) = AveT;
AVETEMP3(m) = AveTc;
POWER(m) = Pow;
POWERAVE(m) = Pave;


end
delete(gcp) %Close parallel pool

%Open aa print data to files
fileID01 = fopen('MaxTemp.txt','a');
fileID02 = fopen('MinTemp.txt','a');
fileID03 = fopen('MaxTempCer.txt','a');
fileID04 = fopen('MinTempCer.txt','a');
fileID05 = fopen('AveTemp.txt','a');
fileID06 = fopen('AveTempCer.txt','a');
fileID07 = fopen('Power.txt','a');
fileID08 = fopen('PowerCalc.txt','a');

for i = 1:length(PowList)
fprintf(fileID01,'%10.10f\r\n',MAXTEMP(i));
fprintf(fileID02,'%10.10f\r\n',MINTEMP(i));
fprintf(fileID03,'%10.10f\r\n',MAXTEMP3(i));
```

```
fprintf(fileID04,'%10.10f\r\n',MINTEMP3(i));
fprintf(fileID05,'%10.10f\r\n',AVETEMP(i));
fprintf(fileID06,'%10.10f\r\n',AVETEMP3(i));
fprintf(fileID07,'%10.10f\r\n',POWER(i));
fprintf(fileID08,'%10.10f\r\n',POWERAVE(i));
end

fclose(fileID01);
fclose(fileID02);
fclose(fileID03);
fclose(fileID04);
fclose(fileID05);
fclose(fileID06);
fclose(fileID07);
fclose(fileID08);
```

```
%PROGRAM: ShortWaveHomo.m
%FUNCTION CALLS: secant.m, TMM.m
%DESCRIPTION: Implements solution of high-frequency homogenization method
%for a 1D lossy laminate with a two-phase cell problem. Determines perturbation
%solutions to the dispersion curves and compares solution to the exact
%solution of the Transfer Matrix Method (TMM)

clear; %Clears all declared parameters and variables

ep1 = 1; %phase 1 real part of dielectric constant
ep2 = 4; %phase 2 real part of dielectric constant
s = sqrt(ep1); %square root of ep1
r = sqrt(ep2); %square root of ep2
epp1 = 0; %phase 1 imaginary part of dielectric constant
epp2 = 1000; %phase 2 imaginary part of dielectric constant
lam = 2; %Nondimensional length of a single cell

%Activates STANDARD METHOD (px=0) or ALTERNATE METHOD (px=1)
%Standard Method yeilds a solution amplitude independent of dielectric loss
%while the Alternate Method has a solution that does giving a better
%approximation for non-zero dielectric loss as it captures the effect of
%reflected waves in the model.
px = 1;

N = 50; %Number of cells. Implies that Macroscale length is L = N*lam*l
eta = 1./(N*lam); %Asymptotic parameter defined by \eta = l/L
i = sqrt(-1); %imaginary unit

%Characterisitc Equation for the periodic case
charZero =@(gam) 2.*r.*s.*(cos(gam*r).*cos(gam*s*(lam-1))-1)-(r.^2+s.^2)...
.*sin(gam.*r).*sin(gam.*s*(lam-1));
%Characterisitc Equation for the antiperiodic case
charPI =@(gam) 2.*r.*s.*(cos(gam*r).*cos(gam*s*(lam-1))+1)-(r.^2+s.^2)...
.*sin(gam.*r).*sin(gam.*s*(lam-1));
%Derivative of the Characteristic Equations (periodic and antiperiodic)
charDiff =@(gam) 2.*r.*s.*(-r.*sin(gam.*r).*cos(gam.*s*(lam-1))...
-s.*(lam-1).*cos(gam.*r).*sin(gam.*s*(lam-1)))-(r.^2+s.^2)...
.*(r.*cos(gam.*r).*sin(gam.*s*(lam-1))+s.*(lam-1).*sin(gam.*r)...
.*cos(gam.*s*(lam-1)));


MaxEval = 40; %Maximum eigenfrequency to search for roots
gam = 0:.001:MaxEval; %eigenfrequency range where to search for roots
```

```
zerotol = 1e-6; %error tolerance for finding zeros
count1 = 1; %counts roots of odd multiplicity for periodic case
count2 = 1; %counts roots of odd multiplicity for antiperiodic case
count3 = 1; %counts roots of even multiplicity for periodic case
count4 = 1; %counts roots of even multiplicity for antiperiodic case

%LOOP: Loops over eigenfrequency discretized range in search of roots
for j = 1:length(gam)-1
    %Finds possible roots of odd multiplicity
    if charZero(gam(j+1))*charZero(gam(j)) <= 0 %Periodic Case
        ZeroTest(count1,1:2) = [secant(charZero,gam(j),gam(j+1),zerotol) 1];
        count1 = count1 + 1;
    end
    if charPI(gam(j+1))*charPI(gam(j)) <= 0 %Antiperiodic Case
        PITest(count2,1:2) = [secant(charPI,gam(j),gam(j+1),zerotol) 1];
        count2 = count2 + 1;
    end

    %Finds possible roots of even multiplicity, change in sign of
    %derivative over consequtive grid points yields local extrema
    if charDiff(gam(j+1))*charDiff(gam(j)) <= 0
        if abs(charZero(0.5*(gam(j+1)+gam(j)))) < 1e-3 %Periodic Case
            ZeroDiffTest(count3,1:2) = [secant(charZero,gam(j)...
            ,gam(j+1),zerotol) 2];
            count3 = count3 + 1;
        elseif abs(charPI(0.5*(gam(j+1)+gam(j)))) < 1e-3 %Antiperiodic Case
            PIDiffTest(count4,1:2) = [secant(charPI,gam(j),gam(j+1)...
            ,zerotol) 2];
            count4 = count4 + 1;
        end
    end
end

%Sorts eigenvalues by value from lowest to highest
if count1 > 1 && count3 > 1
    Zerozeros = sortrows([ZeroTest; ZeroDiffTest(2:length(ZeroDiffTest),:)]);
elseif count1 > 1 && count3 == 1
    Zerozeros = sortrows(ZeroTest);
elseif count1 == 1 && count3 > 1
    Zerozeros = sortrows(ZeroDiffTest);
end
```

```
if count2 > 1 && count4 > 1
    PIzeros = sortrows([PITest; PIDiffTest]);
elseif count2 > 1 && count4 == 1
    PIzeros = sortrows(PITest);
elseif count2 == 1 && count4 > 1
    PIzeros = sortrows(PIDiffTest);
end

%{
%Plots Characteristic Functions and Their Zeros
figure(1) %Periodic Case
plot(gam,charZero(gam),'b',[0 MaxEval],[0 0],'k')
hold on
plot(Zerozeros(:,1),zeros(length(Zerozeros(:,1)),1),'o')
title('Periodic eigenvalues')

figure(2) %Antiperiodic Case
plot(gam,charPI(gam),'r',[0 MaxEval],[0 0],'k')
hold on
plot(PIzeros(:,1),zeros(length(PIzeros(:,1)),1),'ro')
title('Antiperiodic eigenvalues')
%}


%%%%%%%%%%%%%%%%%%%%%%%%%%%%%%%%%%%%%%%%%%%%%%%%%%%%%%%%
%Construct Dispersion Curve Relation for Periodic case
%%%%%%%%%%%%%%%%%%%%%%%%%%%%%%%%%%%%%%%%%%%%%%%%%%%%%%%%

%Set of Preliminary functions needed to construct Dispersion Curves
pZero =@(gam) (r.*sin(gam.*s.*(lam-1)) + s.*sin(gam.*r))...
./(cos(gam.*s.*(lam-1)) - cos(gam.*r));

U1sqZero =@(gam) pZero(gam).^2.*(lam-1)./2 + r.^2.*(lam-1)./2 ...
- pZero(gam).*r./(s.*gam) + pZero(gam).*r.*cos(gam.*s.*(lam-1)).^2./(s.*gam) ...
    -r.^2.*sin(gam.*s.*(lam-1)).*cos(gam.*s.*(lam-1))./(2.*s.*gam) ...
+ pZero(gam).^2.*sin(gam.*s.*(lam-1)).*cos(gam.*s.*(lam-1))./(2.*s.*gam);
U2sqZero =@(gam) pZero(gam).^2./2 + s.^2./2 + pZero(gam).*s./(r.*gam)...
 - pZero(gam).*s.*cos(gam.*r).^2./(r.*gam) ...
    -s.^2.*sin(gam.*r).*cos(gam.*r)./(2.*r.*gam) ...
+ pZero(gam).^2.*sin(gam.*r).*cos(gam.*r)./(2.*r.*gam);

PermU2Zero =@(gam) s.^2.*U1sqZero(gam)+r.^2.*U2sqZero(gam);
LossU2Zero =@(gam) epp2.*U2sqZero(gam);
```

251

```
DiffU2VZero =@(gam) r.*s.*lam.^2.*gam.*(s.*sin(gam.*r).*cos(gam.*s.*(lam-1))...
+r.*cos(gam.*r).*sin(gam.*s.*(lam-1)))./(cos(gam.*s.*(lam-1))-cos(gam.*r)).^2;

epEffZero =@(gam) PermU2Zero(gam)./DiffU2VZero(gam);
eppEffZero =@(gam) LossU2Zero(gam)./DiffU2VZero(gam);

%Functions Defining Perturbation to Dispersion Curves
gammaZ =@(gam,Bloch) gam + Bloch.^2./(2*lam.^2.*gam.*epEffZero(gam))...
 - lam.^2.*gam.^3.*(eta.^2.*eppEffZero(gam)).^2./(8.*epEffZero(gam).*Bloch.^2);
gammaZLoss =@(gam,Bloch) gam - Bloch.^2./(2*lam.^2.*gam.*epEffZero(gam))...
 + lam.^2.*gam.^3.*(eta.^2.*eppEffZero(gam)).^2./(8.*epEffZero(gam).*Bloch.^2);

%%%%%%%%%%%%%%%%%%%%%%%%%%%%%%%%%%%%%%%%%%%%%%%%%%%%%%%%%%%%%%
%Construct Dispersion Curve Relation for Antiperiodic case
%%%%%%%%%%%%%%%%%%%%%%%%%%%%%%%%%%%%%%%%%%%%%%%%%%%%%%%%%%%%%%

%Set of Preliminary functions needed to construct Dispersion Curves
pPi =@(gam) (r.*sin(gam.*s.*(lam-1)) - s.*sin(gam.*r))./(cos(gam.*s.*(lam-1))...
 + cos(gam.*r));

U1sqPi =@(gam) pPi(gam).^2.*(lam-1)./2 + r.^2.*(lam-1)./2 ...
- pPi(gam).*r./(s.*gam) + pPi(gam).*r.*cos(gam.*s.*(lam-1)).^2./(s.*gam) ...
-r.^2.*sin(gam.*s.*(lam-1)).*cos(gam.*s.*(lam-1))./(2.*s.*gam) ...
+ pPi(gam).^2.*sin(gam.*s.*(lam-1)).*cos(gam.*s.*(lam-1))./(2.*s.*gam);
U2sqPi =@(gam) pPi(gam).^2./2 + s.^2./2 + pPi(gam).*s./(r.*gam) ...
- pPi(gam).*s.*cos(gam.*r).^2./(r.*gam)-s.^2.*sin(gam.*r).*cos(gam.*r)...
./(2.*r.*gam) + pPi(gam).^2.*sin(gam.*r).*cos(gam.*r)./(2.*r.*gam);

PermU2Pi =@(gam) s.^2.*U1sqPi(gam)+r.^2.*U2sqPi(gam);
LossU2Pi =@(gam) epp2.*U2sqPi(gam);

DiffU2VPi =@(gam) -r.*s.*lam.^2.*gam.*(s.*sin(gam.*r).*cos(gam.*s.*(lam-1))...
+r.*cos(gam.*r).*sin(gam.*s.*(lam-1)))./(cos(gam.*s.*(lam-1))+cos(gam.*r)).^2;

epEffPi =@(gam) PermU2Pi(gam)./DiffU2VPi(gam);
eppEffPi =@(gam) LossU2Pi(gam)./DiffU2VPi(gam);

%Functions Defining Perturbation to Dispersion Curves
gammaPi =@(gam,Bloch) gam + (Bloch-pi).^2./(2*lam.^2.*gam.*epEffPi(gam))...
 - lam.^2.*gam.^3.*(eta.^2.*eppEffPi(gam)).^2./(8.*epEffPi(gam).*(Bloch-pi).^2);
gammaPiLoss =@(gam,Bloch) gam - Bloch.^2./(2*lam.^2.*gam.*epEffPi(gam)) ...
 + lam.^2.*gam.^3.*(eta.^2.*eppEffPi(gam)).^2./(8.*epEffPi(gam).*Bloch.^2);
```

```
%Linear set of Grid point used in dispersion plot
Z = .01:.001:1;
%Brillouin Zone Grid and Attenuation Grid from .01 to pi/2
%(half the Brillouin Zone) where the application of the Z^4 applies more
%gridpoints near rapid change at 0
BlochZ = (pi/2)*Z.^4;
LossFac = (pi/2)*Z.^4;
%Centers Brillouin Zone for Antiperiodic case around \pi
BlochPi = (pi/2)*(1-Z.^4+1);

%Plots the dispersion curve for the degenerate mode corresponding the
%classical Long-wave case where wavelength is longer than microscale
figure(3)
plot(BlochZ,BlochZ./sqrt(2*(1+r.^2)),'b','LineWidth',2)
hold on

%Defines the number of eigenfrequency base states to plot in both cases
Zmax = 3;
PImax = 3;

%LOOP: Loops over number of base state eigenfrequencies in
%periodic case to plot
for j=2:Zmax
    if Zerozeros(j,2) == 1 %Simple Roots
        figure(3)
        plot(BlochZ,gammaZ(Zerozeros(j,1),BlochZ),'b','LineWidth',2)
        hold on
        plot([0 pi/2],[Zerozeros(j,1) Zerozeros(j,1)],'--ok','LineWidth',2)
        hold on
        figure(4)
        plot(LossFac,gammaZLoss(Zerozeros(j,1),LossFac),'b','LineWidth',2)
        hold on
    elseif Zerozeros(j,2) == 2 %Multiple Roots (degenerate modes)
        cb = (r.^2+s.^2.*(lam-1))./(Zerozeros(j,1).^2.*lam);
        figure(3)
        plot(BlochZ,Zerozeros(j,1)-BlochZ./(2*Zerozeros(j,1)*sqrt(cb))...
        ,'b','LineWidth',2)
        hold on
        plot(BlochZ,Zerozeros(j,1)+BlochZ./(2*Zerozeros(j,1)*sqrt(cb))...
        ,'b','LineWidth',2)
        hold on
```

```
        end
end
axis([0 pi 0 3.1415])
set(gca,'Fontsize',18)

%LOOP: Loops over number of base state eigenfrequencies in periodic case to plot
for j=1:PImax
    if PIzeros(j,2) == 1 %Simple Roots
        figure(3)
        plot(BlochPi,gammaPi(PIzeros(j,1),BlochPi),'r','LineWidth',2)
        hold on
        plot([pi/2 pi],[PIzeros(j,1) PIzeros(j,1)],'--ok','LineWidth',2)
        hold on
        figure(4)
        plot(LossFac,gammaPiLoss(PIzeros(j,1),LossFac),'-r','LineWidth',2)
        hold on
    elseif PIzeros(j,2) == 2 %Multiple Roots (degenerate modes)
        cb = (r.^2+s.^2.*(lam-1))./(PIzeros(j,1).^2.*lam);
        figure(3)
        plot(BlochPi,PIzeros(j,1)-BlochZ./(2*PIzeros(j,1)*sqrt(cb))...
        ,'-r','LineWidth',2)
        hold on
        plot(BlochPi,PIzeros(j,1)+BlochZ./(2*PIzeros(j,1)*sqrt(cb))...
        ,'-r','LineWidth',2)
        hold on
    end
end
figure(3)
axis([0 pi 0 3.1415])
set(gca,'Fontsize',18)
xlabel('Brillouin zone (\lambda\eta k)')
ylabel('eigenfrequency (\gamma)')
title(['\epsilon^{\prime\prime} = ' num2str(epp2) ', \eta = ' num2str(eta)])
figure(4)
axis([0 pi/2 0 3.1415])
set(gca,'Fontsize',18)
xlabel('Attenuation Factor (\lambda\eta \kappa)')
ylabel('eigenfrequency (\gamma)')
title(['\epsilon^{\prime\prime} = ' num2str(epp2) ', \eta = ' num2str(eta)])

%%%%%%%%%%%%%%%%%%%%%%%%%%%%%%%%%%%%%%%%%%%%%%%%%%%%%%%%%%%%%%%%%%%%%%%%%%%%%
%%%%%%%%%%%%%%%%%%%%%%%%% HFH Solution Plots %%%%%%%%%%%%%%%%%%%%%%%%%%%%%%%%
%%%%%%%%%%%%%%%%%%%%%%%%%%%%%%%%%%%%%%%%%%%%%%%%%%%%%%%%%%%%%%%%%%%%%%%%%%%%%
```

```
%Given a particular frequency of an incident wave the dispersion curves
%determine the Bloch number (k) and Attenuation number (\kappa) needed to
%plot the solutions of the high-frequency homogenization method

efreq = 1.91063323; %Incident eigenfrequency (nondimensional wavenumber)

%Sets Bloch number to zero. If no Bloch number found along dispersion curve
%search it implies that the solution is lossless and the frequency is
%within a band gap
Bloch = 0;
%Sets Attenuation number to zero. If no Attenuation number found along dispersion
%curve search it implies that the solution is lossless and the frequency is
%outside a band gap
Atten = 0;

%LOOP: Loops over Dispersion curve nearest incident eigenfrequency.
%Determines Bloch number and Attenuation number that correspond to the
%incident frequency chosen by user. NOTE THIS IS NOT AUTOMATED AND IS
%CURRENTLY CHOSEN SPECIFICALLY BY USER FOR ONE BRANCH IN PARTICULAR.
%WILL NEED TO BE CHANGED AS NEEDED.
for j=1:length(BlochZ)-1
if gammaZ(Zerozeros(2,1),BlochZ(j)) > efreq && ...
gammaZ(Zerozeros(2,1),BlochZ(j+1)) < efreq
    Bloch = (BlochZ(j)+BlochZ(j+1))/2; %Averages over the gridpoints
    break
end
end
for j=1:length(LossFac)-1
if gammaZLoss(Zerozeros(2,1),LossFac(j)) < efreq && ...
gammaZLoss(Zerozeros(2,1),LossFac(j+1)) > efreq
    Atten = (LossFac(j)+LossFac(j+1))/2; %Averages over the gridpoints
    break
end
end


%Construct Solution
k = Bloch/(lam*eta); %k value
kappa = Atten/(lam*eta); %\kappa value
%p parameter
pZero =@(gam) (r.*sin(gam.*s.*(lam-1)) ...
+ exp(-i*lam*eta*(k+sqrt(-1)*kappa)*px).*s.*sin(gam.*r))...
```

```
./(cos(gam.*s.*(lam-1)) - exp(-i*lam*eta*(k+sqrt(-1)*kappa)*px)...
.*cos(gam.*r));
%Leader Order Cell Problem Solution
U =@(xi,gam) (r.*sin(s.*gam.*xi)+pZero(gam)...
.*cos(s.*gam.*xi)).*heaviside(-xi)+(s.*sin(r.*gam.*xi)+pZero(gam)...
.*cos(r.*gam.*xi)).*heaviside(xi);
%Derivative of Cell Problem Solution
DU =@(xi,gam) (r.*s.*gam.*cos(s.*gam.*xi)-pZero(gam).*s.*gam...
.*sin(s.*gam.*xi)).*heaviside(-xi)+(s.*r.*gam.*cos(r.*gam.*xi)...
-pZero(gam).*r.*gam.*sin(r.*gam.*xi)).*heaviside(xi);
%Define complex Bloch parameter
K = k+i*kappa;
%Define macroscale (envelope) function for left-moving wave
f1 =@(xi) exp(i*K.*eta.*xi);
%Define macroscale (envelope) function for right-moving wave
f2 =@(xi) exp(-i*K.*eta.*xi);

%Grid for whole domain in the microscale variable \xi
xi1 = 0:.01:lam*N;
%Grid for the cell problem, bounded between -(lam-1)<\xi<1
xi2 = mod(xi1,lam)-(lam-1);


%%%%%%%%%%%%%%%%%%%%%%%%%%%%%%%%%%%%%%%%%%%%&%%%%%%%%%%%
%Solution to single slab external scattering problem
%%%%%%%%%%%%%%%%%%%%%%%%%%%%%%%%%%%%%%%%%%%%&%%%%%%%%%%%
%Problem solve the external scatering of a single layer of the homogenized
%material being illuminated on one side from the left.

E0 = 1; %Incident electric field amplitude
%Set of solution specific parameters
PP = (i*efreq+i*K*eta).*U(-(lam-1),efreq)+DU(-(lam-1),efreq);
PM = (i*efreq+i*K*eta).*U(1,efreq)-DU(1,efreq);
MP = (i*efreq-i*K*eta).*U(-(lam-1),efreq)+DU(-(lam-1),efreq);
MM = (i*efreq-i*K*eta).*U(1,efreq)-DU(1,efreq);
Q = 1-MP*MM*exp(2*i*K*eta*lam*N)./(PP*PM);

%Coefficients of solution for left and right moving waves
a2 = 2*i*efreq*E0./(PP*Q); %left moving wave
b2 = -MM*exp(2*i*K*eta*lam*N)*a2./PM; %right moving wave

%HFH Solution to scattering problem
Efield = a2.*f1(xi1).*U(xi2,efreq)+b2.*f2(xi1).*U(xi2,efreq);
```

```
%Plot of HFH solution
figure(7)
g1 = plot(xi1,real(Efield),'b','LineWidth',3);
xlabel('\zeta')
ylabel('E^{(0)}(z,\zeta)')
set(gca,'Fontsize',18)
hold on

%Determines and Plots solution in the free space region on the left
xi3 = -(lam-1):.01:0;
a1 = E0;
b1 = -E0 + (a2+b2).*U(-(lam-1),efreq);
E1 = a1*exp(i*efreq*xi3)+b1*exp(-i*efreq.*xi3);
plot(xi3,real(E1),'b','LineWidth',3)
Efield = [E1(1:length(E1)-1) Efield];


%%%%%%%%%%%%%%%%%%%%%%%%%%%%%%%%%%%%%%%%%%%%%%%%%%%%%%%%%%%%%%%%%%%%%%%
%%%%%%%%%%%%%%% Transfer Matrix Method Call %%%%%%%%%%%%%%%%%%%%%%%%%%
%%%%%%%%%%%%%%%%%%%%%%%%%%%%%%%%%%%%%%%%%%%%%%%%%%%%%%%%%%%%%%%%%%%%%%%

%Free space parameters (left hand side)
MatParam(1,1) = 1; %dielectric constant
MatParam(2,1) = 1; %layer width
for j = 2:(2*N+1)
    if mod(j,2) == 1
        %phase 2 dielectric constant
        MatParam(1,j) = ep2-sqrt(-1)*eta^2*epp2;
    else
        %phase 1 dielectric constant
        MatParam(1,j) = ep1-sqrt(-1)*eta^2*epp1;
    end
    MatParam(2,j) = 1; %layer width
end
%Free space parameters (right hand side)
MatParam(1,j+1) = 1; %dielectric constant
MatParam(2,j+1) = 1; %layer width
gam = efreq; %set incident eigenfrequency as the nondimensional wavenumber
Einit = [1 0]; %Set amplitude of incident electric field
[E,Dom] = TMM(MatParam,gam,Einit,"on"); %Function call

%Plot solution to TMM
```

```
figure(7)
h1 = plot(Dom(1:10:length(Dom)),real(E(1:10:length(Dom))),'-ok','LineWidth',1);
hold on
%plot(Dom,Eupper,'r',Dom,Elower,'k')
set(gca,'Fontsize',18)
axis([-1 20 -max(max(real(E)),max(real(Efield))) ...
max(max(real(E)),max(real(Efield)))])
legend([g1 h1],'HFH','TMM')
hold on

%Error Calculation
abserr = abs(real(Efield)-real(E));
relerr = abserr./abs(real(E));
L2normAve = norm(relerr)./length(Dom);
```

```matlab
%PROGRAM: ShortWaveHomo_ErrLoop.m
%FUNCTION CALLS: secant.m, TMM.m
%DESCRIPTION: Finds error plots as a function of the asymptotic parameter
%\eta for various values of the dielectric constant by looping over solutions
%of high-frequency homogenization method for a 1D lossy laminate with a
%two-phase cell problem. Determines perturbation solutions to the dispersion
%curves and compares solution to the exact solution of the Transfer Matrix
%Method (TMM)

clear; %Clears all declared parameters and variables


ep1 = 1; %phase 1 real part of dielectric constant
ep2 = 4; %phase 2 real part of dielectric constant
s = sqrt(ep1); %square root of ep1
r = sqrt(ep2); %square root of ep2
epp1 = 0; %phase 1 imaginary part of dielectric constant
epp2 = 1000; %phase 2 imaginary part of dielectric constant
lam = 2; %Nondimensional length of a single cell

%Activates STANDARD METHOD (px=0) or ALTERNATE METHOD (px=1)
%Standard Method yeilds a solution amplitude independent of dielectric loss
%while the Alternate Method has a solution that does giving a better
%approximation for non-zero dielectric loss as it captures the effect of
%reflected waves in the model.
px = 0;

%Set color markers for error plotting
color = {'-ok','-ob','-og','-or','-om'};


ePrime = 0:250:1000; %Set of dielectric loss vaalues to loop over
colorindex = 0; %Initillize dielectric loss counter
%LOOP: Loops over values of dielectric loss
for epp2 = ePrime
colorindex = colorindex+1; %Update dielectric loss counter

%Clear necessary variables between solution runs within loop
clearvars -except ep1 ep2 s r epp1 epp2 lam px color ePrime colorindex

Cells = 50:50:500; %Set of number of cells to loop over
count = 0; %Initilize cell counter
%LOOP: Loops over different number of cells comprising the medium
for N = Cells
count = count+1 %Update cell counter
```

```
eta = 1./(N*lam); %Asymptotic parameter defined by \eta = l/L
i = sqrt(-1); %imaginary unit

%Characterisitc Equation for the periodic case
charZero =@(gam) 2.*r.*s.*(cos(gam*r).*cos(gam*s*(lam-1))-1)-(r.^2+s.^2)...
.*sin(gam.*r).*sin(gam.*s.*(lam-1));
%Characterisitc Equation for the antiperiodic case
charPI =@(gam) 2.*r.*s.*(cos(gam*r).*cos(gam*s*(lam-1))+1)-(r.^2+s.^2)...
.*sin(gam.*r).*sin(gam.*s.*(lam-1));
%Derivative of the Characteristic Equations (periodic and antiperiodic)
charDiff =@(gam) 2.*r.*s.*(-r.*sin(gam.*r).*cos(gam.*s.*(lam-1))...
-s.*(lam-1).*cos(gam.*r).*sin(gam.*s.*(lam-1)))-(r.^2+s.^2)...
.*(r.*cos(gam.*r).*sin(gam.*s.*(lam-1))+s.*(lam-1).*sin(gam.*r)...
.*cos(gam.*s.*(lam-1)));


MaxEval = 40; %Maximum eigenfrequency to search for roots
gam = 0:.001:MaxEval; %eigenfrequency range where to search for roots


zerotol = 1e-6; %error tolerance for finding zeros
count1 = 1; %counts roots of odd multiplicity for periodic case
count2 = 1; %counts roots of odd multiplicity for antiperiodic case
count3 = 1; %counts roots of even multiplicity for periodic case
count4 = 1; %counts roots of even multiplicity for antiperiodic case

%LOOP: Loops over eigenfrequency discretized range in search of roots
for j = 1:length(gam)-1
    %Finds possible roots of odd multiplicity
    if charZero(gam(j+1))*charZero(gam(j)) <= 0 %Periodic Case
        ZeroTest(count1,1:2) = [secant(charZero,gam(j),gam(j+1),zerotol) 1];
        count1 = count1 + 1;
    end
    if charPI(gam(j+1))*charPI(gam(j)) <= 0 %Antiperiodic Case
        PITest(count2,1:2) = [secant(charPI,gam(j),gam(j+1),zerotol) 1];
        count2 = count2 + 1;
    end

    %Finds possible roots of even multiplicity, change in sign of
    %derivative over consequtive grid points yields local extrema
    if charDiff(gam(j+1))*charDiff(gam(j)) <= 0
        if abs(charZero(0.5*(gam(j+1)+gam(j)))) < 1e-3 %Periodic Case
```

```matlab
                ZeroDiffTest(count3,1:2) = [secant(charZero,gam(j),gam(j+1)...
            ,zerotol) 2];
                count3 = count3 + 1;
            elseif abs(charPI(0.5*(gam(j+1)+gam(j)))) < 1e-3 %Antiperiodic Case
                PIDiffTest(count4,1:2) = [secant(charPI,gam(j),gam(j+1)...
                ,zerotol) 2];
                count4 = count4 + 1;
            end
        end
end

%Sorts eigenvalues by value from lowest to highest
if count1 > 1 && count3 > 1
    Zerozeros = sortrows([ZeroTest; ZeroDiffTest(2:length(ZeroDiffTest),:)]);
elseif count1 > 1 && count3 == 1
    Zerozeros = sortrows(ZeroTest);
elseif count1 == 1 && count3 > 1
    Zerozeros = sortrows(ZeroDiffTest);
end
if count2 > 1 && count4 > 1
    PIzeros = sortrows([PITest; PIDiffTest]);
elseif count2 > 1 && count4 == 1
    PIzeros = sortrows(PITest);
elseif count2 == 1 && count4 > 1
    PIzeros = sortrows(PIDiffTest);
end

%{
%Plots Characteristic Functions and Their Zeros
figure(1) %Periodic Case
plot(gam,charZero(gam),'b',[0 MaxEval],[0 0],'k')
hold on
plot(Zerozeros(:,1),zeros(length(Zerozeros(:,1)),1),'o')
title('Periodic eigenvalues')

figure(2) %Antiperiodic Case
plot(gam,charPI(gam),'r',[0 MaxEval],[0 0],'k')
hold on
plot(PIzeros(:,1),zeros(length(PIzeros(:,1)),1),'ro')
title('Antiperiodic eigenvalues')
%}
```

```matlab
%%%%%%%%%%%%%%%%%%%%%%%%%%%%%%%%%%%%%%%%%%%%%%%%%%%%%%%%%
%Construct Dispersion Curve Relation for Periodic case
%%%%%%%%%%%%%%%%%%%%%%%%%%%%%%%%%%%%%%%%%%%%%%%%%%%%%%%%%

%Set of Preliminary functions needed to construct Dispersion Curves
pZero =@(gam) (r.*sin(gam.*s.*(lam-1)) + s.*sin(gam.*r))...
./(cos(gam.*s.*(lam-1)) - cos(gam.*r));

U1sqZero =@(gam) pZero(gam).^2.*(lam-1)./2 + r.^2.*(lam-1)./2 ...
- pZero(gam).*r./(s.*gam) + pZero(gam).*r.*cos(gam.*s.*(lam-1)).^2./(s.*gam) ...
    -r.^2.*sin(gam.*s.*(lam-1)).*cos(gam.*s.*(lam-1))./(2.*s.*gam) ...
+ pZero(gam).^2.*sin(gam.*s.*(lam-1)).*cos(gam.*s.*(lam-1))./(2.*s.*gam);
U2sqZero =@(gam) pZero(gam).^2./2 + s.^2./2 + pZero(gam).*s./(r.*gam) ...
- pZero(gam).*s.*cos(gam.*r).^2./(r.*gam)-s.^2.*sin(gam.*r).*cos(gam.*r)...
./(2.*r.*gam) + pZero(gam).^2.*sin(gam.*r).*cos(gam.*r)./(2.*r.*gam);

PermU2Zero =@(gam) s.^2.*U1sqZero(gam)+r.^2.*U2sqZero(gam);
LossU2Zero =@(gam) epp2.*U2sqZero(gam);

DiffU2VZero =@(gam) r.*s.*lam.^2.*gam.*(s.*sin(gam.*r)...
.*cos(gam.*s.*(lam-1))+r.*cos(gam.*r).*sin(gam.*s.*(lam-1))) ...
./(cos(gam.*s.*(lam-1))-cos(gam.*r)).^2;

epEffZero =@(gam) PermU2Zero(gam)./DiffU2VZero(gam);
eppEffZero =@(gam) LossU2Zero(gam)./DiffU2VZero(gam);

%Functions Defining Perturbation to Dispersion Curves
gammaZ =@(gam,Bloch) gam + Bloch.^2./(2*lam.^2.*gam.*epEffZero(gam))...
-lam.^2.*gam.^3.*(eta.^2.*eppEffZero(gam)).^2./(8.*epEffZero(gam).*Bloch.^2);
gammaZLoss =@(gam,Bloch) gam - Bloch.^2./(2*lam.^2.*gam.*epEffZero(gam))...
+lam.^2.*gam.^3.*(eta.^2.*eppEffZero(gam)).^2./(8.*epEffZero(gam).*Bloch.^2);

%%%%%%%%%%%%%%%%%%%%%%%%%%%%%%%%%%%%%%%%%%%%%%%%%%%%%%%%%%
%Construct Dispersion Curve Relation for Antiperiodic case
%%%%%%%%%%%%%%%%%%%%%%%%%%%%%%%%%%%%%%%%%%%%%%%%%%%%%%%%%%%

%Set of Preliminary functions needed to construct Dispersion Curves
pPi =@(gam) (r.*sin(gam.*s.*(lam-1)) - s.*sin(gam.*r))...
./(cos(gam.*s.*(lam-1)) + cos(gam.*r));

U1sqPi =@(gam) pPi(gam).^2.*(lam-1)./2 + r.^2.*(lam-1)./2 ...
- pPi(gam).*r./(s.*gam) + pPi(gam).*r.*cos(gam.*s.*(lam-1)).^2./(s.*gam) ...
    -r.^2.*sin(gam.*s.*(lam-1)).*cos(gam.*s.*(lam-1))./(2.*s.*gam) ...
```

```matlab
+ pPi(gam).^2.*sin(gam.*s.*(lam-1)).*cos(gam.*s.*(lam-1))./(2.*s.*gam);
U2sqPi =@(gam) pPi(gam).^2./2 + s.^2./2 + pPi(gam).*s./(r.*gam) ...
- pPi(gam).*s.*cos(gam.*r).^2./(r.*gam)-s.^2.*sin(gam.*r).*cos(gam.*r)...
./(2.*r.*gam) + pPi(gam).^2.*sin(gam.*r).*cos(gam.*r)./(2.*r.*gam);

PermU2Pi =@(gam) s.^2.*U1sqPi(gam)+r.^2.*U2sqPi(gam);
LossU2Pi =@(gam) epp2.*U2sqPi(gam);

DiffU2VPi =@(gam) -r.*s.*lam.^2.*gam.*(s.*sin(gam.*r).*cos(gam.*s.*(lam-1))...
+r.*cos(gam.*r).*sin(gam.*s.*(lam-1)))./(cos(gam.*s.*(lam-1))+cos(gam.*r)).^2;

epEffPi =@(gam) PermU2Pi(gam)./DiffU2VPi(gam);
eppEffPi =@(gam) LossU2Pi(gam)./DiffU2VPi(gam);

%Functions Defining Perturbation to Dispersion Curves
gammaPi =@(gam,Bloch) gam + (Bloch-pi).^2./(2*lam.^2.*gam.*epEffPi(gam))...
-lam.^2.*gam.^3.*(eta.^2.*eppEffPi(gam)).^2./(8.*epEffPi(gam).*(Bloch-pi).^2);
gammaPiLoss =@(gam,Bloch) gam - Bloch.^2./(2*lam.^2.*gam.*epEffPi(gam))...
+ lam.^2.*gam.^3.*(eta.^2.*eppEffPi(gam)).^2./(8.*epEffPi(gam).*Bloch.^2);


%Linear set of Grid point used in dispersion plot
Z = .01:.001:1;
%Brillouin Zone Grid and Attenuation Grid from .01 to pi/2
%(half the Brillouin Zone) where the application of the Z^4 applies more
%gridpoints near rapid change at 0
BlochZ = (pi/2)*Z.^4;
LossFac = (pi/2)*Z.^4;
%Centers Brillouin Zone for Antiperiodic case around \pi
BlochPi = (pi/2)*(1-Z.^4+1);

%{
%Plots the dispersion curve for the degenerate mode corresponding the
%classical Long-wave case where wavelength is longer than microscale
figure(3)
plot(BlochZ,BlochZ./sqrt(2*(1+r.^2)),'b','LineWidth',2)
hold on

%Defines the number of eigenfrequency base states to plot in both cases
Zmax = 3;
PImax = 3;

%LOOP: Loops over number of base state eigenfrequencies in
```

263

```matlab
%periodic case to plot
for j=2:Zmax
    if Zerozeros(j,2) == 1 %Simple Roots
        figure(3)
        plot(BlochZ,gammaZ(Zerozeros(j,1),BlochZ),'b','LineWidth',2)
        hold on
        plot([0 pi/2],[Zerozeros(j,1) Zerozeros(j,1)],'--ok','LineWidth',2)
        hold on
        figure(4)
        plot(LossFac,gammaZLoss(Zerozeros(j,1),LossFac),'b','LineWidth',2)
        hold on
    elseif Zerozeros(j,2) == 2 %Multiple Roots (degenerate modes)
        cb = (r.^2+s.^2.*(lam-1))./(Zerozeros(j,1).^2.*lam);
        figure(3)
        plot(BlochZ,Zerozeros(j,1)-BlochZ./(2*Zerozeros(j,1)*sqrt(cb))...
        ,'b','LineWidth',2)
        hold on
        plot(BlochZ,Zerozeros(j,1)+BlochZ./(2*Zerozeros(j,1)*sqrt(cb))...
        ,'b','LineWidth',2)
        hold on
    end
end
axis([0 pi 0 3.1415])
set(gca,'Fontsize',18)

%LOOP: Loops over number of base state eigenfrequencies in
%periodic case to plot
for j=1:PImax
    if PIzeros(j,2) == 1 %Simple Roots
        figure(3)
        plot(BlochPi,gammaPi(PIzeros(j,1),BlochPi),'r','LineWidth',2)
        hold on
        plot([pi/2 pi],[PIzeros(j,1) PIzeros(j,1)],'--ok','LineWidth',2)
        hold on
        figure(4)
        plot(LossFac,gammaPiLoss(PIzeros(j,1),LossFac),'-r','LineWidth',2)
        hold on
    elseif PIzeros(j,2) == 2 %Multiple Roots (degenerate modes)
        cb = (r.^2+s.^2.*(lam-1))./(PIzeros(j,1).^2.*lam);
        figure(3)
        plot(BlochPi,PIzeros(j,1)-BlochZ./(2*PIzeros(j,1)*sqrt(cb))...
        ,'-r','LineWidth',2)
        hold on
```

```
            plot(BlochPi,PIzeros(j,1)+BlochZ./(2*PIzeros(j,1)*sqrt(cb))...
            ,'-r','LineWidth',2)
            hold on
       end
end
figure(3)
axis([0 pi 0 3.1415])
set(gca,'Fontsize',18)
xlabel('Brillouin zone (\lambda\eta k)')
ylabel('eigenfrequency (\gamma)')
title(['\epsilon^{\prime\prime} = ' num2str(epp2) ', \eta = ' num2str(eta)])
figure(4)
axis([0 pi/2 0 3.1415])
set(gca,'Fontsize',18)
xlabel('Attenuation Factor (\lambda\eta \kappa)')
ylabel('eigenfrequency (\gamma)')
title(['\epsilon^{\prime\prime} = ' num2str(epp2) ', \eta = ' num2str(eta)])
%}


%%%%%%%%%%%%%%%%%%%%%%%%%%%%%%%%%%%%%%%%%%%%%%%%%%%%%%%%%%%%%%%%%%%%%%%
%%%%%%%%%%%%%%%%%%%%%%%%% HFH Solution Plots %%%%%%%%%%%%%%%%%%%%%%%%%%%
%%%%%%%%%%%%%%%%%%%%%%%%%%%%%%%%%%%%%%%%%%%%%%%%%%%%%%%%%%%%%%%%%%%%%%%

%Given a particular frequency of an incident wave the dispersion curves
%determine the Bloch number (k) and Attenuation number (\kappa) needed to
%plot the solutions of the high-frequency homogenization method

efreq = 1.91063323; %Incident eigenfrequency (nondimensional wavenumber)

%Sets Bloch number to zero. If no Bloch number found along dispersion curve
%search it implies that the solution is lossless and the frequency is
%within a band gap
Bloch = 0;
%Sets Attenuation number to zero. If no Attenuation number found along
%dispersion curve search it implies that the solution is lossless and
%the frequency is outside a band gap
Atten = 0;

%LOOP: Loops over Dispersion curve nearest incident eigenfrequency.
%Determines Bloch number and Attenuation number that correspond to the
%incident frequency chosen by user. NOTE THIS IS NOT AUTOMATED AND IS
%CURRENTLY CHOSEN SPECIFICALLY BY USER FOR ONE BRANCH IN PARTICULAR.
%WILL NEED TO BE CHANGED AS NEEDED.
```

```
for j=1:length(BlochZ)-1
if gammaZ(Zerozeros(2,1),BlochZ(j)) > efreq && ...
gammaZ(Zerozeros(2,1),BlochZ(j+1)) < efreq
    Bloch = (BlochZ(j)+BlochZ(j+1))/2; %Averages over the gridpoints
    break
end
end
for j=1:length(LossFac)-1
if gammaZLoss(Zerozeros(2,1),LossFac(j)) < efreq && ...
gammaZLoss(Zerozeros(2,1),LossFac(j+1)) > efreq
    Atten = (LossFac(j)+LossFac(j+1))/2; %Averages over the gridpoints
    break
end
end


%Construct Solution
k = Bloch/(lam*eta); %k value
kappa = Atten/(lam*eta); %\kappa value
%p parameter
pZero =@(gam) (r.*sin(gam.*s.*(lam-1)) ...
+ exp(-i*lam*eta*(k+sqrt(-1)*kappa)*px).*s.*sin(gam.*r))...
./(cos(gam.*s.*(lam-1)) - exp(-i*lam*eta*(k+sqrt(-1)*kappa)*px).*cos(gam.*r));
%Leader Order Cell Problem Solution
U =@(xi,gam) (r.*sin(s.*gam.*xi)+pZero(gam).*cos(s.*gam.*xi))...
.*heaviside(-xi)+(s.*sin(r.*gam.*xi)+pZero(gam).*cos(r.*gam.*xi))...
.*heaviside(xi);
%Derivative of Cell Problem Solution
DU =@(xi,gam) (r.*s.*gam.*cos(s.*gam.*xi)-pZero(gam).*s.*gam...
.*sin(s.*gam.*xi)).*heaviside(-xi)+(s.*r.*gam.*cos(r.*gam.*xi)...
-pZero(gam).*r.*gam.*sin(r.*gam.*xi)).*heaviside(xi);
%Define complex Bloch parameter
K = k+i*kappa;
%Define macroscale (envelope) function for left-moving wave
f1 =@(xi) exp(i*K.*eta.*xi);
%Define macroscale (envelope) function for right-moving wave
f2 =@(xi) exp(-i*K.*eta.*xi);

%Set up gridpoints for the domain
xi1 = 0:.01:lam*N; %Grid for whole domain in the microscale variable \xi
%Grid for the cell problem, bounded between -(lam-1)<\xi<1
xi2 = mod(xi1,lam)-(lam-1);
```

```
%%%%%%%%%%%%%%%%%%%%%%%%%%%%%%%%%%%%%%%%%&%%%%%%%%%%
%Solution to single slab external scattering problem
%%%%%%%%%%%%%%%%%%%%%%%%%%%%%%%%%%%%%%%%%&%%%%%%%%%%
%Problem solve the external scatering of a single layer of the homogenized
%material being illuminated on one side from the left.

E0 = 1; %Incident electric field amplitude
%Set of solution specific parameters
PP = (i*efreq+i*K*eta).*U(-(lam-1),efreq)+DU(-(lam-1),efreq);
PM = (i*efreq+i*K*eta).*U(1,efreq)-DU(1,efreq);
MP = (i*efreq-i*K*eta).*U(-(lam-1),efreq)+DU(-(lam-1),efreq);
MM = (i*efreq-i*K*eta).*U(1,efreq)-DU(1,efreq);
Q = 1-MP*MM*exp(2*i*K*eta*lam*N)./(PP*PM);

%Coefficients of solution for left and right moving waves
a2 = 2*i*efreq*E0./(PP*Q); %left moving wave
b2 = -MM*exp(2*i*K*eta*lam*N)*a2./PM; %right moving wave

%HFH Solution to scattering problem
Efield = a2.*f1(xi1).*U(xi2,efreq)+b2.*f2(xi1).*U(xi2,efreq);

%Determines and Plots solution in the free space region on the left
xi3 = -(lam-1):.01:0;
a1 = E0;
b1 = -E0 + (a2+b2).*U(-(lam-1),efreq);
E1 = a1*exp(i*efreq*xi3)+b1*exp(-i*efreq.*xi3);
Efield = [E1(1:length(E1)-1) Efield];


%%%%%%%%%%%%%%%%%%%%%%%%%%%%%%%%%%%%%%%%%%%%%%%%%%%%%%%%%%%%%%%%%%%%%%%%
%%%%%%%%%%%%%%%% Transfer Matrix Method Call %%%%%%%%%%%%%%%%%%%%%%%%%
%%%%%%%%%%%%%%%%%%%%%%%%%%%%%%%%%%%%%%%%%%%%%%%%%%%%%%%%%%%%%%%%%%%%%%%%

%Free space parameters (left hand side)
MatParam(1,1) = 1; %dielectric constant
MatParam(2,1) = 1; %layer width
for j = 2:(2*N+1)
    if mod(j,2) == 1
        %phase 2 dielectric constant
        MatParam(1,j) = ep2-sqrt(-1)*eta^2*epp2;
    else
        %phase 1 dielectric constant
```

```
        MatParam(1,j) = ep1-sqrt(-1)*eta^2*epp1;
    end
    MatParam(2,j) = 1; %layer width
end
%Free space parameters (right hand side)
MatParam(1,j+1) = 1; %dielectric constant
MatParam(2,j+1) = 1; %layer width
gam = efreq; %set incident eigenfrequency as the nondimensional wavenumber
Einit = [1 0]; %Set amplitude of incident electric field
[E,Dom] = TMM(MatParam,gam,Einit,"on"); %Function call

%Calculates Log base 10 of the absolute error
Error(count) = max(log10(abs(real(Efield)-real(E))));

end

%Plot Error over \eta for a particular dielectric loss
figure(1)
h11(colorindex) = plot(log10(1./(2*Cells)),Error,color{colorindex}...
,'LineWidth',2);
xlabel('log(\eta)')
ylabel('max(log(Absolute Error))')
set(gca,'Fontsize',18)
hold on

legendInfo{colorindex} = {['\overline{\epsilon}^{\prime\prime} = ' ...
num2str(ePrime(colorindex))]};

end

hh = legend(['$$\overline{\epsilon}^{\prime\prime} = $$' num2str(ePrime(1))], ...
    ['$$\overline{\epsilon}^{\prime\prime} = $$' num2str(ePrime(2))], ...
    ['$$\overline{\epsilon}^{\prime\prime} = $$' num2str(ePrime(3))], ...
    ['$$\overline{\epsilon}^{\prime\prime} = $$' num2str(ePrime(4))], ...
    ['$$\overline{\epsilon}^{\prime\prime} = $$' num2str(ePrime(5))]);

set(hh,'Interpreter','latex')
axis([-3 -2 -2.5 0.5])
```

## C.2 function files

```
%File - ParamDeclare.m
%PROGRAM: PowerResponse.m
%INPUT: none
%OUTPUT: Param - String of declared variables (cell array)
%        Fcn - String of declared functions (cell array)
%FUNCTION CALLS: none
%Description - Initilizes parameters and converts them into a string array
%for passing them to other functions and programs where they are redeclared

%{
Place the following block of code to declare parameters for use

% Runs function ParamDeclare.m to pass parameters
[Param,Fcn] = ParamDeclare;

%Initilize parameters for use in desired program
for j=1:length(Param)
    evalc([Param{j,1},'=',Param{j,2}]);
end
for j=1:length(Fcn)
    evalc(Fcn{j});
end
%}

function [Param,Fcn] = ParamDeclare

%%%%%%%%%%%%%%%%%%%%%%%%%%%%%%%%%%%%%%%%%%%%%%%%%%%%%%%%%%%%%%%%%%%%%%%%%%%%
%%%%%%%%%%%%%%%%%%%% USER SPECIFIED PARAMETERS  %%%%%%%%%%%%%%%%%%%%%%%%%%
%%%%%%%%%%%%%%%%%%%%%%%%%%%%%%%%%%%%%%%%%%%%%%%%%%%%%%%%%%%%%%%%%%%%%%%%%%%%
%User chooses values for microscale length (l) and wavelength (lam0)
%The rest of the parameters should be chosen to satisfy the validity
%conditions found from chosing scales of parameter

%GEOMETRY PARAMETERS
lam = 2; %Channel width parameter
l = 1e-5; %Microscale Length (Channel width)
L = 1; %Macroscale Length (Channel length): Chosen to satisfy \delta~\eta^2

%FLUID VELOCITY PARAMETERS
psign = -1; %Sign of pressure gradient (1=downward flow, -1=upward flow)
U = 1e-4; %Characterisitc fluid velocity: Chosen to satisfy Pe~\eta
```

```
mu = 1e-4; %Dynamic fluid viscosity: Chosen to satisfy Br~\eta^3

%THERMAL PARAMETERS
kf = 1.038e-3; %Thermal conductivity of fluid
km = 300; %Thermal conductivity of material
rhof = 1261.34; %Density of fluid
rhom = 3200; %Density of material
cf = 8.775; %Speficfic heat of fluid
cm = 4; %Specific heat of material
h = 1e-6; %Heat transfer coefficient: Chosen to satisfy Bi~\eta^2 (1e-6)
xi = 1e-7; %Emissivity: Chosen to satisfy Q~\eta^2
TA = 300;

%ELECTRIC FIELD PARAMETERS
lam0 = 1e-5*2*pi; %EM Wavelength
E0 = 1e3; %Incident electric field intensity: Chosen to satisfy P~\eta^2
epsilonf = (7*pi/2)^2; %Permittivity of fluid (4)
epsilonm = (1*pi)^2; %Permittivty of material (20)
lossfmag = 0.000; %Magnitude of Fluid Loss at zero Temp
lossfexp = 1; %Exponential Factor of Fluid Loss
lossmmag = 0.001; %Magnitude of Material Loss at zero Temp
lossmexp = 3; %Exponential Factor of Material Loss

%INCIDENT FILEDS (assume field is polarized in x or y completly)
EL = 1; %Left incident wave: x-component polarization
ER = 1; %Right incident wave: x-component polarization

%%%%%%%%%%%%%%%%%%%%%%%%%%%%%%%%%%%%%%%%%%%%%%%%%%%%%%%%%%%%%%%%%%%%%%%%%%%%%
%%%%%%%%%%%%%%%%%%%%% DO NOT CHANGE BEYOND THIS POINT %%%%%%%%%%%%%%%%%%%%%%%
%%%%%%%%%%%%%%%%%%%%%%%%%%%%%%%%%%%%%%%%%%%%%%%%%%%%%%%%%%%%%%%%%%%%%%%%%%%%%

%UNIVERSAL CONSTANTS
i = sqrt(-1); %Complex unit
ep0 = 8.85e-12; %Permittivity of free space
mu0 = 4.*pi.*1e-7; %Permeability of free space
c = 1./sqrt(ep0.*mu0); %Speed of light in free space
s = 5.67e-8; %Stefan-Boltzman constant

%PARAMETER GROUPS
omega = 2*pi*c./lam0; %angular frequency
eta = l./L; %aspect ratio
alphaf = kf./(rhof.*cf); %Thermal diffusivity of fluid
alpham = km./(rhom.*cm); %Thermal diffusivity of material
```

```
sigma0 = omega.*ep0; %characteristic effective conductivity
K = kf./km; %ratio of fluid to material thermal conductivity
alpha = alphaf./alpham; %ratio of fluid to material thermal diffusivity
Ue = -psign.*(lam-1).^3./3; %effective fluid velocity
A = 1+2.*(lam-1).*(K./alpha); %simplifying parameter
B = 1+2.*(lam-1).*K; %simplifying parameter
gamma = 2*pi*l./lam0; %Nondimensional wavenumber
omegabar = (omega.*l.^2)./alpham; %Nondimensional angular frequency

%SCLAED PARAMETER GROUPS
%This may be replaced by specified values for Pe, P, Bi, Q as long as they are
%around order 1 in scale and parameters satisfy the scaling validity
Pe_scale = eta;
P_scale = eta.^2;
Bi_scale = eta.^2;
Q_scale = eta.^2;
Pe = (l.*U./alphaf)./Pe_scale; %Scaled Peclet number
P = ((l.^2.*E0.^2.*sigma0)./(2.*km.*TA))./P_scale; %Scaled Power Parameter
Bi = (h.*l./kf)./Bi_scale; %Scaled Biot number
Q = (s.*xi.*TA.^3.*l./kf)./Q_scale; %Scaled Radiation Parameter

%NONDIMENSIONAL SCALES
tc = l.^2./alpham;

%Redefine Parameters as needed
P = 4;
K = 0.5;
alpha = ((rhom*cm)/(rhof*cf))*K;
Q = 0;
Pe = 2;
B = 1;
gamma = 1;
Bi = 0.5;
K = 0.5;
Q = 0;
lam = 2;
epsilonf = (7*pi/2)^2;
epsilonm = (1*pi)^2;
lossmmag = 0.001;
lossmexp = 3;
lossfmag = 0.000;
lossfexp = 0;
```

```matlab
%Convert Parameters to String Array to pass to other m-files
Param = {
    'lam' num2str(lam); ...              %1
    'gam' num2str(gamma); ...            %2
    'l' num2str(l); ...                  %3
    'L' num2str(L); ...                  %4
    'psign' num2str(psign); ...          %5
    'U' num2str(U); ...                  %6
    'mu' num2str(mu); ...                %7
    'kf' num2str(kf); ...                %8
    'km' num2str(km); ...                %9
    'rhom' num2str(rhom); ...            %10
    'rhof' num2str(rhof); ...            %11
    'cm' num2str(cm); ...                %12
    'cf' num2str(cf); ...                %13
    'h' num2str(h); ...                  %14
    'xi' num2str(xi); ...                %15
    'TA' num2str(TA); ...                %16
    'lam0' num2str(lam0); ...            %17
    'E0' num2str(E0); ...                %18
    'epsilonf' num2str(epsilonf); ...    %19
    'epsilonm' num2str(epsilonm); ...    %20
    'lossfmag' num2str(lossfmag); ...    %21
    'lossfexp' num2str(lossfexp); ...    %22
    'lossmmag' num2str(lossmmag); ...    %23
    'lossmexp' num2str(lossmexp); ...    %24
    'EL' num2str(EL); ...                %25
    'ER' num2str(ER); ...                %26
    'i' num2str(i); ...                  %27
    'ep0' num2str(ep0); ...              %28
    'mu0' num2str(mu0); ...              %29
    'c' num2str(c); ...                  %30
    's' num2str(s); ...                  %31
    'omega' num2str(omega);              %32
    'eta' num2str(eta);                  %33
    'alphaf' num2str(alphaf); ...        %34
    'alpham' num2str(alpham); ...        %35
    'sigma0' num2str(sigma0); ...        %36
    'K' num2str(K); ...                  %37
    'alpha' num2str(alpha); ...          %38
    'Ue' num2str(Ue); ...                %39
    'A' num2str(A); ...                  %40
    'B' num2str(B); ...                  %41
```

```matlab
    'omegabar' num2str(omegabar); ...    %42
    'Pe' num2str(Pe); ...                %43
    'P' num2str(P); ...                  %44
    'Bi' num2str(Bi); ...                %45
    'Q' num2str(Q); ...                  %46
    'tc' num2str(tc)};                   %47


Fcn = {'lossf =@(T) lossfmag.*exp(lossfexp.*T)'; ...
       'lossm =@(T) lossmmag.*exp(lossmexp.*T)';...
       'epf =@(T) epsilonf-i.*lossf(T)'; ...
       'epm =@(T) epsilonm-i.*lossm(T)'};

 %Outputs List of Parameters Used
   fid = fopen('ParamList.txt','wt');
   for j = 1:length(Param(:,1))
       fprintf(fid,[Param{j,1} '=' Param{j,2} '\n']);
   end
   fprintf(fid,'\n');
   for j = 1:length(Fcn)
       fprintf(fid,[Fcn{j} '\n']);
   end
   fclose(fid);

end
```

```
%PROGRAM: Emag3.m
%INPUT: T - Temperature (scalar/vector)
%       Param - String of parameters from ParamDeclare.m function call
%       Fcn - String of inline functions from ParamDecalre.m function call
%OUTPUT: E - L2 Electric Field Norm (scalar/vector)
%FUNCTION CALLS: none
%DESCRIPTION: Calculates the total magnitude (L2 norm) of Electric field
% absorbed by lossy layer in the triple layer laminate

function E = Emag3(T,Param,Fcn)

%Initilize parameters
for j=1:length(Param)
    evalc([Param{j,1},'=',Param{j,2}]);
end
for j=1:length(Fcn)
    evalc(Fcn{j});
end

i = sqrt(-1); %Complex unit
r2 = gam.*sqrt(epf(T)); %Complex wavenumber for region 2
r3 = gam.*sqrt(epm(T)); %Complec wavenumber for region 3
r4 = gam.*sqrt(epf(T)); %Complex wavenumber for region 4

%Construction of a3, b3, coefficients of EM wave in lossy material
Q1 = (1+((gam-r2)./(gam+r2)).*exp(-2.*i.*r2.*(lam-1)))...
./(1-((gam-r2)./(gam+r2)).*exp(-2.*i.*r2.*(lam-1)));
Q2 = (exp(-i.*r4)+((gam-r4)./(gam+r4)).*exp(i.*(r4-2.*r4.*lam)))...
./(exp(-i.*r4)-((gam-r4)./(gam+r4)).*exp(i.*(r4-2.*r4.*lam)));

b3 = (-(i.*r4.*Q2+i.*r3).*(Q1+1).*i.*r2.*(2.*gam./(gam+r2))...
.*exp(i.*(gam-r2).*(lam-1)).*EL+(i.*r2.*Q1-i.*r3).*exp(-i.*r3)...
.*(Q2+1).*i.*r4.*(2.*gam./(gam+r4)).*exp(i.*(gam.*lam+(1-lam).*r4)...
-i*gam).*ER)./((r2.*r4.*Q1.*Q2+r2.*r3.*Q1+r3.*r4.*Q2+r3.^2)...
-(r2.*r4.*Q1.*Q2-r2.*r3.*Q1-r3.*r4.*Q2+r3.^2).*exp(-i.*2.*r3));
a3 = ((i.*r4.*Q2-i.*r3).*exp(-i.*2.*r3).*(Q1+1).*i.*r2.*(2.*gam./(gam+r2))...
.*exp(i.*(gam-r2).*(lam-1)).*EL-(i.*r2.*Q1+i.*r3).*exp(-i.*r3).*(Q2+1)...
.*i.*r4.*(2.*gam./(gam+r4)).*exp(i.*(gam.*lam+(1-lam).*r4)-i*gam).*ER)...
./((r2.*r4.*Q1.*Q2+r2.*r3.*Q1+r3.*r4.*Q2+r3.^2)...
-(r2.*r4.*Q1.*Q2-r2.*r3.*Q1-r3.*r4.*Q2+r3.^2).*exp(-i.*2.*r3));
aa3 = ((i.*r4.*Q2-i.*r3).*exp(-i.*r3).*(Q1+1).*i.*r2.*(2.*gam./(gam+r2))...
.*exp(i.*(gam-r2).*(lam-1)).*EL-(i.*r2.*Q1+i.*r3).*(Q2+1).*i.*r4...
.*(2.*gam./(gam+r4)).*exp(i.*(gam.*lam+(1-lam).*r4)-i*gam).*ER)...
```

```matlab
./((r2.*r4.*Q1.*Q2+r2.*r3.*Q1+r3.*r4.*Q2+r3.^2)...
-(r2.*r4.*Q1.*Q2-r2.*r3.*Q1-r3.*r4.*Q2+r3.^2).*exp(-i.*2.*r3));

%L2 norm of the electric field in regions 3
E = ((aa3.*conj(aa3))./(i.*(r3-conj(r3))))-((a3.*conj(a3))./(i.*(r3-conj(r3))))...
    -((b3.*conj(b3))./(i.*(r3-conj(r3)))).*(exp(-i.*(r3-conj(r3)))-1)...
    +((aa3.*conj(b3))./(i.*(r3+conj(r3)))).*exp(i.*conj(r3))...
    -((a3.*conj(b3))./(i.*(r3+conj(r3))))-((b3.*conj(aa3))./(i.*(r3+conj(r3))))...
.*exp(-i.*r3)+((b3.*conj(a3))./(i.*(r3+conj(r3)))));

end
```

```
%PROGRAM: Efield3.m
%INPUT: T - (vector) temperature
%       z - (vector) spatial domain in region 3
%       Param - (cell array) string of parameters from ParamDeclare.m
%       Fcn - (cell array) string of functions from ParamDecalre.m
%OUTPUT: E - Spatially dependent modulus of the electric field
%FUNCTION CALLS: none
%DESCRIPTION: Calculates the modulus of the electric field for the
%triple-layer laminate problem with temperature dependent dielectric
%constant


function E = Efield3(T,z,Param,Fcn)

%%%%%%%%%%%%%%%%%%%%%%%%%%%%%%%%%%%%%%%%%%%%%%%%%%%%%%%%%%%%%%%%%%%%%%%%%%%
%%%%%%%%%%%%%%%%%%%%%%%%%% DECLARE MODEL PARAMETERS %%%%%%%%%%%%%%%%%%%%%%%%%
%%%%%%%%%%%%%%%%%%%%%%%%%%%%%%%%%%%%%%%%%%%%%%%%%%%%%%%%%%%%%%%%%%%%%%%%%%%%%

%INITIALIZE PARAMETERS FROM Param AND Fcn FOR USE IN PROGRAM
for j=1:length(Param)
    evalc([Param{j,1},'=',Param{j,2}]);
end
for j=1:length(Fcn)
    evalc(Fcn{j});
end

i = sqrt(-1); %imaginary unit
r2 = gam.*sqrt(epf(T)); %Complex wavenumber for region 2
r3 = gam.*sqrt(epm(T)); %Complec wavenumber for region 3
r4 = gam.*sqrt(epf(T)); %Complex wavenumber for region 4

%Construction of a3, b3, coefficients of EM wave in lossy material
Q1 = (1+((gam-r2)./(gam+r2)).*exp(-2.*i.*r2.*(lam-1)))...
./(1-((gam-r2)./(gam+r2)).*exp(-2.*i.*r2.*(lam-1)));
Q2 = (exp(-i.*r4)+((gam-r4)./(gam+r4)).*exp(i.*(r4-2.*r4.*lam)))...
./(exp(-i.*r4)-((gam-r4)./(gam+r4)).*exp(i.*(r4-2.*r4.*lam)));
den = (r2.*r4.*Q1.*Q2+r2.*r3.*Q1+r3.*r4.*Q2+r3.^2).*exp(i.*r3)...
-(r2.*r4.*Q1.*Q2-r2.*r3.*Q1-r3.*r4.*Q2+r3.^2).*exp(-i.*r3);
a3num = (i.*r4.*Q2-i.*r3).*exp(-i.*r3).*(Q1+1).*i.*r2.*(2.*gam./(gam+r2))...
.*exp(i.*(gam-r2).*(lam-1)).*EL-(i.*r2.*Q1+i.*r3).*(Q2+1).*i.*r4...
.*(2.*gam./(gam+r4)).*exp(i.*(gam.*lam+(1-lam).*r4)-i*gam).*ER;
b3num = -(i.*r4.*Q2+i.*r3).*exp(i.*r3).*(Q1+1).*i.*r2.*(2.*gam./(gam+r2))...
.*exp(i.*(gam-r2).*(lam-1)).*EL+(i.*r2.*Q1-i.*r3).*(Q2+1).*i.*r4...
```

```
.*(2.*gam./(gam+r4)).*exp(i.*(gam.*lam+(1-lam).*r4)-i*gam).*ER;
a3 = a3num./den;
b3 = b3num./den;

%Magnitude of Electric Field
E = a3.*conj(a3).*exp(i.*(r3-conj(r3)).*z)...
    +b3.*conj(b3).*exp(-i.*(r3-conj(r3)).*z)...
    +a3.*conj(b3).*exp(i.*(r3+conj(r3)).*z)...
    +b3.*conj(a3).*exp(-i.*(r3+conj(r3)).*z);
%real function used to make sure all of the imaginary parts are set
%identically to zero
E = real(E);

end
```

```
%PROGRAM: secant.m
%INPUT: f - function with zeros (function handle)
%        x0 - initial value less than root (scalar)
%        x1 - initial value greater than root (scalar)
%        tol - error tolerance within which to find the root (scalar)
%OUTPUT: x - root of function f between x0 and x1
%FUNCTION CALLS: none
%DESCRIPTION: Implements the secant method which is a root finding method
%that finds zeros of function f between two initial guesses x0 and x1 to an
%error tolerance determined by tol

function x = secant(f,x0,x1,tol)

relerr = 1; %Initilize relative error

%LOOP: Loops until the relative error is below the specified tolerance
while relerr > tol
    x = (x0.*f(x1)-x1.*f(x0))./(f(x1)-f(x0)); %root estimate
    relerr = max(abs(x-x1)./abs(x1)); %relative error
    x0 = x1; %define new left point
    x1 = x; %define new right point
end
```

```
%PROGRAM: tridiag.m
%INPUT: AL - subdiagonal of matrix
%        AM - main diagonal of matrix
%        AR - superdiagonal of matrix
%        r - right hand side of linear system
%OUTPUT: u - solution to linear system Au=r
%FUNCTION CALLS: none
%DESCRIPTION: Solves the linear system Au=r for A tridiagonal. Tridiagonal
%solver taken from the text Numerical Recipes

function u = tridiag(AL,AM,AR,r)

n = length(r);

bet = AM(1);
u(1) = r(1)/bet;

for j=2:n
   gam(j) = AR(j-1)/bet;
   bet = AM(j)-AL(j)*gam(j);
   if (bet==0) disp('trinumrec failed'), pause, end
   u(j) = (r(j)-AL(j)*u(j-1))/bet;
end

for j=n-1:-1:1
   u(j) = u(j) - gam(j+1)*u(j+1);
end
```

```
%PROGRAM: TMM.m
%INPUT: MatParam - (2 x N+2 matrix) Material parameter array, where Row 1 =
%                     complex dielectric constant, Row 2 = Layer width
%        gam - (scalar) nondimensional free space wavenumber
%              (2\pi\frac{l}{\lambda_0}), l=characteristic microscale,
%              \lambda_0 = free space wavelength
%        Einit - (1x2 vector) Incident field amplitudes from left and right
%                  boundaries
%        bars - (string) String set to "on" or "off" which will plot the
%                  layer boundaries with the solution or not
%OUTPUT: EE - (vector) Electric field across all layers and free space
%        Domain - (vector) Domain across all layers and free space
%FUNCTION CALLS: none
%DESCRIPTION: Solves Helmholtz equation for the scatering problem of two
%waves at normal incidence impinging upon an array of N parallel layers of
%dielectric media by the Transfer Matrix Method (TMM). Material parameters
%for each layer are defined in MatParam where MatParam(1,j) = complex
%dielectric constant and MatParam(2,j) = layer width.

%{
 NOTES ON USING CELL ARRAY FOR SET OF MATRICIES
 M = {[1 1; 2 2] [0 1; 1 0]};
 M{1} = first matrix M{2} = second matrix
 M{1}(1) = first element of first matrix
%}

function [EE,Domain] = TMM(MatParam,gam,Einit,bars)

%Initializations
N = length(MatParam(1,:))-2; %Number of Material layer
z0 = 0;
i = sqrt(-1); %imaginary unit
dc = MatParam(1,:); %redefines dielectric constant
l = MatParam(2,:); %redefines layer widths
L = sum(l(2:N+1)); %total width of material layers
k = gam.*sqrt(dc); %defines wavenumbers from dielectric constant

a = zeros(1,N+2); %allocate space for coefficients of right moving waves
b = zeros(1,N+2); %allocate space for coeeficients of left moving waves

%Initilize coefficients for incident waves (Sommerfeld Radiation Condition)
%Phase change on right wave needed for symmetry
a(1) = Einit(1);
```

```
b(N+2) = Einit(2).*exp(i.*k(N+2).*L);


%Creation of all the Individual Transfer Matrices
M = cell(2,N+1);
for j = 1:N
    plus = (k(j+1)+k(j))./(2.*k(j+1));
    minus = (k(j+1)-k(j))./(2.*k(j+1));
    %Transfer Matrix Across Layer Boundary
    M{1,j} = [plus minus; minus plus];
    %Transfer Matrix Across Layer
    M{2,j} = [exp(i.*k(j+1).*l(j+1)) 0; 0 exp(-i.*k(j+1).*l(j+1))];
end
plus = (k(N+2)+k(N+1))./(2.*k(N+2));
minus = (k(N+2)-k(N+1))./(2.*k(N+2));
M{1,N+1} = [plus minus; minus plus];


%Solution for the outer most coefficients b(1) and a(N+2)
TrMat = eye(2);
for j = 1:N
    TrMat = M{2,j}*M{1,j}*TrMat;
end
TrMat = M{1,N+1}*TrMat;


b(1) = (b(N+2).*exp(-i.*k(N+2).*(z0+L))-TrMat(2,1).*a(1)...
.*exp(i.*k(1).*z0))./(TrMat(2,2).*exp(-i.*k(1).*z0));
a(N+2) = (TrMat(1,1).*a(1).*exp(i.*(k(1).*z0))+TrMat(1,2)...
.*b(1).*exp(-i.*k(1).*z0))./(exp(i.*k(N+2).*(z0+L)));


%Solution for each of the interior coefficients
for m = 1:N
    TrMat = eye(2);
    for j = 1:m-1
        TrMat = M{2,j}*M{1,j}*TrMat;
    end
    TrMat = M{1,m}*TrMat;

    Len = sum(l(2:m));
    a(m+1) = (TrMat(1,1).*a(1).*exp(i.*k(1).*z0)+TrMat(1,2).*b(1)...
.*exp(-i.*k(1).*z0))./exp(i.*k(m+1).*(z0+Len));
    b(m+1) = (TrMat(2,1).*a(1).*exp(i.*k(1).*z0)+TrMat(2,2).*b(1)...
.*exp(-i.*k(1).*z0))./exp(-i.*k(m+1).*(z0+Len));
end
```

```matlab
%Plot Solution
dz = l(1)./100; %define grid length for 100 gridpoints in a layer
LB = z0-l(1); %define left boundary in grid
z = LB:dz:z0; %discretize domain for this layer
E = a(1).*exp(i.*k(1).*z)+b(1).*exp(-i.*k(1).*z); %Electric field solution
Dom = z; %define domain

%LOOP: Loops over each layer defining solution of electric field
for m = 2:N+1
   dz = l(m)./100; %define grid length for 100 gridpoints in a layer
   z = sum(l(2:m-1))+dz:dz:sum(l(2:m)); %discretize domain for this layer
   %Electric field solution
   E = [E a(m).*exp(i.*k(m).*z)+b(m).*exp(-i.*k(m).*z)];
   %Update total domain of all layers
   Dom = [Dom sum(l(2:m-1))+dz:dz:sum(l(2:m))];
end
dz = l(N+2)./100; %define grid length for 100 gridpoints in a layer
RB = z0+L+l(N+2); %define right boundary in grid
z = z0+L+dz:dz:RB; %discretize domain for this layer
EE = E; %Define EE as the electric field without the right freespace solution
Domain = Dom; %Define domain without the right freespace domain

%Right freespace solution
E = [E a(N+2).*exp(i.*k(N+2).*z)+b(N+2).*exp(-i.*k(N+2).*z)];
Dom = [Dom z0+L+dz:dz:RB];

%UNCOMMENT: If you want to plot solution within this function
%{
%Plots the boundaries of the material layers if the condition is true
figure(33)
if bars == "on"
for m = 2:N+1
   dz = l(m)./100;
   z = sum(l(2:m-1)):dz:sum(l(2:m));
   plot([z(1) z(1)],[min([-2 min(real(E))]) max([2 max(real(E))])]...
   ,'r','LineWidth',2)
   hold on
end
end
plot(Dom,real(E),'b','LineWidth',2);
hold on
%}
end
```